VOLUME 3 (1957) No. 3

NUCLEAR PHYSICS

MONTHLY JOURNAL DEVOTED TO THE EXPERIMENTAL AND THEORETICAL STUDY OF ATOMIC NUCLEI, NUCLEAR FIELDS AND THE FUNDAMENTAL ASPECTS OF COSMIC RADIATION

EDITOR: L. ROSENFELD · MANCHESTER

J. O. NEWTON, The Coulomb excitation of U^{235}, Pu^{239} and U^{238} 345
S. NILSSON, A decay of a negative τ' 364
T. LINDQUIST and I. MARKLUND, The influence of *l*-forbiddenness on magnetic dipole transitions in Tl^{203} 367
C. P. SIKKEMA, Scattering of fast neutrons by neon in the energy region 1.9 to 3.5 MeV 375
F. A. EL BEDEWI and M. A. ELWAHAB, An investigation of the reaction $^{23}Na(d, n)\ ^{24}Mg$ 385
K. LANIUS, Über die Zertrümmerung schwerer Kerne der Kernemulsion durch Teilchen der kosmischen Strahlung 391
V. F. WEISSKOPF, The problem of an effective mass in nuclear matter 423
I. M. KHALATNIKOV, Concerning the elastic scattering of high energy particles 433
L. PUZIKOV, R. RYNDIN and J. SMORODINSKY, Construction of the scattering matrix of a two-nucleon system 436
B. D'ESPAGNAT and J. PRENTKI, On symmetries in elementary particle interactions 446
J. S. LEVINGER, N. AUSTERN and P. MORRISON, The dipole sum rule with an approximate Hamiltonian 456
J. SCOBIE, Electron capture in arsenic 74 and arsenic 76 465
B. D'ESPAGNAT, R. OMNES, J. PRENTKI, Some remarks on decay rates of heavy mesons 471
R. E. WHITE and F. J. M. FARLEY, Polarisation in the inelastic scattering of neutrons by helium 476
S. OFER, The energy levels of Hf^{177} and the unified model 479
Book Reviews. 491
News Item 492

NORTH-HOLLAND PUBLISHING COMPANY - AMSTERDAM

May 1957

EDITORIAL BOARD

AUSTRIA: B. Karlik (Vienna), H. Thirring (Vienna)

BELGIUM: M. de Hemptinne (Louvain), J. Verhaeghe (Ghent)

CANADA: G. Volkoff (Vancouver)

DENMARK: C. Møller (Copenhagen), S. Rozental (Copenhagen)

EGYPT & ARAB COUNTRIES: F. El Bedewi (Alexandria), M. G. Nooh (Cairo)

FINLAND: L. Simons (Helsinki)

FRANCE: A. Berthelot (Saclay), S. Gorodetzky (Strasbourg), F. Joliot (Paris)

GERMANY (FED. REP.): W. Gentner (Freiburg i. B.), J. H. D. Jensen (Heidelberg)
GERMANY (DEM. REP.): G. Hertz (Leipzig)

GREAT BRITAIN: S. Devons (Manchester)

HUNGARY: L. Janossy (Budapest)

INDIA: H. Bhabha (Bombay), B. Peters (Bombay), R. Ramanna (Trombay)

IRISH REPUBLIC: J. McConnell (Maynooth)

ISRAEL: G. Racah (Jerusalem)

ITALY: E. Amaldi (Rome)

JAPAN: S. Kikuchi (Tokyo), S. Tomonaga (Tokyo)

NETHERLANDS: H. Brinkman (Groningen), S. R. de Groot (Leiden)

NORWAY: E. Hylleraas (Oslo), A. Lundby (Oslo), H. Wergeland (Trondheim)

POLAND: L. Infeld (Warsaw)

PORTUGAL: J. M. Araújo (Porto), J. R. de Almeida Santos (Coimbra)

SOUTH AMERICA: G. Beck (Saõ Paulo), J. Leite Lopes (Rio de Janeiro)

SPAIN: J. M. Otero (Madrid), C. Sanchez del Rio (Madrid)

SWEDEN: O. Klein (Stockholm), K. Siegbahn (Uppsala), I. Waller (Uppsala)

SWITZERLAND: P. Huber (Basel), P. Scherrer (Zürich)

U.S.S.R.: M. A. Markov (Moscow), I. S. Shapiro (Moscow), D. V. Skobeltzyn (Moscow)

YUGOSLAVIA: I. Supek (Zagreb)

U.S.A. & MEXICO: V. Weisskopf (Cambridge, Mass.)

AUSTRALIA & NEW ZEALAND: H. Messel (Sydney), M. L. Oliphant (Canberra)

CONTRIBUTIONS may be sent to the Editor, Professor L. Rosenfeld, Dept. of Theoretical Physics, The University, Manchester, either directly, or preferably through the intermediary of one of the members of the Editorial Board of the country or region in which the author is working. They may be written in English, French or German.

NUCLEAR PHYSICS is published in monthly issues. The subscription price is fl 57.00; 114s; $ 15.00. Postfree.

SUBSCRIPTIONS should be sent to the publishers, NORTH-HOLLAND PUBLISHING COMPANY, P.O.Box 103, Amsterdam or to any subscription-agent. Subscriptions for U.S.A. are to be sent exclusively to INTERSCIENCE PUBLISHERS, INC., 250 Fifth Avenue, New York 1, N.Y.

BOOKS FOR REVIEW should be sent to Professor Rosenfeld.

No part of this issue may be reproduced in any form, by print, photoprint, microfilm or any other means without written permission from the publisher. Reprints, photoprints or microfilms are obtainable at cost from the publisher.

Printed in the Netherlands

Nuclear Physics **3** (1957) 345—363; *North-Holland Publishing Co., Amsterdam*

THE COULOMB EXCITATION OF U^{235}, Pu^{239}, AND U^{238}

J. O. NEWTON †

Atomic Energy Research Establishment, Harwell

Received 3 January 1957

Abstract: Gamma rays from the Coulomb excitation of U^{235}, Pu^{239} and U^{238} have been observed with a xenon filled proportional counter. Energies of 46.23 ± 0.2, 56.74 ± 0.3 and 103.2 ± 1 keV with U^{235}, 49.6 ± 0.3 and 57.5 ± 0.3 keV with Pu^{239} and 44.7 ± 0.2 keV with U^{238} were obtained. The gamma rays are interpreted as arising from the decay of rotational states. From the absolute cross sections and from the branching ratios of the gamma rays from the second rotational states the reduced transition probabilities B_{E2} and intrinsic quadrupole moments Q_0 were estimated. Mean values for Q_0 of 10.1, 9.2 and 10.3 barns were obtained for U^{235}, Pu^{239} and U^{238} respectively. Possible assignments of single particle states in a deformed potential to the ground states of U^{235} and Pu^{239} are discussed.

1. Introduction

The excitation of nuclei by the Coulomb interaction provides a powerful tool in the study of their energy levels below about 1 MeV in energy. The reduced transition probabilities for excitation and decay of a particular level by the multipolarity of the excitation can be obtained directly from the cross section; information about the spin and multipolarities of decay can be obtained by angular distribution and polarisation measurements of the gamma rays and by measurements of the conversion electrons.

This method has been extensively exploited in the last three years, e.g. Heydenburg and Temmer [1]), Stelson and McGowen [2]), Huus, Bjerregaard and Elbek [3]). With about one exception the multipolarity of the excitation has been electric quadrupole and most of the states excited have been of the collective type. This is at first sight surprising because the cross section for electric dipole excitation is greater than that for electric quadrupole excitation [4, 5]) if the reduced transition probabilities B_{E1} have the single particle (Weisskopf formula) values. However, inspection of the predicted single particle energy levels for nuclei (see for example Nilsson [6])) shows that few low lying states which could be reached by E1 excitation are expected to exist and that these might in general be expected to have values of the B_{E1} much smaller than those for a single particle. On the other hand levels of the collective type may have values of B_{E2} up to 100 times greater than those for a single particle (Bohr and Mottelson [7])).

† At present on leave of absence at the Radiation Laboratory, University of California, Berkeley, California.

The measurements reported here are on the odd mass radioactive nuclei U^{235} and Pu^{239} and the even nucleus U^{236}; further work on U^{233} and Np^{237} is reported in a companion paper (Newton [8])). This region of nuclei has not so far been extensively studied by the Coulomb excitation method.

The principal difficulties of Coulomb excitation experiments on these very heavy nuclei are:

(a) The gamma rays produced have in general energies less than 100 keV. Thus sodium iodide spectrometers give poor resolution ($\approx$ 25 %) whilst the energies of the conversion electrons are so low that they are difficult to detect amongst the general background of scattered electrons [3]).

(b) The conversion coefficients of the gamma rays are high, of the order of 10^2—10^3, so that the observed radiation is correspondingly weak.

(c) The nuclei are radioactive, producing gamma rays of their own.

In view of (a) it was decided to use a xenon filled proportional counter to detect the gamma rays. Such a counter has good resolution and fair efficiency, about 7 % and 12 % respectively at 60 keV.

Three gamma rays were observed from the excitation of U^{235} and two from Pu^{239}. It seems reasonable to attribute these to the decay of rotational states which are found to exist in many nuclei well removed from closed shells [7, 9]).

2. Experimental Method

Targets, in the form of the oxides (U_3O_8 and PuO_2) deposited on 0.005" Ni foil, were bombarded with singly charged helium ions from the Harwell Van de Graaf generator. They were prepared in the Chemistry Division of A.E.R.E. by the method given by Glover and Borrell [10]); deposits which vary in thickness by only a few per cent can be made in this way. They covered an area of diameter 1 cm and had a density of approximately 400 $\mu g/cm^2$. Both the thickness of the target to alpha particles and the amount of radioactive material present was measured by counting and pulse analysis in a standard low geometry proportional counter. The beam of helium ions was approximately 6 mm in diameter and produced a faint darkening where it hit the target. In the alpha measurements a collimator, consisting of a piece of 0.005" Al foil with a 6 mm hole in it, was placed round this region. It was therefore possible to give a good estimate of the average density of target material in the region which was bombarded. Since the targets were "nearly thin" as shown by the pulse analysis, slight variations in thickness over this region were not of importance.

The charge falling on the target was measured by a current integrator, the secondary electrons having been suppressed by a potential of 100 volts.

The proportional counter was of the type described by West and Bradley[11]) and was filled to a pressure of 2.3 atmospheres with xenon; it was of 5 cm

diameter and had an active length of 9 cm. The counter was placed in the 0° position with respect to the incident beam and its axis was 3.2 cm from the target.

It would be difficult to make an accurate calculation of the absolute efficiency of the counter in this geometry. The efficiency of the counter was therefore measured at 59.6 keV by counting the gamma rays from a source of Am^{241}, whose disintegration rate had been measured in a low geometry counter; the number of 59.6 keV gamma rays per alpha particle was taken to be 0.40 ± 0.015 as reported by Beling, Newton and Rose [12]). The efficiency at other energies was then estimated by a graphical integration method which took into account the geometry of the system; the absorption coefficients used were those given by Compton and Allison [13]). The curve of efficiency for the full energy peak as a function of energy is shown in fig. 1; this takes into account the fact that there are no escape peaks for

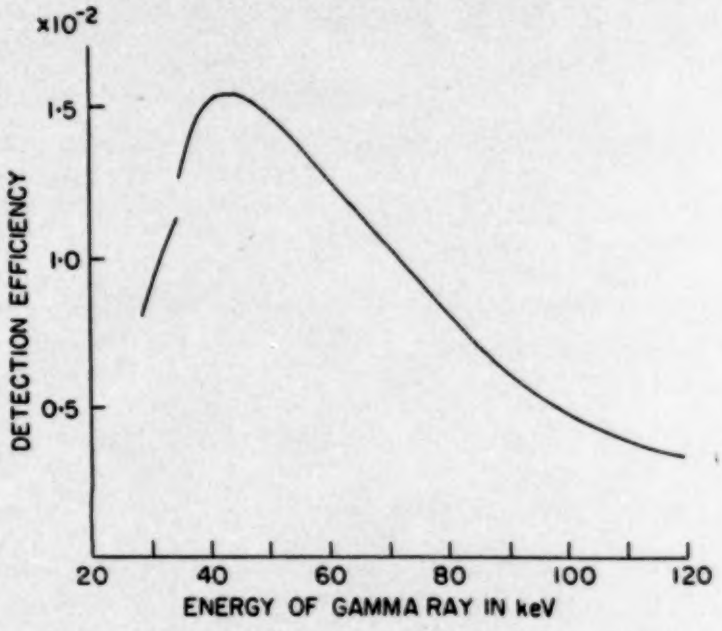

Fig. 1. Overall efficiency for detection of gamma rays in the main peak as a function of gamma ray energy.

gamma rays having energies less than that of the L absorption edge in xenon.

It was thought desirable to make a check on this semi-empirical efficiency curve at a point where the errors might be expected to be greatest, i.e. at the low energy end of the curve. The 29 keV gamma ray from the decay of Np^{237} was convenient for this purpose. A determination of its energy was made with a krypton filled counter by comparing its pulse height distribution with that of the 26.36 keV gamma ray from Am^{241} decay (Day [14])) and with a xenon filled counter by comparing with the

escape peak (29.91 keV) of the 59.57 keV gamma ray from Am^{241} decay [14]). A value of 29.66 ± 0.08 keV was obtained. The absolute intensity of this gamma ray from the source used in the Coulomb excitation experiment was measured by comparing its counting rate in a krypton filled counter with that of the 26.36 keV gamma ray from an Am^{241} source of measured disintegration rate taken in the same geometry. The gamma rays were collimated through a 0.0015″ mica window into the counter so that absorber corrections were negligible. From this value of the intensity and the measured alpha-disintegration rate of the source a value of (0.139 ± 0.016)

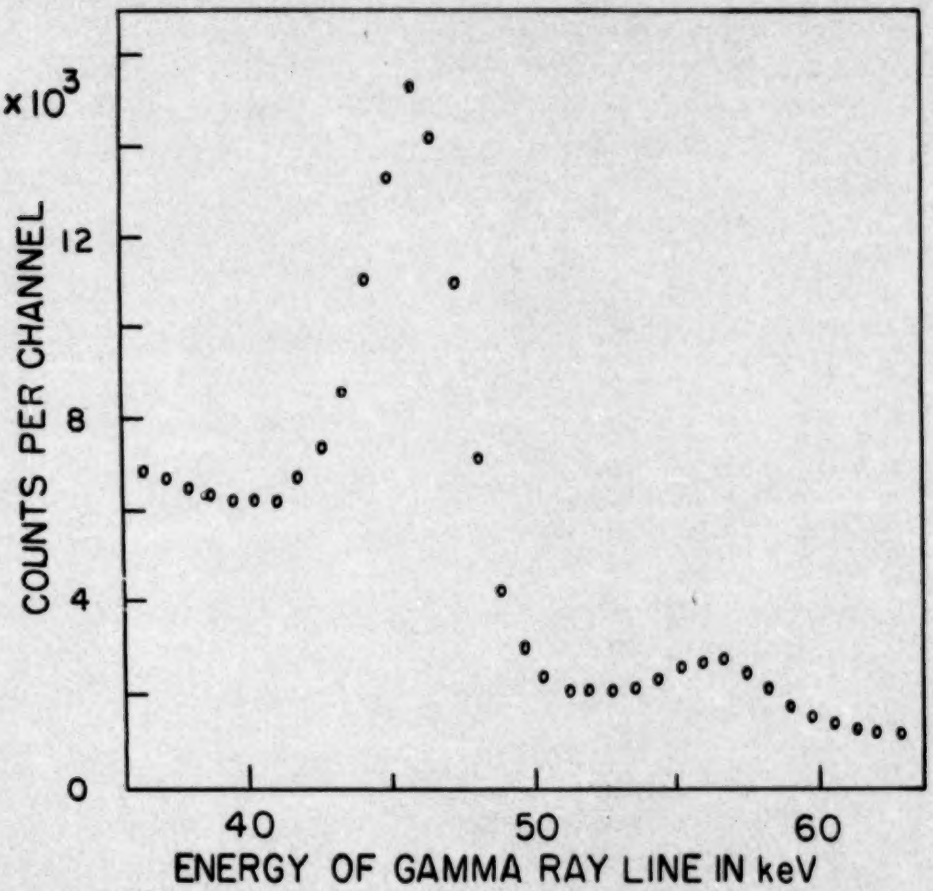

Fig. 2. Pulse height spectrum of the 46.2 and 56.7 keV gamma rays from the Coulomb excitation of U^{235}.

was obtained for the number of 29.7 KeV gamma rays per alpha particle; the value obtained when the Np^{237} was in the target position and the semi-empirical efficiency curve assumed was (0.130 ± 0.015). These results are in satisfactory agreement with one another and with that of 0.14 reported by Magnusson *et al.* [15]).

A thirty channel kicksorter (A.E.R.E. type 1091A) was used to analyse the pulses from the proportional counter and the 59.57 keV gamma ray from the decay of Am^{241} [14]) was used as the energy standard. Both the

full energy and escape peaks were used; the escape peak has an energy equal to the full energy minus the K X-ray energy of xenon (29.66 keV).

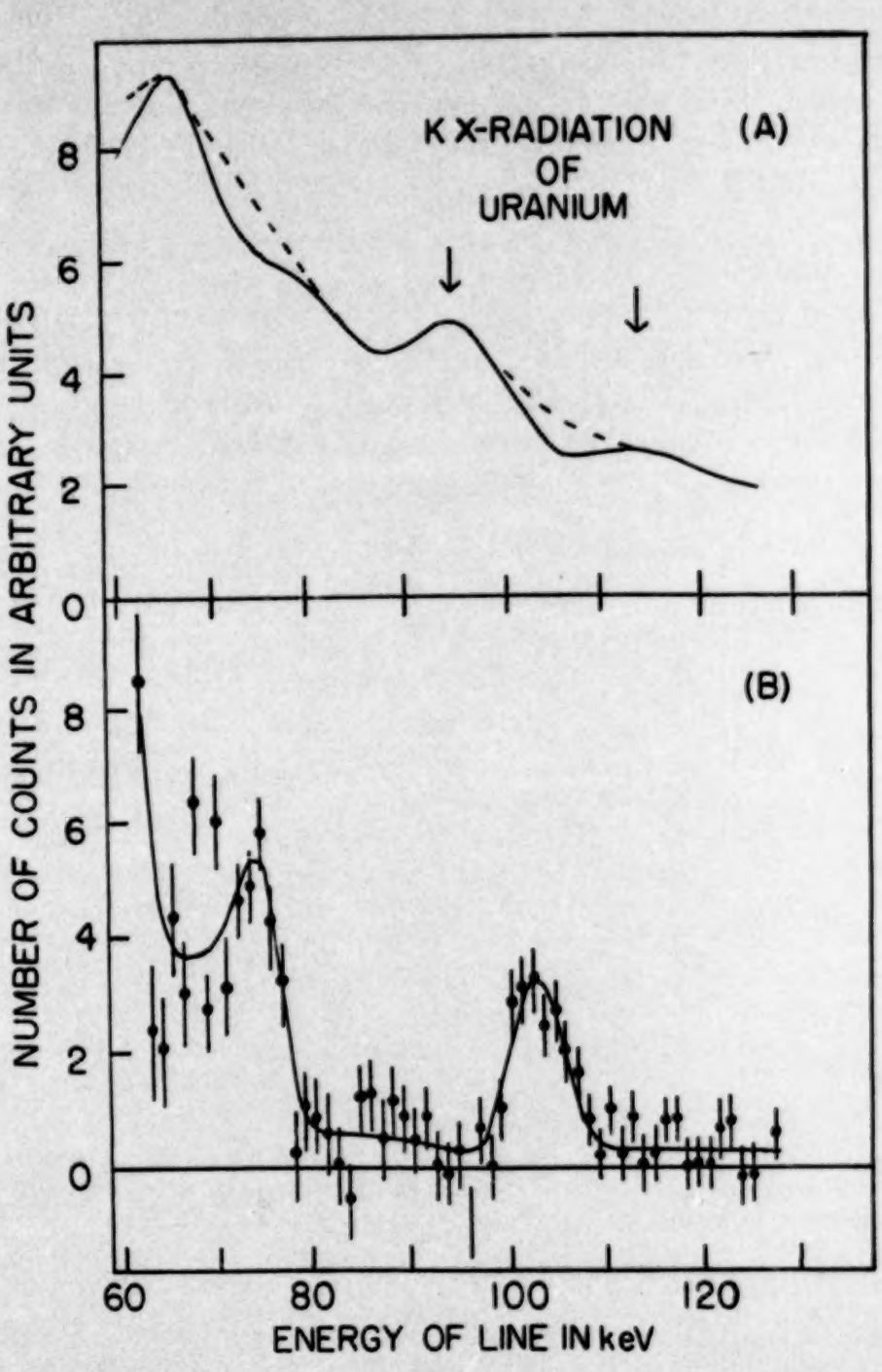

Fig. 3. (A) Full line: pulse height spectrum from the Coulomb excitation of natural uranium. Broken line: pulse height spectrum from the Coulomb excitation of U^{235}.

(B) Difference between the pulse height spectra of (A) above, showing the main and escape peaks of the 103 keV gamma ray. The rise on the extreme left arises from the main peak of the 56.7 keV line.

3. Energies, Relative Intensities and Cross Sections for the Production of Gamma Rays

3.1. THE NUCLEUS U^{238}

One gamma ray with energy 44.7 ± 0.2 keV was observed together with the L and K X-radiation of uranium. The cross section at 2.85 MeV bombarding energy for the 44.7 keV radiation is $(5.7 \pm 1) \times 10^{-29}$ cm^2.

3.2. THE NUCLEUS 3.2 U^{235}

The target contained 79 % of U^{235} and 21 % of U^{238}. It was therefore necessary to subtract out the contribution of the U^{238}. Three gamma rays having energies of 46.23 ± 0.2, 56.74 ± 0.3 and 103.2 ± 1 keV were observed together with uranium X-radiation. Fig. 2 shows a spectrum of the two lower energy lines (escape peaks not shown), whilst in fig. 3b is shown the spectrum of the 103 keV line. In the latter case it was necessary to subtract from the spectrum obtained that produced by bombarding a target of

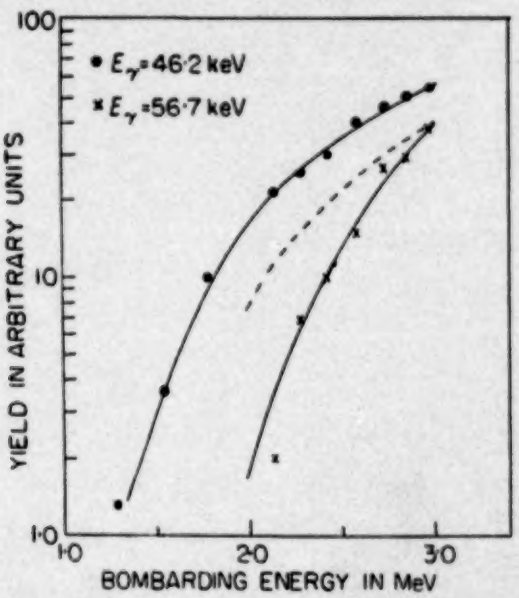

Fig. 4. Excitation functions for the 46.2 and 56.7 keV gamma rays of U^{235}. The full lines are the theoretical curves for excitation of states at 46.2 and 103.0 keV respectively; the broken line is the theoretical curve for excitation of a state at 56.7 keV.

natural uranium with helium ions of the same energy. In this way it was possible to subtract out the effect of the continuous bremsstrahlung spectrum and that of the K X-rays of uranium (fig. 3a). Four separate pairs of runs were made on this spectrum and there seems no doubt that the 103 keV gamma ray exists.

Excitation functions of the 46.2 keV and 56.7 keV gamma rays were measured; they are shown in fig. 4. The full lines are the theoretical curves, arbitrarily normalised, for the excitation of 46.2 keV and 103.0 keV states;

the dotted curve is that for excitation of a state at 56.7 keV. The excitation function for the 103 keV gamma ray was not measured. The results are consistent with these gamma rays arising from the excitation of states at 46.2 keV and 103.0 keV.

The relative intensities of the gamma rays at a bombarding energy of 2.85 MeV are given in table 1; the cross section for the production of the 46.2 keV gamma ray is $(2.56\pm0.3)\times10^{-28}$ cm^2.

TABLE 1

Relative intensities of the gamma rays from the Coulomb excitation of U^{235} by 2.85 MeV helium ions

Energy in keV	46.23 ± 0.2	56.74 ± 0.3	103.2 ± 1
Relative intensity	1	$(6.6\pm0.8)\times10^{-2}$	$(1.6\pm0.2)\times10^{-2}$

3.3 THE NUCLEUS Pu^{239}

The gamma radiation from the decay of this nucleus was sufficiently intense to produce a serious background. Two gamma rays having energies of 49.6 ± 0.3 keV and 57.5 ± 0.3 keV were observed.

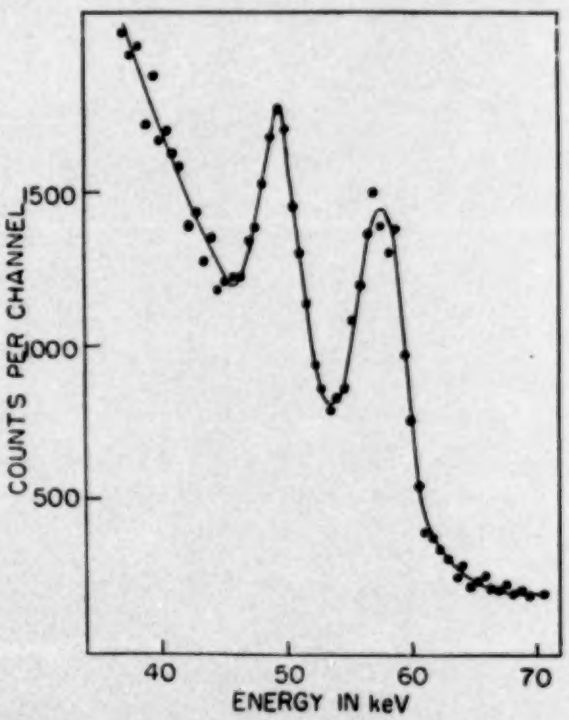

Fig. 5. Pulse height spectrum, with source background subtracted, of the 49.6 and 57.5 keV gamma rays of Pu^{239}.

In fig. 5 is shown the spectrum after subtraction of the background with the beam off. The excitation functions of the two gamma rays were measured and are shown in fig. 6. It was not possible to decide from these whether the two gamma rays originated from one state at 57.5 keV or from

states at 49.6 and 57.5 keV; but it is clear that neither gamma ray comes from a state at 107.1 keV.

The intensity of the 57.5 keV gamma ray relative to that of the 49.6 keV gamma ray at 2.85 MeV bombarding energy is 1.63 ± 0.12; the cross section for production of the 49.6 keV gamma ray is $(2.23 \pm 0.3) \times 10^{-29}$ cm^2.

4. Interpretation

4.1. THEORETICAL CONSIDERATIONS

Since rotational states have been observed to occur systematically in nuclei well removed from closed shells [7, 9]) it is reasonable to suppose that rotational states were excited in these experiments. The ratios of the energies of the levels which were excited support this assumption (see

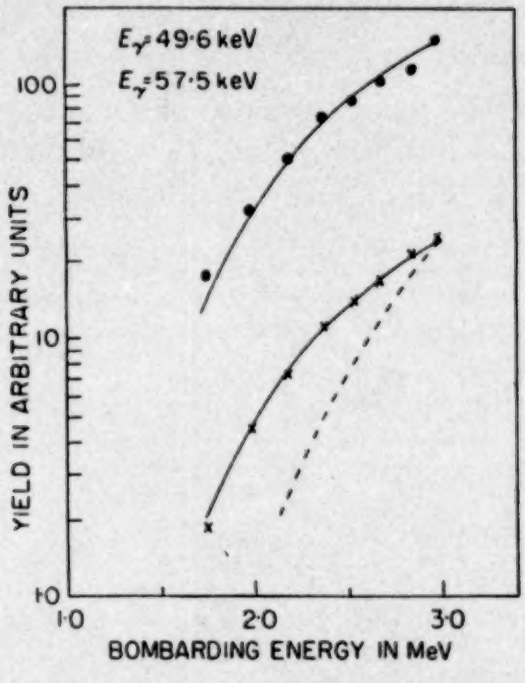

Fig. 6. Excitation functions for the 49.6 and 57.5 keV gamma rays of Pu^{239}. The full lines are the theoretical curves for excitation of a state at 57.5 keV; the broken line is the theoretical curve for excitation of a state at 107 keV.

§ 4.2). The results of these experiments will therefore be used as a check on the theory of rotational states as given by Bohr and Mottelson [7]); Alaga, Alder, Bohr and Mottelson [16]); Nilsson [6]). The results of this theory are now so well known that they will not be reproduced here except where required for reasons of clarity. In addition to the original papers given above an excellent review of the theory from the point of view of the experimentalist has been given by Huus, Bjerregaard and Elbeck [3]).

With E2 Coulomb excitation it is generally possible to reach one rotational state in an even nucleus and two states in an odd mass nucleus. The decay of the two states (1,2) in the case of the odd nucleus with

$K \neq \frac{1}{2}$ gives rise to three gamma rays, one γ_{20}, being a pure E2 transition, the other two, γ_{21} and γ_{10}, being mixed M1, E2 transitions. If the mixing ratios and conversion coefficients are known it is possible to estimate the total cross sections for excitation of the states.

Tables of L conversion coefficients taking into account screening but not finite nuclear size have been circulated by M. E. Rose. It now appears both from the calculations of Sliv and from experimental results [17, 18, 19, 20]) that the assumption of a point nucleus produces a serious error in the results for magnetic dipole transitions. The ratio of the calculated K conversion coefficient for a point nucleus to that for an extended nucleus is not very sensitive to energy or charge number and the corresponding ratio for L conversion probably has about the same value. These experimental results have therefore been worked out (a) with Rose's data and (b) with Rose's M1 data multiplied by a factor of 0.6 estimated from a comparison of Rose's and Sliv's K conversion coefficients. The amount of M+N+ . . . conversion was estimated empirically. (see § 4.3).

It is possible to deduce the mixing ratios from measurements of the conversion lines, by combined angular correlation and polarisation measurements, or, rather more indirectly, by measuring the strength of the pure E2 transition relative to that of the mixed transition from the same state. In the present experiments we have used the last method, even though it is in some ways the least satisfactory. However, if angular distribution measurements had been made there would be some doubt about their interpretation because it is possible that large attenuation coefficients (Abragam and Pound [21])) are involved; these are certainly observed in ($\alpha-\gamma$) angular correlations in this region (see the review article by Newton [22]) for references).

Assuming the result of Alaga, Alder, Bohr and Mottelson [16]) we have

$$\frac{B_{E2}(2 \to 0)}{B_{E2}(2 \to 1)} = \frac{\langle I_2 2K0 | KK \rangle^2}{\langle I_2 2K0 | I_1 K \rangle^2}$$

where $I_i = K+i$ is the spin of the i^{th} rotational state. Thus we may calculate the intensity of the E2 part of the $2 \to 1$ transition if we know that of the $2 \to 0$ transition. The difference between this and the total intensity for the $2 \to 1$ transition then gives the M1 intensity. It can also be shown that if δ_{ij}^2 is the ratio of E2 to M1 quanta in the transition from level i to level j, then

$$\left(\frac{\delta_{10}}{\delta_{21}}\right)^2 = \left(\frac{\Delta E_{10}}{\Delta E_{21}}\right)^2 \cdot \frac{(K+1)(K+3)}{K(K+2)}$$

where ΔE_{10} is the energy difference between state 1 and 0 etc. Experimental evidence supporting these rules for allowed transitions is steadily mounting; some examples are given in ref. [16]) and others in the paper by Stephens,

Asaro and Perlman [23]). With these results and the calculated conversion coefficients we may calculate the total excitation of the two states and hence the $B_{E2}(0 \to 2)$ and $B_{E2}(0 \to 1)$. Then with the relations

$$B_{E2}(0 \to 1) = \frac{15}{16\pi} e^2 Q_0^2(1) \frac{K}{(K+1)(K+2)}$$

and

$$B_{E2}(0 \to 2) = \frac{15}{8\pi} e^2 Q_0^2(2) \frac{1}{(2K+3)(K+2)}$$

we can calculate the effective intrinsic quadrupole moments $Q_0(1)$ and $Q_0(2)$ for the first and second rotational states. According to unified model theory $Q_0(1) = Q_0(2)$ so that we may test the model by seeing whether this relation holds. It should be remembered however that some results of the model have already been assumed in obtaining our values for B_{E2}; in the absence of further data we are in effect testing the self-consistency of the model.

In the case of Pu^{239} it is possible to compare our value for the E2:M1 branching ratio with that obtained from conversion electron data on the 49.6 keV transition by Hollander, Smith and Mihelich [24]) in their work on Np^{239} decay. Our value of 0.29 ± 0.03 agrees well with theirs of 0.27 ± 0.05 [25]) obtained when they use Rose's M1 conversion coefficients multiplied by 0.6. When they use the unmodified coefficients they get 0.43 ± 0.08. This result suggests that the theoretical branching ratios of Alaga *et al.* are not seriously in error in this case at any rate. A further quantity of interest which can be derived from the E2:M1 branching ratios, when $K > \frac{1}{2}$, is $|g_\Omega - g_R|$, where g_Ω and g_R are the gyromagnetic ratios for the particle and the core. On the irrotational model $g_R = +Z/A$; the few experimental values obtained so far [26, 27]) are in some cases nearly a factor of two smaller than Z/A but do not exceed this by a significant factor. The ground state magnetic moment is given by

$$\mu = \frac{K^2}{K+1} g_\Omega + \frac{K}{K+1} g_R \text{ for } K > \tfrac{1}{2}.$$

Thus, if the branching ratio and magnetic moment are known, values for g_Ω and g_R can be obtained; they will not be unique unless the signs of μ and $(g_\Omega - g_R)$ are known.

4.2. THE ROTATIONAL LEVELS

The spin of the U^{235} ground state is reported to be 7/2 [28, 29]) though at the time this experiment was performed it was thought to be 5/2 [30]). From the simple theory of rotational states [7]), which seems to be obeyed fairly well in this region of nuclei [22]), the ratio of the energies of the second

to those of the first excited states are given as 2.286 and 2.222 for ground state spins 5/2 and 7/2 respectively; the measured value of 2.229 ± 0.009 is in good agreement with that expected for spin 7/2.

The spin of Pu^{239} has been given as $\frac{1}{2}$ [31, 32]). The spacing of the rotational states is therefore expected to be irregular. Unfortunately it was not possible to decide from the experimental results whether the two observed gamma rays came from the same state at 57.5 keV or from states at 49.6 and 57.5 keV. The energies of the states of a rotational band with $K = \frac{1}{2}$ are given by [9])

$$E(I) = \frac{\hbar^2}{2\mathscr{I}}\{I(I+1)+a(-1)^{I+\frac{1}{2}}(I+\tfrac{1}{2})\}.$$

The ambiguities in the level positions and in the spins, which could be 3/2 or 5/2, lead to 4 values for the parameters $\hbar^2/2\,\mathscr{I}$ and a. These are listed in table 2.

TABLE 2
Rotational parameters

Level order	A 3/2 5/2	A 5/2 3/2	B 3/2 5/2	B 5/2 3/2
$\hbar^2/2\,\mathscr{I}$ (keV)	6.28	4.62	9.06	8.79
a	−0.57	+3.16	+0.83	+1.18
E, I	75.9, 7/2	52.8, 9/2	173.2, 7/2	169.5, 9/2

A and B refer to levels at 7.9 and 57.5 keV and at 57.5 keV respectively; the spin of the lower state is given on the left. E and I are the energy and spin predicted for the next excited state.

Now it seems to be a general rule, which can be understood on the basis of rotational-particle coupling (Kerman [33])), that the values of $\hbar^2/2\mathscr{I}$ are smaller for odd mass nuclei than for the neighbouring even nuclei [9]). The value for Pu^{238} is 7.34 keV so that if we accept this rule two of the possibilities in table 2 can be ruled out. Further support for this is given by the alpha decay of Pu^{239} [34]). It has been suggested independently by Newton [22]) and by Bohr and Mottelson [35]) that the favoured alpha particle transitions take place between bands having the same value of K and moreover, since the deformation changes slowly with A, that the two bands should be similar. One indeed finds that the alpha decay of Pu^{239} leads to a set of states in U^{235} with energies, relative to the lowest of these states, of 13.5 and 52 keV. Furthermore the relative intensities of the alpha particle groups support the view that the 13.5 keV state has spin 3/2 [35]); it is likely therefore that the 7.9 keV state in Pu^{239} also has spin 3/2. Additional support for this conclusion is given by the work of Graham and Bell [36, 37]), on the beta decay of Np^{239}, who find a gamma ray having an energy of 67 keV which can be interpreted as leading to the 7.9 keV state. A gamma ray of energy (68.0 ± 1) keV leading to this state would be ex-

pected from the decay of the third rotational state of the band given in column 1 of table 2; the decay of the third rotational state of the band given in column 2 would give a gamma ray of energy (44.9±1.3) keV. It seems likely from this evidence that the parameters of the rotational band are as given in column 1; this conclusion was reached independently by Hollander, Smith and Mihelich [24]) from experiments on the beta decay of Np^{239}. Though the evidence in favor of the postulated decay scheme from the beta-decay and Coulomb excitation experiments taken separately cannot be considered strong, the combined evidence is very strong; it does not seem to be possible to fit the beta decay data into a scheme with levels at 49.6 and 57.5 keV. Transitions from higher levels in Pu^{239} to this rotational band are discussed in the above paper [24]) and in the paper, by Newton and Rose [38]).

4.3. THE QUADRUPOLE MOMENTS AND REDUCED TRANSITION PROBABILITIES

These were calculated from the data as explained in § 4.1. The amount of M+N ··· conversion is significant and it was necessary to make an empirical estimate of this from experimental results. The values of (M+N ···)/L for E2 transitions used in this estimate are given in table 3. The scatter may well be due to the considerable experimental difficul-

TABLE 3
Values of (M+N . . .)/L for various E+ transitions.

Nucleus	Th^{228}	Ra^{224}	Np^{237}	Th^{234}	Ra^{226}	Ra^{226}	U^{230}
E (keV)	57	84.2	99	48	67	67	53
$\frac{M+N\ldots}{L}$	0.34	0.36	0.28	0.2	0.33	0.34	0.28
Ref.	[39])	[40])	[41])	[42])	[43])	[44])	[45])

ties. The unweighted mean of these values is 0.304±0.02. Some further values for this quantity, with $E \approx 44$ keV, were collected by Rasmussen, Slatis and Passell [46]); the mean of the 4 results with a β^- spectrometer has a value of 0.301±0.005 in good agreement with the above.

There are few examples of pure M1 transitions in heavy nuclei. Those we have taken are given in table 4. The mean of these results is 0.31±0.02.

TABLE 4
Values of (M+N . . .)/L for various M1 transitions

Nucleus	Th^{228}	Bi^{210}	Bi^{210}	Np^{237}	Np^{237}
E (keV)	184	47	47	208	208
$\frac{M+N\ldots}{L}$	0.3	0.266±0.03	0.345±0.05	0.29	0.33
Ref.	[47])	[48])	[49])	[50])	[51])

A value of 0.3 for $(M+N\cdots)/L$ has been taken for all the transitions in this work. Though there is no good reason for supposing that this quantity is entirely independent of multipolarity, energy and atomic number, it seems unlikely that the assumption of the above value will lead to an error of more than 5 % in the total cross sections.

The L conversion coefficients which were derived from Rose's tables are given in table 5. The M1 coefficients shown here were multiplied by 0.6 in order to allow for the finite nuclear size correction.

TABLE 5

L conversion coefficients used in the calculations.

Nucleus	E2			M1	
	γ_{10}	γ_{21}	γ_{20}	γ_{10}	γ_{21}
U^{238}	500				
U^{235}	420	158	8.3	53.5	29.4
Pu^{239}		405	195		58.7

In table 6 are given the values obtained for the B_{E2}, Q_0 and $g_\Omega - g_R$. The errors given do not include any allowance for the possibility that the conversion coefficients used may be inaccurate. The magnetic moment of U^{235} has been given as 0.31 [29]) and from this we obtain values of -0.015 and 0.45 or -0.19 and 0.27 for g_Ω and g_R respectively, assuming that g_R is positive.

TABLE 6

Values of Q_0, B_{E2} and $|g_\Omega - g_R|$

Nucleus	K	Energy of State (keV)	$(1/e^2)\ B_{E2}$ $\times 10^{48}$	Q_0(R) $\times 10^{24}$	Q_0(C) $\times 10^{24}$	$\lvert g_\Omega - g_R \rvert$
U^{238}	0	44.7	10.7 ± 2	10.3$\pm$1	10.3$\pm$1	
U^{235}	7/2	46.2	7.4 ± 0.7	13.2$\pm$0.7	11.2$\pm$0.6	
		103.0	1.18$\pm$0.16	10.5$\pm$0.7	9.0$\pm$0.6	$(4.6\pm0.9)10^{-1}$
Pu^{239}	1/2	7.9				
		57.5	5.3 ± 0.3	9.4$\pm$0.3	9.2$\pm$0.3	

The B_{E2} and Q_0 (R) were obtained with Rose's conversion coefficients; For Q_0(C), Rose's M1 conversion coefficients were multiplied by 0.6. A further error of ± 10 % for the B_{E2} and ± 5 % for the Q_0 must be combined with those shown above to obtain the error on the absolute values.

The values of $Q_0(1)$ and $Q_0(2)$ for U^{235} are nearly the same, as one would expect from the theory; nevertheless the difference between them is significant if the errors have been correctly estimated.

4.4. INTERPRETATION IN TERMS OF NILSSON's ENERGY LEVELS

The calculations of Nilsson [6]) on energy levels of individual nucleons in strongly deformed nuclei make predictions regarding levels which should exist in the region of U^{235} and Pu^{239}. From the wave functions it is possible to calculate the quantities such as g_Ω; it is of interest to compare these with the values derived from experiment and see which, if any, of these levels can be assigned to the ground states of these nuclei. The energy levels given by Nilsson for the particle numbers greater than 126 are shown in fig. 7; the levels arising from the $j_{15/2}$ spherical state (shown dotted) are guessed. In the notation for a state will be given the state of a spherical nucleus from which it arises, followed by the asymptotic quantum numbers $Nn_z\Lambda$ [6]) (infinite distortion) and the values of Ω and π.

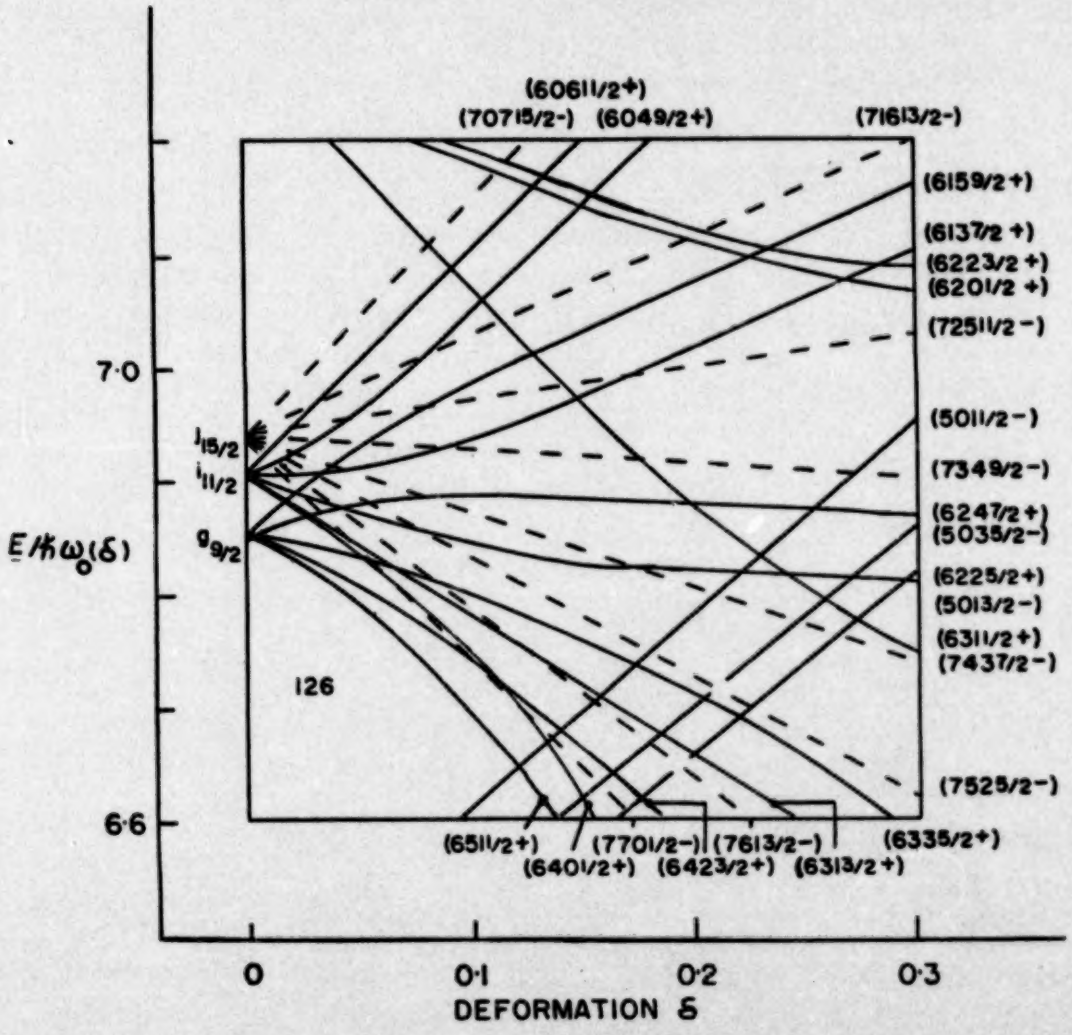

Fig. 7. Energy levels of nucleons in a spheroidal potential for nucleon numbers greater than 126, as given by Nilsson. The levels arising out of the $j_{15/2}$ state of a spherical nucleus were not calculated by Nilsson and are guessed. The energy of the $j_{15/2}$ state is lower here than that given by Nilsson in order to give better agreement with experiment.

(i) *U^{235}*

The possible assignments are the ($j_{15/2}$, 743, 7/2−) and the ($g_{9/2}$, 624, 7/2+) levels. The wave functions for the former levels have unfortunately not been given and it was only possible to calculate g_Ω in the limit of zero and infinite distortions. The values of g_Ω and of μ are plotted as a function of deformation δ in fig. 8. From the approximate formula given by Nilsson [6]) and our value for the Q_0 of U^{235} we obtain a value of 0.22 for δ. Considerably better agreement is given by level ($j_{15/2}$, 743, 7/2−) which therefore seems most likely to be the correct assignment. This view is further supported by the experimental result [52]) that $\mu(U^{233})/\mu(U^{235}) = -1.8$; the only assignment which fits the data for U^{233} ground state [8]) predicts a magnetic

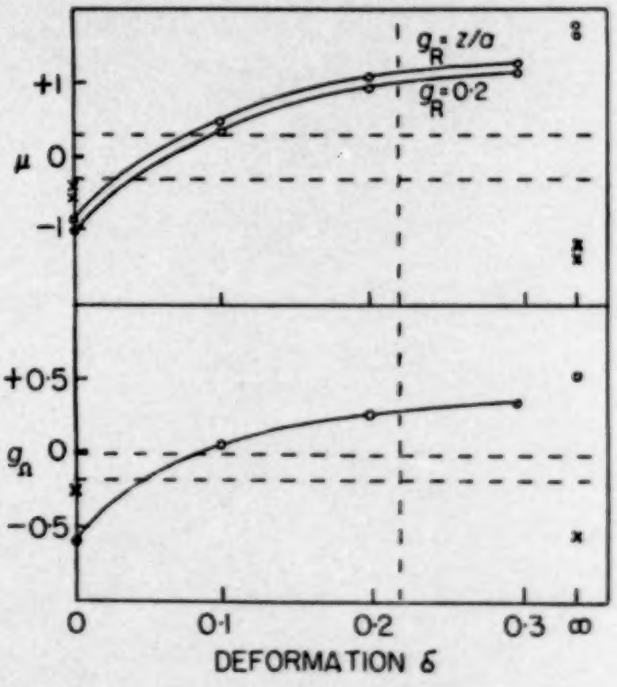

Fig. 8. Calculated values of μ and g_Ω as a function of δ for the states ($j_{15/2}$, 743, 7/2-), denoted by crosses, and for the state ($g_{9/2}$, 624, 7/2+), denoted by open circles. The values of μ, g_Ω and δ for U^{235} derived from the experiments are shown by broken lines.

moment μ of magnitude about +0.8 for that nucleus and hence a μ of about −0.4 for U^{235}.

(ii) *Pu^{239}*

The two possible assignments are ($p_{1/2}$, 501, 1/2−) and the ($d_{5/2}$, 631, 1/2+). In fig. 9 are shown the theoretical values for the decoupling parameter a, μ and the quantity $(g_\Omega - g_R)$ $(1-b_0)$, b_0 being defined in ref. [6]). It can be seen that only the latter state can give agreement with the experimental value of −0.58 for *a*; for this reason, we have not calculated the other quantities for the first possibility. Although the ($d_{5/2}$, 631, 1/2+)

assignment is probably correct it is clearly not possible to obtain agreement with the experimental values for a unique value of δ, the value obtained from the measured Q_0 being 0.195.

It is interesting to note that the value of the decoupling parameter for the $K = \frac{1}{2}$ band in U^{235} is -0.21. From the results shown in fig. 8 one might infer that in this band the nucleus was less distorted than in the

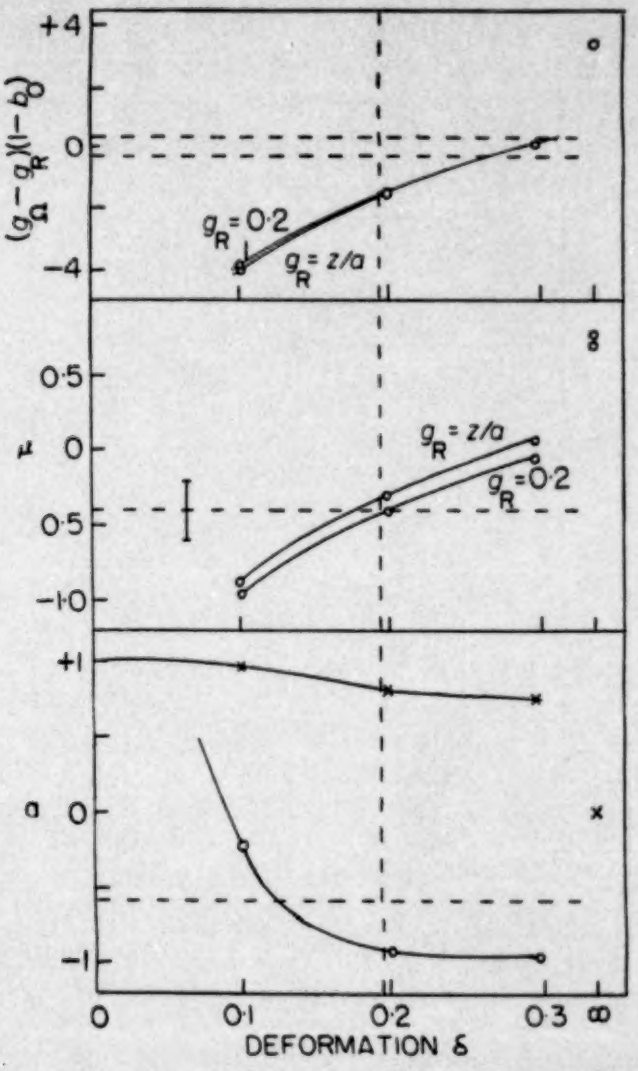

Fig. 9. Calculated values of a, μ and $(g_\Omega - g_R)(1-b_0)$ as functions of δ for the state $(d_{5/2}, 631, 1/2+)$, denoted by open circles, and for the state $(p_{1/2}, 501, 1/2-)$, denoted by crosses. The values derived from epxeriment for Pu^{239} are denoted by broken lines; note that μ is shown as negative here, actually its sign has not yet been determined.

corresponding band of Pu^{239}. In view, however, of the rather poor agreement between the experimental and theoretical results it may not be justifiable to come to this conclusion. From the relative intensities of the 52.0 and the 38.5 keV gamma rays from Pu^{239} decay reported by West, Dawson, and Mandleberg, one finds a value for $|(g_\Omega - g_R)(1-b_0)|$ of 0.27 compared with

0.35 for Pu^{239}. The closeness of the two values is further evidence in favour of the two bands being essentially similar.

4.5. THE ENERGY LEVELS OF U^{235}

The energy levels of U^{235} and Pu^{239} derived from the Coulomb excitation measurements and from the alpha decay data on Pu^{239} [27]) are shown in fig. 10. It seems almost certain, from the discussion in § 4.2 and § 4.4 that

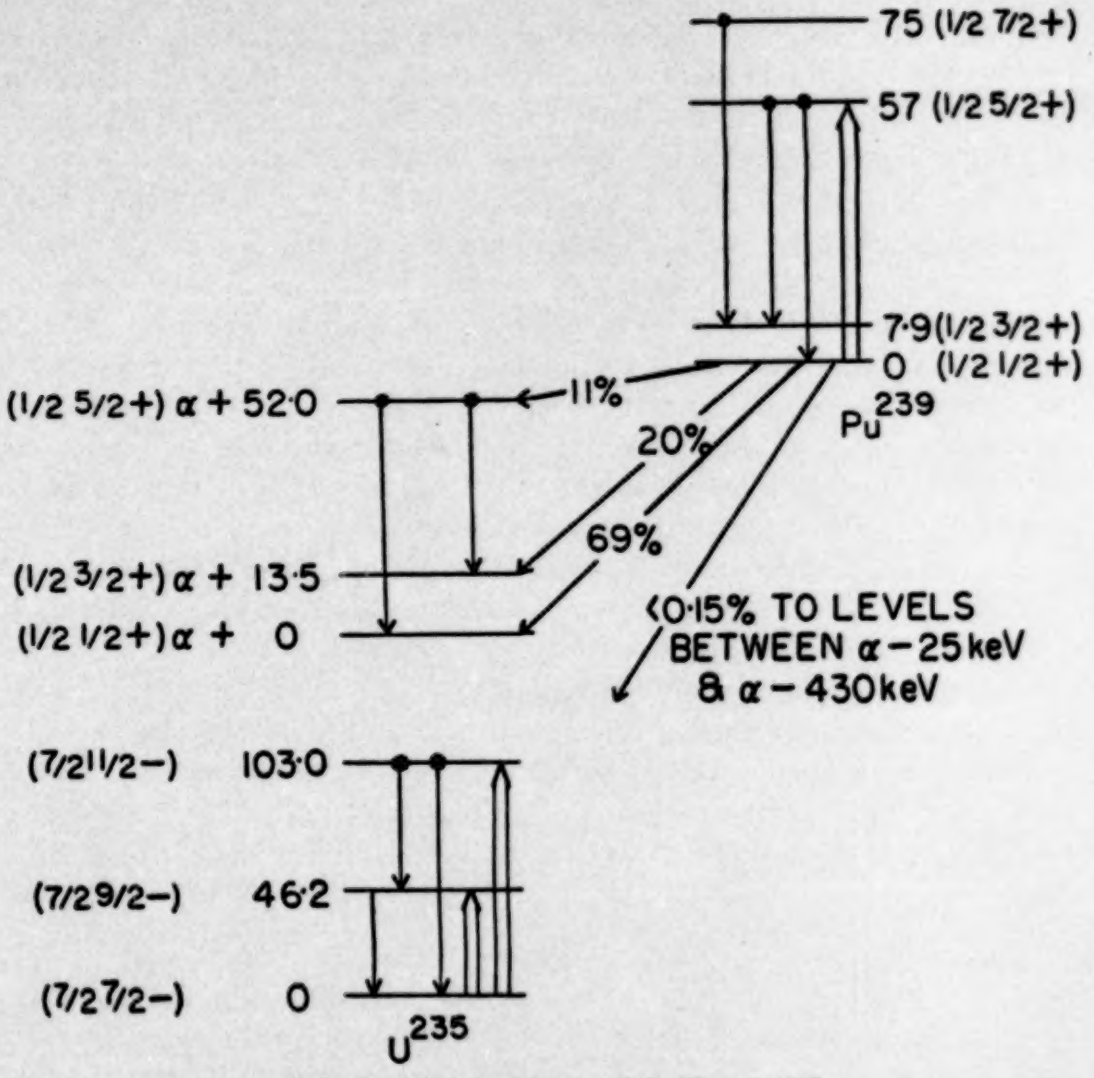

Fig. 10. The energy levels of Pu^{239} and U^{235}.

the favoured alpha particle groups from Pu^{239} lead to a rotational band in U^{235} having $K = \frac{1}{2}$. The $K = I = \frac{1}{2}$ state will presumably decay by means of an octapole transition to the $K = 7/2$ ground state of U^{235} and nearly all of the transitions from Pu^{239} decay must pass through it, but up till the present moment no radiation which can reasonably be assigned to this transition has been observed; the amount of L radiation, for instance [53]), is only enough to account for the decay of states in the $K = \frac{1}{2}$ rotational band.

These results can be accounted for if (a) the state has a lifetime of many years or (b) if it has an energy less than the L_{III} binding energy in uranium (17.16 keV); in this case no LX- radiation could be observed from the transition and the gamma ray itself would be so highly converted that it would be very difficult to see. In principle it should be possible to see the M radiation, but this has low energy, ≈ 4 keV and hence is difficult to observe; it may also have a low fluorescent yield.

The lifetimes given by the Weisskopf single particle formula for 17 keV E3 and M3 transitions are 10^6 sec and 10^9 sec respectively; internal conversion would reduce the lifetime of the state considerably, perhaps by a factor of about 10^6. If our assignments to the 1/2 and 7/2 states are correct, then the transition will be E3. Furthermore, the E3 transition ($d_{5/2}$, 631, $1/2^+$) $\rightarrow$ ($j_{15/2}$, 743, $7/2-$) is forbidden both in the spherical and cylindrical limits. It is likely therefore that it will also be forbidden in the case of intermediate distortion; for E1 transitions which are forbidden in both the limiting cases the retardation factor varies between about 10^{-3} and 10^{-6} (Rasmussen and Strominger [54]).

From the considerations above it seems likely that the $K = I = \frac{1}{2}$ state in U^{235} is an isomeric state which may have a very long lifetime, perhaps even of years. Direct observation of the state will be difficult but it may be possible to see the conversion electrons or M radiation if the transition has high enough energy. Another interesting possibility which would work if the state had a lifetime of the order of a month or more would be to separate out U^{235} grown from uranium-free Pu^{239}. It would then be possible to (a) Coulomb excite the state; gamma rays of 52.0 and 38.5 keV should then be observed (see fig. 10) and the Q_0 could be measured (b) observe the alpha decay spectrum of the metastable state; it should be quite different from that of normal U^{235} since it has $K = 1/2+$ instead of $K = 7/2-$. This would be an interesting case to study from the point of view of the alpha decay rules [22, 35]).

I should like to thank Mr. F. Hudswell and Mr. J. Waldron of the Chemistry Division at Harwell for providing and preparing the targets. I am also grateful to Mr. D. West and Mr. F. Bradley for giving advice on proportional counters.

References

1) N. P. Heydenburg and G. M. Temmer, Phys. Rev. **100** (1955) 150
2) P. H. Stelson and F. K. McGowan, Phys. Rev. **99** (1955) 112
3) T. Huus, J. H. Bjerregaard and B. Elbek, Mat. Fys. Medd. Dan. Vid. Selsk. **30** (1956) No. 150
4) K. Alder and A. Winther, Mat. Fys. Medd. Dan. Vid. Selsk. **29** (1955) No. 19; CERN/T/KA-AW-4 (1955)
5) L. C. Biedenharn, M. Goldstein, J. L. McHale and R. M. Thaler, Phys. Rev. **101** (1956) 662

6) S. G. Nilsson, Mat. Fys. Medd. Dan. Vid. Selsk. **29** (1955) No. 16
7) A. Bohr and B. R. Mottelson, Mat Fys. Medd. Dan. Vid. Selsk. **27** (1953) no. 16
8) J. O. Newton, to be published
9) A. Bohr and B. R. Mottelson, Beta and Gamma Ray Spectroscopy ed. by K. Siegbahn (North Holland Publ. Co., Amsterdam, 1955) Ch. 17
10) K. M. Glover and P. Borrell, J. Nuclear Energy **1** (1955) 214
11) D. West and E. F. Bradley, Phil. Mag. **1** (1956) 97
12) J. K. Beling, J. O. Newton and B. Rose, Phys. Rev. **86** (1952) 757
13) A. H. Compton and S. K. Allison, X-rays in Theory and Experiment (Van Nostrand, 1956)
14) P. P. Day, Phys. Rev. **97** (1955) 689
15) L. B. Magnusson, D. W. Engelkemeir, M. S. Freedman, F. T. Porter and F. Wagner, Bull. Am. Phys. Soc. **30** No. 7 (1955) 10
16) G. Alaga, K. Alder, A. Bohr and B. R. Mottelson, Mat. Fys. Medd. Dan. Vid. Selsk. **29** (1955) no. 9
17) L. A. Sliv and M. A. Listengarten, Zh. eksper, teor. Fiz. **22** (1952) 29
18) A. H. Wapstra and G. J. Nijgh, Nuclear Physics **1** (1956) 245
19) C. Nordling, K. Siegbahn, E. Sokolowski and A. H. Wapstra, Nuclear Physics **1** (1956) 326
20) F. K. McGowan and P. H. Stelson, Phys. Rev. **103** (1956) 1133
21) A. Abragam and R. V. Pound, Phys. Rev. **92** (1953) 943
22) J. O. Newton, Progress in Nuclear Physics **4** (1955) 234
23) F. S. Stephens, F. Asaro and I. Perlman, Phys. Rev. **100** (1955) 1543
24) J. M. Hollander, W. G. Smith and J. W. Mihelich, Phys. Rev. **102** (1956) 740
25) J. M. Hollander, private communication
26) R. J. Blin-Stoyle, Rev. Mod. Phys. **28** (1956) 75
27) F. K. McGowan, privately circulated data
28) K. L. van der Sluis and J. McNally, J. Opt. Soc. Am. **45** (1954) 65
29) C. A. Hutchison Jr., P. M. Llewellyn, E. Wong and P. Dorian, Phys. Rev. **102** (1956) 292
30) K. L. van der Sluis and J. McNally, J. Opt. Soc. Am. **44** (1954) 87
31) B. Bleaney, P. M. Llewellyn and M. H. L. Pryce, Phil. Mag. **45** (1954) 991
32) M. van den Berg, P. F. A. Klinkenberg and P. Regnault, Physica **20** (1954) 37
33) A. K. Kerman, Mat. Fys. Medd. Dan. Vid. Selsk. **30** (1956) no. 15
34) F. Asaro and I. Perlman, Phys. Rev. **88** (1952) 828
35) A. Bohr, P. O. Fröman and B. R. Mottelson, Mat. Fys. Medd. Dan. Vid. Selsk. **29** (1955) no. 10
36) R. L. Graham and R. E. Bell, Phys. Rev. **83** (1951) 222A
37) J. M. Hollander, I. Perlman and G. T. Seaborg, Rev. Mod. Phys. **25** (1953) 469
38) J. O. Newton, B. Rose and J. Milsted, Phil. Mag. **1** (1956) 981
39) W. D. Brodie, Proc. Phys. Soc. A **67** (1954) 265
40) S. Rosenblum, M. Valadares and M. Guillot, Comptes Rendus **235** (1952) 238
41) J. L. Wolfson (1954) private communication
42) B. Zajac, Phil. Mag. **43** (1952) 264
43) C. J. D. Jarvis and M. A. S. Ross, Proc. Phys. Soc. A **63** (1951) 535
44) S. Rosenblum, M. Valadares and R. Bernas, Comptes Rendus **239** (1954) 759
45) Ong Ping Hok, P. Kramer, G. Meijer, J. W. R. Fennema and W. L. Zijp, Physica **21** (1955) 719
46) J. O. Rasmussen, H. Slätis, and T. O. Passell, Phys. Rev. **99** (1955) 42
47) J. Kyles, C. G. Campbell and W. J. Henderson, Proc. Phys. Soc. A **66** (1953) 519
48) D. K. Butt and W. D. Brodie, Proc. Phys. Soc. A **64** (1951) 791
49) L. Cranberg, Phys. Rev. **77** (1950) 155
50) J. M. Hollander, private communication
51) S. A. Baranov and K. N. Shlyagin, Zh. eksper. teor. Fiz. **30** (1956) 225
52) N. I. Kahteovsky and M. P. Chaska, Dok. Ak. Nauk. S. S. S. R. **103** (1955) 49
53) D. West, J. K. Dawson and C. J. M. Mandleberg, Phil. Mag. **43** (1952) 875
54) D. Strominger and J. O. Rasmussen, Nuclear Physics **2** (1956/57) 113

Nuclear Physics **3** (1957) 364—366; *North-Holland Publishing Co., Amsterdam*

A DECAY OF A NEGATIVE τ'

S. NILSSON

Institute of Physics, Uppsala

Received 27 December 1956

Only a few of the modes of negative heavy mesons are established. So far the decay modes $K^-_{\pi 2}$, K^-_{e3} [1]) and τ^- [2]) have been found. Due to the strong absorption of negative K-mesons at rest, it is necessary to observe decays in flight, in order to establish the identity of the K^--meson.

An event, which is consistent with the decay in flight of a negative τ',

$$\tau' \rightarrow \pi^- + \pi^0 + \pi^0,$$

has been found in this laboratory. The stack consists of 60 plates $4'' \times 7'' \times 600\,\mu$m and was exposed to the partially separated negative K-meson beam at the Berkeley Bevatron. The beam momentum was 430 MeV/c.

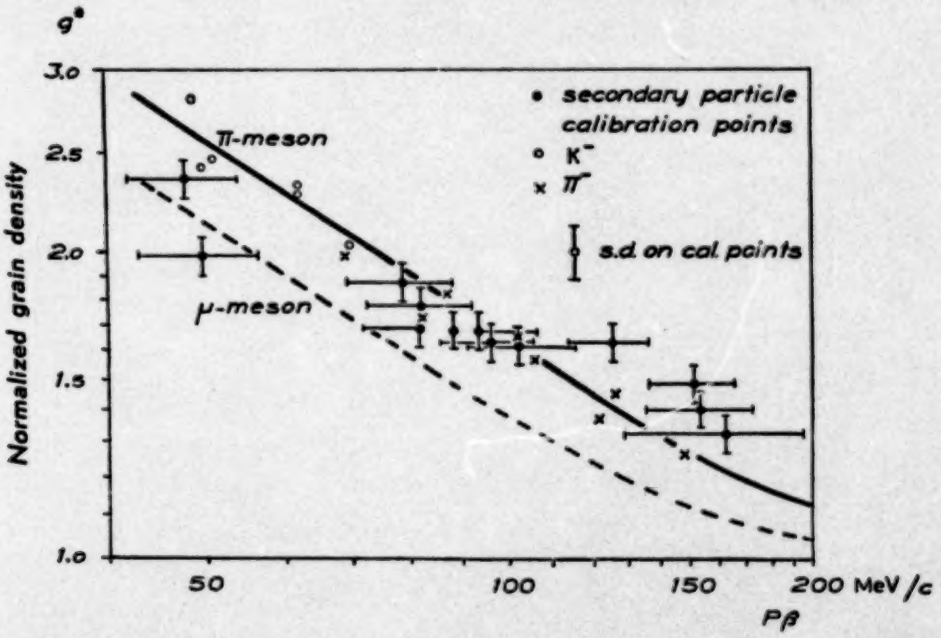

Fig. 1. The normalised grain density g^* versus $p\beta$ for the secondary particle.

The event is unusually suitable for measurements. The secondary is emitted in the forward hemisphere at a space angle of 40.5° with the primary direction. The primary goes 84.9 mm in 3 plates before decaying. No blob or slow electron at the decay point indicates a nuclear reaction. The secondary goes through 29 plates corresponding to a total range of 87.7 mm in emulsion

before leaving the stack. In the first 13 plates it is flat, about 4 mm per plate. It is thus possible to measure g^* (relative to the π^--mesons in the beam) versus $p\beta$ with good accuracy.

In each plate the ionisation measurements were normalised by counting at least 1000 grains on interacting π-mesons in the primary beam. Each $p\beta$-measurement was made with at least 60 basic cells and noise eliminated between $t-2t$ and $t-3t$ overlapping cells and the weighted mean taken.

The masses determined from $g^*-p\beta$ are for the primary $m_p = 1010\pm70\, m_e$ and for the secondary $m_s = 273\pm12\, m_e$. The $g^*-p\beta$-diagram for the secondary is shown in fig. 1. The calibration line has been obtained by grain counting versus residual range on K^-- and π^--mesons giving rise to capture stars at rest.

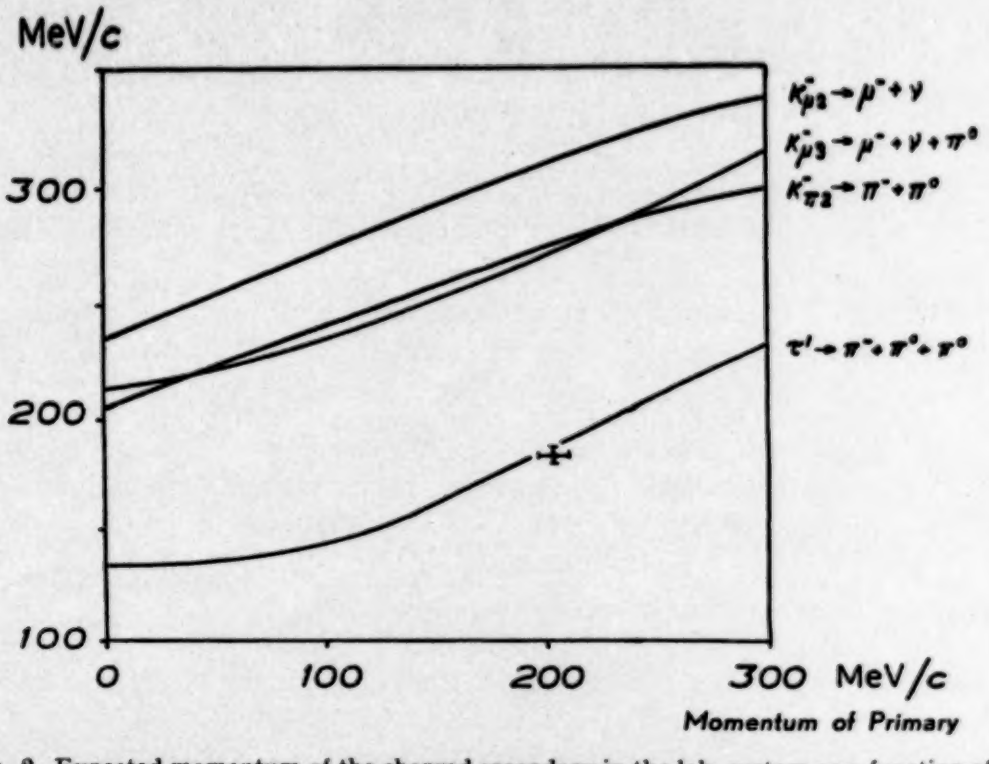

Fig. 2. Expected momentum of the charged secondary in the lab. system as a function of the momentum of the K-meson for 40.5° emission angle. The lines for the three-body decays are lines of maximum momentum. The experimental point is plotted for the assumption that the secondary is a π^-.

The primary track is consistent with a K^--meson, $m_K = 966\, m_e$. The secondary track is consistent with a π^--meson. At the point of decay the momentum of the primary was $p = 203\pm7$ MeV/c, and the momentum of the secondary $p = 184\pm4$ MeV/c assuming it was a π^-. One finds $p\beta = 150\pm5$ MeV/c from multiple scattering and $p\beta = 144\pm3$ MeV/c from g^*. The momentum of the π^--meson in the rest system of the K^--meson is thus given by $p^* = 132\pm3$ MeV/c.

The $K_{\pi 2}$ and $K_{\mu 2}$ modes of decay are dynamically ruled out. The three-

body decays $K_{\pi 3}$ and $K_{\mu 3}$ are possible, the former being favoured by the identification of the secondary.

In fig. 2 the expected momentum of the secondary particle in the lab. system is shown as a function of the K^--meson momentum, assuming $m_K = 966\, m_e$. For the three-body decays the line of maximum momentum is shown and all states below this line are possible. The $K_{\mu 3}$ decay scheme is assumed to be $K_{\mu 3} \rightarrow \mu + \nu + \pi^0$ according to recent results [3]).

The τ' mode of decay is the only one consistent with all information. The kinetic energy of the π^--meson is $T^* = 52 \pm 2$ MeV in the centre- of-momentum system in this case, whereas the maximum kinetic energy for the π^- from a τ decay is $T^*_{max} = 54$ MeV. By analogy with the π^- energy distribution of the positive τ one would expect only a small probability for obtaining events with a high energy π^-. This would make $K_{\mu 3}$ more probable from the point of view of the energy distribution. But, again, the $K_{\mu 3}$ is ruled out by the measurements on the secondary.

No results are available for the relative abundances of negative K-mesons. The amount of positive τ' is stated as 1—4 % in various experiments [4]).

We conclude that negative K-meson decay modes so far observed include the $K^-_{\pi 2}$, K^-_{e3}, τ^- and the negative τ'.

We wish to thank Dr. E. J. Lofgren for exposing the plates at the Bevatron, Berkeley, California. This work is partly sponsored by ARDC.

References

1) A. G. Ekspong and G. Goldhaber, Phys. Rev. **102** (1956) 1187
2) Proceedings of Rochester Conference 1956, V-5
3) Proceedings of Rochester Conference 1956, V-19
4) Ritson *et al.*, Phys. Rev. **101** (1956) 1085; Crussard *et al.*, Nuovo Cimento **3** (1956) 731; Proceedings of Rochester Conference 1956, VI-31

Nuclear Physics **3** (1957) 367—374; *North-Holland Publishing Co., Amsterdam*

THE INFLUENCE OF *l*-FORBIDDENNESS ON MAGNETIC DIPOLE TRANSITIONS IN Tl^{203}

TORSTEN LINDQVIST AND INGVAR MARKLUND

Institute of Physics, Uppsala, Sweden

Received 21 January 1957

Abstract: The angular correlation of the 400 keV—279 keV cascade in Tl^{203} has been measured. The correlation function has the form $w(\theta) = 1-(0.205\pm0.005)\cos^2\theta$. A comparison between the mixing ratio of the 400 keV transition ($d_{5/2} \rightarrow d_{3/2}$) and the mixing ratio of the 279 keV transition ($d_{3/2} \rightarrow s_{1/2}$) is done. The *l*-forbidden M1 transition is retarded by a factor of 1.3×10^{-3} compared to the *l*-allowed M1 transition.

1. Introduction

Among magnetic dipole transitions the so called *l*-forbidden, i.e. orbital momentum forbidden transitions, are of special interest. In the one-particle shell model only spin-flip M1 transitions are allowed, e.g. $p_{3/2} \rightarrow p_{1/2}$ but not $d_{3/2} \rightarrow s_{1/2}$. The *l*-forbidden M1 transitions are characterized by the selection rules $\Delta l = 2$, $\Delta j = 1$. The fact that these transitions do take place, although very much slowed down, is due to extraordinary terms of the magnetic dipole operator. These extraordinary terms appear because of some velocity-dependent interaction, e.g. spin-orbit coupling. Graham and Bell [1]) and recently de Waard and Gerholm [2]) have studied such *l*-forbidden M1 transitions by lifetime measurements. The retardation factor R, i.e. the factor by which an *l*-forbidden M1 transition is slowed down compared to an *l*-allowed one, can be determined from the measured lifetime compared to the theoretical transition probability for an *l*-allowed M1 transition given by Moszkowski [3]). An ideal case for a determination of R is a comparison of an *l*-forbidden and an *l*-allowed M1 transition in the same nucleus. In the following angular correlation experiment such a determination of R is done by measuring the mixing ratios of gamma transitions in Tl^{203}.

2. Decay of Pb^{203}

Pb^{203} decays by electron-capture to excited states in Tl^{203}. The halflife is 53 h. The decay of Pb^{203} has been analyzed among others by Prescott [4]), Wapstra *et al.* [5]) and Varma [6]) with in principle the same result. The decay scheme of Wapstra is shown in fig. 1. The 279 keV level can also be reached from Hg^{203} by beta decay. This fact allows for an absolute measurement of the conversion coefficient of the 279 keV transition. This transition takes

place between a $d_{3/2}$-level and $s_{1/2}$-level, $\Delta j = 1$ and $\Delta l = 2$. The magnetic dipole transition is therefore l-forbidden. The upper transition, the 400 keV

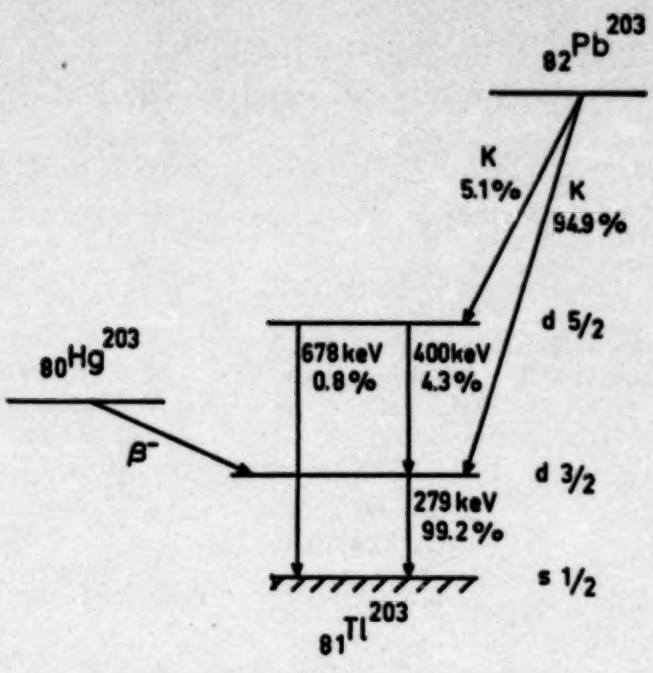

Fig. 1. Decay scheme of Pb^{203} (ref. [5]).

line, occurs between $d_{5/2}$ and $d_{3/2}$ levels, $\Delta j = 1$ and $\Delta l = 0$, wherefore in this case the magnetic dipole transition is l-allowed.

3. Conversion Coefficients

Much attention has been focused on the conversion of the 279 keV transition. The absolute K-conversion coefficient has recently been measured by Wapstra and Nijgh [7]), who give the value $\alpha_K = 0.164 \pm 0.005$, and by Nordling *et al.* [8]), $\alpha_K = 0.159 \pm 0.004$. From Rose's theoretical conversion coefficients the 279 keV transition was identified as an admixture of M1 and E2. If a is the fraction of E2, the mean value of $\alpha_K = 0.162$ gives $a = 81\ \%$. However, by comparing the K/L ratio and α_K Wapstra and Nijgh [7]) found that the fraction a should be 56 % †, which they explained by reducing the theoretical M1 coefficients by about 40 %. Nordling *et al.* [8]) measured the absolute K and L conversion coefficients and found $a = 58\ \%$ and that the M1 coefficients should be reduced by about 47 %. It is well known that Sliv *et al.* [9]) have recalculated the theoretical conversion coefficients taking into account the finite size of the nucleus. They have found that the M1 coefficients should be reduced by an amount of the same order of magnitude as given by Wapstra [7]) and Nordling *et al.* [8]). Sliv's values for the K conversion coefficients of 279 keV and 400 keV

† Note that in ref. [7]) a is the fraction of M1, in ref. [8]) a is the fraction of E2.

lines are given in table 1. From these values it is found that $a = 74\ \%$ for the 279 keV line, still in some disagreement with the a-values determined by Wapstra [7]) and Nordling *et al.* [8]).

TABLE 1

Sliv's conversion coefficients

E_γ (keV)	α_K (M1)	α_K (E2)
279	0.41	0.076
400	0.145	0.032

The K conversion coefficient of the 400 keV line has been measured by Wapstra *et al.* [5]), $\alpha_K = 0.118 \pm 0.015$, and by Varma [6]), $\alpha_K = 0.076$. The reason of this discrepancy is not understood. The measurement of Wapstra *et al.* [5]) seems to be more straightforward and is taken here as more dependable. With $\alpha_K = 0.118$ and the conversion coefficients of Sliv (table 1) it is found that the 400 keV transition is an admixture of M1 and E2, $a = 24\ \%$.

From this discussion it is clear that it is very difficult to determine multipole mixing only from conversion coefficients. A measurement of the angular correlation between the 400 keV and the 279 keV lines will throw some light on this problem. In such an experiment the mixing ratios are independent of the conversion coefficients.

4. Correlation Experiment

The angular correlation of the 400 keV—279 keV cascade in Tl^{203} has been measured by Prescott [4]) and Varma [6]). Their results show a large discrepancy. Prescott finds the correlation function to be

$$w(\theta) = 1 + (0.07 \pm 0.008) \cos^2 \theta$$

and Varma

$$w(\theta) = 1 - (0.152 \pm 0.007) \cos^2 \theta.$$

Our experiment was performed with a scintillation coincidence spectrometer with an effective resolving time of 10^{-7} s. The detectors were $1\frac{1}{2}$ in $\times 1\frac{1}{2}$ in NaI(Tl) crystals with RCA 6342 photomultipliers. One channel accepted the photopeak of the 279 keV line and the other channel was set on the 400 keV photopeak.

The lead activity was obtained from the Nobel Institute in Stockholm, where it was produced by deutron bombardment on a thallium target. Two different sources were investigated. The first was in the form of solid lead chloride and the second was a solution of lead chloride.

Because of the fact that the intermediate level of the cascade has a spin of 3/2, the correlation function does not contain higher order terms than $\cos^2 \theta$. Therefore, it is not necessary to measure more than two angles.

From this information one can calculate directly the coefficients of the correlation function. In one run we measured the asymmetry at 180° and 90°, in another run at 180° and 135°. They both came out with the same correlation function.

The correction for the counter solid angles was done for the proper energies. No other geometrical corrections were done.

5. Results

By evaluating the data for the correlation function

$$w(\theta) = 1 + A_2 P_2(\cos\theta)$$

we obtain for the solid source $A_2 = -0.127$ and for the liquid source $A_2 = -0.128$. The results show that the correlation function is independent of the chemical form of the source. In view of the measured lifetime of the intermediate level, $\tau_\gamma = 5\times 10^{-10}$ sec [10]), one should not expect any attenuation of the correlation. The mean value is $A_2 = -0.128 \pm 0.003$. If this result is transformed into the representation of Prescott [4]) and Varma [6]) we get

$$w(\theta) = 1-(0.205\pm 0.005)\cos^2\theta.$$

This is a considerably larger anisotropy than both the earlier experiments have given.

As mentioned above the 400 and 279 keV lines are admixtures of M1 and E2. In angular correlation work one defines the mixing ratio δ as the ratio of, in this case, the reduced matrix element of the E2 transition to that of the M1 transition, both taken with their signs. Thus δ can be positive or negative. The intensity ratio depends on the squares of the reduced matrix elements, i.e. on δ^2. If both transitions in a cascade are mixed, the coefficients of the correlation function depend on both mixing ratios. With the notation of Ferentz and Rosenzweig [11]) one obtains

$$A_2 = A_2^{(1)}(\delta_1)\cdot A_2^{(2)}(\delta_2)$$

where $A_2^{(1)}(\delta_1)$ and $A_2^{(2)}(\delta_2)$ are known functions [11]), characteristic of each spin sequence. With a known value of A_2 one then gets the relation between the two mixing ratios.

The "subcoefficients" $A_2^{(1)}$ and $A_2^{(2)}$ have been calculated for the spin sequence 5/2 (M1+E2) 3/2 (M1+E2) 1/2 in Tl^{203}. The relation between the mixing ratios is shown in fig. 2. Instead of δ as variable we have chosen the fraction a of E2 in each transition in principle as in ref. [7]). It is obvious that

$$a = \frac{\delta^2}{1+\delta^2}.$$

Let us first consider the a-values obtained from the conversion coefficients, $a_{400} = 24\,\%$ and $a_{279} = 74\,\%$. They define a point that is not

located on any curve branch. (The dashed lines indicate the errors of respective a-values.) This fact might be a new indication that the M1 conversion coefficients by Sliv are a little too high as pointed out by Nielsen *et al.* [12]). The value of a_{279} found by Nordling *et al.* [8]) corresponds to four different values of a_{400}, in fig. 2 marked as I, II, III and IV. It is in the light of the conversion coefficient measurement very unlikely, that the 400 keV transition should have more than 80 % E2. One can therefore exclude III and IV.

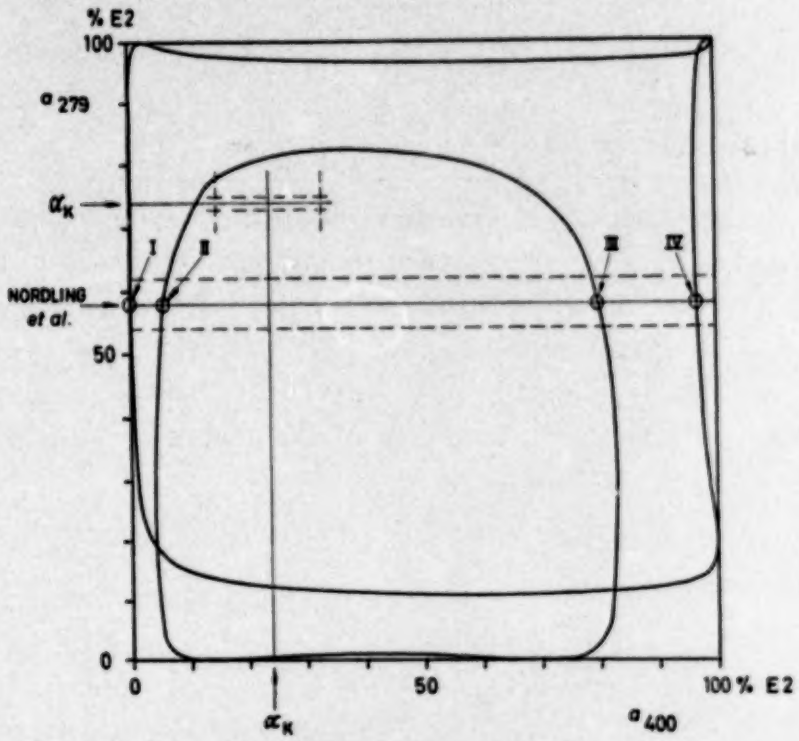

Fig. 2. Relation between a_{400} and a_{279} for the measured correlation (see text).

The value I, $a_{400} = 0.09$ %, means practically pure M1 and is very insensitive to the value of a_{279}. Finally II, $a_{400} = 6$ %, means an admixture of 6 % E2 in the 400 keV transition. It is not possible to choose between the cases I and II. However, the following interesting consideration can be made.

The transition probabilities T of a single proton are, according Moszkowski [3]), for M1 and E2 transitions (with the nuclear radius $r = 1.2\times10^{-13}\cdot A^{1/3}$ cm),

$$T_{M1} = 2.8\times10^{13}\cdot E_\gamma^{\,3}\cdot S(j_1 L j_f) \quad \text{sec}^{-1},$$
$$T_{E2} = 7.4\times10^{7}\cdot E_\gamma^{\,5}\cdot A^{4/3}\cdot S(j_1 L j_f) \quad \text{sec}^{-1},$$

where A is the mass of the nucleus, E_γ the energy of the transition in MeV and $S(j_1 L j_f)$ a statistical factor.

The general expression for $S(j_1 L j_f)$ is [3])

$$S(j_1 L j_f) = (2l_1+1)(2l_f+1)(2L+1)(2j_f+1)$$
$$\times |V(l_1 l_f L;\ 000)|^2\, |W(l_1 j_1 l_f j_f;\ \tfrac{1}{2} L)|^2,$$

where l_i, l_f, j_i and j_f are initial and final, orbital and total angular momentum respectively, L the multipole of the transition, the quantities V are closely related to Clebsch-Gordan coefficients and the quantities W are Racah coefficients. The statistical factors for the actual transitions are tabulated

TABLE 2
Statistical factors

j_i	j_f	L	S	
5/2	3/2	1	6/5	ref. [3])
5/2	3/2	2	2/7	
3/2	1/2	1	1	ref. [3])
3/2	1/2	2	1	

in table 2. The theoretical transition probabilities, based on the single particle shell model, are not expected to represent an l-forbidden M1 transition. We now assume that the l-forbidden M1 transition is retarded by a factor R compared to the l-allowed M1 transition. The electric transitions are known to be independent of the velocity-dependent interaction [13]) that alters the transition probability of the magnetic transitions.

For the 279 keV transition we thus obtain

$$(T_{M1})_{279} = 2.8\times 10^{13}\times (0.279)^3 \cdot R \quad \text{sec}^{-1}.$$

From definition we have

$$\delta_1^2 = \left(\frac{T_{E2}}{T_{M1}}\right)_{400}, \quad \delta_2^2 = \left(\frac{T_{E2}}{T_{M1}}\right)_{279}.$$

Accordingly

$$\frac{\delta_1^2}{\delta_2^2} = \left(\frac{T_{E2}}{T_{M1}}\right)_{400} : \left(\frac{T_{E2}}{T_{M1}}\right)_{279} = \frac{(0.400)^2}{(0.279)^2} \times \frac{2\times 5}{7\times 6} \cdot R$$

or

$$R = \frac{\delta_1^2}{\delta_2^2} \times \left(\frac{279}{400}\right)^2 \times 4.2.$$

In case I we have $a_{400} = 0.09$ %, i.e. $\delta_1^2 = 0.0009 \pm 0.0015$ and $a_{279} = 58$ %, i.e. $\delta_2^2 = 1.38 \pm 0.23$. The result is

$$R_I = (1.3 \pm 2.7)\times 10^{-3}.$$

In case II we have $a_{400} = 6$ %, i.e. $\delta_1^2 = 0.063 \pm 0.011$ and $a_{279} = 58$ %, i.e. $\delta_2^2 = 1.38 \pm 0.23$. Thus

$$R_{II} = 0.09 \pm 0.03.$$

It should be pointed out that the R values determined from the angular correlation experiment do not depend on the absolute transition rates. However, Moszkowski's energy dependence and statistical factors are assumed to be valid.

R can also be determined by comparing the experimental transition rate and theoretical transition rate [3]). We have

$$T_{M1} = \frac{1}{\tau_{M1}} = [(1+\delta^2)\tau_\gamma]^{-1} \text{ sec}^{-1},$$

where τ_{M1} is the lifetime of the M1 transition, δ^2 the ratio of the E2 and M1 intensity fractions and τ_γ, the measured lifetime of the transition. With $\delta^2 = 1.38$ and $\tau_\gamma = (5\pm1)\times10^{-10}$ sec[10]) we obtain for the 279 keV transition

$$T_{M1,\,exp} = (0.8\pm0.2)\times10^{9} \quad \text{sec}^{-1},$$

$$T_{M1,\,theor} = 0.6\times10^{12} \quad \text{sec}^{-1}.$$

Thus

$$\frac{T_{M1,\,exp}}{T_{M1,\,theor}} = R = (1.3\pm0.3)\times10^{-3}.$$

The R value of case I and that of the lifetime measurement agree very well. One is therefore inclined to consider case 1 as giving the right value. Another support for this case is the value of δ_1^2, obtained from the theoretical transitions rates:

$$\delta^2_{1,\,theor} = \frac{T_{E2,\,theor}}{T_{M1,\,theor}} = 0.0004,$$

$$\delta^2_{1,\,exp} = 0.0009+0.0015.$$

It is therefore concluded that an l-forbidden M1 transition is retarded by a factor of 1.3×10^{-3} compared to an l-allowed M1 transition. Further, Moszkowski's theoretical transition rates seem to represent l-allowed transitions very well in this nucleus. The nucleus in question, ${}_{81}Tl^{203}$, is well fitted for this theory, since it has one single proton hole within the closed shell of 82 protons.

Another conclusion of the result obtained is that the 400 keV transition in Tl^{203} is practically pure M1 transition.

The authors are greatly indebted to Professor Kai Siegbahn for his interest in this work. Further our thanks are due to Dr T. R. Gerholm for helpful theoretical discussion and to Dr I. Bergström for pointing out the problem and putting the radioactive source to our disposal.

References

1) R. L. Graham and R. E. Bell, Can. J. Phys. **31** (1953) 377
2) H. de Waard and T. R. Gerholm, Nuclear Physics **1** (1956) 281
3) S. A. Moszkowski, Beta and Gamma Ray Spectroscopy, editor Kai Siegbahn (North Holland Publishing Company, Amsterdam, 1955) Ch XIII, p. 373
4) J. R. Prescott, Proc. Phys. Soc. A **67** (1954) 254
5) A. H. Wapstra, D. Maeder, G. J. Nijgh and L. Th. M. Ornstein, Physica **20** (1954) 169

6) J. Varma, Phys. Rev. **94** (1956) 1688
7) A. H. Wapstra and G. J. Nijgh, Nuclear Physics **1** (1956) 245
8) C. Nordling, K. Siegbahn, E. Sokolowski and A. H. Wapstra, Nuclear Physics **1** (1956) 326
9) L. Sliv and J. Band, privately distributed tables
10) Mean value of three measurements:
a) (Coulomb excit.) R. Barloutaud, T. Grjebine and M. Riou, Comptes Rendus **240** (1955) 1207
b) (res. scatt.) F. R. Metzger, Journ. Franklin Inst. **261** (1956) 219
c) (del. coinc.) J. Ewan and R. L. Graham, private communication
11) M. Ferentz and N. Rosenzweig, ANL-5324 (not published)
12) K. O. Nielsen, O. B. Nielsen and N. A. Waggoner, Nuclear Physics **2** (1956/57) 476
13) R. G. Sachs and N. Austern, Phys. Rev. **81** (1951) 705

Nuclear Physics **3** (1957) 375—384; *North-Holland Publishing Co., Amsterdam*

SCATTERING OF FAST NEUTRONS BY NEON IN THE ENERGY REGION 1.9 TO 3.5 MeV

C. P. SIKKEMA

Natuurkundig Laboratorium der Rijks Universiteit, Groningen

Received 1 February 1957

Abstract: The scattering of monoenergetic neutrons by neon in the neutron energy range 1.9 to 3.5 MeV has been investigated by measuring the neon recoils in a multiple-wire proportional counter with which a γ-ray background can be reduced to a very low value by an anticoincidence technique.

Approximate values for the total cross-section are obtained, which show resonance peaks at 1.94, 2.00, 2.11, (2.45), 2.57, 2.73, 2.88, 3.28, and 3.37 MeV neutron energy. By the study of angular distributions the resonances at 1.94 and 2.00 MeV could be ascribed to a $3/2^+$ and a $3/2^-$ level in the ^{21}Ne nucleus respectively. The strong resonance at 2.11 MeV seems to be due to both a $3/2^+$ and a $3/2^-$ level.

1. Introduction

Fast neutrons with energies up to about 6 MeV may interact with ^{20}Ne nuclei in three different ways:

1. *Elastic scattering*, which will occur at all energies.

2. *Inelastic scattering*. The lowest excited state of ^{20}Ne has an excitation energy of 1.63 MeV above the ground state. Thus inelastic scattering is possible for neutron energies above 1.71 MeV.

3. (n, α) *Reaction*. This reaction is 0.60 MeV endoergic [14]) and is therefore energetically possible for neutrons with an energy above 0.63 MeV. Practically this reaction becomes observable only above 1.9 MeV [5]) because of the influence of the Coulomb barrier.

The elastic scattering has so far been studied in the energy region from 0.8 to 1.75 MeV in which six resonances were found [1, 2, 3]).

Studies of the (n, α) reaction using monoenergetic neutrons in the energy range used in the present work have also been published [4, 5, 6]).

The present paper deals with measurements of the total cross section and differential elastic scattering cross sections in the energy range covered by D+D-neutrons.

2. Experimental Method

The D+D reaction was used as a source of monoenergetic neutrons. Deuterons were accelerated by a cascade generator with voltages between 400 and 550 kV. The current of the magnetically analyzed beam was about 100 μA. Thin heavy ice targets were obtained by evaporating an appropriate quan-

tity of heavy water on a copper strip, cooled by liquid air as indicated in fig. 1. We have used targets with a stopping power of 50 or 25 kV, which was measured by comparing the neutron yield with the thick target yield. After the wearing out of a target under deuteron bombardment, the copper

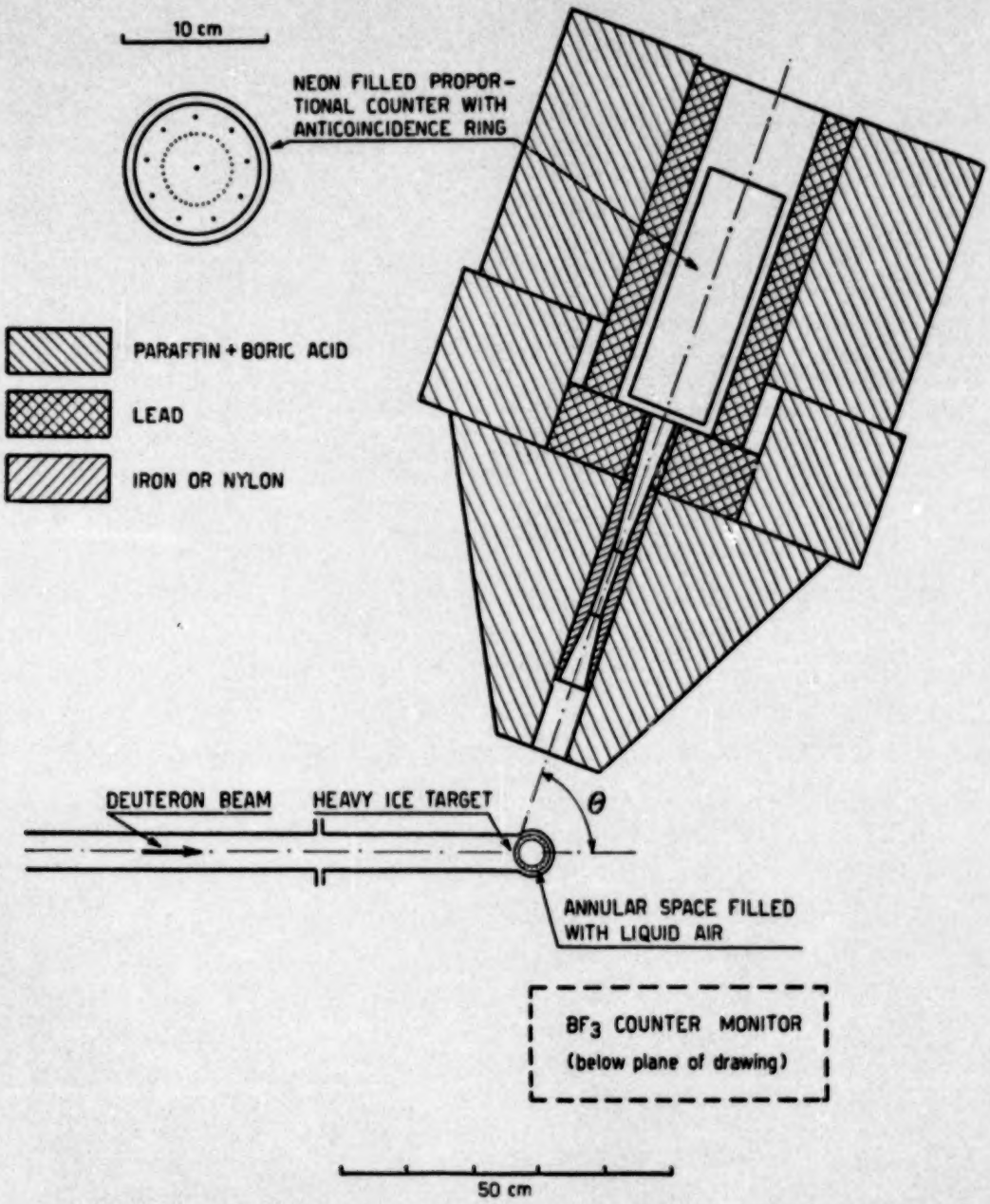

Fig. 1. Experimental arrangement for the measurement of the total and the differential elastic scattering cross sections of neon for D+D neutrons, the energy of which was varied from 1.9 to 3.5 MeV mainly by changing the angle Θ between 0° and 156°.

strip could be displaced a little by rotating the Dewar vessel on which it had been soldered. In this way fifteen fresh targets could be prepared and irradiated during one run of measurements at different neutron energies.

Fig. 1 shows the experimental arrangement. The neutrons enter the de-

tector through a neutron beam collimator, the inner part of which has been made of iron or nylon. The neutron beam passing through the collimator had a divergence in the horizontal plane of 1 to 2 degrees. The collimator system, including the detector is mounted on a large turntable. Thus the energy of the neutrons used could be varied by changing the angle Θ between the collimator axis and the deuteron beam. At extreme positions of the collimator the neutron energy was also varied by variation of the acceleration voltage. The energy spread of the neutrons entering the detector is estimated to be about 25 keV below 2.7 MeV neutron energy and about 40 keV above this value.

A proportional counter filled with 62 or 118 cm Hg of natural neon with 2 % CO_2 was used as a detector for recoil nuclei and reaction products. With

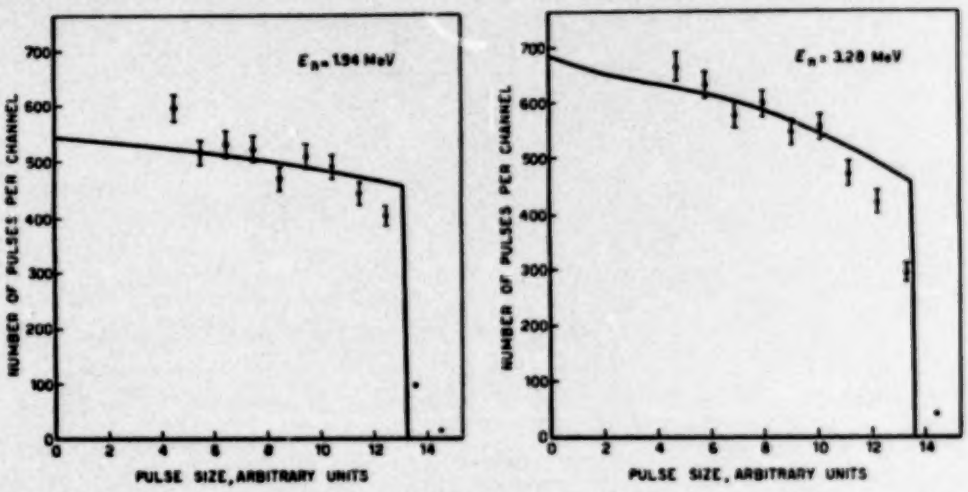

Fig. 2. Typical pulse size distributions of the hydrogen recoil proportional counter. Experimental data are fitted with "theoretical" curves.

a cathode diameter of 5 cm and a wire thickness of 0.15 mm the operating voltage was 1000 to 1500 volts.

Two types of measurements were made. First, in order to obtain an approximate value for the total cross section as a function of neutron energy, pulses were counted with high gas amplification and low bias. In this case, however, many fast electrons produced in the counter walls by γ-radiation would also have been counted. To reduce the γ-ray counting effectively, the counter was built as a multiple wire counter, similar to the one constructed for other purposes by Giles [7]). The central counting volume is surrounded by ten small proportional counters, which are separated from the central volume only by a grid of thin wires. Pulses from the central volume are registered only if there is no coincident pulse from the ring of counters around it. In this way, the counting of γ-quanta through their long-range secondary electrons is reduced to 2 to 3 percent, whereas the pulses from the short-range neon recoil nuclei remain practically unaffected by the anticoincidence. Moreover the counter was heavily shielded with lead bricks.

Secondly, pulse size distributions were taken from the counter at selected neutron energies, to get more information about the nature of the scattering

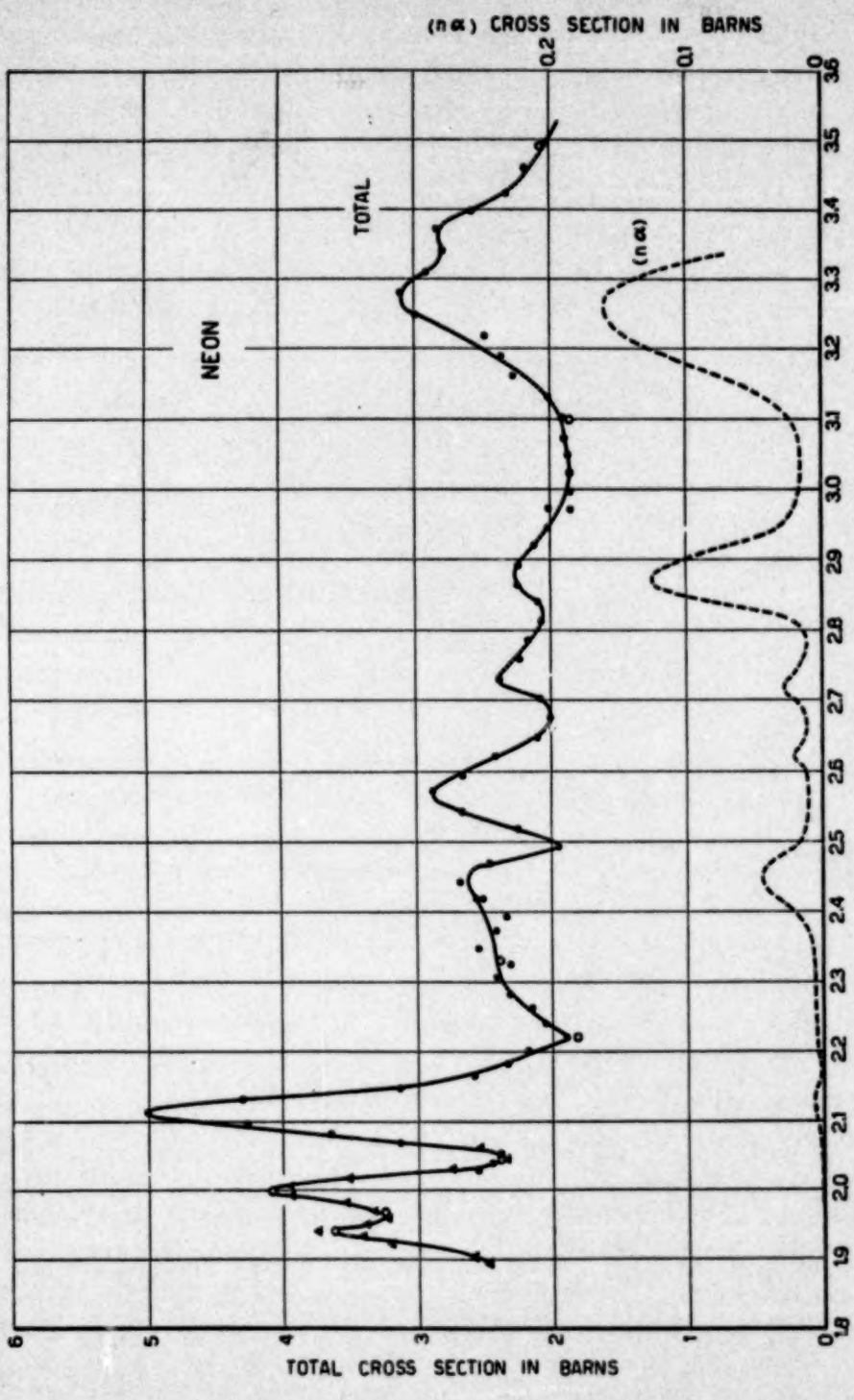

Fig. 3. The total cross section of neon as a function of neutron energy. The dotted curve represents the (n, α) cross section of neon at a 10× enlarged scale, after Johnson *et al.* [5]).

process. Pulses were photographed from the screen of a cathode-ray tube on 35 mm film. They were analyzed manually, by projecting the film on a screen divided into 30 equal parts. A row of microswitches is mounted near the screen, one for each interval, which are connected with 30 registers.

In order to be able to calculate absolute total and differential cross sections the neon counter was, after each series of measurements, replaced by a hydrogen recoil proportional counter which is used as a neutron fluxmeter. The filling gas of this counter consisted of 42 cm of methane and 6.5 atm of argon. With a cathode diameter of 5 cm and a wire thickness of 0.2 mm the operating voltage was 7000 volts. The sensitive volume of this counter, as well as that of the neon counter, was accurately defined without distortion of the electric field by a special construction of the wire [8]). The total number of scattered neutrons in the hydrogen counter was determined from the pulse size distribution. This could be done by graphical extrapolation to zero pulse size. For the most accurate work however, we started from a "theoretical" pulse size distribution, taking into account the wall effects [9, 10]). Such a function with the actual parameters substituted, was fitted to the observed data by least squares analysis, the total number of scattered neutrons being the variable which is determined by this process. The total cross section of hydrogen can then be used to calculate the neutron flux. Fig. 2 shows that the observed pulse size distributions are in reasonable agreement with the theoretical ones. From this it may be concluded that the collimator does not cause a serious degeneration of the neutrons. During all measurements a BF_3 proportional counter surrounded by paraffin served as a neutron monitor.

3. Results

Fig. 3 shows the measured total cross section of neon as a function of neutron energy. Dots represent values obtained by integral pulse counting. The circles have been derived from the pulse height distributions by integration after fitting the experimental data by a polynomial of the 2nd, 3rd or 4th degree. In this case a small correction for the CO_2 content and the remaining γ-ray pulses was applied. Triangles represent cross sections, resulting from integral pulse counting, the scale of which has been corrected to improve the agreement with the more accurate values deduced from pulse size distributions as indicated by the circles. The observed total cross section curve should be regarded as an average for 91 % ^{20}Ne and 9 % ^{22}Ne, since the natural isotope mixture was used. The mean error in the absolute cross sections may be estimated to 10 to 15 percent, except in the neighbourhood of sharp peaks, where the error may be somewhat larger because of insufficient energy resolution.

Figs. 4 and 5 show the results of measurements of pulse size distributions from recoil nuclei. These were carried out at neutron energies for which the total cross section shows a maximum or a minimum and at a few other values as indicated by the arrows in the diagrams added. The distributions observed are presented as differential elastic scattering cross sections as a function of

the cosine of the scattering angle, both in the centre-of-mass system, which can be deduced from the pulse size distributions by a linear transformation[11])

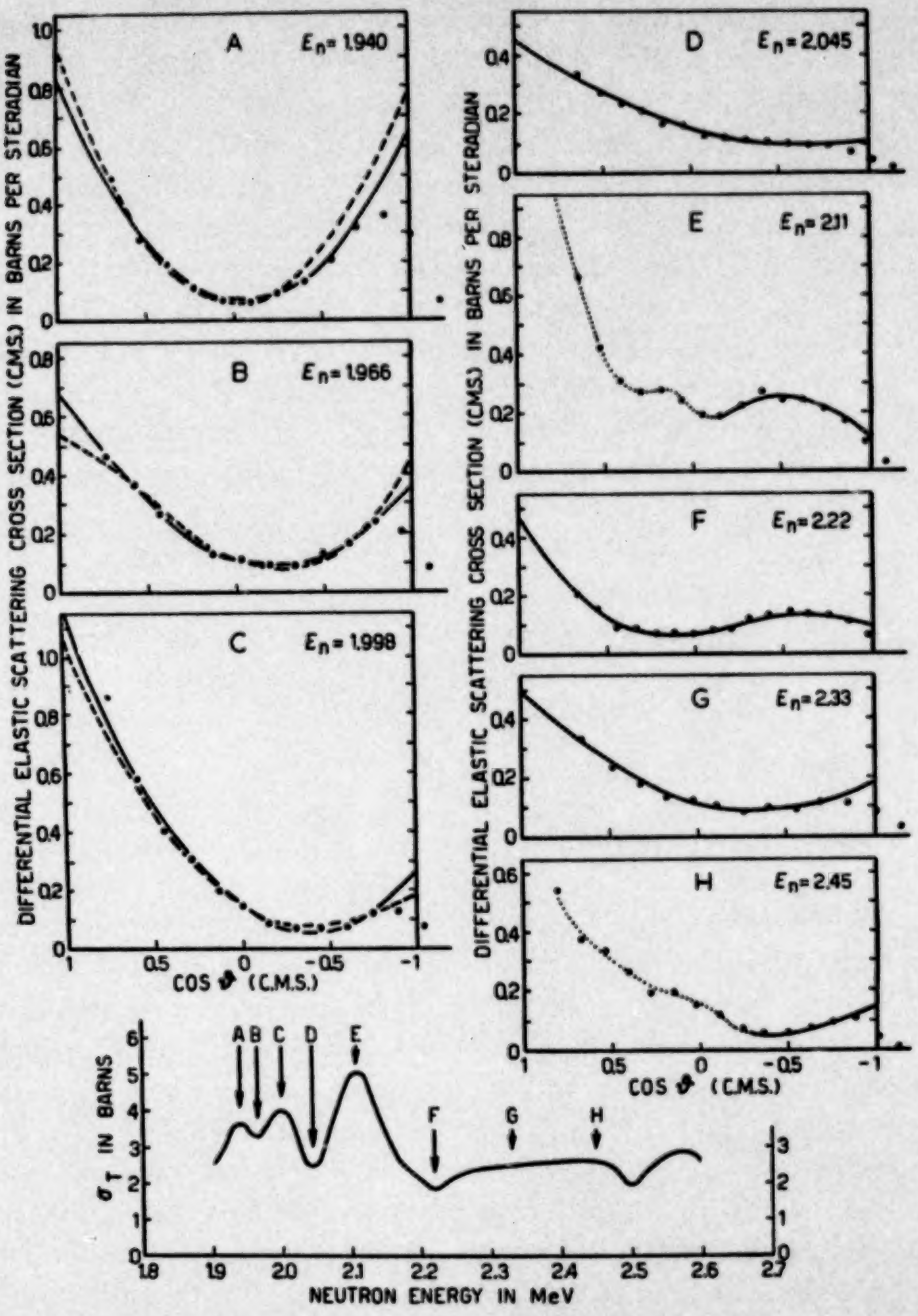

Fig. 4. Differential cross section for elastic scattering of neutrons by neon as a function of scattering angle, both in the centre-of-mass system, at various neutron energies. These neutron energies are indicated in the total cross section curve by the arrows in the lower figure. The full curves are empirically fitted to the data. The dashed curves in figs. A, B and C are theoretical ones for ^{20}Ne, assuming a D 3/2 resonance at 1.94 MeV and a P 3/2 resonance at 2.00 MeV.

The pulse size was assumed to be proportional to the energy of the recoil nuclei, which will only approximately be true. The full curves in figs. 4 A, B,

C, D, F and G represent polynomials of the 2nd or 3rd degree which have been fitted to the experimental data using the method of least squares. The curves in fig. 5 K and M are of 4th degree and have been fitted by trial and error. In the cases of figs. 4 E and H and fig. 5 L inelastic scattering contributes to the pulse size distributions. This is indicated by a step about halfway in the curves, as the corresponding pulse size appears to be about equal

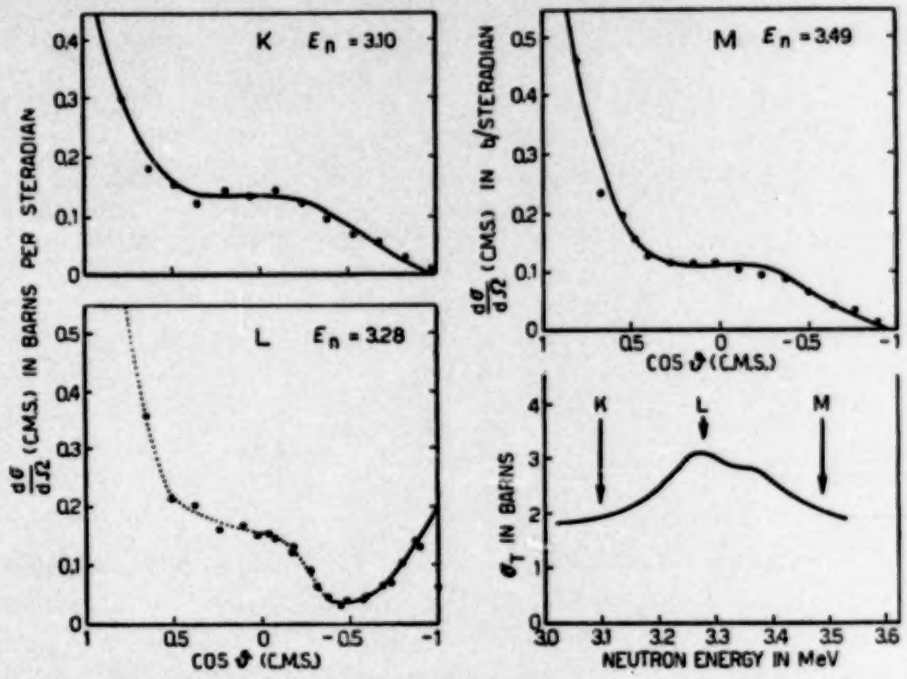
K E_n = 3.10
L E_n = 3.28
M E_n = 3.49
$\frac{d\sigma}{d\Omega}$ (C.M.S.) IN BARNS PER STERADIAN
$\frac{d\sigma}{d\Omega}$ (C.M.S.) IN b/STERADIAN
COS ϑ (C.M.S.)
σ_T IN BARNS
NEUTRON ENERGY IN MeV

Fig. 5. The same as fig. 4, in the energy range 3.1 to 3.5 MeV.

to the one expected in the case of a head-on inelastic collision with ^{20}Ne. Consequently the parts of the curves to the left of this step have been dotted in the figures because they do not represent a differential elastic scattering cross section. The dashed curves in figs. 4 A, B and C are theoretical ones (see section 4).

4. Discussion of the Results

The gross structure of the total cross section as a function of neutron energy, as represented by the full curve in fig. 3 will be due to the most abundant isotope ^{20}Ne. The same will be the case for the pulse size distributions. A theoretical account of the experimental results should therefore be given in terms of resonances corresponding to levels in the compound nucleus ^{21}Ne. A determination of these levels as to their energies, widths and quantum numbers from the present information is, however, not possible for the greater part of the energy range under consideration, for two reasons. First, it may be concluded from fig. 3 and from further considerations given in this section, that we have to do with overlapping resonances in many cases. Second-

ly, the results are complicated by the occurrence of inelastic scattering and (n, α) reactions. A satisfactory analysis can therefore only be carried out for the two resonances at 1.94 and 2.00 MeV neutron energy, at which almost pure elastic scattering occurs. The results are given at the end of this section.

It is of interest to compare the total cross section curve with the (n, α) reaction cross section which has been measured separately before [4, 5]) and is shown by the dotted curve in fig. 3 at a 10× enlarged scale. The peaks in the (n, α) cross section correspond in part to maxima in the total cross section, which is illustrated by table 1.

TABLE 1

Maxima in the total cross section of neon, compared with resonances in the (n, α) reaction.

	Neutron energy (MeV)									
Maxima in σ_T from the present work	1.94	2.00	2.11	(2.45)	2.57		2.73	2.88	3.28	(3.37)
Maxima in $\sigma(n, \alpha)$ according to ref. [5])			2.12	2.45		2.62	2.72	2.87	3.26	

No clear maxima appear in σ_T at 2.45 and 2.62 MeV, possibly because resonances are masked by neighbouring resonances which are not accompanied by an (n, α) reaction. At 2.45 MeV evidence for this is given by the pulse size distribution (fig. 4H) which is much different from the one at 2.33 MeV (fig. 4G) especially because of the contribution of inelastic scattering.

Pulse size distributions are also shown in the neighbourhood of the broad resonance at 3.28 MeV (fig. 5). The curve at 3.28 MeV differs from the other ones again by the evidence of strong inelastic scattering and also by a strong backward elastic scattering.

4.1. ANALYSIS OF THE RESONANCES AT 1.94, 2.00 AND 2.11 MeV

Formulas for the differential elastic scattering cross section of particles with spin $\frac{1}{2}$ on nuclei with zero spin, taking into account spin orbit coupling have been given by Bloch [12]) and others. For our purpose, taking into account angular momentum quantum numbers l not higher than 2, we write these formulas as follows:

$$k^2 \frac{\mathrm{d}\sigma}{\mathrm{d}\Omega} = |A|^2 + |B|^2,$$

with

$$\begin{aligned} A &= \zeta_0 + (\zeta_1^{1/2} + 2\zeta_1^{3/2}) \cos\vartheta + (2\zeta_2^{3/2} + 3\zeta_2^{5/2})(\tfrac{3}{2}\cos^2\vartheta - \tfrac{1}{2}) \\ B &= -i(\zeta_1^{3/2} - \zeta_1^{1/2}) \sin\vartheta - 3i(\zeta_2^{5/2} - \zeta_2^{3/2}) \sin\vartheta \cos\vartheta; \end{aligned} \qquad (1)$$

here $k = 2\pi/\lambda$, λ being the "reduced" wavelength of the incoming neutron,

$d\sigma/d\Omega$ is the elastic scattering cross section per unit solid angle in the centre-of-mass system, ϑ the scattering angle of the neutrons in the same system. The quantities ζ_l^J are related to the phase-shifts of the scattered waves δ_l^J by $\zeta_l^J = \sin\delta_l^J \exp(i\delta_l^J)$, J being equal to $l+\frac{1}{2}$ or $l-\frac{1}{2}$. The total cross section is given by

$$\frac{k^2}{4\pi}\sigma_T = |\zeta_0^{1/2}|^2+|\zeta_1^{1/2}|^2+2|\zeta_1^{3/2}|^2+2|\zeta_2^{3/2}|^2+3|\zeta_2^{5/2}|^2. \qquad (2)$$

In case of a resonance, one phase-shift, the resonant phase-shift, has to be put nearly equal to 90°. In order to determine which resonant phase-shift gives the best agreement with the observed total and differential cross sections, the potential scattering contribution should be known. In our measurements, however, no region of pure potential scattering occurs in the neighbourhood of the resonances to be analyzed. We therefore start by assuming an s-wave potential scattering phase-shift of about −60° and a small negative p-wave phase-shift, as may be expected from hard-sphere scattering. Fortunately the angular distributions predicted by formula (1) show large differences for the various possible types of resonances. Hence the values of the non-resonant phase-shifts need not be exactly known.

In the case of the peak at 1.94 MeV, the angular distribution is well represented by a parabola which is nearly symmetrical with respect to $\vartheta = \frac{1}{2}\pi$ (fig. 4 A). This corresponds to a $D_{3/2}$ resonance. The angular distribution at 2.00 MeV has the shape of an asymmetric parabola (fig. 4 C), the forward scattering being much larger than the backward scattering. This corresponds to a $P_{3/2}$ resonance, a $P_{1/2}$ resonance being excluded by the magnitude of the forward scattering.

The dashed curves in figs. 4 A, B and C represent angular distributions following from formula (1), using the above resonance parameters. Potential scattering phase-shifts used are $\delta_0 = -55°$ and $\delta_1 = -15°$. It should be noted however that because of the experimental uncertainties, no accurate values for the phase-shifts can be deduced from the observed angular distributions. The widths of the resonances, following from the $\delta_1^{3/2}$ and $\delta_2^{3/2}$ values used in fig. 4 B and from the total cross section curve, are also only approximate ones. The widths estimated are 20 ± 10 keV and 50 ± 10 keV for the 1.94 and 2.00 MeV resonances respectively.

The strong peak at 2.11 MeV could not be explained as a single resonance on the basis of the observed angular distribution (fig. 4 E). The curve seems to be of the 3rd degree, which means that considerable $P_{3/2}$ as well as $D_{3/2}$ scattering must be present. We are therefore inclined to assume a $P_{3/2}$ and a $D_{3/2}$ resonance in this region, which overlap for the greater part. A detailed analysis is made difficult, however, by the occurrence of inelastic scattering.

Table 2 gives the parameters of the excited states in the ^{21}Ne nucleus which

correspond to the above resonances. Bracketed values have not been well established. The binding energy of the neutron to the ^{20}Ne nucleus is assumed to be 6.75 MeV above the ground state of ^{21}Ne, as calculated from the mass values [13, 14]).

TABLE 2

Levels in ^{21}Ne

E_n (MeV)	Excitation energy (MeV)	Spin	Parity	Width (keV)
1.94	8.60	3/2	+	20±10
2.00	8.66	3/2	−	50±10
2.11	8.76	(3/2)	(+)	
		(3/2)	(−)	

The author wishes to express his thanks to Professor H. Brinkman, the Director of this laboratory, for his stimulating support of this work. His thanks are further due to Mr. P. J. Pasma for his help in the operation and maintenance of the neutron generator, to Mr. H. H. van Barneveld for his aid in taking the data and to Mr. R. v. Wageningen for theoretical discussions.

The work was part of the research program of the "Stichting voor Fundamenteel Onderzoek der Materie" (F.O.M.), financially supported by the Netherlands Organization for Pure Scientific Research (Z.W.O.).

References

1) H. O. Cohn and J. L. Fowler, Phys. Rev. **99** (1955) 1625(A); Bull. Am. Phy. Soc. **1** (1956) 175, F6
2) J. L. Fowler, Short communication at the International Conference on nuclear reactions, Amsterdam, July 1956; Physica **22** (1956) 1136(A)
3) J. L. Fowler, Private communication
4) C. P. Sikkema, Nature **165** (1950) 1016
5) C. H. Johnson, C. K. Bockelman and H. H. Barschall, Phys. Rev. **82** (1951) 117 (L)
6) F. C. Flack and J. B. Warren, Proc. Roy. Soc. Canada **47** (1953) 131(A)
7) R. Giles, Rev. Sci. Instr. **24** (1953) 986
8) C. P. Sikkema, Nuclear Instruments (1957) to be published
9) B. B. Rossi and H. H. Staub, Ionization chambers and counters (McGraw-Hill, 1949) 154
10) T. H. R. Skyrme, P. R. Tunnicliffe and A. G. Ward, Rev. Sci. Instr. **23** (1952) 204
11) H. H. Barschall and M. H. Kanner, Phys. Rev. **58** (1940) 590
12) F. Bloch, Phys. Rev. **58** (1940) 829
13) E. Segrè, Experimental Nuclear Physics, Part I (Wiley, 1952)
14) F. Ajzenberg and T. Lauritsen, Revs. Modern Phys. **27** (1955) 77

Nuclear Physics **3** (1957) 385—390; *North-Holland Publishing Co., Amsterdam*

AN INVESTIGATION OF THE REACTION ^{23}Na (d,n) ^{24}Mg

F. A. EL BEDEWI and M. A. EL WAHAB
Faculty of Science, University of Alexandria

Received 18 December 1956

Abstract: The photographic plate technique has been used to investigate the neutrons emitted from the disintegration of sodium by 8 MeV deuterons. The angular distributions of some neutron groups have been compared with curves calculated from the known deuteron stripping theories.

A new level in ^{24}Mg at 10.46$\pm$0.10 MeV is found to have even parity and spin 1 or 2.

1. Introduction

The nuclear properties of the low lying energy levels of ^{24}Mg have been studied rather extensively by different nuclear reactions [1, 2]. Above an excitation energy of 5.26 MeV some few levels have also been reported from either inelastic scattering of protons and deuterons or from ^{23}Na (d, n) ^{24}Mg reaction. Since magnesium naturally exists as a mixture of three isotopes while sodium is only found as a single isotope, experiments on (d, n) reaction are recommended for a direct investigation of the energy levels in ^{24}Mg. In this high energy region Mandeville [3]) used 1.4 MeV deuterons to bombard a thick target of metallic sodium. The neutrons emitted at 90° were detected by photographic plates and two levels at 7.70 MeV and 8.64 MeV were observed. The angular distribution of neutrons belonging to these groups were recently reported by Calvert *et al.* [4]) using a fast neutron spectrometer.

The present investigation was made to study this reaction at a deuteron energy of 8 MeV in the hope to observe new energy levels as well as to confirm previous results.

2. Method

A thin layer of sodium iodide painted on to gold backing was bombarded by deuterons of mean energy 7.75$\pm$0.07 MeV. The neutrons were detected by nine 2 in.$\times$2 in. Ilford C_2 600μ nuclear plates mounted vertically at angles ranging from $-5°$ to 55° with respect to the direction of the incident beam. The exposure was made with the 37 in. cyclotron at the Nuclear Physics Research Laboratory, Liverpool, employing the experimental arrangement described by Middleton, El Bedewi and Tai [5]). Investigation of the plates was carried out at the University of Alexandria, Egypt.
The criterion for selecting recoil protons was as follows:

a) In each plate, search was only made in a strip of emulsion of width 4 mm and length 9 mm centred about the line joining the centres of the target and plate and commenced 8 mm from the inner edge of the plate.

b) All tracks of ranges greater than 150 μ and subtending a horizontal angle $\leqq 12°$ with the centre line and having a dip of less than 10 μ in a length of 100 μ at the beginning of the track were recorded.

The neutron energy corresponding to each recoil proton was calculated from some geometrical considerations and using the range energy relation reported by El Bedewi [6]).

3. Results and Discussion

A total of about 5000 tracks was measured from plates exposed at all angles of observation. A representation histogram at angle 0° to indicate the number of tracks recorded in successive intervals of 100 keV in neutron energy is shown in fig. 1. From an analysis of such histograms at all angles

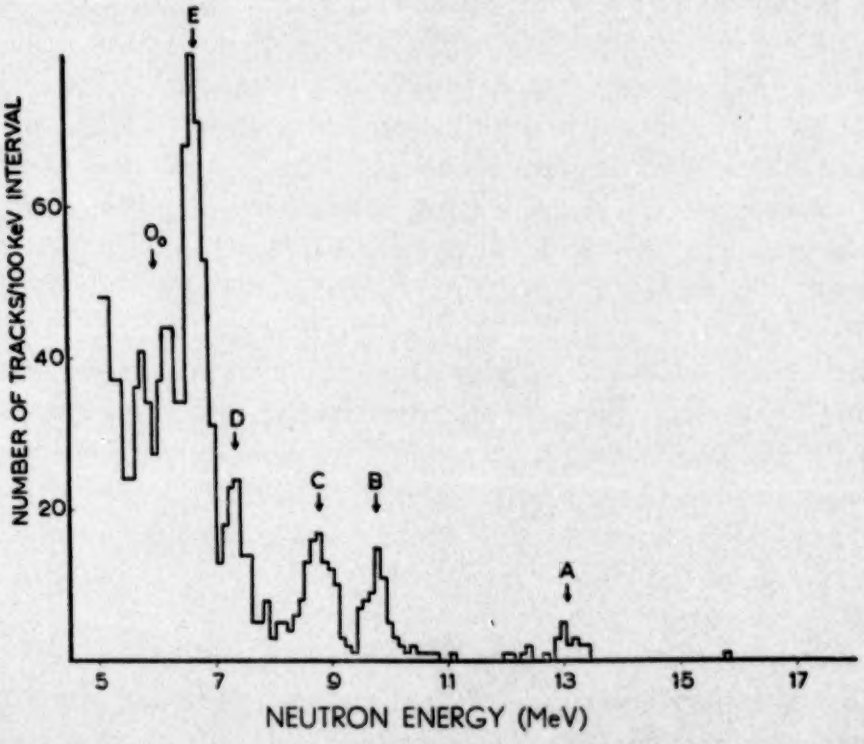

Fig. 1. Spectrum of neutron groups from the deuteron bombardment of sodium at an angle of observation of 0°.

of observation the existence of groups A, B, C, D and E were established. Other groups may exist, but since they are of weak intensity they have been neglected.

Assuming the Q-value of this reaction to be 9.478 MeV [1]) no track was found to represent a transition to the ground state of ^{24}Mg. Very few tracks

of energy ≈ 16 MeV have been observed which may represent a transition to the first excited state known at 1.368 MeV. Assuming that the group A represents the well known doublet at 4.13 and 4.24 MeV, one can then calculate the effective energy of the incident deuteron. On this assumption,

TABLE 1

^{23}Na (d, n) ^{24}Mg		^{24}Mg (p, p') ^{24}Mg Ref. [7])
Present	Ref. [3])	
7.45±0.10	7.70	7.32±0.3
8.48±0.10	8.64	8.30±0.4
(9.85±0.20)	—	—
10.46±0.10	—	—

the groups B, C, D and E were found to correspond to transitions to excited states of ^{24}Mg at 7.45±0.10 MeV, 8.48±0.10 MeV, (9.85±0.20 MeV) and 10.46±0.10 MeV respectively. We are not certain that group D belongs to the present reaction since its position nearly coincides with a possible group of neutrons emitted from the ^{12}C (d, n)^{13}N reaction, leaving the residual nucleus at its ground state. The carbon as well as oxygen may exist as contamination in the exposed target. The position of the oxygen ground state is indicated by the arrow at 0°. The present results are compared with the possible levels previously reported in this energy region as shown in table 1.

The angular distribution of the neutron groups A, B, C and E were obtained by estimating the number of tracks belonging to each group from the plotted histograms. The relative intensities of each group were corrected for the variation of the cross section of the (n, p) scattering with neutron energy [8]). These results were transferred to the centre of mass system and represented, in the same units of intensity, as shown in fig. 2. The experimental errors are the statistical standard deviation. The theoretical curves are calculated from the Butler stripping theory [9]) using the Gamow radius $(1.7\pm1.22)\ A^{\frac{1}{3}} \times 10^{-13}$ cm as the radius of interaction. In all these groups the agreement between the theoretical and experimental distribution was achieved when assuming the angular momentum transferred by the absorbed proton to be mainly $l_p = 0$. In case of the groups A and C a better fit could be obtained by adding up in suitable proportions curves with $l_p = 0$ and $l_p = 2$. In general, the distributions for the groups A, B and C agree with those reported by Calvert *et al.* [4]).

Since the ground state of ^{23}Na is known [1]) to have spin $3/2^+$ the value of $l_p = 0$ for the transition to the 7.45 MeV and 10.46 MeV levels of ^{24}Mg indicates that each of these levels has even parity and spin 1 or 2. It is of interest to point out that if the first level of isobaric spin $T = 1$ appears

at ≈ 9.4 MeV [10]) the new level at 10.46 MeV in ^{24}Mg may then be the analogue to the 1.34 MeV level in ^{24}Na. El Bedewi and El Wahab [11]) have investigated the ^{23}Na (d, p) ^{24}Na reaction using deuterons of mean energy 8.60 MeV. It is found that the angular momentum of the absorbed nucleon

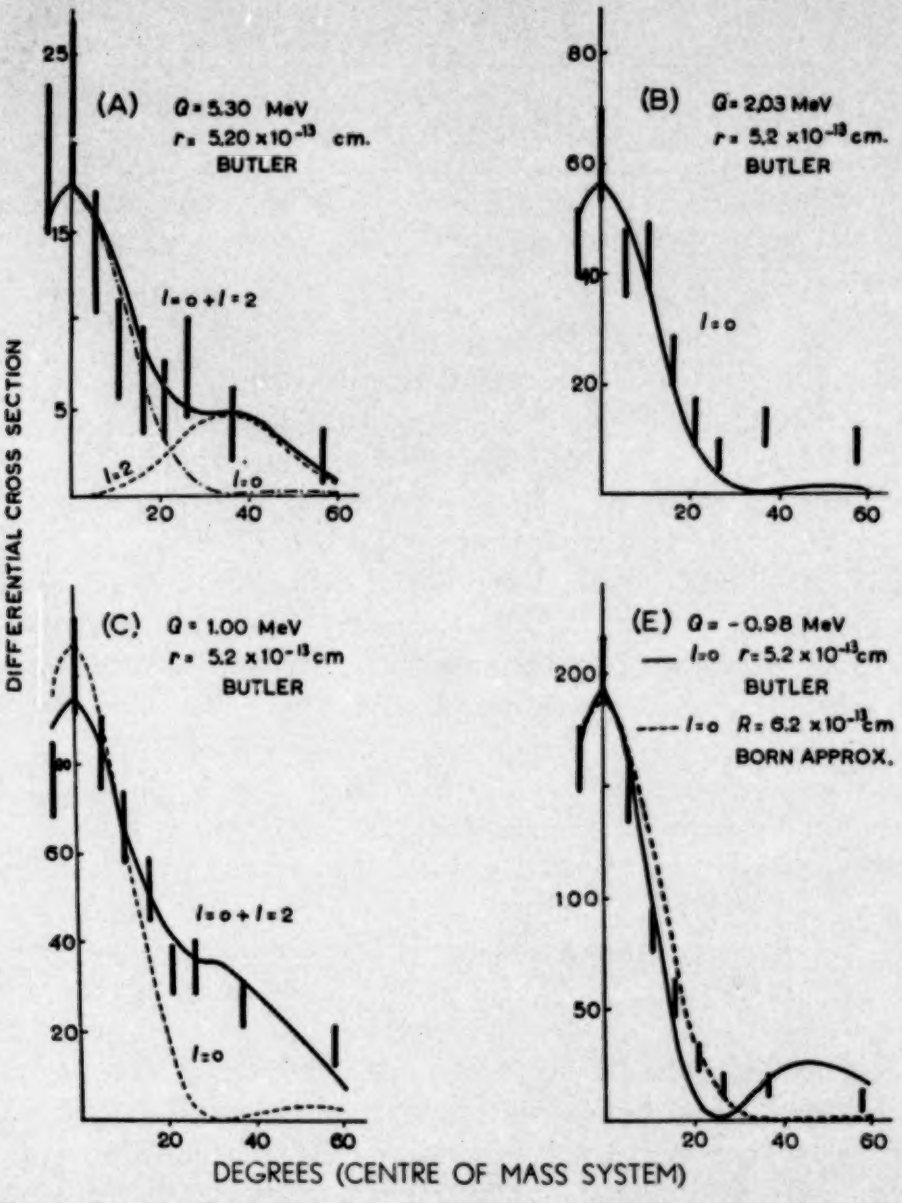

Fig. 2. Angular distribution of neutron groups emitted from ^{23}Na (d, n) ^{24}Mg.

forming either of these levels in ^{24}Mg and ^{24}Na is equal to zero and the corresponding groups have a considerably large cross section in comparison to that of the neighbouring levels. Braid [12]) has recently reported the spin of the 1.34 MeV level in ^{24}Na to be 2^+. If these levels are in fact identical then on account of the isobaric spin selection rule the assignment of spin 1 to the 10.46 MeV level in ^{24}Mg is excluded and it would then have spin 2 and even parity.

The level corresponding to group A was proved by Hausman *et al.* [13]) to be a doublet of 4.13 MeV and 4.24 MeV having spin 4^+ and 2^+ respectively [14]). The fact that the distribution pattern shows a mixture of $l_p = 0$ and $l_p = 2$ indicates that the 4.13 MeV level should be formed by d-wave protons while the adjacent level is formed by the capture of *s*-wave protons. As shown in table 2, it seems worth while to draw the attention to the fact that although both levels have nearly the same value of reduced width yet the capture probability of the lower level is six times its value for the higher one.

Finally, the mixture of $l_p = 0$ and $l_p = 2$ for the level at 8.48 MeV indicates that it has even parity and spin 1 or 2 if it exists as a single level. However, this level may be also a doublet since this group, when compared with the neighbouring ones, has a large half width. In this case the spin of one of these levels may be 1^+ or 2^+ while the other can have a spin 0, 1, 2, 3 or 4.

A summary of the nuclear properties of the examined levels is given in table 2.

TABLE 2

Neutron group	Energy level (MeV)	*l*-value	possible level spins	parity	relative reduced width	Relative capture probability
A	4.13	2	4	even	1	1
	4.24	0	2	even	1.3	0.17
B	7.45	0	1 or 2	even	3.4	0.22
C	8.48	0	1 or 2	even	5.1	0.32
		2	0—4	even	2.0	2.90
E	10.46	0	2	even	36	0.72

One of the authors (F.B.) is grateful to Professor H. W. B. Skinner for his encouragement and advice during the performance of this experiment at the Nuclear Physics Research Laboratory, Liverpool.

The authors would also like to express their gratitude to Professor M. A. El Sherbini for his interest and discussion.

References

1) P. M. Endt and J. C. Kluyver, Rev. Mod. Phys. **26** (1954) 95
2) P. J. Grant, J. G. Rutherglen, F. C. Flack and G. W. Hutchinson, Proc. Phys. Soc. A **68** (1955) 369
3) C. E. Mandeville, Phys. Rev. **76** (1949) 436
4) J. M. Calvert, A. A. Jaffe, A. E. Litherland and E. E. Maslin, Proc. Phys. Soc. A **68** (1955) 1008
5) R. Middleton, F. A. El Bedewi and C. T. Tai, Proc. Phys. Soc. A **66** (1953) 95
6) F. A. El Bedewi, Proc. Phys. Soc. A **64** (1951) 1079
7) H. W. Fulbright and R. R. Bush, Phys. Rev. **74** (1948) 1323
8) R. K. Adair, Rev. Mod. Phys. **22** (1950) 249

9) S. T. Butler, Proc. Roy. Soc. A **208** (1951) 559
10) E. Goldberg, W. Haeberli, A. I. Galonsky and R. A. Douglas, Phys. Rev. **93** (1954) 799
11) F. A. El Bedewi and M. A. El Wahab, to be published
12) T. H. Braid, Phys. Rev. **102** (1956) 1109
13) H. J. Hausman, A. J. Allen, J. S. Arthur, R. S. Bender and C. J. Mc Dole, Phys. Rev. **88** (1952) 1296
14) J. C. Newton, Phys. Rev. **96** (1954) 241

Nuclear Physics **3** (1957) 391—422; *North-Holland Publishing Co., Amsterdam*

ÜBER DIE ZERTRÜMMERUNG SCHWERER KERNE DER KERNEMULSION DURCH TEILCHEN DER KOSMISCHEN STRAHLUNG

K. LANIUS

Institut Miersdorf
der Deutschen Akademie der Wissenschaften zu Berlin
Zeuthen/Berlin

Received 19 December 1956

Abstract: A detailed investigation of 1020 desintegration stars, with 1 to 5 prongs, of the heavy nuclei in nuclear emulsion is reported and the results compared with the theoretical model of a nucleon cascade followed by evaporation. The observed frequencies of the emitted α particles and deuterons are many times larger than the theoretical expectation. The angular distributions and angular correlations as well as the energy spectra of these particles are also in disagreement with the theoretical model. The behaviour of the protons is approximately explained by the model. 70 % of the stars have recoil tracks with range < 6 μ. Their range distribution, angular distribution and angular correlations are only partially accounted for by the theory.

1. Einleitung

In dieser Arbeit soll der Gültigkeitsbereich der Theorie, die zur Erklärung der Zertrümmerung schwerer Kerne durch hochenergetische Nukleonen entwickelt wurde, im Detail untersucht werden.

Viele Autoren haben die Kernzertrümmerungen mit Kernemulsionen untersucht, die entweder durch Teilchen der kosmischen Strahlung oder vor allem in letzter Zeit durch künstlich beschleunigte Teilchen hervorgerufen wurden.

Die theoretische Beschreibung gliedert den Prozeß in zwei aufeinanderfolgende Stadien. Während des ersten Stadiums entwickelt sich, ausgelöst durch das primäre Teilchen, eine Nukleonenkaskade im Kern. Ein Teil der angestoßenen Nukleonen wird den Kern direkt verlassen, während der andere Teil im zweiten Stadium zu einer Anregung des Restkerns führt. Diese Anregungsenergie wird durch Teilchenemission abgegeben.

Beide Schritte lassen sich im Detail analysieren; der erste mit Hilfe einer statistischen Methode — der Monte-Carlo-Methode — und der zweite mit Hilfe der Verdampfungstheorie.

Bei der Untersuchung großer Sterne, das sind Zertrümmerungen durch Teilchen hoher Energie (> 500 MeV), wurden von mehreren Autoren Erscheinungen beobachtet, die nicht mit dem oben skizzierten Mechanismus zu erklären waren. Das führte zu folgenden Hypothesen:

1) *Die Spaltung*

Durch das primäre Nukleon wird der Kern in zwei oder mehrere Bruchstücke gespalten.

Im Radiation Laboratory (Berkeley) wurden systematische Untersuchungen der Spaltung schwerer Kerne durch hochenergetische Teilchen mit radiochemischen Methoden durchgeführt. Für die Spaltung von Ag durch 340 MeV Protonen fand Kofstadt [1]) einen Wirkungsquerschnitt von 10^{-1} bis 10^{-2} mb.

Beschränken wir daher unsere Untersuchungen auf Sterne, die durch Nukleonen mit Energien $\lesssim 340$ MeV ausgelöst sind, so können wir die Zahl der Spaltungsprozesse von Ag- und Br-Kernen der Emulsion gegenüber der Zahl der Zertrümmerungen vernachlässigen.

2) *Die Lokale Verdampfung*

Ein Teil des Kerns wird auf eine höhere Temperatur als die des Kernrestes erhitzt.

Kind und Patergnani [2]) haben diesen Prozeß analysiert. Sie zeigten, daß die Zeit, die zur Verteilung der Anregungsenergie über den ganzen Kern notwendig ist, größer sein kann als die Zeit, die zur Auslösung einer lokalen Verdampfung gebraucht wird. Dieser Fall kann eintreten, wenn die Anregungsenergie > 7 MeV ist. Also wird auch dieser Prozeß nur bei großen Sternen zu einem nachweisbaren Effekt führen.

3) *Die Mesonen-Erzeugung*

Mit wachsender Energie der sternauslösenden Nukleonen kann eine Erzeugung von π-Mesonen im Kern stattfinden. Auch dieser Prozeß läßt sich bei kleinen Sternen vernachlässigen.

Um diese drei Möglichkeiten auszuschließen, beschränken sich unsere Untersuchungen auf kleine Sterne, d.h. auf geringe Energien der sternauslösenden Nukleonen.

Leider standen uns zur Durchführung der Arbeit keine an einer Beschleunigungsmaschine exponierten Platten zur Verfügung. Die von uns untersuchten kleinen Sterne sind zum überwiegenden Teil durch Neutronen der kosmischen Strahlung ausgelöst worden.

2. Experimentelle Ergebnisse

2.1. EXPERIMENTELLE BEDINGUNGEN

Die Untersuchungen wurden mit 400 μ dicken Agfa-K2-Platten (3×6 cm) durchgeführt. Die Platten wurden in zwei Gruppen zu je drei Platten auf der Zugspitze (3000 m) exponiert. Die Exponierungsdauer der ersten Gruppe betrug 48 Tage, die der zweiten Gruppe 29 Tage. In beiden Fällen waren die Platten vertikal aufgestellt. Die Temperatur betrug im Mittel 15° C, die relative Luftfeuchtigkeit im Mittel 50 %.

Die Entwicklung der Emulsionen erfolgte nach dem Temperaturentwicklungsverfahren [3]). Die Platten wurden unter dem Mikroskop bei 300-facher Vergrößerung abgesucht. Alle Spuren mit Reichweiten $< 6\,\mu$ wurden als Rückstoßspuren gezählt. Diese Spuren gelten nach der üblichen Klassifizierung nicht als Arm. In Tabelle I ist die Sterngrößenverteilung der untersuchten Sterne angegeben.

TABELLE I

Zahl der Arme	1	2	3	4	5
Zahl der Sterne m.r. †	159	348	211	113	44
Zahl der Sterne o.r.	—	160	209	174	45
Zahl der Sterne m.2r.	12	14	8	—	2

Bei den zweiarmigen Ereignissen o.r. wurden, um Streuungen auszuschließen, nur solche Ereignisse mitgezählt, bei denen aus dem Verlauf der Spuren klar ersichtlich war, daß es sich um Sterne handelt. Fälle von Proton-Proton-Streuungen in der Gruppe der dreiarmigen Sterne o.r. wurden nicht gezählt.

In einigen Zertrümmerungen war aus dem Korndichteverlauf längs der Spuren zu erkennen, daß es sich um ältere durch Fading beeinflußte Sterne handelte. Solche Sterne wurden durchweg nicht gezählt. Ihre Anwesenheit erklärt sich daraus, daß die Platten bereits vor der Exponierung mehrere Wochen in Meereshöhe lagerten.

Die Identifizierung der in der Emulsion endenden Spuren, die Messung ihrer Horizontal- und Vertikal-Projektionen und die Winkelmessungen wurden bei 1350-facher Vergrößerung durchgeführt.

Die Reichweite der in der Emulsion endenden Spuren wurde durch Messung der Horizontal- und der Vertikal-Projektion, l und h, bestimmt. Die erstere wurde mit einem Okular-Mikrometer gemessen. Zur Messung der Vertikal-Projektion wurde ein am Mikroskop angebrachtes Zeiß-Orthotest benutzt. Dieses hat einen Teilungswert von $1\,\mu$ und eine Meßgenauigkeit von $\pm\,0.5\,\mu$. Der Schrumpfungsfaktor S wurde für jede der sechs Platten gemessen. Mit diesen Daten wurde die Reichweite $R = \sqrt{(l^2+S^2h^2)}$ der endenden Spuren bestimmt.

2.2 DIE IDENTIFIZIERUNG DER SPUREN

Das Unterscheidungsvermögen der Agfa-K2-Platte entspricht etwa dem der Ilford-C2-Platte. Für einen erfahrenen Beobachter ist es also ohne Schwierigkeit möglich, in der Emulsion endende Spuren einfach geladener Teilchen von α-Teilchen zu unterscheiden. Voraussetzung hierfür ist, daß

a) der Winkel γ, den die Spur mit der Emulsionsebene einschließt, nicht zu groß ist, und daß

† d.h. mit Rückstoßspur; entsprechend heißt o.r. ohne Rückstoßspur.

b) die Spur in der Emulsion eine hinreichende Länge besitzt.

Zu a): an den untersuchten Sternen wurden 3586 Spuren (einschließlich Rückstoßspuren) beobachtet, die in der Emulsion endeten. Unter diesen befanden sich 105 Spuren mit einer Reichweite $R > 40\ \mu$, die nicht identifiziert werden konnten. Ein großer Teil dieser Spuren schloß einen Winkel $\gamma > 70°$ mit der Emulsionsebene ein. Daraus folgernd, wurde der Grenzwinkel bis zu dem eine Spuridentifizierung bei hinreichender Länge möglich ist, zu $\gamma' = 70°$ festgestezt. Es kommt hinzu, daß Spuren, die nahezu senkrecht zur Emulsionsebene verlaufen, leicht übersehen werden können. Die nachfolgenden Reichweite-Verteilungen beschränken sich daher auf den Winkelbereich $+70° \leqq \gamma \leqq -70°$.

Zu b): zur Ermittlung der hinreichenden Länge wurde folgender Endentest durchgeführt. In willkürlicher Reihenfolge wurden α-Teilchen und einfach geladene Teilchen, die auf Grund ihrer Lage und Reichweite mit Sicherheit identifiziert werden konnten, herausgegriffen. Durch einen Beobachter wurden diese Spuren im Mikroskop so eingestellt, daß nur das Ende der Spur im Gesichtsfeld sichtbar war. Ein zweiter Beobachter mußte feststellen, ob es sich um ein einfach geladenes Teilchen oder ein α-Teilchen handelte.

Tabelle II

Anzahl der Spurenden	eingestellte Restreichweite (μ)	richtig identifizierte Spuren (%)	falsch identifizierte Spuren (%)	
			einfach geladene als α	α als einfach geladene
600	40	88.3	4.2	7.5
300	21	75.7	6.3	18

In den drei Versuchen wurde etwa die gleiche Anzahl aus den beiden Spurengruppen eingestellt. Die Ergebnisse dieser Messungen führten zur Festsetzung der zur Identifizierung hinreichenden Spurenlänge auf $40\ \mu$.

Bei jeder Messung der Reichweite-Verteilung einer beliebigen Spurengruppe aus Sternen muß der Bruchteil der die Emulsion verlassenden Spuren durch eine sog. „geometrische Korrektion" berücksichtigt werden. Es ist also die Wahrscheinlichkeit zu berechnen, daß eine Spur der Länge R ganz in einer Emulsion der Dicke d liegt und mit der Emulsionsebene einen Winkel $\gamma < \gamma'$ einschließt. Setzt man voraus, daß die Teilchen in den Sternen isotrop emittiert wurden, so ergibt sich für $R \sin \gamma' > d$ die Wahrscheinlichkeit zu

$$f = \frac{d}{2R \sin \gamma'}. \tag{1}$$

Für $R \sin \gamma' < d$ erhält man

$$f = 1 - \frac{R \sin \gamma'}{2d}. \tag{2}$$

Um den Anteil der einfach geladenen Teilchen mit Reichweiten $< 40\,\mu$ an der Gesamtzahl der Spuren abschätzen zu können, wurde die Reichweite-Verteilung der einfach geladenen Teilchen oberhalb $40\,\mu$ gemessen. In Abb. 1 ist die geometrisch korrigierte $\sqrt{R}$-Verteilung der einfach geladenen Teilchen oberhalb $40\,\mu$ gezeichnet. In Tabelle III ist die Reichweite-Verteilung unter-

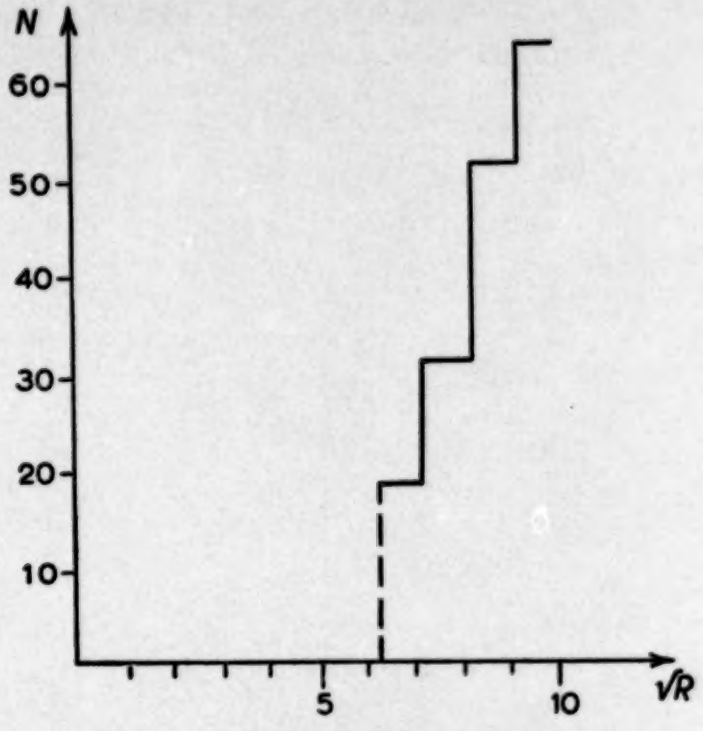

Abb. 1. $\sqrt{R}$-Verteilung der einfach geladenen Teilchen aus allen Sternen.

halb $40\,\mu$ für alle Spuren angegeben. Zum besseren Vergleich ist die Zahl der einfach geladenen Teilchen oberhalb $40\,\mu$ angefügt.

TABELLE III

	alle Spuren		einfach geladene Teilchen	
Reichweite [μ]	10–19.9	20–39.9	40–59.9	60–79.9
Spurenzahl	204	207.9	29.7	57.6

Bei 8.3 der in der zweiten Spalte angegebenen Spuren kann man auf Grund des Korndichteverlaufs annehmen, daß es sich um einfach geladene Teilchen handelt. Diese Zahl entspricht ungefähr dem Erwartungswert, wenn man den Verlauf der Treppenkurve in Abb. 1 gegen Null extrapoliert. Aus diesen Daten folgt, daß die Zahl der einfach geladenen Teilchen mit Reichweiten $< 20\,\mu$ gegenüber den α-Teilchen und Rückstoßkernen vernachlässigt werden kann.

Unter den 3586 in der Emulsion endenden Spuren wurden sechs „Hammerspuren" beobachtet. Das sind Spuren des instabilen ^{8}Li-Kerns, der nach

einem β-Zerfall in zwei α-Teilchen zerfällt. Der Bruchteil der Teilchen mit der Ladung $3e$ ist gegenüber der Zahl der emittierten Teilchen mit der Ladung e bzw. $2e$ vernachlässigbar klein. Diese geringe Emissionswahrscheinlichkeit schwerer Bruchstücke aus kleinen Sternen, d. h. aus Zertrümmerungen kleiner Anregungsenergie, entspricht den Beobachtungen mehrerer Autoren [4, 5, 6]). Wir werden daher im folgenden die Emission von Teilchen mit einer Ladung $\geqq 3e$ vernachlässigen, soweit es sich nicht um Rückstoßspuren handelt.

2.3. DIE TRENNUNG IN ZERTRÜMMERUNGEN LEICHTER UND SCHWERER KERNE

Bei der Analyse kleiner Sterne in der Photoplatte muß man mit Hilfe geeigneter Verfahren die Zertrümmerungen leichter Kerne der Emulsion (C,

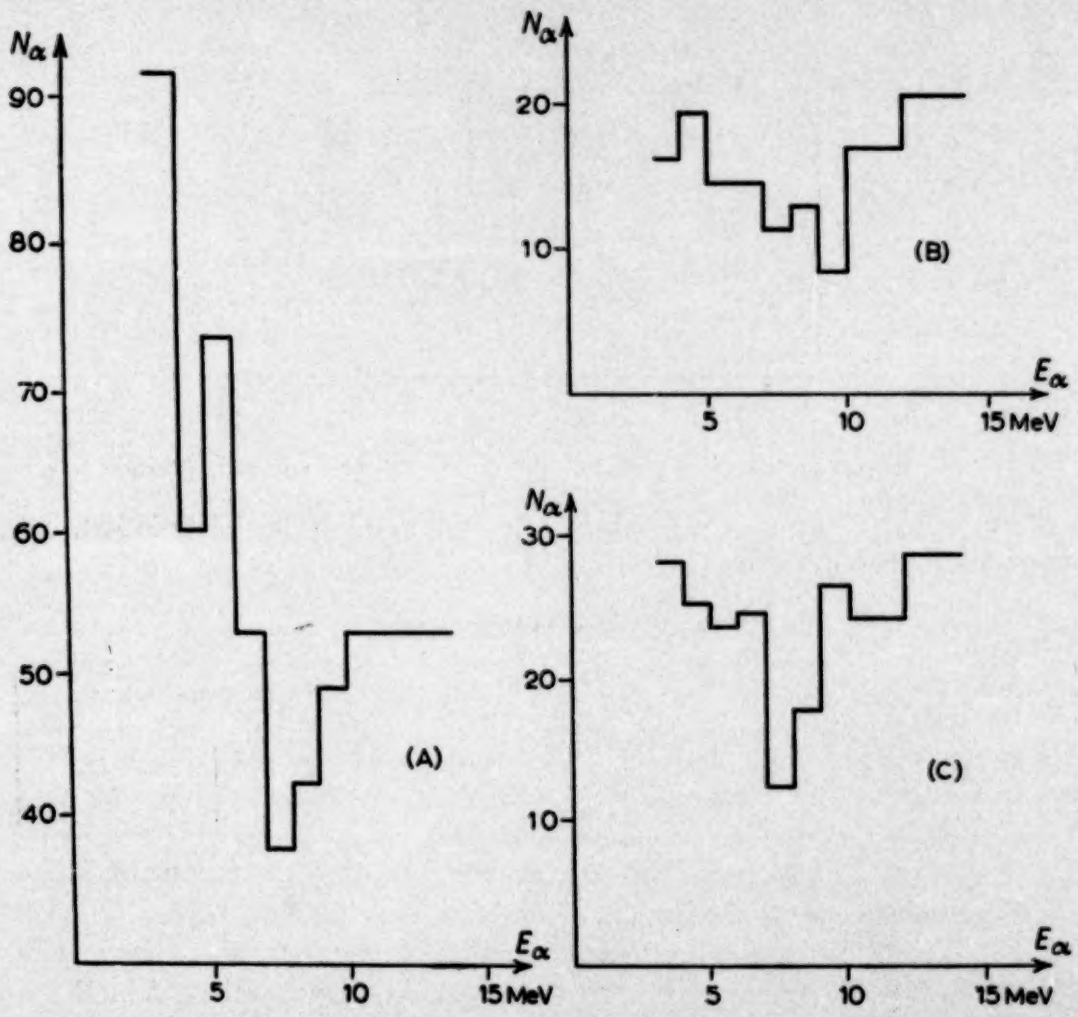

Abb. 2. Energiespektrum der α-Teilchen aus (A) drei- bis fünfarmigen Sternen (B) zweiarmigen Sternen (C) drei- bis fünfarmigen Sternen m. r.

N und O) von den Zertrümmerungen schwerer Kerne (Ag und Br) trennen. Das von uns benutzte Separierungsverfahren beruht auf der unterschiedlichen Höhe des Potentialwalls der leichten und schweren Kerne gegenüber

α-Emission. Bei einem nicht angeregten Kern ist die Höhe im ersten Fall ≈ ≈ 5 MeV, im zweiten Fall ≈ 13 MeV. Betrachtet man die Energieverteilung der α-Teilchen aus Zertrümmerungen kleiner Anregungsenergie, wie sie bei kleinen Sternen vorliegen, so findet man zwei durch ein Minimum klar voneinander zu trennende Maxima. Die Trennmethode besteht darin, daß man alle Sterne mit mindestens einem α-Teilchen, dessen Energie kleiner als der Wert im Minimum, der „Grenzwert", ist, als Zertrümmerungen leichter Kerne zählt.

Perkins [7]) benutzte das Verfahren zur Trennung von σ-Sternen mit 1 bis 4 Armen. Er bestimmte den Grenzwert im Energiespektrum der α-Teilchen zu 10 MeV. Hodgson [8, 9]) benutzte die Methode zur Trennung kleiner Sterne, ausgelöst durch die kosmische Strahlung, bzw. von Sternen, die durch den Beschuß der Emulsionen mit 50 bis 125 MeV-Protonen erzeugt wurden. Für die dreiarmigen Sterne im ersten Falle bestimmte er den Grenzwert zu 8 MeV und bei den vierarmigen Sternen zu 6 MeV. Für die durch künstlich beschleunigte Protonen erzeugten Sterne fand er den Grenzwert zu 9 MeV.

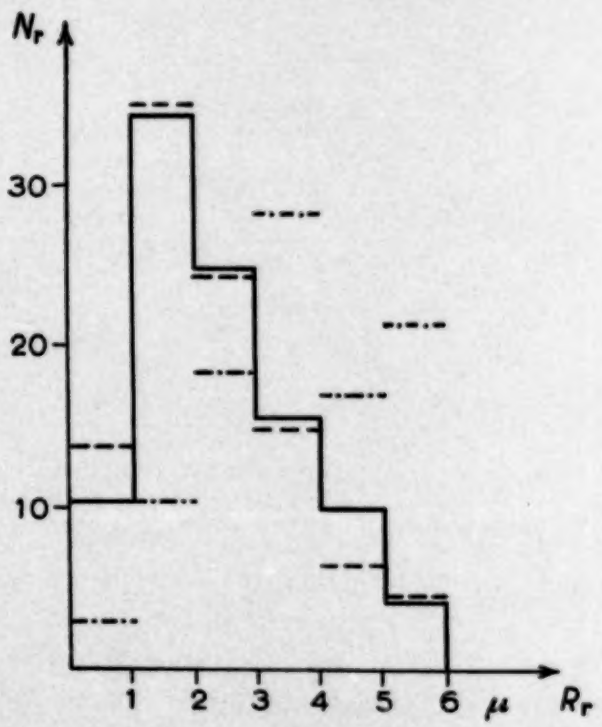

Abb. 3. Reichweite-Verteilung der Rückstoßspuren.
—— = noch nicht klassifizierte Sterne (451 Spuren)
– – – = Zertrümmerung schwerer Kerne (241 Spuren)
–·–·– = Zertrümmerungen leichter Kerne (161 Spuren)

Wie die bisherigen Arbeiten mit Hilfe dieses Separierungsverfahrens zeigten, ist die Methode genügend zuverlässig, um die hauptsächlichen Merkmale der Zertrümmerungen leichter bzw. schwerer Kerne zu untersuchen.

In den Abbildungen 2a bis c sind die korrigierten Energieverteilungen der

α-Teilchen innerhalb des für die Festsetzung des Grenzwertes interessanten Bereiches gezeichnet. Auf Grund dieser Kurven wurden alle zweiarmigen Sterne mit und ohne r, aus denen mindestens ein α-Teilchen mit einer Energie < 9 MeV emittiert wurde und alle drei-, vier- und fünfarmigen Sterne mit und ohne r, aus denen mindestens ein α-Teilchen einer Energie < 8 MeV emittiert wurde, als Zertrümmerungen leichter Kerne klassifiziert.

Neben diesen Sternen mit einer oder mehreren in der Emulsion endenden α-Spuren gibt es eine größere Zahl von Sternen, die keine in der Emulsion

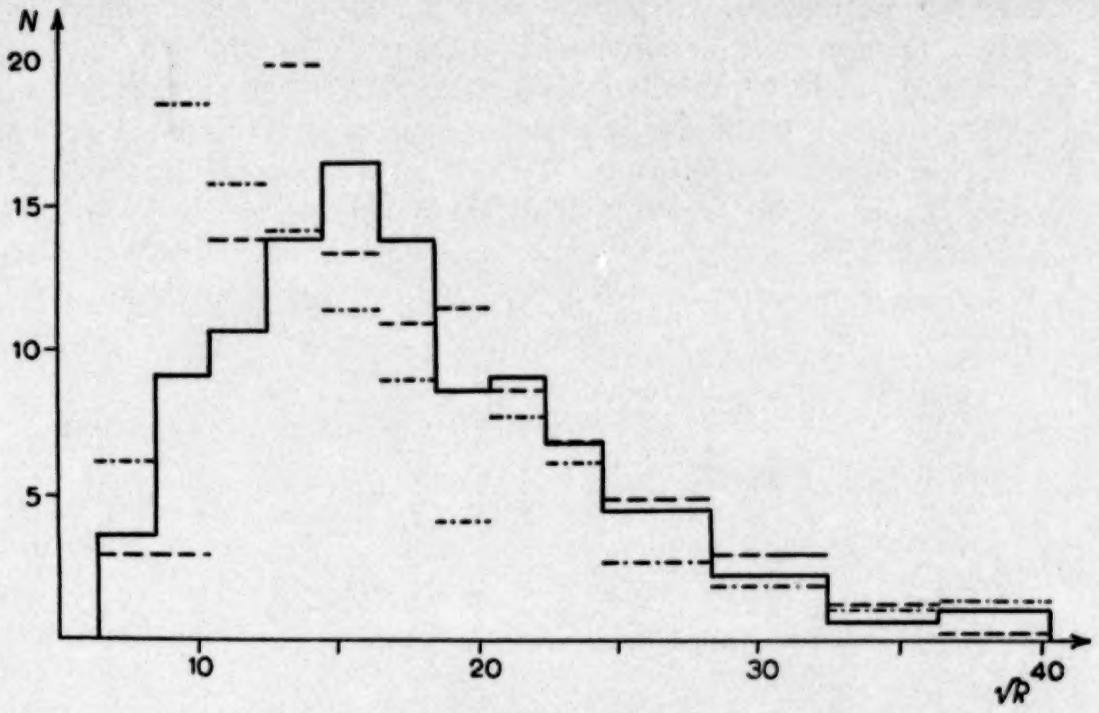

Abb. 4. $\sqrt{R}$-Verteilung der einfach geladenen Teilchen.
——— = noch nicht klassifizierte Sterne (593 Spuren)
– – – = Zertrümmerung schwerer Kerne (228 Spuren)
–·–·– = Zertrümmerungen leichter Kerne (263 Spuren)

endenden α-Spuren besitzen. Um auch diese Sterne als Zertrümmerungen leichter oder schwerer Kerne klassifizieren zu können, wurde die Reichweite-Verteilung der Rückstoßspuren dieser Gruppe mit den entsprechenden Reichweite-Verteilungen der bereits als leicht oder schwer klassifizierten Sterne verglichen.

In Abb. 3 sind die auf gleiche Gesamtzahlen normierten Verteilungen gezeichnet. Die angegebene Zahl der Spuren mit Reichweiten $< 1\,\mu$ ist sehr unsicher, da derart kurze Spuren schwer zu erkennen sind.

Ein Vergleich der drei Verteilungen zeigt, daß die nicht klassifizierten Sterne offensichtlich als Zertrümmerungen schwerer Kerne betrachtet werden können.

Ein weiteres Kriterium für die Richtigkeit dieser Zuordnung ist ein Ver-

gleich der Reichweite-Verteilungen der in der Emulsion endenden Spuren einfach geladener Teilchen. In Abb. 4 sind die auf gleiche Gesamtzahlen normierten $\sqrt{R}$-Verteilungen gezeichnet. Bei diesen Verteilungen wurde keine geometrische Korrektion angebracht.

Auch dieser Vergleich scheint die Identifizierung der nicht klassifizierten Sterne als Zertrümmerungen schwerer Kerne zu unterstützen. Zu seiner Sicherung wurden die Durchschnitte der drei $\sqrt{R}$-Verteilungen statistisch verglichen. Für diesen Vergleich wurden die neun ersten Meßwerte jeder Verteilung benutzt.

TABELLE IV

Art der Sterne	Zahl der Meßwerte	$R^{\frac{1}{2}}$ [$\mu^{\frac{1}{2}}$] Durchschnitt	$s^2[\mu^2]$ Streuung
„schwer"	190	15.7	17.1
„leicht"	229	14.0	21.4
„nicht klassifiziert"	506	15.5	18.9

Der Vergleich „schwer" — „nicht klassifiziert" ergibt, daß eine derartige Abweichung der Durchschnitte in 50 % aller Stichproben zu erwarten ist. Beim Vergleich „leicht" — „nicht klassifiziert" dagegen wird die Abweichung in weniger als 1 % aller Stichproben zu erwarten sein. Dieser Unterschied zwischen den nicht klassifizierten Sternen und den Zertrümmerungen leichter Kerne kann als statistisch gesichert betrachtet werden.

Beide Methoden, — der Vergleich der Reichweite-Verteilungen der Rückstoßspuren und der der Reichweite-Verteilungen der einfach geladenen Teilchen —, führen also zur Einordnung der Sterne ohne endende α-Spur in die Klasse der Zertrümmerungen schwerer Kerne.

Damit erhalten wir die in Tabelle V angegebene Sterngrößenverteilung für die in den schweren Kernen der Emulsion gebildeten Sterne.

TABELLE V

Zahl der Arme	1	2	3	4	5
Zahl der Sterne m.r.	157	273	162	86	35
Zahl der Sterne o.r.	—	123	104	59	21

Das sind insgesamt 1020 Sterne, d. h. 68 % aller Sterne mit einem bis fünf Armen. 70 % dieser Sterne haben eine Rückstoßspur.

Die Häufigkeit der in den schweren Kernen der Emulsion gebildeten Sterne gestattet eine rohe Abschätzung der Energie der sternauslösenden Nukleonen. Grilli u. a. [10]) geben in ihrer Arbeit über die Kernzertrümmerung durch künstlich beschleunigte Protonen die Abhängigkeit der relativen

Häufigkeit der in schweren Elementen der Emulsion gebildeten Sterne von der Protonenenergie an:

TABELLE VI

Energie [MeV]	50	100	150	450
Relative Haufigkeit [%]	40	61	67	74

Aus diesen Werten läßt sich die mittlere Energie der sternauslösenden Nukleonen in unserem Fall zu $\approx$ 200 MeV abschätzen. Es ist jedoch sicher, daß wir es mit einem breiten Energiespektrum der auslösenden Strahlung zu tun haben.

2.4. DIE EMISSIONSWAHRSCHEINLICHKEITEN DER WASSERSTOFF- UND DER HELIUMISOTOPE

Unter den bei der Zertrümmerung eines schweren Kerns der Emulsion emittierten einfach geladenen Teilchen können sich Protonen, Deuteronen und Tritonen befinden.

Zur Identifizierung dieser Teilchen in der Agfa-K2-Emulsion benutzten wir die, vom „committee for the standardization of measurements" [11]) empfohlene „constant sagitta"-Methode, für die in der Emulsion endenden Spuren.

Für einfach geladene Teilchen der Masse M ergibt sich der Mittelwert der absoluten Beträge der zweiten Differenzen, den wir im folgenden mit $\overline{D}$ bezeichnen wollen, zu

$$\overline{D} = \frac{K}{2a} t^{3/2} R^{-n} M^{n-1}. \tag{3}$$

Bei der „constant-sagitta"-Methode wird nun ein Zellenlängenschema berechnet, in dem die Zellenlänge t in Abhängigkeit von der Restreichweite R derart variiert wird, daß $\overline{D}$ konstant bleibt.

Zur Berechnung des Zellenlängenschemas ist die Kenntnis des Streufaktors K und der Energie — Reichweite-Beziehung, d. h. des Faktors a und des Exponenten n, notwendig. Für die K2-Platte wurden diese Größen bestimmt und damit ein Zellenschema für Protonen bei einem $D_p = 0.500\ \mu$ berechnet. Der entsprechende Erwartungswert für Deuteronen ist dann $D_d = 0.370\ \mu$ [12]).

Die durch den Meßprozeß ermittelte zweite Differenz $\overline{D}$ setzt sich aus dem Betrag der „echten" und dem der „unechten" Streuung zusammen:

$$\overline{D}^2 = \overline{D}_e^2 + \overline{D}_u^2.$$

Die unechte Streuung hat im wesentlichen 3 Fehleranteile:

$$\overline{D}_u^2 = d_1^2 + d_2^2 + d_3^2,$$

wobei d_1 von der asymmetrischen Verteilung der entwickelten Silberkörner

um den wahren Weg des Teilchens, d_2 von den persönlichen Ablesefehlern und d_3 von der unregelmäßigen Bewegung des Mikroskoptisches (stage noise) herrühren.

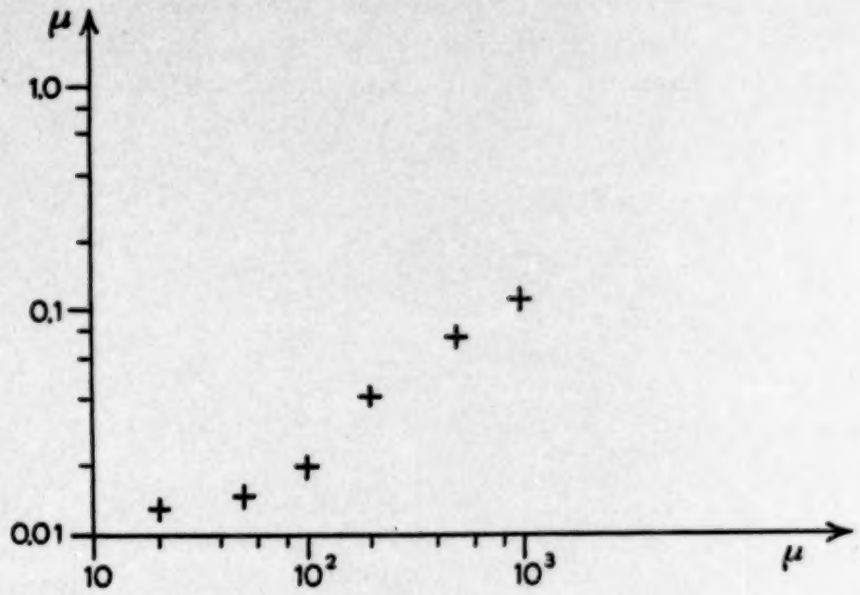

Abb. 5. Variation des stage noise mit der Zellenlänge.

Die Streumessungen wurden mit einem von VEB C. Zeiß, Jena, für diesen Zweck umgebauten Universal-Meßmikroskop durchgeführt. Eine interferometrische Untersuchung der Bewegung des Mikroskopschlittens in Abhängigkeit von der Zellenlänge ergab den in Abb. 5 dargestellten Zusammenhang. Die Eichmessungen wurden an langen endenden Protonenspuren (> 0.5 cm) in der K2-Emulsion vorgenommen. Sie ergaben für Protonen eine echte Streuung $\overline{D}_p = 0.515\,\mu$. Die unechte Streuung wurde zu $\overline{D}_u = 0.12\,\mu$ bestimmt [12]).

Streumessungen wurden an 293 endenden Spuren einfach geladener Teilchen der ein- bis fünfarmigen Sterne aus schweren Kernen durchgeführt. Die Reichweite dieser Spuren lag im Intervall $300\,\mu \leqq R \leqq 2440\,\mu$. Einer Reichweite von $2440\,\mu$ entspricht in der K2-Platte eine Deuteron-Energie von 30 MeV bzw. eine Protonenenergie von 22.3 MeV. Die Spuren hatten einen Neigungswinkel $\gamma \leqq 30°$ gegen die Emulsionsebene. Die gemessenen Mittelwerte der zweiten Differenzen für jede Spur wurden korrigiert

1) in bezug auf die Neigung der Spur,
2) in bezug auf die unechte Streuung.

Eine Glättungskorrektur erwies sich als überflüssig. Um eine Verfälschung der Mittelwerte der Streuung durch die großen von Einzelstreuakten herrührenden Ablenkungen zu vermeiden, wurde die Verteilung der D-Werte bei $D_{co} = 4\overline{D}$ abgeschnitten (cut off).

In Abb. 6 ist die gemessene Häufigkeitsverteilung der Mittelwerte $\overline{D}_e$ der

echten Streeung für die 293 Spuren dargestellt. Durch diese Verteilung ist die theoretisch zu erwartende Gauss-Verteilung um den anderweitig gesicherten Wert $\overline{D}_p = 0.515\,\mu$ gelegt, die der Hypothese entspricht, daß alle Spuren durch Protonen hervorgerufen wurden. Die experimentelle Verteilung der $\overline{D}_e$-Werte um $\overline{D}_p$ deutet jedoch darauf hin, daß ein Teil der links von $\overline{D}_p$ liegenden $\overline{D}_e$-Werte Deuteronen oder Tritonen zuzuschreiben ist.

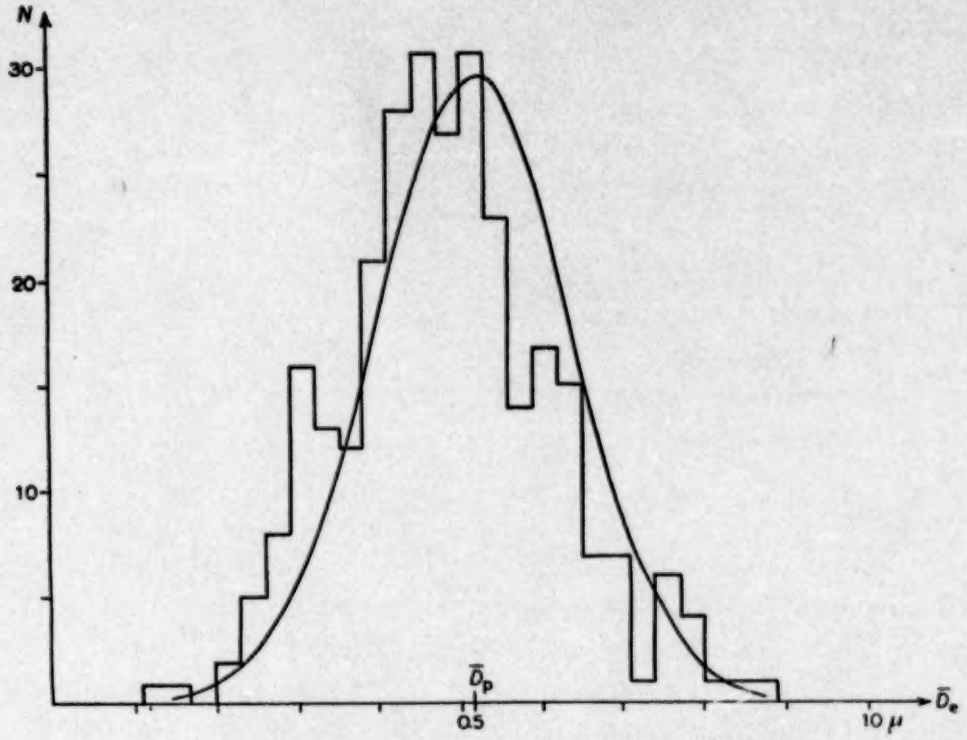

Abb. 6. Häufigkeitsverteilung der Mittelwerte $\overline{D}_e$ der echten Streuung.

Zur Berechnung der Gauss-Verteilung wurde daher die sinnvolle Annahme gemacht, daß in Abb. 6 alle rechts von $\overline{D}_p$ liegenden Mittelwerte der zweiten Differenzen Protonen zuzuschreiben sind. So kann man aus der beobachteten Verteilung oberhalb von $0.515\,\mu$ die mittlere quadratische Abweichung der Gauss-Verteilung berechnen. Es ergab sich $\sigma_p = 0.119\,\mu$. Vergleicht man die experimentell beobachtete mit der theoretisch zu erwartenden Verteilung mittels χ^2-Test, so erhält man $\chi^2 = 42$ bei 16 Freiheitsgraden. Daraus folgt $P < 0.05\,\%$, d. h., die experimentelle Verteilung kann nur in $< 0.05\,\%$ aller Fälle als zufällige Abweichung von der theoretischen Verteilung auftreten. Man kann daher den Unterschied zwischen den Verteilungen als statistisch gesichert betrachten.

Um die experimentelle Verteilung statistisch analysieren zu können, wurden folgende plausible Annahmen gemacht:

a) Der Anteil der Tritonen ist gegenüber den Protonen und Deuteronen vernachlässigbar klein.

Hadley und York [13]) untersuchten mittels magnetischer Analyse die Isotopenhäufigkeiten der bei Zertrümmerung von C-, Cu- und Pb-Kernen durch 90 MeV-Neutronen gebildeten einfach geladenen Teilchen. Aus ihren Messungen läßt sich die Zahl der Tritonen auf etwa 1/10 der Deuteronenzahl schätzen. Leider überdeckt sich der von ihnen untersuchte Energiebereich nur zu einem kleinen Teil mit dem von uns untersuchten.

Unsere Hypothese findet eine weitere Bestätigung durch die kürzlich publizierten Daten von Currie u. a. [14]). Sie haben Ag mit 450 MeV-Protonen beschossen und radiochemisch das gebildete Tritium nachgewiesen. Die mittlere Zahl der pro Stern emittierten Tritonen beträgt 0.032.

b) Die Mittelwerte der zweiten Differenzen für die Deuteronen bilden eine Gauss-Verteilung um ihren theoretischen Mittelwert $\overline{D}_d = 0.370\,\mu$. Die Streuung dieser Verteilung läßt sich folgendermaßen bestimmen:

Die Grundgesamtheit aller zweiten Differenzen ist eine Normalverteilung um den Mittelwert 0 mit der Streuung σ^2. Für den Mittelwert der Beträge der zweiten Differenzen gilt die Beziehung

$$\overline{D}_m = \sqrt{\frac{2}{\pi}}\,\sigma.$$

Die Verteilung der Durchschnitte der Beträge der zweiten Differenzen $\overline{D}$ aus jeweils n Einzelmessungen ($n > 10$) ist eine normale um den Mittelwert $\overline{D}_m$ mit der Streuung (siehe [15]))

$$\sigma_{\overline{D}} = \sqrt{1-\frac{2}{\pi}}\,\frac{\sigma}{\sqrt{n}} = \frac{0.76}{\sqrt{n}}\,\overline{D}.$$

Analoges gilt für die unechte Streuung

$$\sigma_{\overline{D}_u} = \frac{0.76}{\sqrt{n}}\,\overline{D}_u.$$

Da $\overline{D}_e = \sqrt{(\overline{D}^2 - \overline{D}_u^{\,2})}$ ist, so erhält man nach dem Fehlerfortpflanzungsgesetz

$$\sigma_{\overline{D}_e} = \frac{0.76}{\sqrt{n}}\left(\frac{(\overline{D}_e^{\,2}+\overline{D}_u^{\,2})^2+\overline{D}_u^{\,4}}{\overline{D}_e^{\,2}}\right)^{\frac{1}{2}}. \tag{4}$$

Mit den bekannten Werten von $\overline{D}_e$ für Protonen und Deuteronen und $\overline{D}_u$ sowie dem gemessenen Wert von $\sigma_{\overline{D}_e} = 0.119\,\mu$ für Protonen läßt sich aus Gleichung (4) $\sigma_{\overline{D}_e}$ für Deuteronen bestimmen. Man erhält $\sigma_d = 0.088\,\mu$.

Mit diesen Werten läßt sich für ein vorgegebenes p : d-Verhältnis durch Überlagerung der beiden Normalverteilungen eine resultierende Verteilung gewinnen (Abb. 7). Die Güte der Anpassung dieser resultierenden Verteilung an die Meßwerte kann man mit dem χ^2-Test feststellen. In Tabelle VII sind die Ergebnisse für verschiedene Protonenhäufigkeiten angegeben.

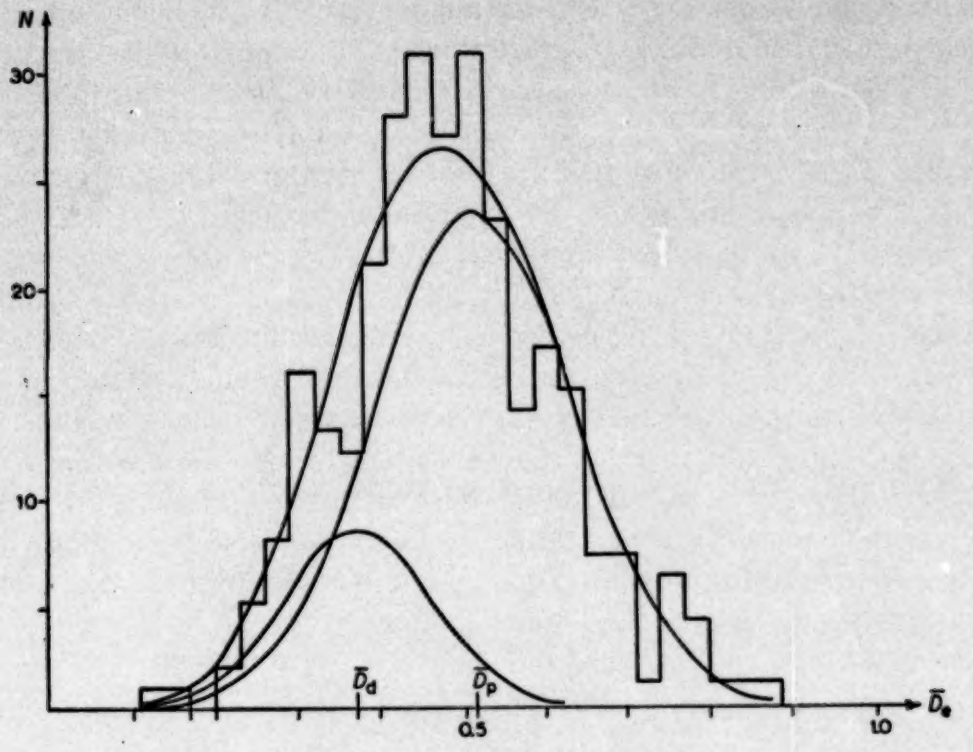

Abb. 7. Anpassung der gemessenen Häufigkeitsverteilung der $\bar{D}_e$-Werte durch Überlagerung zweier Gauss-Verteilungen.

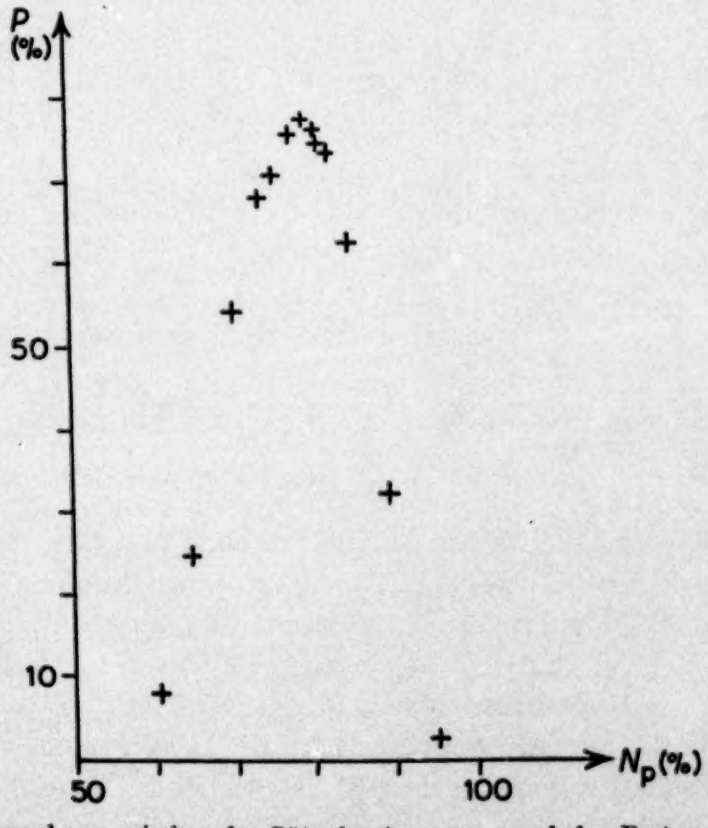

Abb. 8. Zusammenhang zwischen der Güte der Anpassung und der Protonenhäufigkeit N_p.

TABELLE VII

N_p[%]	95.3	89.9	84.8	82.1	81.0	80.1	79.1	77.4	75.0	73.6	69.9	64.8	60.1	55.1
P [%]	2.4	32.6	62.5	73.4	74.7	76.6	77.7	75.6	70.6	67.9	54.2	24.9	8.0	0.6

Die obere Reihe enthält die angenommenen Protonenhäufigkeiten. In der unteren Reihe ist die Wahrscheinlichkeit P dafür angegeben, daß die beobachtete Verteilung innerhalb der statistischen Schwankungen der theoretischen Verteilung liegt. Der Zusammenhang zwischen P und N_p ist in Abb. 8 dargestellt. Da er symmetrisch ist, läßt sich durch Mittelwertbildung als beste Anpassung an die gemessene Verteilung der $\overline{D}_e$ die Protonenhäufigkeit zu $N_p = 78.2\,\%$ bestimmen †.

Zur Untersuchung der Frage, ob für diesen N_p-Wert Spuren einer bestimmten Klasse verantwortlich sind, wurden die 293 Spuren in folgende Gruppen unterteilt:

1) 166 Spuren aus drei-, vier- und fünfarmigen Sternen,

2) 163 Spuren, deren Reichweiten im Intervall $500\,\mu \leqq R \leqq 2440\,\mu$ liegen,

3) 189 Spuren aus Sternen mit Rückstoßspur.

Führt man für jede dieser Gruppen eine Analyse analog der vorstehend beschriebenen durch, so erhält man die in Tabelle VIII zusammengefaßten Ergebnisse:

TABELLE VIII

Armzahl der Sterne	mittlere Sterngröße	σ_p [μ]	σ_d [μ]	P [%]	N_p [%]	$\overline{R}_p$ [μ]	$\overline{R}_d$ [μ]	P_p
1–5	2.8	0.119	0.088	<0.05	78.2	637	753	0.70 ± 0.03
3–5	3.6	0.113	0.084	≈ 0.5	80.0	655	667	0.79 ± 0.03
1–5	2.9	0.092	0.068	$\ll 0.05$	73.4	868	861	0.74 ± 0.03
1–5 m.r.	3.2	0.112	0.084	<0.05	74.3	646	694	0.71 ± 0.03

In Spalte 5 ist die Wahrscheinlichkeit dafür angegeben, daß die experimentelle Verteilung als zufällige Abweichung der theoretischen Verteilung auftreten kann, wenn man annimmt, daß alle Spuren nur durch Protonen hervorgerufen sind. In Spalte 6 gibt N_p die Protonenhäufigkeit an, bei der man die beste Anpassung an die experimentelle Verteilung gewinnt. Um daraus die wahre relative Häufigkeit P_p der Protonen bestimmen zu können, muß man

† Nach Abschluß der Arbeit wurde von Bebel [12]) als endgültiges Resultat der Eichmessungen $\overline{D}_p = 0.518\pm0.012\,\mu$ angegeben. Um den Einfluß dieses Fehlers zu untersuchen, haben wir die vorstehende Analyse auch für $\overline{D}_p = 0.506\,\mu$ bzw. $\overline{D}_p = 0.530\,\mu$ durchgeführt. Die Untersuchung der Nullhypothese — d. h. alle Spuren wurden durch Protonen hervorgerufen — ergab im ersten Fall $P < 0.5\,\%$ und im zweiten Fall $P \ll 0.05\,\%$. Die beste Anpassung erhielten wir für $N_p \approx 84\,\%$ bzw. $N_p \approx 75\,\%$.

die mittleren Reichweiten der Protonen und Deuteronen kennen. Nimmt man an, daß in jeder Gruppe die Teilchen mit $\overline{D}_e > 0.500\,\mu$ Protonen sind, so läßt sich eine mittlere Reichweite $\overline{R}_p$ berechnen. Entsprechend erhält man eine mittlere Reichweite $\overline{R}_{p,d}$ für die Teilchen mit $\overline{D}_e < 0.500\,\mu$. Da der Bruchteil der Protonen bzw. Deuteronen bekannt ist, kann man $\overline{R}_d$ für jede Gruppe bestimmen (Spalte 7 und 8). Unter Berücksichtigung der unterschiedlichen geometrischen Korrektionsfaktoren für die mittleren Reichweiten wurden die in der letzten Spalte angegebenen relativen Häufigkeiten der Protonen berechnet. Als Fehler ist die mittlere quadratische Abweichung angegeben.

Die relative Häufigkeit P_α der zweifach geladenen Teilchen aus den Zertrümmerungen schwerer Kerne wurde für die einzelnen Sterngruppen bestimmt.

Als obere Grenze für die α-Teilchen wählten wir $E_\alpha = 30$ MeV und für die einfach geladenen Teilchen $R = 2440\,\mu$. Zur Bestimmung von P_α sind die in der Emulsion endenden Spuren mit einem Neigungswinkel $\gamma \leqq 30°$ benutzt worden. Die Reichweite-Verteilung der einfach geladenen Teilchen bzw. die der α-Teilchen wurde nach Gleichung (1) und (2) geometrisch korrigiert.

Die so erhaltenen Ergebnisse sind in Tabelle IX zusammengefaßt. Als Fehler sind die mittleren quadratischen Abweichungen der relativen Häufigkeiten angegeben.

TABELLE IX

Armzahl der Sterne	P_α
2	0.22 ± 0.02
3	0.31 ± 0.03
4	0.31 ± 0.03
5	0.32 ± 0.05
2–5 m.r.	0.29 ± 0.02
2–5 o.r.	0.27 ± 0.03
2–5	0.28 ± 0.02

Diese Ergebnisse befinden sich in befriedigender Übereinstimmung mit den in letzter Zeit publizierten Werten. Hodgson [3]) beschoß Platten mit Protonen verschiedener Energie (45 bis 122 MeV) und bestimmte für ein- bis fünfarmige Sterne, die durch Zertrümmerung schwerer Kerne entstanden waren, P_α zu 0.22 ± 0.02. Er fand keine merkliche Variation von P_α mit der auslösenden Protonenenergie bzw. mit der Sterngröße. Grilli u.a.[10]) bestimmten ebenfalls P_α bei Zertrümmerung schwerer Kerne durch künstlich beschleunigte Protonen ($E = 50$ bis 450 MeV). Auch ihre Werte zeigen keine merkliche Variation mit der Energie der auslösenden Protonen und stimmen annähernd mit unseren Werten überein.

2.5. DIE WINKELVERTEILUNG DER SPUREN

Die Winkelverteilung der emittierten Teilchen ist ein weiterer experimenteller Test zur Untersuchung des Zertrümmerungsprozesses. Die nachfolgenden Ergebnisse beziehen sich nur auf die ein- bis fünfarmigen Sterne, die durch Zertrümmerung der schweren Kerne der Emulsion entstanden sind.

Die Projektion der Winkel auf die Emulsionsebene wurde mit einem Winkelmeßokular gemessen.

Im folgenden werden nachstehende Bezeichnungen benutzt:

β = Projektion des Winkels zwischen der Vertikalen und dem Arm,

β_r = Projektion des Winkels zwischen der Vertikalen und der Rückstoßspur,

$(\beta-\beta_r)$ = Projektion des Winkels zwischen dem Arm und der Rückstoßspur,

β_α = Projektion des Winkels zwischen 2 α-Teilchen,

β_p = Projektion des Winkels zwischen 2 einfach geladenen Teilchen,

$\beta_{\alpha,p}$ = Projektion des Winkels zwischen α-Teilchen und einfach geladenen Teilchen,

$$R = \frac{\text{Sterne mit } 90^\circ \leqq \beta_r \leqq 180^\circ}{\text{Sterne mit } 0^\circ \leqq \beta_r < 90^\circ},$$

$$C = \frac{\text{Arme mit } 90^\circ \leqq (\beta-\beta_r) \leqq 180^\circ}{\text{Arme mit } 0^\circ \leqq (\beta-\beta_r) < 90^\circ},$$

$$D = \frac{90^\circ \leqq \beta_{\alpha,p} \leqq 180^\circ}{0^\circ \leqq \beta_{\alpha,p} < 90^\circ},$$

$$E = \frac{90^\circ \leqq \beta_p \leqq 180^\circ}{0^\circ \leqq \beta_p < 90^\circ},$$

$$G = \frac{90^\circ \leqq \beta_\alpha \leqq 180^\circ}{0^\circ \leqq \beta_\alpha < 90^\circ},$$

F = die relative Häufigkeit der nach vorn emittierten Teilchen.

In Abb. 9a ist die gemessene β-Verteilung für alle endenden Spuren einfach geladener Teilchen gezeichnet, die eine Reichweite $\leqq 2440\,\mu$ besitzen und einen Winkel $\gamma \leqq 70^\circ$ mit der Emulsionsebene einschließen. Abb. 9b zeigt die β-Verteilung aller α-Teilchen mit einer Energie $\leqq 30$ MeV und einem Winkel $\gamma \leqq 70^\circ$.

TABELLE X

	α-Teilchen	Einfach geladene Teilchen
alle Sterne	0.56 ± 0.02	0.54 ± 0.02
Sterne m.r.	0.52 ± 0.03	0.53 ± 0.02
Sterne o.r.	0.63 ± 0.03	0.58 ± 0.03

In der Tabelle X sind die F-Werte für diese Arme angegeben.

Der angegebene Fehler ist hierbei und in den nachfolgenden Fällen die mittlere quadratische Abweichung der relativen Häufigkeit.

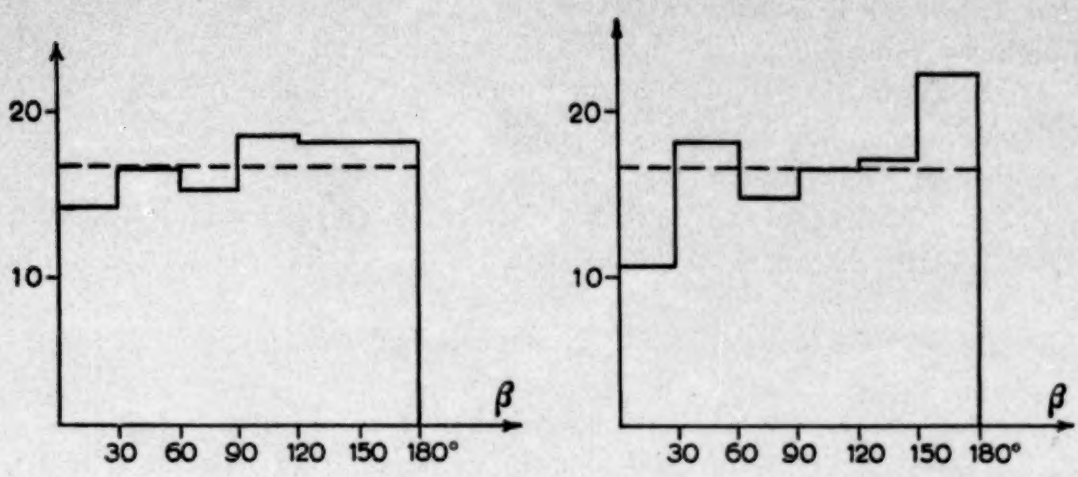

(A) einfach geladene Teilchen (841 Spuren) (B) α-Teilchen (478 Spuren)

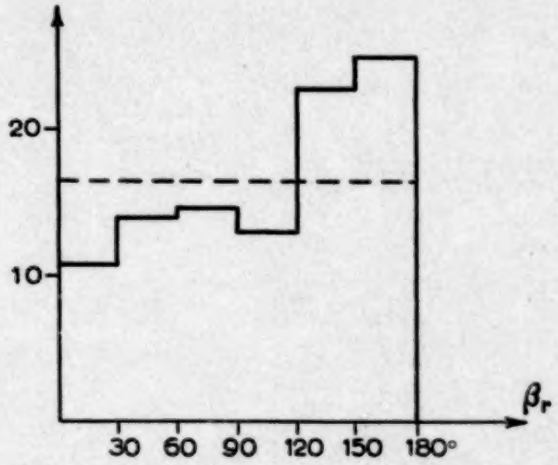

(C) Rückstoßspuren (703 Spuren)

Abb. 9. Winkelverteilung der emittierten Spuren

Ein direkter Vergleich unserer experimentellen Ergebnisse mit Werten aus Platten, die an Beschleunigungsmaschinen exponiert wurden, ist nicht möglich. Da der überwiegende Teil der von uns untersuchten Sterne durch Neutronen der kosmischen Strahlung ausgelöst worden ist, kann die Vertikale nur näherungsweise als die Vorzugsrichtung der sternauslösenden Strahlung betrachtet werden. Daher liegen unsere Werte unter den entsprechenden Daten für künstlich erzeugte Sterne.

Aus den experimentellen Ergebnissen erkennt man:

1) α-Teilchen und einfach geladene Teilchen des betrachteten Energie- bzw. Reichweiteintervalls haben eine anisotrope Winkelverteilung.

2) Die Anisotropie ist in beiden Fällen für Teilchen aus Sternen ohne Rückstoßspur ausgeprägter als für Teilchen aus Sternen mit Rückstoßspur.

Zur Untersuchung der Frage, ob sich diese Anisotropie vorwiegend auf Teilchen höherer Energie beschränkt, wurden die Arme jeweils in zwei Gruppen unterteilt und für jede dieser Gruppen die β-Verteilung ermittelt. Die so erhaltenen F-Werte sind in Tabelle XI angegeben.

TABELLE XI

	α-Teilchen		einfach geladene Teilchen	
	$E = 8-14$ MeV	$E = 14-30$ MeV	$R = 20-500\,\mu$	$R = 500-2440\,\mu$
F	0.55 ± 0.03	0.58 ± 0.03	0.53 ± 0.02	0.60 ± 0.04

Eine Restreichweite von 500 μ entspricht einer Protonenenergie von 9 MeV bzw. einer Deuteronenenergie von 12 MeV.

Aus den experimentellen Ergebnissen erkennt man:

1) Für α-Teilchen und einfach geladene Teilchen wächst die Anisotropie mit zunehmender Energie.

2) In beiden Fällen zeigen auch die Teilchen der gering energetischen Gruppen noch eine merkliche Anisotropie.

Die Untersuchung der Isotopenhäufigkeit der einfach geladenen Teilchen im Reichweiteintervall von 300 μ bis 2440 μ ergab, daß man die Spuren mit einer Streuung $\overline{D}_e > 0.500\,\mu$ als Protonen betrachten kann. Die Untersuchung der β-Verteilung für diese Protonenspuren führt zu einer relativen Häufigkeit der nach vorn emittierten Protonen von $F = 0.59\pm0.04$. Für die Teilchen mit $\overline{D}_e < 0.500\,\mu$ bestimmten wir die relative Häufigkeit zu $F = 0.57\pm 0.04$. Macht man die plausible Annahme, daß die Protonen mit $\overline{D}_e > 0.500\,\mu$ den gleichen F-Wert haben wie die Protonen mit $\overline{D}_e < 0.500\,\mu$ so läßt sich aus dem bekannten Häufigkeitsverhältnis der Protonen zu den Deuteronen der F-Wert für die Deuteronen zu $F = 0.54$ abschätzen.

Dieses Ergebnis zeigt, daß sowohl für die Deuteronen als auch für die Protonen eine Anisotropie vorhanden ist.

In Abb. 9c ist die β_r-Verteilung der Rückstoßspuren mit Reichweiten $< 6\,\mu$ und einem Neigungswinkel $\gamma \leqq 70°$ dargestellt. Aus diesen Daten wurde der R-Wert zu 1.55 ± 0.03 bestimmt. Auch dieser Wert läßt sich wegen der Unbestimmtheit der Richtung der sternauslösenden Neutronen nicht unmittelbar mit den Werten vergleichen, die an künstlich erzeugten Sternen erhalten wurden. An Sternen, die durch Teilchen der kosmischen Strahlung etwa der gleichen Energie erzeugt wurden, fanden Grilli und Vitale [16]) in guter Übereinstimmung mit uns einen Wert von $R = 1.6$.

Unterteilt man die Sterne nach ihrer Größe in zwei Gruppen und bestimmt

für jede dieser Gruppen den R-Wert, so erhält man die nachstehenden Resultate:

TABELLE XII

	ein- und zweiarmige Sterne	drei-, vier- und fünfarmige Sterne
R	1.35 ± 0.03	1.93 ± 0.04

Eine weitere Unterteilung der Rückstoßspuren nach ihrer Länge führt zu den folgenden R-Werten:

TABELLE XIII

Reichweite der Rückstoßspur	$0-1.9\,\mu$	$2.0-5.9\,\mu$
R	1.50 ± 0.04	1.61 ± 0.04

Aus den experimentellen Ergebnissen erkennt man:

1) Auch für die Rückstoßspuren besteht eine ausgeprägte Vorwärtsbündelung.

2) Diese Vorwärtsbündelung ist für die größeren der von uns untersuchten Sterne wesentlich ausgeprägter als für die kleineren.

3) Die Vorwärtsbündelung der längeren Rückstoßspuren ist kaum merklich ausgeprägter als die der kürzeren.

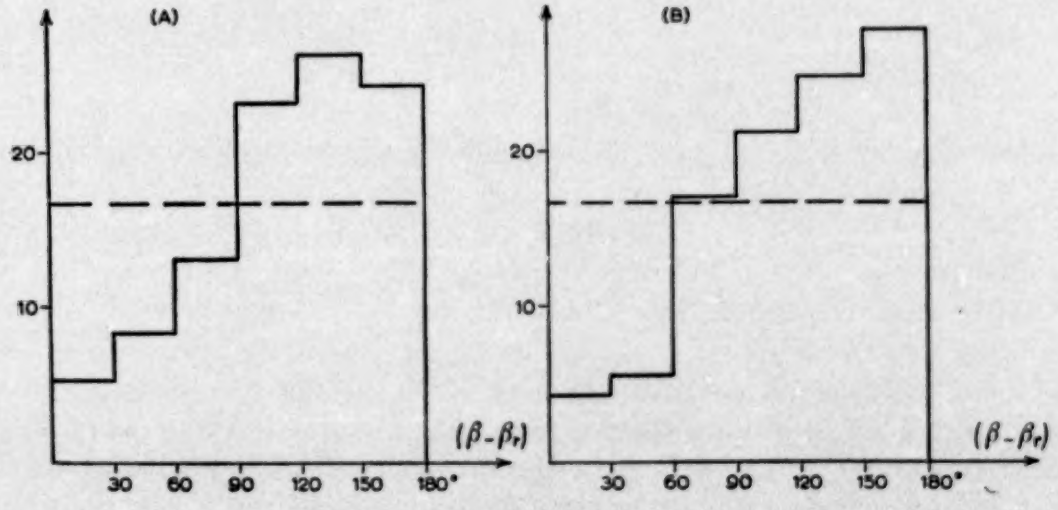

Abb. 10.

In den Abb. 10a und 10b sind die $(\beta-\beta_r)$-Verteilungen für einfach geladene Teilchen und für α-Teilchen des untersuchten Reichweite- bzw. Energieintervalle dargestellt. Die C-Werte sind in der nachfolgenden Tabelle angegeben:

TABELLE XIV

	α-Teilchen	einfach geladene Teilchen
ein- bis fünfarmige Sterne	2.78±0.04	2.77±0.03
ein- bis zweiarmige Sterne	3.31±0.06	3.10±0.03
drei- bis fünfarmige Sterne	2.57±0.04	2.43±0.04

Berücksichtigen wir die unterschiedlichen Längen der Rückstoßspuren, so erhalten wir folgende C-Werte:

TABELLE XV

	Länge der Rückstoßspuren	
	0—1.9 μ	2—5.9 μ
α-Teilchen	3.03±0.05	2.51±0.05
Einfach geladene Teilchen	2.68±0.04	2.72±0.04

Aus den experimentellen Ergebnissen erkennt man:

1) Zwischen Rückstoßspuren und α-Teilchen bzw. einfach geladenen Teilchen besteht eine ausgeprägte Winkelkorrelation.

2) Die C-Werte für α-Teilchen und einfach geladene Teilchen haben etwa die gleiche Größe.

3) Die Anisotropie ist für die kleineren Sterne wesentlich ausgeprägter als für die größeren.

4) Zwischen α-Teilchen und den kurzen wie auch den längeren Rückstoßspuren besteht eine ausgeprägte Anisotropie. Für die kurzen Rückstoßspuren ist sie etwas größer.

5) Zwischen den einfach geladenen Teilchen und den beiden Gruppen der Rückstoßspuren ist die Anisotropie etwa gleich groß.

Der von uns gemessene C-Wert für die α-Teilchen befindet sich in guter Übereinstimmung mit dem entsprechenden Wert von Grilli u. a. [10]).

Zur Beantwortung der Frage, ob zwischen den Armen, die von einem Stern ausgehen, eine Winkelkorrelation besteht, wurden Verteilungen der Winkel $\beta_{\alpha,p}$, β_p und β_α gemessen. Die Messungen beschränken sich auch wieder auf einfach geladene Teilchen mit $R \leqq 2440\,\mu$ und α-Teilchen mit $E_\alpha \leqq 30$ MeV ($\gamma \leqq 70°$). Die Resultate sind in den Abb. 11a bis 11c dargestellt. Daraus ergeben sich folgende Werte:

$$D = 0.96 \pm 0.04, \qquad E = 0.79 \pm 0.05, \qquad G = 1.56 \pm 0.06.$$

Der Unterschied zwischen diesen Werten der Sterne mit bzw. ohne Rückstoßspur lag innerhalb der mittleren quadratischen Abweichungen.

Aus den experimentellen Ergebnissen erkennt man:

1) Zwischen den α-Teilchen und den einfach geladenen Teilchen existiert offenbar keine Winkelkorrelation.

2) Die einfach geladenen Teilchen zeigen untereinander eine Bevorzugung kleiner Winkel.

3) Die α-Teilchen schließen anscheinend bevorzugt Winkel $> 90°$ miteinander ein.

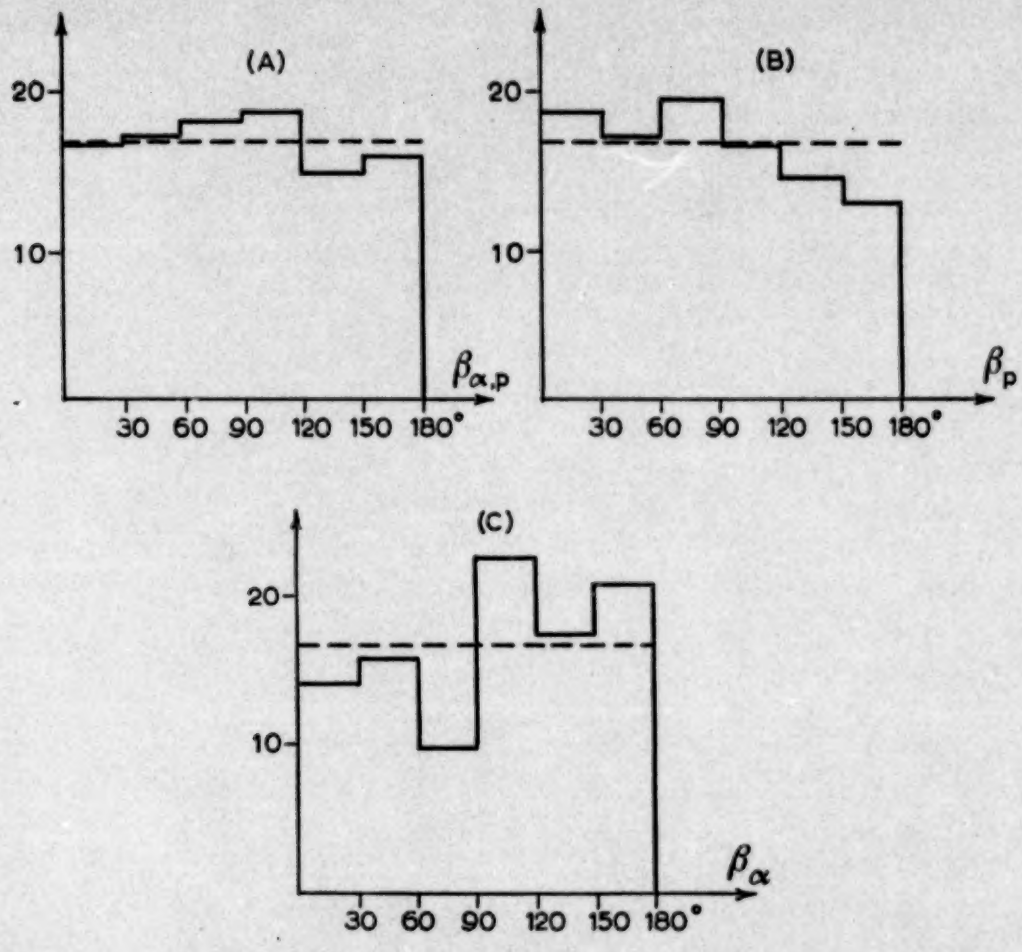

Abb. 11. Winkelkorrelationen zwischen
(A) α-Teilchen und einfach geladenen Teilchen (262 Winkel)
(B) den einfach geladenen Teilchen untereinander (238 Winkel)
(C) den α-Teilchen untereinander (115 Winkel).

Dieses letzte Ergebnis wurde durch Messungen an solchen Sternen gewonnen, bei denen mindestens zwei α-Spuren der geforderten Art vorhanden waren. Die in Abb. 9b dargestellte β-Verteilung aller α-Teilchen zeigte eine Vorwärtsbündelung der Spuren. Um festzustellen, ob diese Vorwärtsbündelung auch für die Gruppe der α-Spuren gilt, mit deren Hilfe die β_α-Verteilung gewonnen wurde, ist für diese Spuren die β-Verteilung nochmals gesondert untersucht worden. Als Ergebnis erhielten wir $F = 0.53 \pm 0.04$. Eine Bündelung der α-Teilchen deutet sich also auch hier an.

2.6. DIE ENERGIEVERTEILUNG DER EMITTIERTEN TEILCHEN.

Weitere den Zertrümmerungsprozeß charakterisierende Merkmale sind die Energieverteilungen der emittierten Teilchenarten. Sie sind nachstehend für die Zertrümmerungen der schweren Kerne mit einem bis fünf Armen angegeben. Alle Verteilungen beziehen sich auf endende Spuren, die einen Neigungswinkel $\gamma \leqq 30°$ mit der Emulsionsebene einschließen. Die Verteilungen wurden nach Gleichung (1) und (2) geometrisch korrigiert. Die

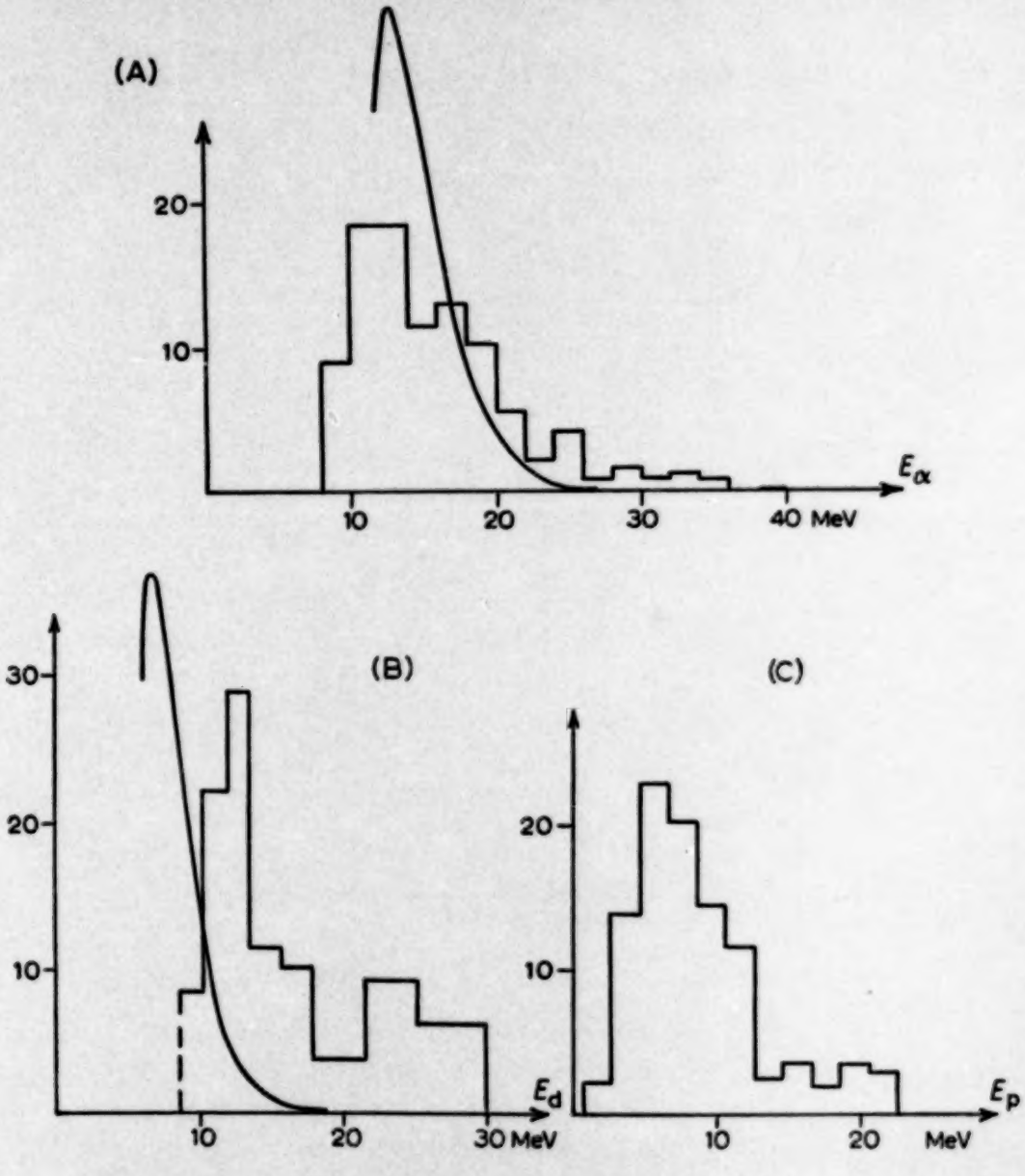

Abb. 12. Energieverteilungen der
(A) α-Teilchen (304 Spuren)
(B) Deuteronen (60 Spuren)
(C) Protonen (458 Spuren)
In die gemessene Verteilung ist die nach der Verdampfungstheorie berechnete Verteilung eingezeichnet.

Energie-Reichweite-Beziehungen wurden mit dem von Vigneron [17]) angegebenen Verfahren für die K2-Emulsion bestimmt [12]).

In Abb. 12a ist die Energieverteilung der α-Teilchen dargestellt.

Ausgehend von der bereits wiederholt gemachten Annahme, daß die einfach geladenen Teilchen mit einer Streuung $\overline{D}_e > 0.500\,\mu$ im Reichweiteintervall 300 bis 2440 μ Protonen sind, läßt sich eine Energieverteilung der

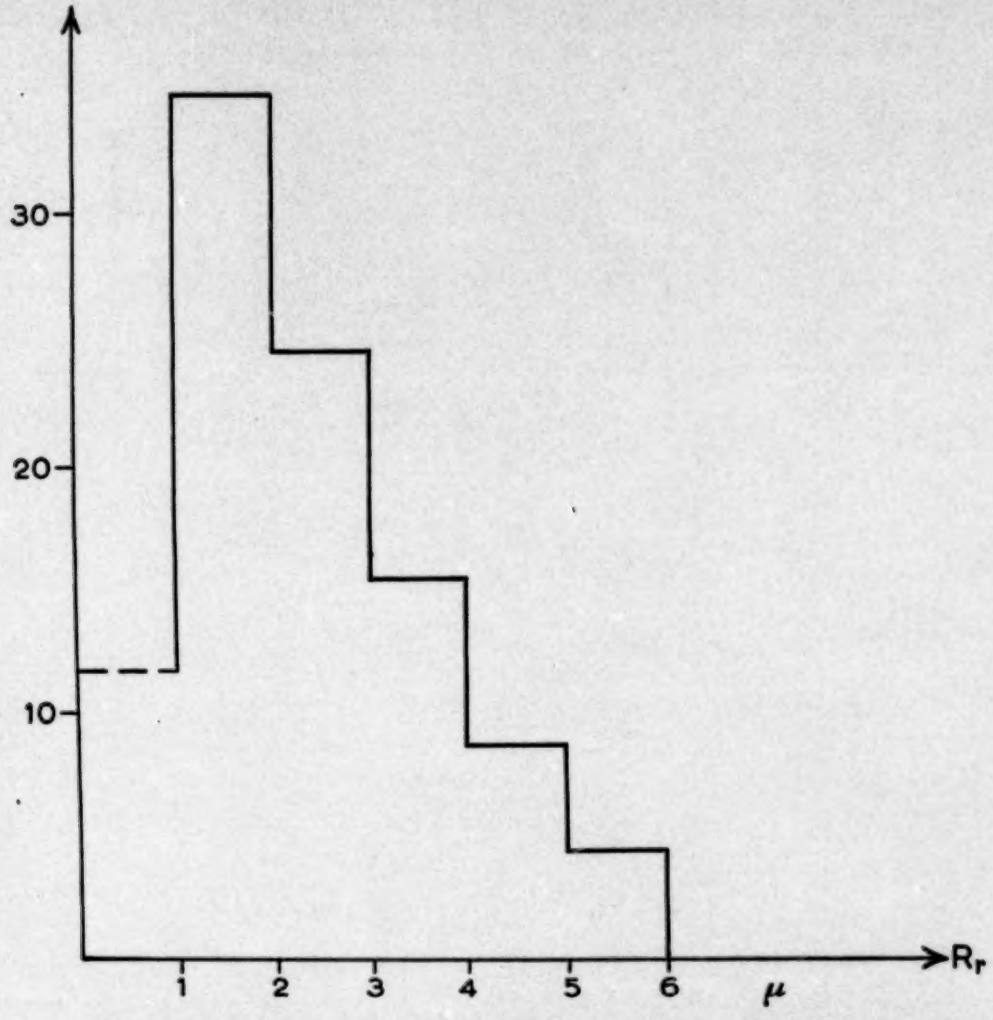

Abb. 13. Reichweite-Verteilung der Rückstoßspuren (692 Spuren)

Deuteronen gewinnen. Die einfach geladenen Teilchen mit $\overline{D}_e < 0.500\,\mu$ setzen sich in einem bekannten Verhältnis aus Protonen und Deuteronen zusammen. Macht man die sinnvolle Annahme, daß die Protonen dieser Gruppe die gleiche Reichweiteverteilung besitzen wie die Protonen mit $\overline{D}_e > 0.500\,\mu$, so erhält man durch Subtraktion nach einer entsprechenden Normierung die Reichweiteverteilung der Deuteronen. Mit Hilfe der Energie-Reichweite-Beziehung für die Deuteronen gewinnt man daraus die zugehörige Energieverteilung. Sie ist in Abb. 12b dargestellt. Aus ihrem Verlauf folgt, daß die Zahl der Deuteronen mit Energien < 8.8 MeV (das entspricht einer

Reichweite von 300 μ) vernachlässigbar klein gegenüber der Zahl der Protonen mit Reichweiten $< 300\,\mu$ ist. Alle einfach geladenen Teilchen mit einer Reichweite $< 300\,\mu$ wurden daher als Protonen betrachtet und mit ihrer Hilfe das in Abb. 12c dargestellte Protonenenergiespektrum gewonnen.

Das von uns gemessene Verhältnis der Zahl der Protonen zu der der Deuteronen läßt sich nur mit einem von Deutsch [18]) gemessenen Wert vergleichen. Der Autor beschoß Ag mit Protonen von 332 MeV und untersuchte mit einem magnetischen Analysator die Häufigkeit der emittierten Isotope. Für eine Energie von ≈ 9.5 MeV fand er ein Verhältnis d : p $\approx$ 1 : 12 der nach vorn emittierten Teilchen. Bei etwa der gleichen Energie (2 MeV Intervallbreite) erhalten wir d : p $\approx$ 1 : 11. Dieser Wert bezieht sich auf den gesamten Raumwinkel. Die Übereinstimmung ist unter Berücksichtigung der statistischen Schwankungen in beiden Fällen als befriedigend zu bezeichnen.

Tabelle XVI enthält die aus den von uns gemessenen Energieverteilungen sich ergebenden mittleren Energien für die verschiedenen Teilchenarten. Die obere Energiegrenze wurde in allen drei Verteilungen zu 30 MeV gewählt.

TABELLE XVI

Teilchenart	p	d	α
Energie [MeV]	10.0	15.2	15.3

In Abb. 13 ist die Reichweite-Verteilung der Rückstoßspuren gezeichnet. Es sei an dieser Stelle nochmals darauf hingewiesen, daß die Zahl der Rückstoßspuren mit Reichweiten $< 1\,\mu$ sehr unsicher ist, da derart kurze Spuren schwer zu identifizieren sind. Als mittlere Reichweite ergibt sich $R = 2.4\,\mu$.

3. Diskussion der Ergebnisse

Das Modell der Nukleonenkaskade ist bereits mehrfach zur Berechnung von Sternen unter Verwendung der sog. Monte-Carlo-Methode benutzt worden [19, 20, 21, 22]).

Bernardini und Mitarbeiter [20]) sowie Morrison und Mitarbeiter [21]) haben die Kaskadenrechnungen auch auf Nukleonen ausgedehnt, die nach Verlassen des Kerns kinetische Energien < 30 MeV haben. Obwohl für diese Teilchen die Voraussetzungen der Stoßnäherung nicht mehr voll erfüllt sind, sehen die Autoren die Berechtigung dieses Versuches in der von ihnen gefundenen Übereinstimmung mit dem Experiment. Sie konnten damit die Vorwärtsbündelung der Protonen mit Energien < 30 MeV in bezug auf die Richtung des sternauslösenden Nukleons und den Verlauf des Energiespektrums der Protonen befriedigend erklären.

In der nachfolgenden Tabelle sind einige Ergebnisse der Monte-Carlo-Methode für Sterne aus Ag und Br wiedergegeben.

TABELLE XVII

Primäres Nukleon	E [MeV]	U [MeV]	Mittlere Zahl der Kaskaden-Protonen pro Stern		Autor
			Alle Energien	< 30 MeV	
n, p	400	50	1.6	0.6 ± 0.1	[20]
p	140	44	1.3	0.5	[21]
n	90	42	0.4		[22]
p	90	42	0.6		
n	400	52	0.8		
p	400	52	1.87 ± 0.25		
n	700	50	1.5		
p	700	50	2.2		

Die schwache Veränderlichkeit der mittleren Anregungsenergie mit der Primärenergie deutet darauf hin, daß die betreffenden Autoren nur die elastische Nukleon-Nukleon-Streuung berücksichtigt haben. Bei einer Primärenergie von 700 MeV ist eine Vernachlässigung der Mesonenerzeugung offensichtlich nicht mehr zulässig. Bei 657 MeV verhält sich der Wirkungsquerschnitt für elastische p-p-Streuung zu dem für unelastische Streuung wie $1 : 0.8$ [23].

Wie in den vorhergehenden Abschnitten über die experimentellen Ergebnisse gezeigt wurde, sind die von uns untersuchten Sterne vorwiegend durch Neutronen mit einer Energie von ≈ 200 MeV ausgelöst. Wir schätzen daher die mittlere Zahl der Kaskaden-Protonen mit Energien < 30 MeV auf ≈ 0.3 pro Stern. Die Anregungsenergie der Restkerne schätzen wir im Mittel auf $U = 50$ MeV pro Stern. Dieser Wert ist eher zu hoch als zu niedrig angesetzt.

Die Verdampfungstheorie beschreibt das Verhalten eines angeregten Kerns mit thermodynamisch-statistischen Methoden. Sie erlaubt die Berechnung der Emissionswahrscheinlichkeit γ_x pro Zeiteinheit für Teilchen beliebiger Energie. Die Relativwahrscheinlichkeit, daß ein Teilchen x mit einer Energie zwischen ε und $\varepsilon + d\varepsilon$ emittiert wird, ergibt sich zu

$$\omega_x(\varepsilon)d\varepsilon = \frac{(\varepsilon - V'_x)}{T^2}\, d\varepsilon\, e^{-\frac{\varepsilon - V'_x}{T}} \qquad (5)$$

Dabei sind T die Temperatur und V'_x die effektive Potentialschwelle des angeregten Kerns.

Zur experimentellen Nachprüfung eignen sich gut die Emissionsverhältnisse der verschiedenen Teilchenarten. Diese lassen sich durch die bei einer bestimmten mittleren Temperatur gebildeten Verhältnisse der Emissionswahrscheinlichkeiten γ_x/γ_y ersetzen. Wir haben diese Verhältnisse für die

schweren Kerne der Agfa-K2-Emulsion berechnet. Es wurde eine mittlere Nukleonenzahl $A = 85$ zugrunde gelegt. In Abb. 14 sind diese Verhältnisse als Funktion der Temperatur dargestellt. Bei der Berechnung von $(\gamma_d+\gamma_t)/\gamma_p$ haben wir berücksichtigt, daß einem Reichweiteintervall von 300 bis 2440 μ unterschiedliche Energieintervalle für Protonen und Deuteronen entsprechen. Auf dieses Reichweiteintervall beschränkten sich unsere Messungen der Emissionswahrscheinlichkeiten der Protonen und Deuteronen.

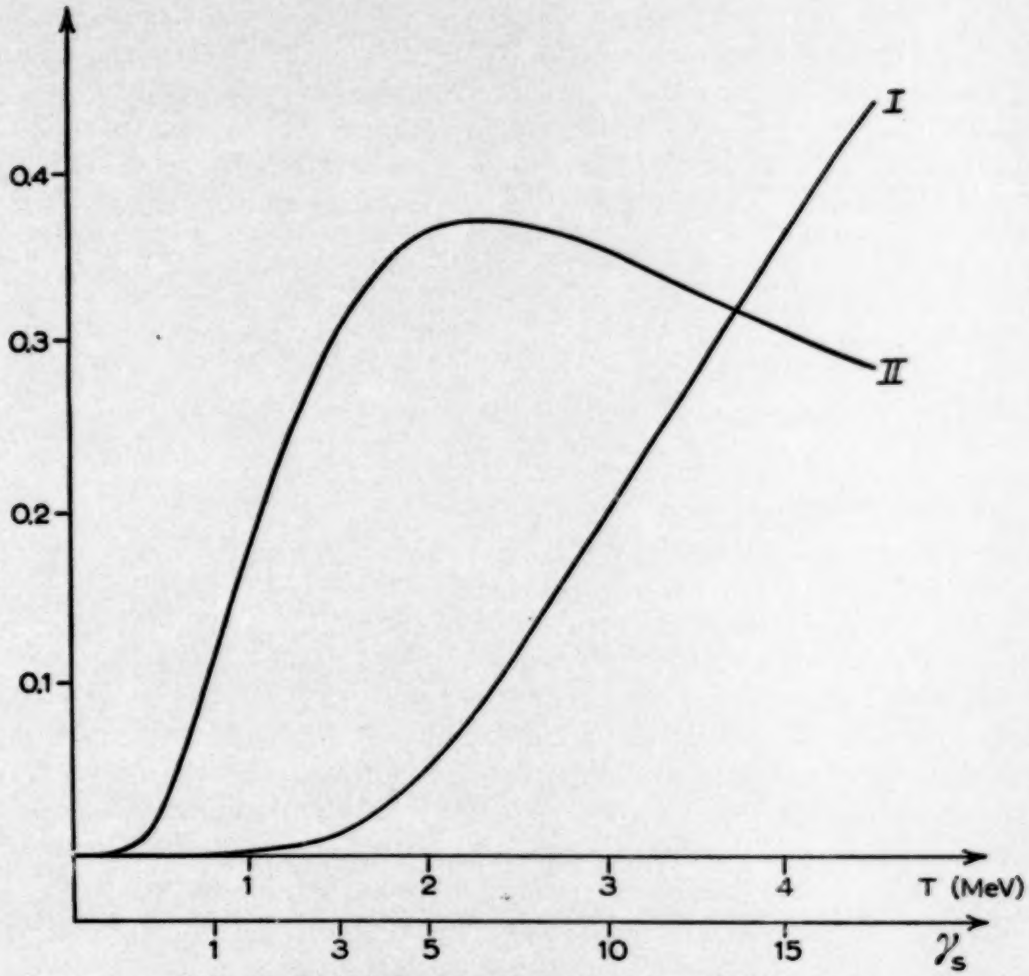

Abb. 14. Verhältnisse der Emissionswahrscheinlichkeiten.

I: $\frac{\gamma_d+\gamma_t}{\gamma_p}$ II: $\frac{\gamma_{He^3}+\gamma_{He^4}}{\gamma_p+\gamma_d+\gamma_t}$

Die Untersuchung der sukzessiven Verdampfung gestattet die Berechnung der Zahl ν_s der im Mittel pro Stern verdampften geladenen Teilchen als Funktion der Anfangstemperatur T_a und der mittleren Temperatur $\overline{T}$ bzw. der Anregungsenergie U des Kerns. In diese Berechnung geht das Emissionshältnis γ_n/γ_p ein. In der Darstellung der Verdampfungstheorie nach Hagedorn

und Macke [25]) wird für dieses Verhältnis für alle Temperaturen ein Mittelwert von etwa 1.5 angenommen, während Le Couteur [24]) die Variation von γ_n/γ_p mit der Temperatur berücksichtigt. Darin liegt die Ursache für den unterschiedlichen Verlauf von $\nu_s = f(\overline{T})$ bzw. $\nu_s = f(U)$ in den beiden Darstellungen. Unsere Berechnung ergab für eine Anregungsenergie von 50 MeV im ersten Fall $\nu_s = 1.5$ und im zweiten Fall $\nu_s < 0.5$. In Abb. 14 ist als zweite Abszisse ν_s eingetragen. Diese Werte wurden durch Anwendung des Verfahrens von Hagedorn und Macke gewonnen.

Unsere Berechnung mittels der Verdampfungstheorie ergab bei einer Anregungsenergie des Restkerns von 50 MeV die in Tabelle XVIII angegebenen Erwartungswerte der im Mittel pro Stern emittierten Teilchen.

Aus der mittleren Größe der untersuchten Sterne und den gemessenen relativen Häufigkeiten der verschiedenen emittierten Teilchenarten erhielten wir die in Tabelle XVIII angegebenen mittleren Spurenzahlen pro Stern.

Tabelle XVIII

	α(+He³)	d(+t)	p	
			Kaskade	Verdampfung
Theorie	0.25	0.01	0.3	1.25
Experiment	0.8±0.05	0.6±0.06	1.4±0.06	

Ein Vergleich dieser Werte zeigt, daß das theoretische Modell der Nukleonenkaskade mit anschließender Verdampfung nicht in der Lage ist, die beobachteten Häufigkeiten zu erklären. Die α-Häufigkeit und besonders die Häufigkeit der Deuteronen überschreitet die theoretischen Erwartungswerte um ein mehrfaches. Bei diesem Vergleich muß man berücksichtigen, daß wir bei der Verdampfungstheorie die Annahme von Hagedorn und Macke benutzt haben. Nach der Annahme von Le Couteur wird der Unterschied zwischen Theorie und Experiment noch größer. Da wir es nur mit einer relativ geringen Anregungsenergie zu tun haben, ist es sogar sehr wahrscheinlich, daß der von uns benutzte Wert von $\nu_s = 1.5$ zu groß gewählt ist.

Vergleichen wir nun unsere Messungen der Winkelverteilung und der Winkelkorrelation mit den Voraussagen der Theorie.

Für alle verdampften Teilchen müßten wir eine isotrope Winkelverteilung beobachten. Dieses Bild sollte sich nur für die Protonen ändern, zu denen der Anteil der Kaskadenteilchen hinzukommt. Man sollte also eine Vorwärtsbündelung in bezug auf die Vertikale, die näherungsweise die Richtung der sternauslösenden Nukleonen ist, erwarten. Ferner müßten die Protonen untereinander eine Bevorzugung kleiner Winkel zeigen, während für die anderen Arme keine Winkelkorrelationen auftreten sollten.

Eine Impulsübertragung auf den getroffenen schweren Kern kann bei einer

Primärenergie von etwa 200 MeV nicht zu einer beobachtbaren Anisotropie führen. Diese Aussage erhält man durch einfache Abschätzung der Schwerpunktsgeschwindigkeit im Vergleich zur Geschwindigkeit der emittierten Teilchen.

Ein Vergleich mit unseren experimentellen Ergebnissen zeigt, daß eine näherungsweise Übereinstimmung mit den theoretischen Voraussagen nur für die Protonen vorhanden ist. Die Vorwärtsbündelung der Deuteronen und der α-Teilchen sowie die Winkelkorrelation der α-Teilchen untereinander vermag die Theorie des Fermigasmodells nicht zu erklären.

Das theoretische Modell der Nukleonenkaskade mit anschließender Verdampfung wurde in einer ausführlichen Arbeit von Grilli und Vitale [16]) zur Analyse der Rückstoßspuren verwandt. Auf Grund dieser Arbeit lassen sich folgende Voraussagen über das Verhalten der Rückstoßspuren bzw. der Sterne mit und ohne Rückstoßspuren machen:

1) Bestimmenden Einfluß auf den Rückstoßkern hat der resultierende Impuls der Nukleonenkaskade. Nur einige der kürzesten Rückstoßspuren können durch den resultierenden Rückstoßimpuls der Verdampfungsteilchen hervorgerufen worden sein.

Die Winkelverteilung der Rückstoßspuren, bezogen auf die Vertikale, muß daher eine ausgeprägte Vorwärtsbündelung zeigen. Diese Vorwärtsbündelung muß für die längeren Rückstoßspuren wesentlich stärker sein.

2) Die Winkelverteilung der Protonen mit $E < 30$ MeV aus Sternen o.r. muß stärker anisotrop sein als die aus Sternen m.r.

3) Die Winkelverteilungen der α-Teilchen aus Sternen mit und ohne sichtbare Rückstoßspur müssen praktisch übereinstimmen.

4) Die $(\beta - \beta_r)$-Beziehung soll folgende Merkmale zeigen:

für α-Teilchen aus Sternen mit kurzer Rückstoßspur eine Bevorzugung großer Winkel;

für α-Teilchen aus Sternen mit längerer Rückstoßspur eine nahezu isotrope Verteilung;

für Protonen aus Sternen mit kurzer Rückstoßspur eine starke Bevorzugung großer Winkel;

für Protonen aus Sternen mit längerer Rückstoßspur eine schwächere Bevorzugung großer Winkel.

Vergleichen wir diese Voraussagen des Modells mit unseren experimentellen Ergebnissen:

Zu 1): Eine ausgeprägte Vorwärtsbündelung der Rückstoßspuren ist vorhanden. Eine Verstärkung der Vorwärtsbündelung für die längeren Rückstoßspuren konnte nicht festgestellt werden.

Zu 2): Diese Voraussage befindet sich in Übereinstimmung mit den Beobachtungen.

Zu 3): Die α-Teilchen zeigen nicht das geforderte Verhalten. Der Unter-

schied scheint sogar noch etwas ausgeprägter zu sein als für die einfach geladenen Teilchen.

Zu 4): Die experimentell gefundenen C-Werte für die α-Teilchen, aber auch für die einfach geladenen Teilchen, entsprechen nicht den Erwartungen des Modells. Bei den letzteren muß aber berücksichtigt werden, daß sich unsere Meßwerte auf Protonen + Deuteronen beziehen.

Vergleichen wir als letztes die beobachteten Energiespektren mit den theoretischen Voraussagen.

Der Verlauf der Energiespektren der Deuteronen und α-Teilchen müßte durch die Gleichung (5) beschrieben werden, da es sich um Verdampfungsteilchen handeln soll. Einer Anregungsenergie des Kerns $U = 50$ MeV entspricht nach der Verdampfungstheorie eine mittlere Temperatur $\overline{T} = 1$ MeV bzw. eine Anfangstemperatur $T_a = 2.5$ MeV. Zur Berechnung des Energiespektrums der α-Teilchen haben wir eine mittlere Temperatur von 2 MeV und zur Berechnung des Deuteronenspektrums eine Temperatur von 1.5 MeV gewählt. Für die effektive Potentialschwelle V'_x wurden für die α-Teilchen 11 MeV und für die Deuteronen 5.5 MeV eingesetzt. Die so gewonnenen Energiespektren sind in die Abb. 12 eingezeichnet. Es wurde kein Wert auf eine genaue Berechnung des Verlaufs des Spektrums in der Nähe der Potentialschwelle gelegt. Der Vergleich des gemessenen mit dem berechneten α-Energiespektrum zeigt einen Überschuß an α-Teilchen höherer Energie. Der experimentelle Verlauf ließe sich als Überlagerung zweier Anteile, eines Verdampfungsanteils und eines vorwiegend für die α-Teilchen höherer Energie verantworlichen Anteils, verstehen. Das Deuteronenspektrum dagegen kann nur zu einem kleinen Bruchteil durch Verdampfung verursacht worden sein.

Bei dem Vergleich von Theorie und Experiment muß man berücksichtigen, daß die zur Berechnung gewählten Temperaturen beide über der mittleren Temperatur von 1 MeV liegen. Hätten wir mit dieser Temperatur gerechnet, so wäre die Übereinstimming noch schlechter. Die Wahl höherer Werte der mittleren Temperatur läßt sich folgendermaßen begründen: Aus Abb. 14 geht hervor, daß sich das Emissionsverhältnis mit wachsender Sterngröße zugunsten der Emission schwererer Teilchen verschiebt, d.h., zu Beginn der Verdampfung ist der Prozentsatz der emittierten α-Teilchen und Deuteronen größer als am Ende.

Das Energiespektrum der Protonen läßt sich durch Überlagerung eines Verdampfungsanteils und eines Kaskadenanteils beschreiben.

Das Ergebnis unseres Vergleiches kann folgendermaßen zusammengefaßt werden:

1) Die Häufigkeit der emittierten Protonen, ihre Winkelverteilung, ihre Winkelbeziehungen untereinander und ihr Energiespektrum lassen sich näherungsweise durch die Theorie erklären.

2) Die Häufigkeit der emittierten α-Teilchen, ihre Winkelverteilung, ihre Winkelbeziehungen untereinander und ihr Energiespektrum sind nicht in Übereinstimmung mit den Voraussagen der Theorie.

3) Die Häufigkeit der emittierten Deuteronen, ihre Winkelverteilung und ihr Energiespektrum befinden sich ebenfalls nicht in Übereinstimmung mit den Voraussagen der Theorie.

4) Die Winkelbeziehungen zwischen Rückstoßspuren und Armen sind nur zum Teil in Übereinstimmung mit den Voraussagen des Modells.

Das theoretische Modell der Nukleonenkaskade mit anschließender Verdampfung aus dem angeregten Restkern ist also zum Verständnis der experimentellen Ergebnisse nicht ausreichend.

Zum Schluß wollen wir noch zwei Hypothesen auf ihre Eignung zur Beseitigung dieser Widersprüche diskutieren.

Zur Erklärung der Vorwärtsbündelung der α-Teilchen wurde von Grilli u. a. [10]) die Hypothese untersucht, daß ein Teil der α-Teilchen während des Kaskadenprozesses den Kern verläßt. Diese Annahme setzt die zeitweilige Existenz einer α-Unterstruktur im Kern voraus. Ihre mittlere Lebensdauer im Kern müßte mindestens von der gleichen Größenordnung sein wie die Zeit, in der ein Nukleon den Kern durchläuft, damit es zu elastischen Nukleon-α-Stößen und damit zur Emission direkt angestoßener α-Teilchen kommen kann.

Die von uns beobachtete Winkelkorrelation der α-Teilchen untereinander läßt sich mit dieser Annahme kaum erklären. Für die α-Teilchen sollte man — ähnlich wie für die Protonen — eine Bevorzugung kleiner Winkel untereinander erwarten.

Beim Beschuß von C- und Cu-Targets mit Neutronen einer Energie von 90 MeV fanden Hadley und York [13]) unter den Zertrümmerungsprodukten Deuteronen, die eine ausgeprägte Vorwärtsbündelung zeigten und deren Energiespektrum ein breites Maximum bei 50 bis 60 MeV hatte. Chew und Goldberger [26]) interpretierten diese Beobachtung als einen „Pick-up-Prozeß" der Neutronen beim Kerndurchgang. Ihre theoretische Analyse mit Hilfe der Bornschen Näherung gilt nur für Deuteronen, deren Energie oberhalb von $\approx$ 50 MeV liegt.

Man könnte eventuell die Entstehung der von uns beobachteten Deuteronen als ein pick-up von Nukleonen im Oberflächenbereich des Kerns durch Kaskadennukleonen deuten. Die Brauchbarkeit dieser Hypothese müßte jedoch durch eine theoretische Untersuchung geprüft werden.

Als Ergebnis der Arbeit läßt sich zusammenfassend feststellen, daß bei der Zertrümmerung schwerer Kerne durch Nukleonen mit einer Energie von einigen 100 MeV die direkten Prozesse im Kern offenbar eine wesentlich stärkere Rolle gegenüber den Compound-Prozessen spielen, als man bisher annahm.

Ick danke der Direktion des Institutes Miersdorf der Deutschen Akademie der Wissenschaften zu Berlin für ihr förderndes Interesse an der Arbeit und ihre Unterstützung bei deren Durchführung.

Ferner danke ich Frau I. Hauser und Herrn S. Schwabe für die Entwicklung der Platten und Herrn D. Bebel für seine Unterstützung bei der Durchführung der Streumessungen.

Vor allem möchte ich Frau S. Stösser, Fräulein K. Ragnick, Fräulein Ch. Wagner und den Herren P. Landrock, J. Langer und H. Engelhardt für ihre große Hilfe bei der Auswertung der Platten danken.

Literaturverzeichnis

1) P. Kofstadt, Report UCRL — 2265 (1953)
2) A. Kind und G. Patergnani, Nuovo Cimento **10** (1953) 1375
3) C. C. Dilworth, G. P. S. Occhialini und R. M. Payne, Nature **162** (1948) 102
4) D. H. Perkins, Proc. Roy. Soc. A **203** (1950) 399
5) P. E. Hodgson, Phil. Mag. **42** (1951) 207
6) S. O. Sörensen, Phil. Mag. **42** (1951) 188
7) D. H. Perkins, Phil. Mag. **40** (1949) 601
8) P. E. Hodgson, Phil. Mag. **43** (1952) 934
9) P. E. Hodgson, Phil. Mag. **45** (1954) 190
10) M. Grilli, B. Vitale, P. E. Hodgson und M. Ladu, Nuovo Cimento **1** (1955) 314
11) Nuovo Cimento Suppl. **1** (1954) 228
12) D. Bebel, Diplomarbeit 1956
13) J. Hadley und H. York, Phys. Rev. **80** (1950) 345
14) L. A. Currie, W. F. Libby und R. L. Wolfgang, Phys. Rev. **101** (1956) 1557
15) M. G. Kendall, The Advanced Theory of Statistics, Vol. 1 (1945) 215
16) M. Grilli und B. Vitale, Nuovo Cimento **10** (1953) 1047
17) L. Vigneron, J. Phys. Rad. **14** (1953) 145
18) M. Deutsch, Phys. Rev. **97** (1955) 1110
19) M. L. Goldberger, Phys. Rev. **74** (1948) 1269
20) G. Bernardini, E. T. Booth und S. J. Lindenbaum, Phys. Rev. **88** (1952) 1017
21) G. C. Morrison, H. Muirhead und N. G. V. Rosser, Phil. Mag. **44** (1953) 1326
22) H. Mc. Manus, W. T. Sharp und H. Gellman, Phys. Rev. **93** (1954) 924
23) M. G. Mesčerjakov, N. P. Bogačev und B. S. Neganov, Nuovo Cimento Suppl. **1** (1956) 119
24) K. J. Le Couteur, Proc. Phys. Soc. A **63** (1950) 259
25) R. Hagedorn und W. Macke in Heisenberg, Kosmische Strahlung (1953) 201
26) G. F. Chew und M. L. Goldberger, Phys. Rev. **77** (1950) 470

Nuclear Physics **3** (1957) 423—432; *North-Holland Publishing Co., Amsterdam*

THE PROBLEM OF AN EFFECTIVE MASS IN NUCLEAR MATTER

VICTOR F. WEISSKOPF

Department of Physics and Laboratory of Nuclear Science
Massachusetts Institute of Technology, Cambridge, Massachusetts

Received 26 January 1957

Abstract: It is shown that the existence of nuclear matter and the independent particle description of its properties implies by itself that the average potential energy is momentum dependent. If this momentum dependence is expressed in terms of an effective mass m^*, one gets $m/m^* = 3/2+(5/2)(P/T_f)$, where P is the packing fraction and T_f the Fermi kinetic energy. The Van Vleck calculation of the average potential energy in the independent particle model is discussed as an example. The photonuclear effect is discussed in terms of a velocity dependent potential.

1. Momentum Dependence of Average Potential

Two generalizations can be made from our present experimental knowledge of nuclear properties:

A. The concept of "nuclear matter." We believe that, if the Coulomb repulsion were removed, an arbitrarily large number of neutrons and protons would form a stable configuration having a particle density and energy density which are both independent of the number of particles involved. The inner part of all nuclei, except the lightest, are samples of such nuclear matter. Experimental evidence suggests that, for an equal number of protons and neutrons, the equilibrium density ϱ and the binding energy P per particle are given by

$$\begin{aligned} \varrho &= 1.72\times 10^{38} \text{ particles/cm}^3 \\ P &= 14 \text{ MeV}. \end{aligned} \tag{1}$$

The former number is the nuclear density at the center as measured by Hofstadter *et al.* [1]); the latter value is the volume term of the Weizsäcker semi-empirical mass formula.

B. The dynamical properties of nuclear matter can be described in fair approximation by an independent particle model. This means that the effect of the nuclear forces upon a given particle can be expressed in the form of a potential energy which is independent of the position of all other particles and depends only upon the coordinates of the particle itself. In the case of infinite nuclear matter, this potential energy would be constant in space (the depth of the potential well), and the resulting many-body wave function would be a product of plane waves duly anti-symmetrized

in order to fulfil the Pauli principle. The experimental evidence for this generalization comes mainly from the successes of the shell model and of the optical model of nuclear reactions.

It will be shown in this note that, as a consequence of the assumptions A and B, the potential energy of each particle must be a function of its momentum and that some properties of this function can be determined.

We consider a piece of nuclear matter containing A particles and assume A to be very large so that we can neglect surface effects. The particles are distributed over many levels α; each of them is characterized by a momentum p_α. The largest momentum, the Fermi momentum p_f, and its kinetic energy T_f are determined by the density ϱ. If neutrons and protons are equally numerous we get

$$p_f = \hbar(\tfrac{3}{2}\pi^2\varrho)^{1/3}, \qquad T_f = \frac{p_f^2}{2m} \tag{2}$$

where m is the mass of the nucleon.

A particle in the level α is under the influence of the forces from all other particles and this, we have assumed, can be expressed in terms of a potential U_α, which is negative and constant within nuclear matter. It is the negative well depth for a particle in the state α. The index α indicates the possibility that the potential energy might depend on the level α. We then get for the total energy of our system

$$E = \sum_\alpha T_\alpha + \tfrac{1}{2}\sum_\alpha U_\alpha, \qquad T_\alpha = \frac{p_\alpha^2}{2m}. \tag{3}$$

The factor $\frac{1}{2}$ in the second term comes about as follows: We assume that the nuclear interactions act between pairs; that is, we assume in the actual Hamiltonian of the system a potential energy of the form

$$V = \sum_{\text{pairs}} V(i, k)$$

where $V(i, k)$ depends on the coordinates of the ith and kth particle and the sum is extended over all pairs. The potential energy U_α of the particle in the state α is the effect of all interactions with the other particles. Hence, if no factor $\frac{1}{2}$ were present, the interaction between our particle in α and another one in β would be counted twice, once in U_α and then again in U_β.

From (3) we get an expression for the packing fraction:

$$P = -\overline{T_\alpha} - \tfrac{1}{2}\overline{U_\alpha} \tag{4}$$

where the bar signifies an average value over the occupied states α.

Next we determine the separation energy S, which is the energy necessary to remove a particle from our system and to leave the residual system in its lowest state. It will be the energy needed to remove a particle from the

highest level $\alpha = f$. (f symbolizes a level on top of the Fermi distribution.) Hence, we get

$$S = -(T_f + U_f). \tag{5}$$

In stating this equation the following point must be watched: When a particle is removed from the state f, the total system is left in a state R′ which, strictly speaking, is not the equilibrium state R of the residual system.† Hence, the energy difference $E(\mathrm{R}) - E(\mathrm{R}')$ (rearrangement energy) should have been added to S in (5). However, this difference is zero as seen in the following way: Where does any difference between R′ and R come from? The state R′ arises when a particle is removed from the level f and nothing else in changed. Hence, R′ occupies the same volume Ω as the original system. However, according to our premise A, the equilibrium state of the residual nucleus has the volume $((A-1)/A)\Omega$. This change of volume has no influence on the energy since a small change of volume away from the equilibrium volume does not change the energy of the system, the equilibrium condition being $(\partial E/\partial \Omega) = 0$. Furthermore, if the spatial distribution of each particle were not uniform (if its location were more-or-less defined within the nucleus), then the removal of a particle would have left a "hole" in the residual system, which would make R′ different from R. Our premise B, however, excludes†† such non-uniformity of position. Hence $E(\mathrm{R}) - E(\mathrm{R}') = 0$.

The disappearance of the rearrangement energy comes from the following cancellation: A small decrease of the volume actually raises all kinetic energies, but it also will decrease the potential energy because more particles get within the ranges of the forces. These two effects must cancel completely when the density is near equilibrium.

The separation energy S is closely connected to the packing fraction P. In fact, the two energies are equal in the limit of large particle numbers. This follows directly from the premise A: The removal of a number n of particles will require an energy $n \cdot S$ and the energy difference of the initial and the final system is equal to $n \cdot P$. Hence, $S = P$.

We now obtain the following relation from (4) and (5):

$$2P - S = S = T_f - 2\overline{T_\alpha} - \overline{U_\alpha} + U_f.$$

† Capital letters as R or R′ are used for the states of the total system, small letters as α or f used for the levels of the single particles.

†† The vanishing of the rearrangement energy is connected with our rather stringent assumption B. The independent particle approximation will deviate from the actual wave function, in particular, at those points in the configuration space where two or more particles are close together. The removal of one particle has an influence upon these deviations at those points at which the particle was close to its partners. This would give rise to a rearrangement energy $\Delta = E(\mathrm{R}') - E(\mathrm{R}) > 0$. If Δ is carried along, one obtains instead of (12): $U_f - \overline{U}_\alpha = \frac{1}{3}T_f + S - \Delta$ and therefore also a somewhat larger m^* than from (10).

The kinetic energy is known; T_f is given by (2), and it is easily shown that in a system of free Fermi particles at lowest energies $\overline{T_\alpha} = (3/5)T_f$. We then get

$$S = -\tfrac{1}{5}T_f - \overline{U_\alpha} + U_f. \tag{6}$$

This shows immediately that U_α must depend upon the state α. If it did not, S would be negative. Equation (5) gives a connection between the average value of U_α and the value U_f of U_α for the highest state. This is all that can with certainty be deduced from our premises A and B.

We now can make some special assumptions about the dependence of U_α on α. The simplest function would be a quadratic one:

$$U_\alpha = U_0 + \frac{p_\alpha^2}{p_f^2} U_1 \tag{7}$$

with two constants, U_0 and U_1. Such a dependence can be expressed in terms of an effective mass m^*:

$$\frac{p_\alpha^2}{2m} + U_\alpha = \frac{p_\alpha^2}{2m^*} + U_0, \qquad m^* = m(1+U_1/T_f)^{-1}. \tag{8}$$

If expression (8) is put into (6) and (5) we get

$$U_0 = -\tfrac{1}{2}(7P+3T_f), \qquad U_1 = -\tfrac{1}{2}(5P+T_f) \tag{9}$$

and

$$\frac{m}{m^*} = \frac{3}{2} + \frac{5}{2}\frac{P}{T_f}. \tag{10}$$

Although these relations should only serve as a first qualitative orientation it is, nevertheless, interesting to put in some numbers. Using the data as given in (1), we obtain from (2)

$$T_f = 38 \text{ MeV},$$

and get

$$U_0 = -106 \text{ MeV}, \qquad U_1 = -54 \text{ MeV}, \qquad \frac{m}{m^*} = 2.42. \tag{11}$$

It must be remembered that the introduction of an effective mass is based upon the doubtful assumption of a quadratic momentum dependence of U_α. The only relation which follows with certainty from our premises is eq. (6):

$$U_f - \overline{U_\alpha} = \tfrac{1}{5}T_f + S. \tag{12}$$

2. The Van Vleck Potential

A good illustration of a momentum dependent average potential is found in a classical paper by Van Vleck in which he calculates the average energies

of nucleons in a nucleus on the basis of the independent particle model. We quote some of these calculations. We consider a system of A particles of four different kinds: protons and neutrons of either spin. They are distributed over A single particle states $\alpha_1 \ldots \alpha_i \ldots \alpha_A$ with the single particle wave functions φ_{α_i}. The total wave function is then

$$\psi = \frac{1}{\sqrt{N_P}} \sum_P (-1)^P P\left(\prod_i \varphi_{\alpha_i}(\mathbf{r}_i)\right) \tag{13}$$

where Π is a product of all φ_{α_i}, P is a permutation among equal particles, N_P is the number of such permutations. We calculate the expectation value E of the energy operator H:

$$H = \sum_i T_i + \tfrac{1}{2} \sum_{i,k} V(\mathbf{r}_i, \mathbf{r}_k),$$

which contains only forces between pairs of particles. The forces are assumed to be spin independent. E can be written in the form

$$E = (\psi|H|\psi) = \sum_\alpha T_\alpha + \tfrac{1}{2} \sum_\alpha U_\alpha. \tag{14}$$

Here the sum is taken over all occupied states (if a state is occupied by two particles of unlike kind, it is counted as two different states in this consideration). T_α is the expectation value of the kinetic energy in the state α:

$$T_\alpha = \int \varphi_\alpha^*(\mathbf{r}_i) T_i \varphi_\alpha(\mathbf{r}_i) \mathrm{d}\mathbf{r}_i, \tag{15}$$

and U_α can be regarded as the average value of the potential energy in the state α. In order to express U_α, we assume that the potential energy $V(\mathbf{r}_1, \mathbf{r}_2)$ is partially an ordinary force and partially an exchange force of the same shape, with the relative strength a_{W} and a_{M}, respectively:

$$V(\mathbf{r}_1, \mathbf{r}_2) = (a_{\mathrm{W}} + a_{\mathrm{M}} X) J(\mathbf{r}_1, \mathbf{r}_2).$$

where X is the exchange operator. We then can express U_α in the form

$$U_\alpha = a_{\mathrm{W}} \sum_\beta (D_{\alpha\beta} - \delta_{\alpha\beta} E_{\alpha\beta}) + a_{\mathrm{M}} \sum_\beta (E_{\alpha\beta} - \delta_{\alpha\beta} D_{\alpha\beta}). \tag{16}$$

Here $E_{\alpha\beta}$ and $D_{\alpha\beta}$ are the following "exchange" and "direct" integrals:

$$\begin{aligned} D_{\alpha\beta} &= \int \varphi_\alpha^*(\mathbf{r}_1) \varphi_\beta^*(\mathbf{r}_2) J(\mathbf{r}_1, \mathbf{r}_2) \varphi_\alpha(\mathbf{r}_1) \varphi_\beta(\mathbf{r}_2) \mathrm{d}\mathbf{r}_1 \mathrm{d}\mathbf{r}_2, \\ E_{\alpha\beta} &= \int \varphi_\alpha^*(\mathbf{r}_1) \varphi_\beta^*(\mathbf{r}_2) J(\mathbf{r}_1, \mathbf{r}_2) \varphi_\alpha(\mathbf{r}_2) \varphi_\beta(\mathbf{r}_1) \mathrm{d}\mathbf{r}_1 \mathrm{d}\mathbf{r}_2, \end{aligned} \tag{17}$$

and †

$\delta_{\alpha\beta} = 1$ if α and β are occupied by particles of the same kind,

$\delta_{\alpha\beta} = 0$ if α and β are occupied by particles of different kinds.

† It is important to remember that we consider states occupied by two different particles as *different* states even if they look formally alike.

It is interesting to calculate these expressions for infinite nuclear matter. In this case, the average potential energy U_α would be equal to the actual potential energy as used in the previous section since no dependence on the position is possible. The wave functions φ_α are plane waves, and the integrals (17) are directly calculable. The direct term $D_{\alpha\beta}$ becomes a constant, and the exchange term $E_{\alpha\beta}$ depends upon the momentum difference between the two states:

$$\begin{aligned} D_{\alpha\beta} &= \Omega^{-1} J(0), \\ E_{\alpha\beta} &= \Omega^{-1} J(\mathbf{p}_\alpha - \mathbf{p}_\beta), \end{aligned} \tag{18}$$

where Ω is the volume of the nuclear matter which we consider and $J(\mathbf{p})$ is the Fourier component of $J(\mathbf{r})$ corresponding to the momentum $\mathbf{p}$.

Let us now assume that among the A particles in the volume Ω we have exactly $A/4$ of each type, and they occupy the lowest possible states. Then the $\delta_{\alpha\beta}$ are easily determined in each case and we get from (16) and (18):

$$U_\alpha = (4a_W - a_M)\frac{AJ(0)}{4\Omega} + (4a_M - a_W)\frac{1}{4\Omega}\sum_\beta J(\mathbf{p}_\alpha - \mathbf{p}_\beta) \tag{18}$$

where the sum in taken over all states † β:

$$\sum_\beta J(\mathbf{p}_\alpha - \mathbf{p}_\beta) = 4\Omega \int_0^{p_f} J(\mathbf{p}_\alpha - \mathbf{p}_\beta)\frac{p^2\,\mathrm{d}p}{(2\pi\hbar)^3} \tag{19}$$

and p_f is the Fermi momentum (1).

The momentum dependence of U_α appears in the second term of (18). Clearly this form does not give rise to a quadratic dependence on p_α since, for very high p_α, the Fourier component $J(\mathbf{p}_\alpha - \mathbf{p}_\beta)$ vanishes and U_α becomes

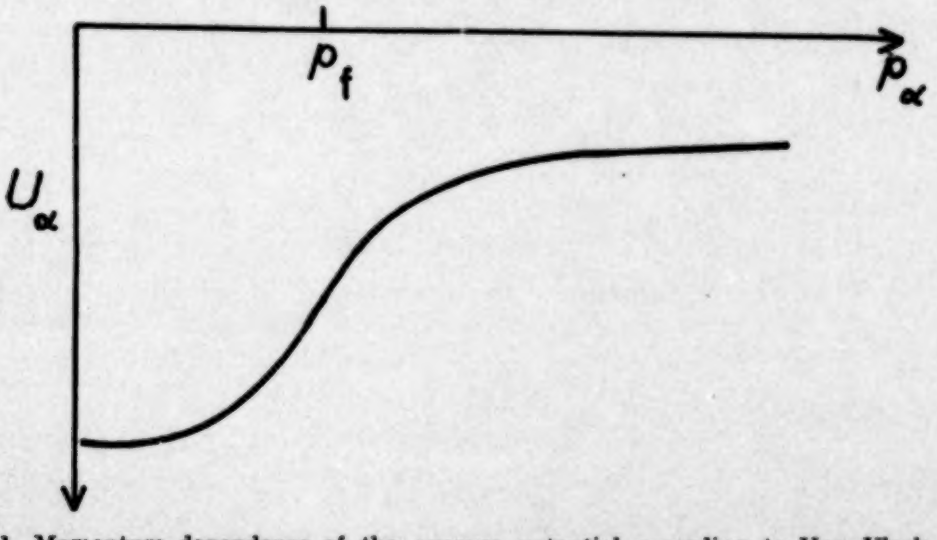

Fig. 1. Momentum dependence of the average potential according to Van Vleck, for a potential with a range equal to Fermi wave length and with $4a_W > a_M$.

† Again we note that we consider here each plane wave of given momentum p_α as being *four* states, one for each particle.

a constant. Only for low values of p_α ($p_\alpha \ll p_f$), U_α is parabolic in p_α. The shape of the p-dependence is qualitatively shown in fig. 1, for a $J(r)$ with a range of the same order as $\hbar/p_f$, and for $4a_W > a_M$. If the Wigner saturation conditions are fulfilled ($4a_W = a_M$), U_α goes to zero for $p_\alpha \to \infty$. There is a point of inflection near $p_\alpha = p_f$. It should be noted that there would be a momentum dependence of U_α also in the case of pure Wigner forces ($a_M = 0$). Of course, such forces would not give rise to the existence of stable nuclear matter.

These calculations are highly approximative and serve only to illustrate a mechanism which leads to a momentum dependent potential as decuded in the previous section. It is obvious that the wave function (13) cannot be a very good approximation when two particles are close to each other. These are just the regions of the configuration space which contribute importantly to the expectation value of the potential energy. Better methods for treating this problem have been devised recently by Brueckner [3]), Bethe and Goldstone [4, 5]) and others.

3. Excited States and Nuclear Photo-Effect

We now consider the excited states of a large nucleus described by a system of independent particles with momentum dependent potential energies. We are looking for a "model"-Hamiltonian, H_M, whose eigenstates are states made up of independent particles and whose eigenvalues are the approximate energy levels of the nucleus. We therefore write

$$H_M = \sum_i \left[\frac{p_i^2}{2m} + V(\mathbf{r}_i, \mathbf{p}_i)\right] \tag{20}$$

where $V(\mathbf{r}_i, \mathbf{p}_i)$ is a single particle potential which is given by

$$\begin{aligned} V(r, p) &= U_\alpha \qquad \text{for } r < R, \\ V(r, p) &= 0 \qquad \text{for } r > R. \end{aligned} \tag{21}$$

In the interior of the nucleus the potential for the momentum p is equal to the average value U_α in nuclear matter for a particle with a momentum $p = p_\alpha$, and it vanishes outside. We leave the potential undetermined in the immediate neighborhood of R, since we are not interested in surface effects.

A momentum and space-dependent potential is not necessarily a hermitian operator. In order to obtain a hermitian Hamiltonian one must symmetrize $V(r, p)$. This can be done in several ways, e.g. as follows. One expands $V(r, p)$ in powers of p^2 (only even powers will occur) and then writes

$$V(r, p) = \sum_{n=0}^{\infty} p^n a_n(r) p^n.$$

Another way of symmetrizing would be

$$V(r, p) = \tfrac{1}{2} \sum_{n=0}^{\infty} (p^{2n} a_n(r) + a_n(r) p^{2n}).$$

All problems deriving from this difficulty appear only in connection with surface effects and are therefore not considered here. The Hamiltonian (20) will give rise to stationary states in which A particles are distributed over single-particle levels as given by the Schroedinger equation

$$\left[\frac{p^2}{2m} + V(r, p)\right] \varphi_\alpha(r) = \varepsilon_\alpha \varphi_\alpha(r). \tag{22}$$

The wave function Ψ of the total nucleus is a solution of

$$H_M \Psi = E\Psi$$

and has the form (13) and an energy

$$E = \sum_\alpha \varepsilon_\alpha \tag{23}$$

where the sum is taken over the occupied states †.

Here we are running into a difficulty which is characteristic of this problem. The energy of a nucleus should be given by (14), which is different from (23). If we neglect the effects of the surface, we get

$$\varepsilon_\alpha = T_\alpha + U_\alpha \tag{24}$$

and, hence, (14) differs from (23) by $\frac{1}{2} \Sigma_\alpha U_\alpha$. It comes from the fact that the interaction between each pair has been counted twice in (20). One can correct approximately for this effect in the following way. Let us call ψ_0 the state of H_M with the lowest energy. We introduce the expectation value of the potential energy in that state:

$$V_0 = (\psi_0 | \sum_i V(r_i, p_i) | \psi_0).$$

Then we contend that the following Hamiltonian gives the correct approximation wave functions and eigenvalues for states of not too high excitations:

$$H_M = \sum_i \left(\frac{p_i^2}{2m} + V(r_i, p_i)\right) - \tfrac{1}{2} V_0. \tag{25}$$

The wave functions are the same as for H_M, but the energies differ †† by the constant $\frac{1}{2} V_0$. The reasons for the approximative validity of (25) are obvious: Each particle is under the influence of all other particles, and this influence is expressed by the potential energy $V(r_i, p_i)$. It moves in this

† See footnote on page 428.

†† One might think that the addition of a constant to the Hamiltonian (2) is not any significant change at all. However, it must be remembered that the Hamiltonian is already gauged by the assumption that the energy of A nucleons at rest and at large distances from each other is set to be zero.

potential and, therefore, can assume all the different stationary levels α given by (21). Hence, the excited states must have excitation energies, which are equal to the sum of the excitations of single particles, as it would follow from (25). However, the following effects are neglected in (25):

The potential $V(r, p)$ is calculated with the assumption that the rest be in the lowest possible energy states (Fermi distribution). Therefore, if more than one particle are in excited states (higher than their state in the Fermi distribution), the potential $V(r, p)$ is no longer correct. This error is small, however, as long as only very few particles are excited. Hence, (25) ought to be a correct approximative Hamiltonian for states in which one or a few particles are excited. If many particles are excited, one can no longer neglect the change in the potential $V(r, p)$, and the model Hamiltonian (25) becomes invalid.

The Hamiltonian (25) can be compared with experiments, in order to determine the actual momentum dependence of the potential. The most direct way would be to study the nuclear spectra and to find indications that the potential well depth is momentum dependent. Actually, if the dependence is given by (7) with an effective mass m^*, the distance between levels should be (m/m^*) times larger than calculated with the normal mass. The best known part of nuclear spectra are the low-lying spectra. Unfortunately, the low excitation energies are determined by energy differences within one shell and depend on the finer details of the well, like the shape of the boundary, the strength of the spin-orbit coupling, etc.; they cannot be used for the determination of the effective mass. The energy distance between different shells would be a more significant magnitude, but it cannot be deduced directly from nuclear spectroscopy.

The nuclear photoeffect with its characteristic "giant" resonance has been recently interpreted by Wilkinson [6]) as being mainly a transition from one shell to the next. If this interpretation is correct, it represents one of the most direct proofs of a momentum-dependent potential. All one has to do is to calculate the optical transitions from the ground state on the basis of the independent particle model and compare it with observed photonuclear absorption. This was done by D. Wilkinson [6]) and S. Rand [7]), and they found that the observed cross sections and their energy dependence can be fairly well reproduced with an effective mass $m^* \approx \frac{1}{2}m$.

It is perhaps useful to make this result understandable by the following qualitative analysis. We first assume that the nuclear well is an oscillator potential $U = \frac{1}{2}m\omega_0^2 r^2$. We adjust the frequency such that the radial extension R of the particle density is $R = r_0 A^{1/3}$, if $\frac{1}{4}A$ equal particles are filled into this potential well. This leads for $A \gg 1$ to the following relation:

$$\hbar\omega_0 = \frac{\hbar^2}{m r_0^2}\left(\tfrac{3}{2}\right)^{1/3}\tfrac{5}{4}A^{-1/3} = \frac{41}{A^{1/3}}\,\text{MeV}. \tag{26}$$

In this simplified model the dipole absorption is all concentrated into one frequency ω_0. If we improve our model by replacing the oscillator potential by the usual potential trough and by introducing the spin-orbit coupling, we expect that the monochromatic absorption will be broadened into a spectrum with a broad maximum near the frequency ω_0.

Hence one can understand that the independent particle model indeed gives rise to a giant resonance in the photonuclear absorption, and we expect (26) to hold for the frequency of the maximum. The relation (26) reproduces well the observed A dependence, but the observed factor is different. According to Fuller and Hayward [8]) the measured frequencies of the maxima in different nuclei can be fairly well represented by the formula $\hbar\,\omega_{\max} = 82/A^{-1/3}$ MeV. Obviously, a momentum dependent potential, e.g. in the form of an effective mass $m^* = \frac{1}{2}m$ would bring theory and experiment in better agreement, as seen from the mass dependence of (26).

References

1) R. Hofstadter, Revs. Mod. Phys. **28** (1956) 214
2) J. Van Vleck, Phys. Rev. **48** (1935) 367
3) K. Brueckner and C. Levinson, Phys. Rev. **97** (1955) 1344
4) H. A. Bethe, Phys. Rev. **103** (1956) 1353
5) H. A. Bethe and J. Goldstone, Proc. Roy. Soc. in preparation (1956)
6) D. Wilkinson, Proceedings of the 1954 Glasgow Conference (Pergamon Press, 1954) p. 161
7) S. Rand, Phys. Rev. (1956) to be published
8) F. Fuller and H. Hayward, Phys. Rev. **101** (1956) 692

Nuclear Physics **3** (1957) 433—435; *North-Holland Publishing Co., Amsterdam*

CONCERNING THE ELASTIC SCATTERING OF HIGH ENERGY PARTICLES

I. M. KHALATNIKOV

Institute for Physical Problems, USSR Academy of Sciences, Moscow

Received 9 January 1957

The problem of elastic scattering of particles whose energy appreciably exceeds the scattering potential $v(\mathbf{r}) = \hbar^2 V/2m$ has been extensively discussed in the literature [1]). In a recent paper by L. Schiff [2]) (cf. also ref. [3])) a new derivation of the formula for the scattering amplitude is presented which is valid under the conditions mentioned above. Although more complicated than the previous derivations Schiff's derivation has the advantage of displaying the necessary symmetry in the initial $\mathbf{k}_0$ and final momenta $\mathbf{k}_f$ of the particle in the intermediate as well as in the final stages of the calculation. Schiff performed the calculations separately for large and small scattering angles. However, the final formulae do not go over into each other. We would like to point out that this is actually due to an error in the derivation of the scattering amplitude formula for large angles.

We first consider (as was done in ref. [2])) the case of the Schroedinger equation; generalization to the Dirac equation encounters no difficulties.

Schiff started from the well known formula for the scattering amplitude in the form of a Born series:

$$f(\mathbf{k}_f, \mathbf{k}_0) = \sum_{n=1}^{\infty} \int \ldots \int \exp(-i\mathbf{k}_f \cdot \mathbf{r}_n) V(\mathbf{r}_n) G(\mathbf{r}_n - \mathbf{r}_{n-1}) V(\mathbf{r}_{n-1}) G(\mathbf{r}_{n-1} - \mathbf{r}_{n-2}) \\ V(\mathbf{r}_{n-2}) \ldots V(\mathbf{r}_2) G(\mathbf{r}_2 - \mathbf{r}_1) V(\mathbf{r}_1) \exp(i\mathbf{k}_0 \cdot \mathbf{r}_1) \mathrm{d}\tau_1 \ldots \mathrm{d}\tau_n, \tag{1}$$

G being the Green function of the operator $\nabla^2 + k^2$:

$$G(\boldsymbol{\rho}) = -(4\pi\varrho)^{-1} \exp(ik\varrho). \tag{2}$$

The next step was to use the stationary phase method for approximating at large k integrals of the type

$$I = \int \varrho^{-1} g(\boldsymbol{\rho}) \exp[i(k\varrho - \mathbf{k} \cdot \boldsymbol{\rho})] \mathrm{d}\tau \tag{3}$$

by integrals having the form

$$I = (2\pi i/k) \int_0^{\infty} g(\mathbf{n}\varrho) \mathrm{d}\varrho \tag{4}$$

($\mathbf{n}$ is the unit vector along $\mathbf{k}$). We introduce the variables $\boldsymbol{\rho}_1 = \mathbf{r}_2 - \mathbf{r}_1, \ldots$ $\boldsymbol{\rho}_{n-1} = \mathbf{r}_n - \mathbf{r}_{n-1}$ and represent the difference $-\mathbf{k}_f \cdot \mathbf{r}_n + \mathbf{k}_0 \cdot \mathbf{r}_1$ as

$$-\mathbf{k}_f\cdot\boldsymbol{\rho}_{n-1}-\mathbf{k}_f\cdot\boldsymbol{\rho}_{n-2}\ldots-\mathbf{k}_f\cdot\boldsymbol{\rho}_m+\mathbf{q}\cdot\mathbf{r}_m-\mathbf{k}_0\cdot\boldsymbol{\rho}_{m-1}\ldots-\mathbf{k}_0\cdot\boldsymbol{\rho}_2-\mathbf{k}_0\cdot\boldsymbol{\rho}_1,$$

where m can take any value between 1 and n.

By using (4), we obtain

$$f(\mathbf{k}_f,\mathbf{k}_0)=-(4\pi)^{-1}\sum_{n=1}^{\infty}(-i/2k)^{n-1}\int d\tau_m\int_0^\infty d\varrho_1\ldots\int_0^\infty d\varrho_{n-1}\exp(i\mathbf{q}\cdot\mathbf{r}_m)\cdot$$
$$V(\mathbf{r}_m+\mathbf{n}_f(\varrho_{n-1}+\ldots+\varrho_m))\ldots V(\mathbf{r}_m+\mathbf{n}_f\varrho_m)V(\mathbf{r}_m)V(\mathbf{r}_m-\mathbf{n}_0\varrho_{m-1})\ldots \quad (5)$$
$$V(\mathbf{r}_m-\mathbf{n}_0(\varrho_{m-1}+\ldots+\varrho_1)).$$

If we put here, e.g., $m=1$, we arrive, after simple integration and summation, at the well known expression for the scattering amplitude:

$$f(\mathbf{k}_f,\mathbf{k}_0)=\int d\tau\exp(i\mathbf{q}\cdot\mathbf{r})V(\mathbf{r})\exp\Big[(-i/2k)\int_0^\infty V(\mathbf{r}-\mathbf{n}_0 s)ds\Big]. \quad (6)$$

In eq. (5) L. Schiff, however, erroneously performed the summation over the values of m between 1 and n.

Thus Schiff's formula differs from (5) in that it contains $\sum_{n=1}^{\infty}\sum_{m=1}^{n}$, a double summation, instead of $\sum_{n=1}^{\infty}$ and the result is his erroneous formula (13).

Formula (6) has the disadvantage of being asymmetrical with respect to the momenta $\mathbf{k}_f$ and $\mathbf{k}_0$. In order to get a symmetrical expression we perform the summation over all values of m and divide the result by n, the number of equivalent terms, i.e., we replace $\sum_{n=1}^{\infty}$ in eq. (5) by a double sum $\sum_{n=1}^{\infty}n^{-1}\sum_{m=1}^{n}$. After a simple integration and summation we obtain the following symmetrical formula:

$$f(\mathbf{k}_f,\mathbf{k}_0)=(ik/2\pi)\int d\tau\exp(i\mathbf{q}\cdot\mathbf{r})V(\mathbf{r})$$
$$\frac{1-\exp\Big[(-i/2k)\Big(\int_0^\infty V(\mathbf{r}-\mathbf{n}_0 s)ds+\int_0^\infty V(\mathbf{r}+\mathbf{n}_f s)ds\Big)\Big]}{\int_0^\infty V(\mathbf{r}-\mathbf{n}_0 s)ds+\int_0^\infty V(\mathbf{r}+\mathbf{n}_f s)ds}. \quad (7)$$

It is evident that formulae (7) and (6) are equivalent within the approximation considered here. Formula (7) has the advantage of being symmetrical: $f(\mathbf{k}_f,\mathbf{k}_0)=f(-\mathbf{k}_0,-\mathbf{k}_f)$.

For small angles we can neglect q_z in $\exp(i\mathbf{q}\cdot\mathbf{r})$ and the integrals in eq. (7) are equal to $\int_0^\infty V(\mathbf{r}-\mathbf{n}_0 s)ds=\int_{-\infty}^{z}V(\mathbf{r})dz$, $\int_0^\infty V(\mathbf{r}+\mathbf{n}_f s)ds=\int_z^\infty V(\mathbf{r})dz$.

The well known formula for the case of small angles then follows from eq. (7):

$$f(\mathbf{k}_f,\mathbf{k}_0)=(ik/2\pi)\iint dx\,dy\exp(iq_x x+iq_y y)V(r)\Big[1-\exp(-i/2k)\int_{-\infty}^{\infty}V(\mathbf{r})dz\Big]. \quad (8)$$

L. Schiff has derived this formula independently and obtained the correct result.

In the case of the Dirac equation the scattering amplitude can be expressed in a simple way through the Schroedinger amplitude (7) [2]).

I wish to express my thanks to Professor L. D. Landau for valuable discussions.

References

1) L. Landau (unpublished); I. Gol'dman and A. Migdal, J. Exptl. Theor. Phys. USSR **28** (1954) 394
2) L. I. Schiff, Phys. Rev. **103** (1956) 443
3) Proceedings of the Sixth Annual Rochester Conference, April 1956

Nuclear Physics **3** (1957) 436—445; *North-Holland Publishing Co., Amsterdam*

CONSTRUCTION OF THE SCATTERING MATRIX OF A TWO-NUCLEON SYSTEM

L. PUZIKOV
USSR Academy of Sciences, Moscow
R. RYNDIN and J. SMORODINSKY
Joint Institute of Nuclear Research

Received 3 January 1957

Abstract: The problem of the number of experiments which are necessary for the determination of the elements of the elastic scattering matrix is discussed. It is shown that in virtue of the unitarity condition the required number of experiments equals the number of complex functions entering the scattering matrix. In the case of nucleon-nucleon scattering the elastic scattering matrix can be determined on basis of 5 experiments: measurement ot the cross section, polarization, normal component of the polarization correlation tensor and the normal components of the triple scattering tensor (for both particles). It is shown that experiments with rotation of polarization by the external magnetic field are not necessary for phase-shift analysis.

1. Introduction

At the present a large amount of experimental data on nucleon-nucleon scattering in a very broad energy region has been published †.

A number of papers have appeared which are devoted to phase analysis of the experimental results. However, it has invariably been found in these investigations that the phase-shift analysis is not unique and usually the authors give several sets of phase-shifts consistent with the experimental results. Phase-shift analysis in these works starts by restricting the number of states involved in scattering. The next step is to set up algebraic equations for a finite number of phases. However, for particles possessing a spin it remains unclear which experimental data should be used to write the equations. A good example is proton-proton scattering at not too high energies.

In this case two states — $^1S_0$ and $^3P_0$ — are predominant in the scattering. These states cannot be separated on the basis of cross section measurements or polarization measurements. On the other hand, they can easily be differentiated by measuring the polarization correlation. The necessity of more intricate experiments is apparent in this case. In other cases, when scattering is not isotropic and it may formally be possible to determine a finite number of phases, the question still remains whether the same phases are sufficient to describe more complex scattering phenomena, such as plural scattering.

In this connection it seemed important to attempt an analysis of all possible types of experiments and to find out which of them are independent in

† A good review of recent data has been written by Wolfenstein [1]). The authors take the opportunity to thank Prof. Wolfenstein for sending his manuscript prior to publication.

the sense that complete reconstruction of the scattering matrix would be possible if the results of these experiments were known. In order to illustrate the line of reasoning applied here we shall start with the two simplest cases, scattering of zero spin particles in a central force field and scattering of spin $\frac{1}{2}$ particles on zero spin nuclei. After this, scattering of nucleons by nucleons will be considered.

The case of arbitrary spin, which at present is only of theoretical interest, and photon scattering will be considered in further communications. We shall moreover restrict our attention to a scattering matrix for a given energy. Further investigation is required to clarify the problem of the energy dependence of the matrix elements.

2. Scattering of Spin Zero Particles

Measurement of the differential cross section of a zero spin particle yields a function $\sigma(\vartheta)$, which is the square of the modulus of the scattering amplitude

$$\sigma(\vartheta) = |f(\vartheta)|^2. \tag{2.1}$$

Evidently, if this quantity is measured at only one value of energy and angle ϑ the phase of the complex function $f(\vartheta)$ will remain completely indeterminate.

If, however, scattering is measured at all angles and is known to be elastic, the phase of $f(\vartheta)$ can also be determined. Indeed, the unitarity relation for the amplitude $f(\vartheta)$ can be written as follows [2]):

$$4\pi \operatorname{Im} f(\vartheta) = k \int \mathrm{d}\omega f^*(\vartheta'')f(\vartheta'). \tag{2.2}$$

Here ϑ' is the angle between $\mathbf{k}$ (initial wave vector) and the variable vector $\mathbf{k}''$ over the direction of which the integration $(\mathrm{d}\omega)$ is carried out; ϑ'' is the angle between the final wave vector $\mathbf{k}'$ and vector $\mathbf{k}''$. Denoting

$$f(\vartheta) = \sqrt{\sigma(\vartheta)}\, \exp\,[i\alpha(\vartheta)], \tag{2.3}$$

we obtain from (2.2), if $\sigma(\vartheta)$ is known, an integral equation for the function $\alpha(\vartheta)$:

$$4\pi \sin \alpha(\vartheta) = k \int \left[\frac{\sigma(\vartheta')\sigma(\vartheta'')}{\sigma(\vartheta)}\right]^{\frac{1}{2}} \cos\,[\alpha(\vartheta')-\alpha(\vartheta'')]\mathrm{d}\omega. \tag{2.4}$$

The solution of the set of equations (2.1) and (2.2) or equation (2.4) is an operation which is equivalent to phase-shift analysis. It is evident that representation of $f(\vartheta)$ in the form of a finite sum of Legendre polynomials is only one possible method of solving the problem which is useful when it is known that only a few phase-shifts are involved in the solution. In the general case straightforward solution of (2.4) may turn out to be a more convenient procedure.

It can be seen from (2.4) that the equation is invariant with respect to the substitution

$$f(\vartheta) \to -f^*(\vartheta) \tag{2.5}$$

or, what is the same,

$$\alpha(\vartheta) \to \pi - \alpha(\vartheta).$$

This transformation corresponds to change of the signs of all scattering phase shifts. Its existence signifies that there are two ways of reconstructing the scattering amplitude on the basis of its modulus. As is well known, this ambiguity can be removed by considering interference with Coulomb scattering (for charged particles) or by studying the energy dependence of scattering at low energies. Thus, measurement of the scattering cross section at a given energy is complete in the sense that it permits one to completely reconstruct the scattering amplitude (perhaps with the aforementioned two possibilities remaining).

3. Scattering of Particles of Spin $\frac{1}{2}$

The scattering amplitude of a particle of spin $\frac{1}{2}$ can be written, as usual, in the form

$$M = a(\vartheta) + b(\vartheta)\boldsymbol{\sigma} \cdot \mathbf{n} \tag{3.1}$$

where $\boldsymbol{\sigma}$ is the Pauli matrix and $\mathbf{n} = \mathbf{k}\times\mathbf{k}'/|\mathbf{k}\times\mathbf{k}'|$ is the normal to the scattering plane.

Experimentally, the cross section and polarization (double scattering) are measured, this yielding two functions

$$\begin{aligned} \sigma(\vartheta) &= |a|^2 + |b|^2 = \tfrac{1}{2}(|f_+|^2 + |f_-|^2), \\ \sigma(\vartheta)P(\vartheta) &= 2\,\mathrm{Re}\, ab^* = \tfrac{1}{2}(|f_+|^2 - |f_-|^2). \end{aligned} \tag{3.2}$$

Evidently, (3.2) defines two moduli †

$$\begin{aligned} |f_+|^2 &= |a+b|^2, \\ |f_-|^2 &= |a-b|^2. \end{aligned} \tag{3.3}$$

If the measurements are carried out at all possible angles and scattering is elastic the phase shifts of the complex functions f_+ and f_- will again be defined by the unitarity conditions

$$\begin{aligned} 4\pi\,\mathrm{Im}\, a(\vartheta) &= k\int d\omega \left[a^*(\vartheta'')a(\vartheta') + b^*(\vartheta'')b(\vartheta') \frac{\cos\vartheta - \cos\vartheta'\cos\vartheta''}{\sin\vartheta'\sin\vartheta''} \right], \\ 4\pi\,\mathrm{Re}\, b(\vartheta) &= k\int d\omega \left[2\,\mathrm{Im}\, a^*(\vartheta'')b(\vartheta') \frac{\cos\vartheta\cos\vartheta' - \cos\vartheta''}{\sin\vartheta\sin\vartheta'} \right. \\ &\left. + b^*(\vartheta'')b(\vartheta') \frac{1 + 2\cos\vartheta\cos\vartheta'\cos\vartheta'' - \cos^2\vartheta - \cos^2\vartheta' - \cos^2\vartheta''}{\sin\vartheta\sin\vartheta'\sin\vartheta''} \right]. \end{aligned} \tag{3.4}$$

† It should be noted that (3.3) are the scattering cross sections for polarized particles with spins directed "up" or "down" (with respect to $\mathbf{n}$).

Equations (3.2) and (3.4) are also amenable to an invariant transformation.

In order to find the latter, we note that the transformation (inversion of sign of the scattering phase shifts)

$$a(\vartheta) \to -a^*(\vartheta), \qquad b(\vartheta) \to b^*(\vartheta) \tag{3.5}$$

does not alter the cross sections or unitarity conditions, but reverses the sign of the polarization.

The same statement also applies to the Minami transformations [3, 4])

$$\begin{aligned} a(\vartheta) &\to a(\vartheta)\cos\vartheta + ib(\vartheta)\sin\vartheta \\ b(\vartheta) &\to -b(\vartheta)\cos\vartheta - ia(\vartheta)\sin\vartheta. \end{aligned} \tag{3.6}$$

Thus, the product of the two transformations

$$\begin{aligned} a(\vartheta) &\to -a^*(\vartheta)\cos\vartheta + ib^*(\vartheta)\sin\vartheta \\ b(\vartheta) &\to -b^*\cos\vartheta + ia^*(\vartheta)\sin\vartheta \end{aligned} \tag{3.7}$$

leaves all the quantities invariant †.

Therefore, in the case of particles of spin $\frac{1}{2}$ a complete experiment consists in measurement of the cross section and polarization. Ambiguity in phase shift determinations due to the presence of transformation (3.7) can be removed by studying the energy dependence of the cross section at low energies. It should be mentioned that (as previously noted by Wolfenstein [5])) the ambiguity can also be removed by studying triple scattering (in which the scattering planes are mutually perpendicular).

4. Scattering of Nucleons by Nucleons

Nucleon-nucleon scattering is described by the matrix

$$\begin{aligned} M = \alpha(\vartheta) &+ \beta(\vartheta)(\boldsymbol{\sigma}_1\cdot\mathbf{n})(\boldsymbol{\sigma}_2\cdot\mathbf{n}) + \gamma(\vartheta)(\boldsymbol{\sigma}_1+\boldsymbol{\sigma}_2)\cdot\mathbf{n} \\ &+ \delta(\vartheta)(\boldsymbol{\sigma}_1\cdot\mathbf{m})(\boldsymbol{\sigma}_2\cdot\mathbf{m}) + \varepsilon(\vartheta)(\boldsymbol{\sigma}_1\cdot\mathbf{l})(\boldsymbol{\sigma}_2\cdot\mathbf{l}). \end{aligned} \tag{4.1}$$

Here $\boldsymbol{\sigma}_1$ and $\boldsymbol{\sigma}_2$ are the Pauli matrices of the two particles and $\mathbf{m}$, $\mathbf{l}$, $\mathbf{n}$ are Cartesian unit vectors which are parallel to $\mathbf{k}-\mathbf{k}'$, $\mathbf{k}+\mathbf{k}'$, $\mathbf{k}\times\mathbf{k}'$ respectively (in the c.m.s.) [6]). That this system is a convenient one can be seen from the fact that its unit vectors will be parallel to the laboratory system wave vectors of the two particles after scattering and to the normal to the scattering plane.

Expression (4.1) differs from the general scattering matrix for two spin $\frac{1}{2}$ particles by the absence of a term which is proportional to $\boldsymbol{\sigma}_1-\boldsymbol{\sigma}_2$. This follows from identity of the particles of the p—p system and from charge invariance of the n—p system.

For identical particles the coefficients of matrix (4.1) possess the property

† In terms of the phase shifts $\delta(j, l)$ this transformation corresponds to

$$\delta(j, j-\tfrac{1}{2}) \rightleftarrows -\delta(j, j+\tfrac{1}{2}).$$

of symmetry with respect to the substitution $\vartheta \to \pi - \vartheta$. This can be conveniently formulated by introducing new functions which will also be useful in the future [7]):

$$\begin{gathered} a = \alpha+\beta, \quad b = \alpha-\beta, \quad c = \delta+\varepsilon, \\ d = \delta-\varepsilon, \quad e = 2\gamma. \end{gathered} \tag{4.2}$$

It can then be shown that for identical particles

$$\begin{gathered} a(\pi-\vartheta) = -a(\vartheta), \quad b(\pi-\vartheta) = -c(\vartheta), \\ c(\pi-\vartheta) = -b(\vartheta), \quad d(\pi-\vartheta) = d(\vartheta), \\ e(\pi-\vartheta) = e(\vartheta). \end{gathered} \tag{4.3}$$

Thus for identical particles the measurements may be carried out only for angles $0 \longleftrightarrow \frac{1}{2}\pi$. In the case of scattering of neutrons by protons the measurement range should be doubled to $0 \longleftrightarrow \pi$, which exactly corresponds to the doubling of the number of states in this system.

Before using the unitarity condition we shall briefly describe the experiments required for a two-nucleon system.

Suppose we are dealing with an unpolarized nucleon beam; the first scattering on hydrogen will define a differential cross section which is connected with the scattering matrix elements by the formula †

$$\sigma(\vartheta) = \tfrac{1}{2}(|a|^2+|b|^2+|c|^2+|d|^2+|e|^2). \tag{4.4}$$

The first scattering produces a beam polarized along $\mathbf{n}$. The magnitude of this polarization is measured on the second scattering:

$$\sigma(\vartheta)P(\vartheta) = \mathrm{Re}\, ae^*. \tag{4.5}$$

Evidently any target with known properties (polarizer) can be used for measuring or for producing the polarization. (In all experiments only one target need be a hydrogen one.)

The polarization of recoil particles is also equal to $P(\vartheta)$ (absence of $\boldsymbol{\sigma}_1-\boldsymbol{\sigma}_2$ in M) and hence need not be measured.

The third target may be added in two ways.

Measurement of the component P_{nn} of the correlation tensor yields

$$\sigma(\vartheta)P_{nn}(\vartheta) = \tfrac{1}{2}(|a|^2-|b|^2-|c|^2+|d|^2+|e|^2). \tag{4.6}$$

In these measurements all three scattering events occur in a single plane. Moreover, the polarization after the second scattering on the hydrogen target can be measured. By using a third target to measure it (any analyser can be used for this) we obtain two quantities corresponding to the two particles participating in the second scattering ††. If all three arrangements

† The formulae of this section are familiar ones.

†† Since the incident particle in this scattering was polarized, the polarization of the two particles after scattering will now be different.

of scattering events occur in a single plane, the measured quantities will be

$$\sigma(\vartheta)D_{nn}(\vartheta) = \tfrac{1}{2}(|a|^2+|b|^2-|c|^2-|d|^2+|e|^2) \quad (4.7)$$

(for the scattered particle),

$$\sigma(\vartheta)K_{n\,n}(\vartheta) = \tfrac{1}{2}(|a|^2-|b|^2+|c|^2-|d|^2+|e|^2) \quad (4.8)$$

(for the recoil particle).

The difference between these two quantities is obvious in the case of neutron scattering: for identical particles the first quantity corresponds to measurement in the angular interval $0 \longleftrightarrow \frac{1}{2}\pi$ and the second in the interval $\frac{1}{2}\pi \longleftrightarrow \pi$.

The aforementinoed experiments yield five equations from which the moduli of the five functions $a+e$, $a-e$, b, c, d can easily be determined and we have to apply considerations similar to the case of spin $\frac{1}{2}$ particles.
In order to determine the phases of these complex functions measured at the various angles one appeals to the unitarity relation. It can be shown (see ref. [8])) that exactly five such relations exist. These relations (see appendix 2) are invariant with respect to the substitution $\alpha(\vartheta) \to -\alpha^*(\vartheta)$, $(\beta\vartheta) \to -\beta^*(\vartheta)$, $\gamma(\vartheta) \to \gamma^*(\vartheta)$, $\delta(\vartheta) \to -\delta^*(\vartheta)$, $\varepsilon(\vartheta) \to -\varepsilon^*(\vartheta)$, which is equivalent to simultaneous reversal of the signs of all phase shifts (as in the preceding case this substitution changes the polarization sign); in the case of nucleon-nucleon scattering no substitution corresponding to the Minami transformation exists [9]). This signifies that the set of experiments indicated above is a complete set.

An important feature of the preceding considerations is the conclusion that in order to determine the scattering matrix measurement of fourfold scattering or application of a magnetic field are not necessary and it should suffice to perform experiments with three targets and with parallel scattering planes.

Up to the present no such complete set of experiments has been performed for any single energy value and this is the reason of the ambiguity encountered in analyzing these experiments.

In connection with the problem of determining the scattering matrix, the question arises as to its connection with the potential. A salient feature is that the number of independent functions in the scattering amplitude is equal to the number of scalar functions in the interaction hamiltonian. Indeed, it is not difficult to show that the general form of interaction of (say) two protons is

$$V = V_1(r)+V_2(r)(\boldsymbol{\sigma}_1\cdot\boldsymbol{\sigma}_2)+V_3(r)(\boldsymbol{\sigma}_1\cdot\mathbf{r})(\boldsymbol{\sigma}_2\cdot\mathbf{r})$$
$$+V_4(r)(\boldsymbol{\sigma}_1+\boldsymbol{\sigma}_2)\cdot\mathbf{L}+V_5(r)(\boldsymbol{\sigma}_1\cdot\mathbf{L})(\boldsymbol{\sigma}_2\cdot\mathbf{L})$$

where $\mathbf{L}$ is the orbital angular momentum. It would be very interesting to ascertain what restrictions are imposed on the scattering matrix if one or several $V_i(r)$ are zero. In other words, one is interested to ascertain whether

any qualitative conclusions regarding the form of V can be made on basis of the scattering matrix properties.

In conclusion the authors wish to thank Prof. E. Segre and Prof. O. Chamberlain for numerous interesting and enlightning discussion of nucleon scattering experiments, carried out in the summer of 1956.

Appendix 1

LIST OF FORMULAE FOR POSSIBLE NUCLEON-NUCLEON SCATTERING EXPERIMENTS

As the set of experiments (five in all) mentioned above for determination of the nucleon-nucleon scattering matrix is not the only possible one we shall present here a short survey of all conceivable experiments. The latter may differ from each other first of all with respect to the state of polarization of the primary beam and target and, secondly, in the nature of the measured quantities (cross section, polarization of scattered particle, polarization of recoil particle, correlation of polarization). Schematically, they may be represented by the following table:

Initial spin state / Result of experiment	A. Unpolarized beam, unpolarized target	B. Polarized beam, unpolarized target	C. Unpolarized beam, polarized target	D. Polarized beam, polarized target
1. Cross section	σ *	$\sigma_i^{(1)}$	$\sigma_k^{(2)}$	σ_{ik}
2. Polarization of scattered particle	$P_p^{(1)}$ *	$D_{ip}^{(1)}$ *	K'_{kp}	$T_{ikp}^{(1)}$
3. Polarization of recoil particle	$P_q^{(2)}$	K_{iq} *	$D_{kq}^{(2)}$	$T_{ikq}^{(2)}$
4. Correlation of polarizations	P_{pq} *	P_{ipq} *	$P_{kpq}^{(2)}$	T_{ikpq} *

Here each column corresponds to a certain initial spin state of the two-nucleon system and the scattering process characteristics to be measured are given in the horizontal rows. Subscript i indicates the direction of initial polarization of the projectile, k refers to the initial target polarization, p refers to the measured component of the scattered particle polarization and q the measured component of the recoil particle polarization. In the future we shall denote each experiment by a letter (column) and number (row) which will indicate the initial spin state of the system and the measured characteristic of the scattering process. Experiment B2, for example, consists in the measurement of a set of quantities $D_{ip}^{(1)}$ which determine the influence of

the i-polarization component of the incident particles on the p-polarization component of the scattered particles, etc.

Not all experiments in the table are different. Due to the symmetry property some of them are actually identical. Thus, in the absence of singlet-triplet transitions (absence of term $\boldsymbol{\sigma}_1-\boldsymbol{\sigma}_2$) experiments A2 and A3, B1 and C1, B4 and C4, D2 and D3, B2 and C3 are essentially the same. In the case of identical particles (see symmetry properties (4.3)), experiments B2 and B3 yield the same quantities (B2) but for complementary angles (ϑ and $\pi-\vartheta$). A similar relation exists between experiments C3 and C2.

In virtue of the invariance of matrix M with respect to reversal of time, the sets of experiments in those table cells which are symmetrical with respect to the main diagonal are equivalent (equivalency of experiments A2 and B1, A4 and D1, etc.). Thus the only experiments which are different are those denoted by the asterisk in the table. It can immediately be seen that a polarized target is required only in the most complicated experiment. However, for actual determination of the scattering matrix these experiments are also superfluous.

Consider now the different characteristics determined in the various experiments.

A1. Measurement of cross section

$$\sigma = \tfrac{1}{4}\,\mathrm{tr}\,(MM^+) = \tfrac{1}{2}\{|a|^2+|b|^2+|c|^2+|d|^2+|e|^2\}.$$

A2. Measurement of polarization

$$\sigma P = \tfrac{1}{4}\,\mathrm{tr}\,(\boldsymbol{\sigma}_1\cdot\mathbf{n}MM^+) = \mathrm{Re}\,ae^*.$$

B2. Determination of the tensor

$$\sigma D_{ip} = \tfrac{1}{4}\,\mathrm{tr}\,(M\sigma_{1i}M^+\sigma_{1p}) = \tfrac{1}{2}\{|a|^2+|b|^2-|c|^2-|d|^2+|e|^2\}n_i n_p$$
$$+\,\mathrm{Re}\,(ab^*+cd^*)m_i m_p + \mathrm{Re}\,(ab^*-cd^*)l_i l_p - \mathrm{Im}\,b^* e(m_i l_p - l_i m_p).$$

From experiments on triple scattering with parallel and perpendicular planes, respectively, the following components are determined:

$$\sigma D_{nn} = \tfrac{1}{2}\{|a|^2+|b|^2-|c|^2-|d|^2+|e|^2\}$$
$$\sigma D_{zm} = -\cos\tfrac{1}{2}\vartheta\,\mathrm{Re}\,(a^*b+c^*d) + \mathrm{Im}\,b^*e\sin\tfrac{1}{2}\vartheta.$$

For determination of the components

$$\sigma D_{zm} = \sin\tfrac{1}{2}\vartheta\,\mathrm{Re}\,(a^*b+c^*d) + \cos\tfrac{1}{2}\vartheta\,\mathrm{Im}\,b^*e,$$
$$\sigma D_{zl} = \sin\tfrac{1}{2}\vartheta\,\mathrm{Re}\,(a^*b-c^*d) + \cos\tfrac{1}{2}\vartheta\,\mathrm{Im}\,b^*e$$

either fourfold scattering must be measured or else triple scattering with a magnetic field between the targets. Unit vectors z and x are directed along $\mathbf{k}$ and $\mathbf{n}\times\mathbf{k}$ respectively.

B3. Measurement of tensor

$$\sigma K_{iq} = \tfrac{1}{4}\,\mathrm{tr}\,(M\sigma_{1i}M^{+}\sigma_{2q}) = \tfrac{1}{2}(|a|^2-|b|^2+|c|^2-|d|^2+|e|^2)n_i n_q$$
$$+ \mathrm{Re}\,(a^*c+b^*d)m_i m_q + \mathrm{Re}\,(a^*c-b^*d)l_i l_q - \mathrm{Im}\,c^*e(m_i l_q - l_i m_q).$$

Components K_{nn} and K_{s-l} can be determined from triple scattering and K_{sm} and K_{s-l} from fourfold scattering.

In the case of identical particles this is equivalent to measurement of the corresponding D_{ip} components at complementary angles ($\vartheta \to \pi-\vartheta$), where $D_{nn}(\pi-\vartheta) = K_{nn}(\vartheta)$, $D_{sm}(\pi-\vartheta) = K_{s-l}(\vartheta)$, $D_{sm}(\pi-\vartheta) = -K_{s-l}(\vartheta)$, $D_{sl}(\pi-\vartheta) = +K_{s-m}(\vartheta)$.

A4. The tensor of polarization correlation is measured:

$$\sigma P_{pq} = \tfrac{1}{4}\,\mathrm{tr}\,(\sigma_{1p}\sigma_{2q}MM^{+}) = \tfrac{1}{2}(|a|^2-|b|^2-|c|^2+|d|^2+|e|^2)n_p n_q$$
$$+ \mathrm{Re}\,(ad^*+bc^*)m_p m_q + \mathrm{Re}\,(b^*c-a^*d)l_p l_q + \mathrm{Im}\,de^*(l_p m_q + l_q m_p).$$

The component

$$\sigma P_{nn} = \tfrac{1}{2}(|a|^2-|b|^2-|c|^2+|d|^2+|e|^2)$$

can be determined in an experiment in which the planes of the analyzing scatterings coincide with the plane of predominant scattering.

In order to determine the components

$$\sigma P_{ml} = \mathrm{Im}\,de^*$$

an experiment is required in which the planes of the analyzing scatterings are perpendicular to those of predominant scattering.

Experiments in which the planes of the analyzing scatterings are perpendicular to the plane of predominant scattering and in which a magnetic field perpendicular to the first scattering plane is applied in front of one of the analyzers, yield the components

$$\sigma P_{mm} = \mathrm{Re}\,(a^*d+b^*c)$$
$$\sigma P_{ll} = -\mathrm{Re}\,(a^*d-b^*c).$$

B4. Measurement of tensor

$$\sigma P_{ipq} = \tfrac{1}{4}\,\mathrm{tr}\,(M\sigma_{1i}M^{+}\sigma_{1p}\sigma_{2q})$$
$$= n_i n_p n_q\,\mathrm{Re}\,ae^* + [m_i m_p n_q + l_i l_p n_q]\,\mathrm{Re}\,be^* + m_i l_p n_q\,\mathrm{Im}\,(a^*b-c^*d)$$
$$- l_i m_p n_q\,\mathrm{Im}\,(a^*b+c^*d) - l_i n_p m_q\,\mathrm{Im}\,(a^*c+b^*d)$$
$$+ n_i l_p m_q\,\mathrm{Im}\,(a^*d+b^*c) + n_i m_p l_q\,\mathrm{Im}\,(a^*d-b^*c)$$
$$+ m_i n_p l_q\,\mathrm{Im}\,(a^*c-b^*d) + [m_i n_p m_q + l_i n_p l_q]\,\mathrm{Re}\,e^*c$$
$$+ [n_i m_p m_q - n_i l_p l_q]\,\mathrm{Re}\,e^*d.$$

D4. In order to perform this experiment a polarized target is required. The components of the following tensor are measured:

$$
\begin{aligned}
\sigma T_{ikpq} = \tfrac{1}{4}\,\mathrm{tr}\,(M\sigma_{1i}\sigma_{2k}M^{+}\sigma_{1p}\sigma_{2q}) &= n_i n_k n_p n_q \tfrac{1}{2}(|a|^2+|b|^2+|c|^2+|d|^2+|e|^2)\\
&+ [m_i m_k m_p m_q + l_i l_k l_p l_q]\,\tfrac{1}{2}(|a|^2+|b|^2+|c|^2+|d|^2-|e|^2)\\
&+ [n_i m_k n_p m_q + m_i n_k m_p n_q]\,\mathrm{Re}\,(ab^*+cd^*)\\
&+ [n_i l_k n_p l_q + l_i n_k l_p n_q]\,\mathrm{Re}\,(ab^*-cd^*)\\
&+ [m_i l_k m_p l_q + l_i m_k l_p m_q]\,\tfrac{1}{2}(|a|^2+|b|^2-|c|^2-|d|^2-|e|^2)\\
&+ [m_i m_k l_p l_q + l_i l_k m_p m_q]\,\tfrac{1}{2}(-|a|^2+|b|^2+|c|^2-|d|^2+|e|^2)\\
&+ [l_i m_k m_p l_q + m_i l_k l_p m_q]\,\tfrac{1}{2}(|a|^2-|b|^2+|c|^2-|d|^2-|e|^2)\\
&+ [l_i n_k n_p l_q + n_i l_k l_p n_q]\,\mathrm{Re}\,(a^*c+b^*d)\\
&+ [n_i m_k m_p n_q + m_i n_k n_p m_q]\,\mathrm{Re}\,(a^*c-b^*d)\\
&- [l_i l_k n_p n_q + n_i n_k l_p l_q]\,\mathrm{Re}\,(b^*c+a^*d)\\
&- [n_i n_k m_p m_k + m_i m_k n_p n_q]\,\mathrm{Re}\,(b^*c-a^*d)\\
&+ [m_i n_k n_p l_q - n_i l_k m_p n_q - l_i n_k n_p m_q + n_i m_k l_p n_q]\,\mathrm{Im}\,(e^*c)\\
&+ [n_i n_k m_p l_q + n_i n_k l_p m_q - m_i l_k n_p n_q - l_i m_k n_p n_q]\,\mathrm{Im}\,(e^*d)\\
&+ [l_i m_k m_p m_q + m_i l_k m_p m_q + l_i l_k m_p m_q + l_i l_k l_p m_q\\
&\qquad - m_i l_k l_p l_q - l_i m_k l_p l_q - m_i m_k m_p l_q - m_i m_k l_p m_q]\,\mathrm{Im}\,(a^*e)\\
&+ [l_i n_k m_p n_q + n_i l_k n_p m_q - n_i m_k n_p l_q - m_i n_k l_p n_q]\,\mathrm{Im}\,(b^*e).
\end{aligned}
$$

Appendix 2

UNITARITY RELATION

We present below the unitarity relation for nucleon-nucleon scattering:

$$
\begin{aligned}
4\pi\,\mathrm{Im}\,\alpha(\vartheta) &= k\int \tfrac{1}{4}\,\mathrm{tr}\,(M^{+}(\mathbf{k}',\mathbf{k}'')M(\mathbf{k},\mathbf{k}'')]\mathrm{d}\omega_{\mathbf{k}''},\\
4\pi\,\mathrm{Im}\,\beta(\vartheta) &= k\int \tfrac{1}{4}\,\mathrm{tr}\,[M^{+}(\mathbf{k}',\mathbf{k}'')M(\mathbf{k},\mathbf{k}'')\boldsymbol{\sigma}_1\cdot\mathbf{n}\,\boldsymbol{\sigma}_2\cdot\mathbf{n}]\mathrm{d}\omega_{\mathbf{k}''},\\
4\pi\,\mathrm{Re}\,\gamma(\vartheta) &= ik\int \tfrac{1}{8}\,\mathrm{tr}\,[M^{+}(\mathbf{k}',\mathbf{k}'')M(\mathbf{k},\mathbf{k}'')(\boldsymbol{\sigma}_1+\boldsymbol{\sigma}_2)\cdot\mathbf{n}]\mathrm{d}\omega_{\mathbf{k}''},\\
4\pi\,\mathrm{Im}\,\delta(\vartheta) &= k\int \tfrac{1}{4}\,\mathrm{tr}\,[M^{+}(\mathbf{k}',\mathbf{k}'')M(\mathbf{k},\mathbf{k}'')\boldsymbol{\sigma}_1\cdot\mathbf{m}\,\boldsymbol{\sigma}_2\cdot\mathbf{m}]\mathrm{d}\omega_{\mathbf{k}''},\\
4\pi\,\mathrm{Im}\,\varepsilon(\vartheta) &= k\int \tfrac{1}{4}\,\mathrm{tr}\,[M^{+}(\mathbf{k}',\mathbf{k}'')M(\mathbf{k},\mathbf{k}'')\boldsymbol{\sigma}_1\cdot\mathbf{l}\,\boldsymbol{\sigma}_2\cdot\mathbf{l}]\mathrm{d}\omega_{\mathbf{k}''}.
\end{aligned}
$$

Evaluation of the traces involved in the unitarity relation is elementary but yields cumbersome expressions which will not be given here. It should be mentioned that if one uses the expression for M given in ref. [5]) the unitarity relation for coefficient $B(\vartheta)$ (singlet scattering) takes the form of the unitarity relation for scattering of spinless particles.

References

1) L. Wolfenstein, Ann. Rev. Nucl. Sci. **6** (1956)
2) R. Glauber and V. Schomaker, Phys. Rev. **89** (1953) 667
3) S. Minami, Progr. Theor. Phys. **11** (1954) 213
4) R. Ryndin and J. Smorodinsky, Doklady **103** (1955) 69
5) L. Wolfenstein, Phys. Rev. **96** (1954) 1654
6) R. Oehme, Phys. Rev. **98** (1955) 147
7) R. Oehme, Phys. Rev. **98** (1955) 216
8) R. Ryndin and J. Smorodinsky, JETP (in print)
9) R. Ryndin and J. Smorodinsky, CERN Symposium Proc., vol. 2 (1956)

Nuclear Physics **3** (1957) 446—455; *North-Holland Publishing Co., Amsterdam*

ON SYMMETRIES IN ELEMENTARY PARTICLE INTERACTIONS

B. D'ESPAGNAT and J. PRENTKI
CERN, *Geneva*

and

ABDUS SALAM
Imperial College of Science and Technology, London

Received 22 January 1957

Abstract: It is investigated how far the number of independent coupling constants in the interaction Lagrangian of elementary particles can be reduced by various covariance requirements in [3]- and [4]-manifolds.

1. Introduction

The hypothesis of charge-independence considerably restricts the number of possible interactions between N, Λ, Σ and Ξ hyperons, and π and K-mesons. Even assuming only 3-field couplings and no parity-degeneracy for K-mesons, there are still 8 possible coupling-constants in the interactions. The interaction Lagrangian is [1, 2] †

$$\begin{aligned}\mathscr{L} = {} & g_1 \bar{\mathrm{N}} i\gamma_5 \boldsymbol{\tau} \cdot \boldsymbol{\pi} \mathrm{N} - g_2(\bar{\Lambda} i\gamma_5 \boldsymbol{\pi} \cdot \boldsymbol{\Sigma} + \mathrm{h.c.}) \\ & - g_3(i\bar{\boldsymbol{\Sigma}} i\gamma_5 \times \boldsymbol{\Sigma}) \cdot \boldsymbol{\pi} + g_4 \bar{\Xi} i\gamma_5 \boldsymbol{\tau} \cdot \boldsymbol{\pi} \Xi \\ & + g_5(\bar{\mathrm{N}} \mathrm{K} \Lambda + \mathrm{h.c.}) + g_6(\bar{\mathrm{N}} \boldsymbol{\tau} \cdot \boldsymbol{\Sigma} \mathrm{K} + \mathrm{h.c.}) \\ & + g_7(\bar{\Xi} \tau_2 \mathrm{K}^* \Lambda + \mathrm{h.c.}) + g_8(\bar{\Xi} \boldsymbol{\tau} \cdot \boldsymbol{\Sigma} \tau_2 \mathrm{K}^* + \mathrm{h.c.}).\end{aligned}$$

The number of coupling constants increases to 13 if τ and θ mesons have opposite intrinsic parities [3] ††, and to 26 if Λ and Σ hyperons are also parity degenerate [4]. It is essential to exploit all possible symmetries which the interaction Lagrangian may possess if one wants to limit the magnitudes of these constants. Some attempts have already been made in this direction [3, 5]. We wish here to reconsider the problem.

2. Substitution Invariance

a) Consider the Lagrangian (1.1) where parity-degeneracy of K, Λ and Σ particles is not taken into account. By inspection, this Lagrangian is invariant for the substitutions †††

† We use the notation of ref. [2]).

†† Schwinger [3]) first pointed out the possible existence of a direct KKπ coupling, existing only if θ and τ have opposite intrinsic parities.

††† To see that $\bar{\Lambda}\boldsymbol{\pi} \cdot \boldsymbol{\Sigma}$+h.c. is substitution-invariant, write this interaction as $\frac{1}{2}\bar{\Lambda}\delta_{\alpha\beta}\boldsymbol{\pi} \cdot \boldsymbol{\tau}_{\beta\gamma}\boldsymbol{\tau}_{\gamma\alpha} \cdot \boldsymbol{\Sigma}$+h.c.

$$\begin{aligned} &\delta_{\alpha\beta}\Lambda \to (\boldsymbol{\tau}\cdot\boldsymbol{\Sigma})_{\alpha\beta} \\ &m_\Lambda \to m_\Sigma \\ &g_5 \to g_6 \\ &g_7 \to g_8 \end{aligned} \tag{2.1}$$

provided $g_3 = 0$.

In the approximation $m_\Lambda = m_\Sigma$, one may infer

$$g_5 = g_6, \qquad g_7 = g_8.$$

b) Similarly the substitutions

$$\begin{aligned} &\mathrm{N} \to \Xi, \quad \pi \to \pi \\ &\Xi \to -\mathrm{N}, \quad \mathrm{K} \to \tau_2 \mathrm{K}^* \\ &\Lambda \to \Lambda, \quad \Sigma \to \Sigma \\ &m_\mathrm{N} \to m_\Xi \end{aligned} \qquad \begin{aligned} &g_1 \to g_4 \\ &g_5 \to g_7 \\ &g_6 \to g_8 \end{aligned} \tag{2.2}$$

leave the Lagrangian invariant. Once again in the (poor) approximation $m_\mathrm{N} = m_\Xi$, one may infer

$$g_1 = g_4, \quad g_5 = g_7, \quad g_6 = g_8,$$

and combining (2.1) and (2.2),

$$g_5 = g_6 = g_7 = g_8, \quad g_1 = g_4, \quad g_3 = 0.$$

With this choice of coupling constants there is nothing in the theory to produce (Σ, Λ) or (N, Ξ) mass differences.

It would be desirable to seek a geometrical basis for these and similar substitutions. This is attempted in the §§ 3 and 4. In § 3, we consider a [3]-isobaric space and particularly the role of reflections in this space. In the §§ 4 and 5, the [3]-isobaric manifold is enlarged to [4], considering both Lorentz and Euclidian metrics. In § 6, we consider a [4]-Euclidian space with a structure different from those in § 4 and § 5. A summary of the results appears in § 7.

3. 3-Dimensional Isobaric Space

Assume N, Ξ, K are iso-spinors, π, Σ iso-pseudo-vectors, Λ an iso-scalar, and all interactions are rotation invariant.

To introduce reflections [1, 2]) we notice that the charge-conserving gauge-transformation $\exp(iQ\alpha)$ for the particular angle $\alpha = \pi$ acquires the significance of a parity-operation $(z \to -z)$, provided the iso-spinors N and Ξ are considered to transform as $\mathrm{N} \to -\tau_3 \mathrm{N}$, and $\Xi \to \tau_3 \Xi$. Reflection invariance is a gift in this scheme, but the interpretation of the operation $\exp(iQ\pi)$ as reflection confers the following distinct advantages:

(1) The degeneracy of N and Ξ (as iso-spinors) is removed. These transform differently for reflections.

(2) If charge $|Q| \leqq 1$, no particles other than those already discovered can

be accomodated in the scheme (apart from a possible isoscalar π_0') without introducing degeneracies in the isobaric space. This is equivalent to the statement that $|U| = |\text{iso-fermion number} - \text{anti-iso-fermion number}| \leqq 1$.

Assuming that $m_\Lambda = m_\Sigma$, it is possible to combine a scalar (Λ) and a pseudo-vector (Σ) into a (reducible) second-rank spinor $a_{\dot{k}l}$, where

$$\begin{aligned} a_{\dot{1}1} &= \Lambda - \Sigma_3 & a_{\dot{2}2} &= \Lambda + \Sigma_3 \\ a_{\dot{1}2} &= -\Sigma_1 - i\Sigma_2 & a_{\dot{2}1} &= -\Sigma_1 + i\Sigma_2. \end{aligned} \tag{3.1}$$

Write

$$\begin{aligned} b_{\dot{1}1} &= \tfrac{1}{2}\overline{\mathrm{N}}(1+\tau_3)\mathrm{K} = b^{\dot{2}2} \\ b_{\dot{2}2} &= \tfrac{1}{2}\overline{\mathrm{N}}(1-\tau_3)\mathrm{K} = b^{\dot{1}1} \\ b_{\dot{1}2} &= \tfrac{1}{2}\overline{\mathrm{N}}(\tau_1 + i\tau_2)\mathrm{K} = -b^{\dot{2}1} \\ b_{\dot{2}1} &= \tfrac{1}{2}\overline{\mathrm{N}}(\tau_1 - i\tau_2)\mathrm{K} = -b^{\dot{1}2}. \end{aligned} \tag{3.2}$$

In this notation the $\mathrm{NK}\Lambda$ and $\mathrm{NK}\Sigma$ interactions can be combined into the invariant form $a_{\dot{k}l}b^{\dot{k}l}$, provided

$$g_5 = g_6.$$

Similarly one may infer the possibility

$$g_7 = g_8.$$

Clearly this combination of Λ and $\boldsymbol{\Sigma}$ fields is equivalent to the substitution (2.1). The π-field, in this notation, is represented by a spinor $C_{\dot{k}l}$ with $\mathrm{tr}\, C_{\dot{k}l} = 0$.

Besides the reflection discussed above, the Lagrangian is invariant also for the so-called charge-parity operation. This operation combines particle-antiparticle conjugation with an operation in the isobaric space and the invariance of the Lagrangian implies the reality of the coupling constants $g_1, \ldots, g_8$ [2]. Schwinger has chosen to designate this as isobaric reflection, considering π as an iso-vector (rather than iso-pseudo-vector) and ascribing parity to the hermitian components of other fields. We shall return to this in § 5.

4. Approach to Four Dimensions

As emphasized in § 3, all present experiments are explained by requiring (i) charge conservation and (ii) invariance of the Lagrangian for rotations in a [3] isobaric space, while reflection-invariance (in at least one form of the theory) is a gift conferred by (i). Notice that while with the conventional tensor representation of $\boldsymbol{\pi}$ and $\boldsymbol{\Sigma}$ fields (π_1, π_2, π_3 etc. rather than π^+, π^-, π^0) the invariance of the Lagrangian for isobaric rotations is always manifest, the invariance for the charge-conserving gauge-transformation $\exp(iQ\alpha)$ is not.

The approach to four dimensions can be made in three ways:

a) One recognises that (with the approximation $m_\Lambda = m_\Sigma$) there is the possibility of combining four fields Σ and Λ into a 4-vector in a Lorentz space †.

b) One may do the same in a Euclidian space: then there is, moreover, the possibility of treating $\boldsymbol{\pi}$ with its 3 components as an antisymmetric self dual tensor in [4].

c) To the set of [3] isobaric rotations, one may adjoin [3] rotations in what may be called the "strangeness space". In the resulting [4] manifold, (N, Ξ) and $(\mathrm{K}, \overline{\mathrm{K}})$ form 4-vectors. This is the theory of Salam and Polkinghorne and is discussed in § 6.

Approaches a) and c) both dispense with the explicit requirement of gauge invariance $\exp(iQ\alpha)$; while this is somewhat accidental in a), in c) it comes from the structure of the [4]-space itself. In b) the additional requirement of charge conservation will be satisfied by making identifications where appropriate with the Lagrangian (1.1).

4.1. LORENTZ SPACE – ROTATIONS ONLY

Rotations in Lorentz space can be described using two-component spinors (whereas 4-component spinors are required for reflexions).

Lemma 1. Given four different two-component spinors ϕ, ψ and u, v transforming as ††

$$\phi, \psi \to s\phi, s\psi,$$
$$u, v \to s^{\dagger -1} u, s^{\dagger -1} v,$$

with $\det s = 1$, then $(\phi^* \boldsymbol{\tau} \psi, -\phi^* \psi)$, $(u^* \boldsymbol{\tau} \tau_2 \psi^*, +u^* \tau_2 \psi^*)$ and $(u^* \boldsymbol{\tau} v, +u^* v)$ are 4-vectors, while $(\phi \boldsymbol{\tau} \tau_2 \phi)$, $(u^* \boldsymbol{\tau} \phi)$ are self-dual tensors.

a) $(\boldsymbol{\Sigma}, \Lambda)$ *a 4-vector.* Identifying $\phi = \mathrm{N}$, $\psi = \mathrm{K}$, $u = \Xi$, we may infer

$$g_5 = g_6, \qquad g_7 = -g_8. \tag{4.1}$$

b) π *as self dual tensor.* If $\phi = \mathrm{N}$, we notice that $\mathrm{N}(\boldsymbol{\tau} \cdot \boldsymbol{\pi})\tau_2 \mathrm{N}$ does not conserve charge nor the quantity $N =$ number of baryons minus number of antibaryons. The only remaining possibility is to take $v = \phi$ (i.e. $s^{\dagger -1} = s$ or consider space-rotations only). It is thus impossible to introduce the self dual π tensor genuinely as a [4]-entity.

c) Assuming the existence of π_0', invariance in [4] requires $g_2 = g_3 = 0$.

4.2. LORENTZ-SPACE – ROTATIONS AND REFLECTIONS

Lemma 2. With the notation of Lemma 1, let

$$\begin{aligned} \phi &\to u, \qquad u \to -\phi \\ \psi &\to v, \qquad v \to -\psi \end{aligned} \tag{4.2}$$

† It is here also possible to introduce a neutral isoscalar π_0' and to treat $\boldsymbol{\pi}, \pi_0'$ as a 4-vector.

†† The matrix $s^\dagger$ is hermitian conjugate to s. One can show that $s^{\dagger -1} = \tau_2 s^* \tau_2$, where s^* is the complex conjugate matrix. Thus $\tau_2 \phi^*$ transforms similarly to u.

for reflections. Then $(\phi^*\tau\psi - u^*\tau v)$, $-(\phi^*\psi + u^*v)$ is a 4-vector for Lorentz transformations including reflections. Each of

$$\Psi = \begin{pmatrix}\phi\\ u\end{pmatrix} \text{ and } \Psi' = \begin{pmatrix}\psi\\ v\end{pmatrix}$$

can be written as a 4-component spinor.

Assuming $m_\Lambda = m_\Sigma$, $m_N = m_\Xi$ and identifying

$$\Psi = \begin{pmatrix}N\\ \Xi\end{pmatrix}, \quad \Psi' = \begin{pmatrix}K\\ \tau_2 K^*\end{pmatrix} = \mathcal{K}$$

with further $\Sigma_\mu = (\boldsymbol{\Sigma}, \Lambda)$ as a 4-vector, we infer $g_5 = g_6 = g_7 = -g_8$. Using the representation

$$\boldsymbol{\Gamma} = \begin{pmatrix}\cdot & \tau\\ \tau & \cdot\end{pmatrix}, \quad \Gamma_0 = \begin{pmatrix}\cdot & 1\\ -1 & \cdot\end{pmatrix},$$

the interaction can be written compactly as $\overline{\Psi}\Gamma_\mu \mathcal{K} \Sigma_\mu$. Since Σ_μ is a 4-vector in this space, i.e.

$$\Lambda \to \Lambda, \quad \boldsymbol{\Sigma} \to -\boldsymbol{\Sigma} \text{ for reflections,} \tag{4.3}$$

the [3]-manifold considered in § 3, with its reflection ($\Lambda \to \Lambda$, $\boldsymbol{\Sigma} \to +\boldsymbol{\Sigma}$) is not embedded in the [4]-space considered here. There is no compelling reason from the present point of view to limit the number of particles as was the case in § 3 †.

4.3. EUCLIDIAN SPACE – ROTATIONS

Lemma 3. Given 4 two-component spinors φ, ψ and u, v transforming as

$$\phi, \psi \to s\phi, s\psi, \qquad u, v \to tu, tv,$$

with

$$\det s = \det t = 1, \qquad ss^\dagger = 1, \qquad tt^\dagger = 1,$$

where s and t are 2 independent matrices ††, then $(\phi^*\tau v, -i\phi^* v)$ and $(\phi^*\tau\tau_2 v^*, -i\phi^*\tau_2 v^*)$ are 4-vectors and $\phi^*\,\tau\,\phi$ is a self-dual tensor.

Identify ††† $\phi = N$, $v = K$ and form a 4-vector $^*\boldsymbol{\Sigma}, i\Lambda$. This gives $g_5 = g_6$. Similarly with $\psi = \Xi$ (or with $\psi = \tau_2\Xi^*$ and the 4-vector $\boldsymbol{\Sigma}^*, -i\Lambda^*$), we obtain $g_7 = g_8$. It is interesting that the sequence of relative signs for (g_5, g_6) and (g_7, g_8) is not the same as for the Lorentz case.

Unlike the Lorentz case, there is no difficulty in treating π as self-dual tensor (though no relation between g_1 and g_4 can be deduced). From the

† The work of Matthews and Salam [5]) with its treatment of Λ and Σ as isobaric tensors arose from a desire to limit the number of particles, as well as to exploit the symmetries of [4]-formulation. This is another alternative for obtaining the results of the present paper.

†† Note s and t are unitary (3-parameter) matrices. In the Lorentz case there is only one non-unitary (6-parameter) matrix s. In contrast to the Lorentz case ϕ and $\tau_2\phi^*$ transform similarly ($\tau_2 s^*\tau_2 = s^{\dagger -1} = s$).

††† Unless this identification is made, the rotations do not span the entire [4]-manifold.

* It is desirable that the 4-vectors (here and in the Lorentz case) should be real. $\boldsymbol{\Sigma}$ and Λ fields should therefore be split into their hermitian parts (see next section).

4-vectors $(\boldsymbol{\Sigma}, i\Lambda)$ and $(\Sigma^*, -i\Lambda^*)$, self-dual tensors can be formed so that $\Lambda\Sigma\pi$ and $\Sigma\Sigma\pi$ interactions can be combined covariantly, provided $g_2 = -g_3$.

4.4. REFLECTIONS IN EUCLIDIAN SPACE

For completeness we write down the result for reflections though no useful identifications seem possible.

Lemma 4. With the notation of Lemma 3, define reflection

$$\phi \to u, \quad u \to -\phi; \qquad \psi \to -v, \quad v \to \psi.$$

Then $\phi^*\boldsymbol{\tau}v - \psi^*\boldsymbol{\tau}u$, $-i(\phi^*v + \psi^*u)$ is a 4-vector and

$$\Psi = \begin{pmatrix}\phi\\ u\end{pmatrix}, \quad \Psi' = \begin{pmatrix}v\\ \psi\end{pmatrix}$$

can be considered as 4-spinors.

Why no simple identifications are possible is connected with the fact that K and $\tau_2 K^*$ transform similarly. Thus, unlike the Lorentz-case, for the 4-spinors $\binom{K}{\tau_2 K^*}$ the rotations do not span the entire [4]-space but really refer only to a [3]-part of it.

The following distinction between Lorentz and Euclidian cases (rotations only) may be pointed out. If A_μ is a 4-vector, the two invariants for the Lorentz case are (Lemma 1)

$$\phi^*\boldsymbol{\tau}\phi \cdot \boldsymbol{A} - \phi^*\phi A_0, \qquad u\tau_2\boldsymbol{\tau}\phi \cdot \boldsymbol{A} - u\tau_2\phi A_0$$

while for the Euclidian case these are (Lemma 3)

$$u^*\boldsymbol{\tau}\phi \cdot \boldsymbol{A} + u^*\phi A_4, \qquad u^*\boldsymbol{\tau}\tau_2 \cdot \phi^*\boldsymbol{A} + u^*\tau_2\phi^* A_4.$$

Both Lorentz expressions are also invariant for the gauge-transformation $\phi \to [\exp(i\alpha)]\phi$, $u \to u \exp(-i\alpha)$, $A_\mu \to A_\mu$. There is no corresponding gauge-transformation for *both* Euclidian expressions. This gauge-transformation (with $\alpha = \pi/2$) made U-conservation possible in § 3 leading on to charge-conservation. Summarizing then, the Euclidian space allows a number of invariants (formed from 4-vectors) for which charge-conservation may not hold. This is not the case for the Lorentz-space.

When comparing the Lorentz and Euclidian formulation it should, however, be stressed that, in the former, $\mathscr{L}_{\text{free}}$ is obviously not an iso-scalar (e.g. for nucleons the only iso-scalar is $\varphi\tau_2\varphi$ while $\varphi^* \ldots \varphi$ is the 4th component of an iso-4-vector). This formulation should thus be viewed as describing a purely formal substitution carried exclusively on $\mathscr{L}_{\text{int.}}$, whereas the Euclidian formulation, where $\mathscr{L}_{\text{free}}$ and $\mathscr{L}_{\text{int}}$ are iso-scalars, provides a consistent theory to which some amount of physical meaning can, maybe, be attached. This, of course, gives a strong preference to the Euclidian approach,

5. Schwinger Approach in 4-Dimensional Space

In this § we use a Majorana representation of ordinary γ matrices, so that quite generally ψ^* is the charge-conjugate field to ψ, and the split of a non-hermitian field ψ into its hermitian components ψ_1, ψ_2 ($\psi = \psi_1 + i\psi_2$) is independent of the space-time frame of reference. With the notations of subsection 4.2 the quantity

$$\phi^* \boldsymbol{\tau} \psi \cdot \boldsymbol{\Sigma} - u^* \boldsymbol{\tau} v \cdot \boldsymbol{\Sigma}^* + \varphi^* \psi \Lambda + u^* v \Lambda^* \tag{5.1}$$

is an invariant provided ($\boldsymbol{\Sigma}$, Λ) behaves as a 4-vector under rotations and transforms as

$$\boldsymbol{\Sigma} \to -\boldsymbol{\Sigma}^*, \qquad \Lambda \to \Lambda^* \tag{5.2}$$

under reflections. With the identifications

$$\begin{pmatrix} \phi \\ u \end{pmatrix} = \begin{pmatrix} \mathrm{N} \\ \tau_2 \mathrm{N}^* \end{pmatrix} = \mathcal{N}, \qquad \begin{pmatrix} \psi \\ v \end{pmatrix} = \begin{pmatrix} \mathrm{K} \\ \tau_2 \mathrm{K}^* \end{pmatrix} = \mathcal{K}$$

this gives $g_5 = g_6$. As mentioned in § 3, (5.2) is conventionally known as charge-parity operation. It is a non-linear operation as it stands. Schwinger's theory differs from those in § 4, by designating this rather than (4.3) as isobaric reflection. (5.2) can be put in a more familiar form by setting

$$\boldsymbol{\Sigma} = 2^{-\frac{1}{2}}(\boldsymbol{\Sigma}^{(1)} + i\boldsymbol{\Sigma}^{(2)}); \qquad \Lambda = 2^{-\frac{1}{2}}(\Lambda^{(1)} + i\Lambda^{(2)}); \tag{5.3}$$

then $\boldsymbol{\Sigma}^{(1)}$, $\Lambda^{(1)}$ transforms as a 4-vector and $\boldsymbol{\Sigma}^{(2)}$, $\Lambda^{(2)}$ as a pseudo-vector. Using the representation

$$\Gamma_i = \begin{pmatrix} \cdot & \tau_i \\ \tau_i & \cdot \end{pmatrix}, \qquad \Gamma_4 = i \begin{pmatrix} \cdot & 1 \\ -1 & \cdot \end{pmatrix}, \tag{5.4}$$

(5.1) can be written in the manifestly covariant form

$$i[\overline{\mathcal{N}} \Gamma_\mu \mathcal{K} \Sigma_\mu^{(1)} + \overline{\mathcal{N}} \Gamma_\mu \Gamma_5 \mathcal{K} \Sigma_\mu^{(2)}]$$

with

$$\Sigma_4 = i\Lambda, \qquad (m_\Lambda = m_\Sigma). \tag{5.5}$$

A similar consideration is possible for the Ξ field provided $g_7 = -g_8$.

We have used a Majorana representation for space-time γ's but not for isobaric Γ's. Also the $\Sigma^{(1)}$, $\Sigma^{(2)}$ fields appearing in (5.5) are hermitian, but this is not true for the $\mathcal{N}$ field. It can be shown that a change of representation of Γ's to the Majorana form $\Gamma' = S\Gamma S^{-1}$ also ensures the hermiticity of the transformed field $\mathcal{N}' = S\mathcal{N}$. Explicitly one can verify that with the choice

$$\Gamma_1' = \begin{pmatrix} \cdot & \tau_1 \\ \tau_1 & \cdot \end{pmatrix}, \quad \Gamma_2' = \begin{pmatrix} 1 & \cdot \\ \cdot & -1 \end{pmatrix}, \quad \Gamma_3' = \begin{pmatrix} \cdot & \tau_3 \\ \tau_3 & \cdot \end{pmatrix}, \quad \Gamma_4' = i \begin{pmatrix} \cdot & 1 \\ -1 & \cdot \end{pmatrix},$$

the matrix S equals

$$\frac{1}{\sqrt{2}} \begin{pmatrix} 1 & \tau_2 \\ -\tau_2 & +1 \end{pmatrix},$$

so that

$$\mathcal{N}' = S\mathcal{N} = \frac{1}{\sqrt{2}} \begin{pmatrix} p+p^* \\ n+n^* \\ -in^*+in \\ ip^*-ip \end{pmatrix}.$$

It may be pointed out that the same kind of approach can be used in a Euclidian [4] space (rotations only [3]), leading to $g_5 = g_6$, $g_7 = g_8$.

The Schwinger approach suffers from the same drawback as noted in § 4.2; there is no limitation on the number of particles that can be introduced. The reflexion operation is a distinctly different operation from those considered in the §§ 3 and 4. The one advantage of the Schwinger formalism is that charge conjugation invariance of the theory is manifest.

6. The Alternative [4] Formulation

In the Salam-Polkinghorne formulation [7]) as in the Lorentz space formulation, charge-conservation is guaranteed and does not have to be imposed as an additional requirement on the Lagrangian. The [4]-space splits into the conventional [3]-isobaric space (I^+) and what may be called a [3]-"strangeness" space (I^-).

Identify $\boldsymbol{\pi}$, $\boldsymbol{\Sigma}$ with the tensor (1, 0), Λ with the scalar (0, 0), K and (N, Ξ) with the vector $(\frac{1}{2}, \frac{1}{2})$ representation, (assuming $m_N = m_\Xi$) †.

Using the well-known spinor representations identify

$$\begin{aligned}
&\mathcal{N}_{1\dot{1}} = p \qquad \mathcal{N}^{1\dot{1}*} = \bar{\Xi}^- \qquad \mathcal{K}_{1\dot{1}} = K^+ \\
&\mathcal{N}_{2\dot{1}} = n \qquad \mathcal{N}^{2\dot{1}*} = -\bar{\Xi}^0 \qquad \mathcal{K}_{2\dot{1}} = K^0 \\
&\mathcal{N}_{1\dot{2}} = \Xi^0 \qquad \mathcal{N}^{1\dot{2}*} = -\bar{n} \qquad \mathcal{K}_{1\dot{2}} = -iK^{0*} \\
&\mathcal{N}_{2\dot{2}} = \Xi^-, \qquad \mathcal{N}^{2\dot{2}*} = \bar{p}; \qquad \mathcal{K}_{2\dot{2}} = iK^{+*}; \\
&-\Sigma^{11} = 2^{\frac{1}{2}}\Sigma^+, \quad \Sigma^{12} = \Sigma^{21} = \Sigma^0, \quad \Sigma^{22} = 2^{\frac{1}{2}}\Sigma^-,
\end{aligned}$$

and similarly for π, the interactions †† can be written in the usual manner

† The requirements that $|Q| \leqq 1$ and that only single-valued representations be considered limits the possible number of particles. In addition to the presently known particles, there may exist (0, 1) Fermions and (0, 1) Bosons.

†† The relation of spinor-indices with the representation $D(I^+, I^-)$ is given by the well-known relation [8])

$$V^{I^+, I^-}_{I_3^+, I_3^-} = \frac{(\phi^1)^{I^+ + I_3^+} (\phi^2)^{I^+ - I_3^+}}{[(I^+ + I_3^+)!(I^+ - I_3^+)!]^{\frac{1}{2}}} \frac{(u^{\dot{1}})^{I^- + I_3^-} (u^{\dot{2}})^{I^- - I_3^-}}{[(I^- + I_3^-)!(I^- - I_3^-)!]^{\frac{1}{2}}}.$$

Here ϕ and u are spinors transforming (in Euclidian space) as in Lemma 3. (The dotting of u indices does not have the significance of complex conjugation in Euclidian space and is only a concession to the conventional notation.) The crucial point (and the one which distinguishes a Lorentz from a Euclidian metric) is the behaviour of $(V^{I^+, I^-}_{I_3^+, I_3^-})^*$ (physically, for example, that of $\bar{K}^0$, K^- in relation to K^+, K^0). For Euclidian metric $(\tau_2\phi^*)$ transforms similarly to ϕ, while this is not the case for Lorentz-space. Thus $(V^{I^+, I^-}_{I_3^+, I_3^-})^*$ transforms similarly to $(-1)^{I_3^+ + I_3^-} (V_{-I_3^+, -I_3^-}^{I^+, I^-})$ for the Euclidean case and to $V^{I^-, I^+}_{I_3^-, I_3^+}$ for the Lorentz-case. (Here $\phi \to s\phi$, $u \to s^*u$ for the Lorentz-case.) A Lorentz-metric is clearly unsuited to represent $(K^+, K^0, \bar{K}^0, -K^-)$. In the Euclidian case $\mathcal{N}^{A\dot{B}}$ transforms similarly to $\mathcal{N}_{A\dot{B}^*}$.

$(\mathcal{N}^{A\dot{B}}\pi_A^C\mathcal{N}_{C\dot{B}}$, for example [9])) † giving $g_1 = g_4$, $g_5 = g_7$, $g_6 = +g_8$.

Here Σ_A^B is a spinor with zero trace. Alternatively it is possible to combine Λ and Σ into a reducible second-rank spinor, where $\Lambda = -\frac{1}{2}$ tr Σ_A^B in the manner of § 3, obtaining $g_5 = g_6$, $g_7 = g_8$.

It is possible to use the tensor (rather than spinor) representations for all these particles and this has been indicated in ref. [7]) ††.

7. Conclusions

We conclude that at the present stage nothing deep or fundamental is achieved by extending the manifold to 4 dimensions. We consider that the 3-dimensional formulation of ref. [1, 2]) and the remarks about substitution invariance in the §§ 2 and 3 suffice to give all possible relations between coupling constants.

If an extension to 4 dimensions must be made there are roughly speaking two distinct ways in which this may be done. The approach in § 6 is the more economical one in that the extension of the manifold guarantees charge conservation, limits the possible number of particles (assuming $|Q| \leqq 1$), and also it is unnecessary to consider reflexions in 4 dimensions. The manifold must be Euclidian in structure.

The second approach also guarantees charge conservation in the Lorentz formulation (§§ 4.1, 4.2 and 5), but not in the Euclidian (§ 4.3) where it is an additional requirement. In the table below we summarize the relations obtained between the coupling constants.

TABLE 1

§ 2: *From substitutions*

If $m_\Lambda = m_\Sigma$, $g_5 = g_6$, $g_7 = +g_8$, $g_3 = 0$.
If $m_N = m_\Xi$, $g_1 = g_4$, $g_5 = g_7$.

§ 4: *Lorentz space* a) *Rotations*

If $m_\Lambda = m_\Sigma$, $g_5 = g_6$, $g_7 = -g_8$.
If π_0' exists, $g_2 = g_3 = 0$.

b) *Reflections*

If $m_N = m_\Xi$, $g_5 = g_7$.
If π_0' exists, $g_1 = g_4$.

It is not possible to introduce π as self-dual tensor.

† See similar considerations by Duimio [8]).

†† In §4, §5, N and Ξ correspond to $D(\frac{1}{2}, 0)$ or $D(0, \frac{1}{2})$ representations; here they correspond to $D(\frac{1}{2}, \frac{1}{2})$. The results of § 4 are readily understood in the light of the preceding footnote. If N corresponds to $D(\frac{1}{2}, 0)$ representation, N* corresponds to $D(\frac{1}{2}, 0)$ for Euclidian and to $D(0, \frac{1}{2})$ for the Lorentz metric. Thus a genuine [4] NNπ interaction with π corresponding to $D(1, 0)$ is impossible for a Lorentz metric ($D(\frac{1}{2}, 0) \times D(0, \frac{1}{2})$ does not give $D(1, 0)$). Similar arguments explain many results of §4.

Euclidian space — Rotations

If $m_\Lambda = m_\Xi$, $g_5 = g_6$, $g_7 = g_8$.
If π is treated as self-dual tensor, $g_2 = -g_3$.

§ 5: *Schwinger* [4]*-space approach* (*Lorentz form*)

If $m_\Lambda = m_\Sigma$, $g_5 = g_6$, $g_7 = -g_8$.

§ 6: *Salam-Polkinghorne* [4]*-space approach*

If $m_N = m_\Xi$, $g_5 = g_7$, $g_6 = g_8$, $g_1 = g_4$.
If $m_\Lambda = m_\Sigma$, $g_5 = g_6$, $g_2 = g_3$.

The interesting conclusions are the differences of relative signs of g_8: the sign is + in § 2 and in the Euclidian space (§§ 4.3 and 6), it is − in the Lorentz space (§§ 4.1, 4.2 and 5). The Lorentz space requires $g_2 = g_3 = 0$, the Euclidian space does not.

We have not commented on the approximations $m_\Lambda = m_\Sigma$ and $m_N = m_\Xi$ which are essential to the entire work. Schwinger has suggested that, perhaps owing to π interactions, there is a preferred axis in the 4-dimensional space. In the Lorentz formulations (§ 4.1, 4.2, 5) this fact can be simply attributed to the non-existence of π_0', then $g_1 \neq g_4$, producing the $N_1\Xi$ mass difference; similarly the Λ, Σ mass difference can be attributed to $g_3 \neq 0$. In the Euclidian formulations (§§ 4.3 and 6), π can always be considered as an antisymmetric self-dual tensor and therefore in § 6 the mass-differences cannot be accounted for in this straightforward fashion. Thus the too great symmetry of the Salam-Polkinghorne theory raises an essential difficulty.

Our thanks are due to Dr. F. Mandl for a helpful discussion. One of us (A. S.) would like to offer his sincere thanks to Professor Bakker for the hospitality of the CERN where this work was done.

References

1) B. d'Espagnat and J. Prentki, Nuclear Physics **1** (1956) 33
2) Abdus Salam, Nuclear Physics **2** (1956/57) 173
3) J Schwinger, Phys. Rev. **104** (1956) 1164, and mimeographed notes by L. S. Rodberg
4) C. N. Yang and T. D. Lee, Phys. Rev. **102** (1956) 290
M. Gell Mann, Rochester Conference Report, 1956 (Interscience publishers, New York)
5) P. T. Matthews and Abdus Salam, Nuclear Physics **2** (1956/57) 582
6) C. N. Yang and T. D. Lee, Nuovo Cimento **3** (1956) 749
7) Abdus Salam and J. C. Polkinghorne, Nuovo Cimento **2** (1955) 685
8) E. M. Corson, Introduction to tensors and spinors (Hafner Publ. Co, New-York, 1953) p. 46
9) F. Duimio, Nuovo Cimento **3** (1956) 595

Nuclear Physics **3** (1957) 456—464; *North-Holland Publishing Co., Amsterdam*

THE DIPOLE SUM RULE WITH AN APPROXIMATE HAMILTONIAN

J. S. LEVINGER

Department of Physics and Astronomy,† Louisiana State University, Baton Rouge, La.

N. AUSTERN

Sarah Mellon Scaife Radiation Laboratory,†† University of Pittsburgh, Pittsburgh, Pa.

P. MORRISON

Newman Laboratory of Nuclear Studies, Cornell University, Ithaca, N.Y.

Received 26 January 1957

Abstract: The familiar f sum rule for the electric dipole interaction of a complex charge-current system with the electromagnetic field is known to be simply applicable even when exchange forces and other non-classical dynamical effects are present. Evaluation of the f sum for absorption from the ground state can be made knowing only the Hamiltonian and the ground state wave function. For complex systems the exact wave function is rarely known. Two methods of estimating the f sum are then attractive whenever an independent particle model is empirically favored: (i) use of the best IPM wave functions and the true Hamiltonian, or (ii) use of the same wave functions but the equivalent one-body potential found to give best energy levels for the IPM. In the first calculation, dynamical correlations are neglected; in the second, a spurious contribution to the sum arises from the velocity dependent form typical of an equivalent one-body potential.

We compute the f sum by both methods in a nuclear example. The results show the differences of principle which arise, though the numerical agreement is rather close. Physical arguments are given for the origin of this close agreement, which can be expected only in particular cases. No criterion for the reliability of such IPM sum rule calculations is known.

1. Introduction

The sum rules specifying the overall interaction of the electromagnetic field with a dynamical system very often have been used in lieu of more detailed models of complicated systems. They suggest themselves for such studies because they appear less dependent on the details of the interaction among the particles. Moreover, for the most important of the sum rules, the f sum rule for the electric dipole interaction, it has been shown by Siegert [1]) that the electric dipole operator retains the classical form

$$\mathbf{D} = \sum_i e_i \mathbf{r}_i \tag{1}$$

even in the presence of exchange interactions and other non-classical dynamical effects. We shall discuss this sum rule exclusively, primarily because of

† Supported in part by the National Science Foundation.

†† Supported in part by the joint program of the Office of Naval Research and the Atomic Energy Commission.

its relevance to the nuclear photoeffect at energies up to some 50 MeV.

The dipole sum rule is essentially a classical result, depending on the conservation laws of current and of energy. For a set of harmonically bound particles each of mass M and of charge $f_i e$, the classical theory of scattering[2]) gives for the electric dipole absorption cross section, integrated over all frequencies ω,

$$\int_0^\infty \sigma(\omega)\mathrm{d}\omega = (2\pi^2 e^2/Mc) \sum_i f_i. \tag{2}$$

Here the dynamics of the system plainly does not enter. But it has been known for a long time [3]) that the extension of this simple result to a more complicated multiply-periodic system demanded the use of at least this general feature of a dynamical system: that the momenta enter the hamiltonian only through a homogeneous quadratic form, the kinetic energy. The presence of other momentum-dependent terms in the hamiltonian modifies the classical sum.

The general relation of the dipole sum rule to the momentum-dependence of the hamiltonian was given by Sachs and Austern [4]) who derived it from the requirements of gauge invariance. One may write [5])

$$\int_0^\infty \sigma(W)\mathrm{d}W = (2\pi^2 e^2 \hbar/Mc) \sum_n f_{0n}. \tag{3}$$

(The appearance of $\hbar$ in this otherwise classical formula comes simply from the use of the photon energy $W = \hbar\omega$ for the integration.) For gauge invariance, the f sum must be given by the expression

$$\sum_n f_{0n} = -\frac{M}{\hbar^2}\langle\psi_0|[[\mathscr{H}, D_z], D_z]|\psi_0\rangle. \tag{4}$$

The sum is just the ground state expectation value of the double commutator of the hamiltonian with the z component of the dipole operator (1). If we write the hamiltonian as $\mathscr{H} = T+V$, the kinetic energy term involves the momenta of all the particles in the familiar quadratic way, and leads to the familiar Thomas-Reiche-Kuhn result (see ref. [5])). The term arising from V demands special treatment.

For a nuclear system in which the hamiltonian contains the coordinates and momenta of N neutrons and Z protons, but those of no other particles (such as mesons), the kinetic energy term leads to a contribution NZ/A, and (4) reduces to

$$\sum_n f_{0n} = NZ/A + \sum_n{}' f_{0n}. \tag{4'}$$

The second term will vanish if the nuclear interaction depends only upon the coordinates (including spin or isobaric spin) of the nucleons. But if exchange terms occur in V, or indeed any other form of explicit or implicit

dependence on $\mathbf{p}_i$, then V and $\mathbf{r}_i$ do not commute, and contributions to the sum beyond that of the kinetic energy are to be expected.

2. Independent Particle Models and the Sum Rule

2.1. ATOMS AND METALS

The description of many-particle systems by the use of independent particle wave functions, with the substitution of an equivalent one-body potential for the true interactions, is the basis of much of the work on these systems. It was Fock [6]) who first showed that the dipole sum rule for the Hartree-Fock atom departed from the T-R-K value, because the exchange interactions, arising from the effects of the Pauli principle, are dependent upon the state of the system under study, and amount to a velocity-dependent potential. Since the true interactions, however, are electrostatic and velocity-independent, the true value of the atomic dipole sum rule is just the familiar result

$$\sum_n f_{0n} = Z. \tag{5}$$

The departure comes from the use of the Hartree-Fock wave functions instead of the real, somewhat correlated wave functions

In a similar way the motion of an electron in a degenerate electron gas is governed by an equivalent one-body potential, say $V_{\mathrm{eq}}(\mathbf{r}, \mathbf{p})$, which is velocity-dependent because of the exchange energy terms required by the exclusion principle, in a way analogous to that of the Hartree-Fock atom. The case of the metal is indeed simpler, in that the surface effects are neglected, so that the equivalent potential depends only upon the electron momentum, and not on its spatial position: $V_{\mathrm{eq}} = V(\mathbf{p})$. If now we evaluate the second term of the appropriate analogue to (4′) using

a) single-particle Fermi gas wave functions, and

b) the equivalent potential,

it makes a finite contribution to the sum. But it is clear that the true pairwise-interacting electrostatic hamiltonian contains no momentum-dependent part except T, so that, using exact antisymmetric wave functions and the true hamiltonian, the f sum should contain no contribution from the second term. The former procedure using V_{eq} is in error. Whether the inaccuracies of the wave function might tend to cancel those of the use of V_{eq} is an open question.

It is, moreover, physically plausible that such approximations as we have just mentioned *ought* to give incorrect estimates of the f sum. For they all substitute a non-local potential, $V_{\mathrm{eq}}(\mathbf{r}, \mathbf{p})$, to represent the effect of correlations imposed on the electron wave function both by Coulomb interactions and by the Pauli principle. Such correlations in general give rise to currents, which are ignored in using the one-body approximations. These currents

influence the dipole sum, and must precisely cancel the effect on the sum of the equivalent velocity-dependent potentials used. The total f sum for any system of electrons moving in a Coulomb field must be just the Thomas-Reiche-Kuhn value for the system considered. Only for photon momenta which are so low as not to be influenced by the momentum space effects of the spatial correlations between electrons, can the individual oscillator strengths f_{0n} be approximated by the independent particle model predictions. (See Wilkinson [7]).

2.2. THE DIPOLE PHOTOEFFECT IN NUCLEI

It is physically clear that not all the currents which flow in nuclei need arise from actual nucleon motion, but that some are caused by the exchange of charged mesons. No such currents exist in systems of electrons. These currents must show up at some photon frequency as a contribution to electromagnetic absorption. Experiments indeed tend to show that the f sum for nuclei is larger than NZ/A. With the correction to the f sum no longer spurious, it is necessary to develop a reliable method for computing the second term of eq. (4'). A correct phenomenological calculation of this term must use the explicit exchange forces, and with them a correct ground state wave function ψ_0, which describes both the nucleon correlations which arise from the exclusion principle and those which have an independent dynamical origin in virtual meson exchange †. This approach is hardly practical, however. In analogy to the simple methods discussed for electronic systems, we therefore might instead consider calculating (4') by using

(I) the most plausible, phenomenological two-body potentials, but with the simple wave functions suggested by the independent particle model, or

(II) the independent particle model wave functions, but together with them the equivalent velocity-dependent one-body potential of which they are eigenstates.

Levinger and Bethe [5]) followed the first method (I) listed above in their study of the photonuclear dipole giant resonance. They evaluated the f sum using a Fermi gas wave function for ψ_0, and for V a sum of two-body potentials, partly of Majorana space-exchange type. The Majorana parts of V do not commute with $\mathbf{D}$, so contribute to $\Sigma' f_{0n}$ an amount proportional to the amount of exchange force. Using a pure Majorana potential of strength sufficient to bind the deuteron, they found the second term of (4') about equal to the first term. An adequate fit to experiment is achieved if $\Sigma' f_{0n}$ is about half NZ/A, so implying that the Majorana part of the nucleon-

† All this presupposes that in some approximation the nucleons retain an identity within the nucleus; if this is not true, the radiation interaction will be given correctly only from the many-body hamiltonian of the meson theory.

nucleon potential has a relative strength of about 50 %, in agreement with several other lines of evidence †.

In the last years the independent particle model for nuclei has gained much success. In the present context this suggests the evaluation of the f sum by following the second listed procedure above. D. H. Wilkinson [7]) particularly has called attention to the impressive success of the shell model in describing the width of the photoeffect giant resonance, and its narrowing near magic numbers. To be sure, the resonance position is too low on the models so far used, as Burkhardt [11]) has shown directly. Whether this is to be remedied by the use of a more suitable velocity-dependent shell model potential to give the position of the higher states, as experiment now suggests, or whether this is a sign of the importance of nucleon correlation in favoring high momentum components in the true ground state wave function, is not known.

But it is interesting to formulate the sum rule study of the photonuclear dipole giant resonance as completely as possible in the shell model context. The term $\Sigma' f_{0n}$ is to be evaluated with the shell model wave function Φ_0 and the effective potential V_{eff}. This will produce an increase in Σf_{0n} over NZ/A.

3. An Example of f Sum Evaluation in the Shell Model

We propose to illustrate the two methods of f sum evaluation in a simple approximate version of the shell model. We shall specialize to the case of mirror nuclei, with $N = Z = A/2$, and consistently neglect the Coulomb forces as well as any other difference between the neutron and proton wave functions. Any spin dependence of the nuclear forces will be neglected as well.

Now the z component of the electric dipole moment operator can be written as

$$D_z = \tfrac{1}{2}(\sum_i z_i - \sum_j z_j). \tag{6}$$

where the subscript i refers to protons, j to neutrons. (This notation will be maintained throughout the discussion.) Use of the general formula (4) now yields the f sum value. The TRK result as usual arises from the kinetic energy terms of the hamiltonian.

The contribution of the potential energy to the f sum is first computed using the actual two-body nucleon interactions, in the way employed by Levinger and Bethe [5]). It is plain that ordinary forces between nucleons will

† LB not only considered the dipole f sum rule, but also several other sum rules, from which they hoped to be able to estimate the shape of the absorption curve. They found results which were in very serious disagreement with experiment, so remarked on a possible need to use wave functions which express strong correlations between the nucleons; independent particle wave functions, like that of the Fermi gas, presumably being very inaccurate. But subsequent work [8, 9, 10]) showed that they had made inadequate use of the Pauli principle, which does not explicitly influence the f sum, and that the correct evaluation of these other sums with the use of independent particle model wave functions also can be made to give results in agreement with experiment.

give no additional contribution to the f sum because such potentials will commute with the coordinates. Exchange forces of Majorana type between like particles (neutron-neutron or proton-proton) will not contribute because the terms will cancel in pairs when we sum over all the nucleons to form D_x (cf. LB, eq. (8)). If we insert into (4) a *purely Majorana* exchange force between protons and neutrons, which we may write

$$V(\mathbf{r}_i, \mathbf{r}_j) = \sum_i \sum_j J(|\mathbf{r}_{ij}|) P^{\mathrm{M}}_{ij}, \quad \text{with } P^{\mathrm{M}}_{ij} f(\mathbf{r}_{ij}) = f(-\mathbf{r}_{ij}), \tag{7}$$

the evaluation of the f sum, as in LB, leads to four terms, each a double commutator of the form

$$[[V, \sum_\alpha z_\alpha], \sum_\beta z_\beta] \tag{8}$$

but differing in that the four include all combinations of the sums $\Sigma_i z_i$ over protons and $\Sigma_j z_j$ over neutrons. These reduce to identical values, and relying upon the assumption of similar neutron and proton wave functions, the triple sum in (8) reduces [10]) to the double sum †

$$\Sigma' f_{0n} = -\frac{M}{\hbar^2} \langle \psi_0 | \sum_i \sum_j J(r_{ij}) (z_i - z_j)^2 P^{\mathrm{M}}_{ij} | \psi_0 \rangle. \tag{9}$$

This can be evaluated using, say, the simple plane-wave Fermi wave functions,

$$\psi_0^* P^{\mathrm{M}}_{ij} \psi_0 = \prod_i \prod_j \exp(-i\mathbf{k}_i \cdot \mathbf{r}_{ij}) \exp(i\mathbf{k}_j \cdot \mathbf{r}_{ij})$$

We now proceed to make the computation in the other order: first constructing an equivalent one-body potential, which will be velocity-dependent, then evaluating the finite commutator of this potential with the coordinate of each particle, and finally summing over all particles. We cannot of course construct from specified two-body interactions a true one-body equivalent potential. We shall instead make use of the suggestion of Van Vleck [12]) He averaged the given two-body interactions over the occupied states of a Fermi gas. This is a kind of first Born approximation of the true many-body problem, at least if one looks apart from all effects of a finite nuclear volume. It has recently been given some small support by the more powerful methods of Brueckner and others (cf. Bethe [13]) † †).

We write first the Van Vleck potential $\overline{V}_i$ arising from Majorana interaction of a single proton with all the neutrons of the nucleus:

$$\overline{V}_i(\mathbf{k}_i) = \sum_j \int \psi_j^* J(r_{ij}) P^{\mathrm{M}}_{ij} \psi_j \, \mathrm{d}^3 \mathbf{r}_j. \tag{10}$$

† *Note added in proof:* The approximation procedure discussed in ref. [10]) is required only because the nuclear centre of mass motion was introduced approximately in ref. [5]). Eq. (9) actually is exact, and is given as (A-17) of the paper by N. Austern and R. G. Sachs, Phys. Rev. 81 (1951) 710. That equation, in turn, was derived from eq. (35) of ref. [4]).

† † *Editor's note.* Cf. also Weisskopf [18]).

A similar sum will apply for the nuclear neutrons, and the total equivalent one-body potential will be just

$$\overline{V} = \sum_i \overline{V}_i(\mathbf{k}_i) + \sum_j \overline{V}_j(\mathbf{k}_j). \tag{11}$$

If the sum in (10) is evaluated with Fermi-gas wave functions, as in (9), the potential $\overline{V}_i$ shows a marked dependence on the proton wave number $\mathbf{k}_i$. For a typical case, $|\overline{V}_i(\mathbf{k}_i)|$ decreases by about a factor of two from $\mathbf{k}_i = 0$ to the Fermi surface, $\mathbf{k}_i = \mathbf{k}_F$. These results are computed using a nuclear radius $1.2A^{1/3} \times 10^{-13}$ cm, and a gaussian neutron-proton potential completely Majorana in character. It is the velocity dependence of this part of the equivalent one-body potential which makes the main addition to the f sum.

There is an additional contribution to the Van Vleck potential arising from the like-particle forces. Van Vleck found that the effective potential for a proton, $\overline{V}_i$, was increased by 3/8 of its value when proton-proton forces with the same potential function $J(r_{ij})$ were considered.

Now the contribution which such a velocity-dependent one-body potential makes to the f sum follows from the general relation of (4). The double commutator of a coordinate with a function of its conjugate momentum can be evaluated by making the usual operator substitution, $\hbar\mathbf{k}_i = \mathbf{p}_i = (\hbar/i)\nabla_i$, and using the fundamental commutation rules for conjugate variables. In this way the terms of this contribution may be written

$$[\overline{V}, \sum_i z_i], \sum_j z_j] \propto \sum_i \sum_j \partial^2 \overline{V}/\partial k_{zi}\, \partial k_{zj} = 0. \tag{12}$$

Here the value of the mixed commutator, combining a proton with a neutron sum, is plainly zero. Let us compare this result with that of the first method of calculation. For the case here considered, the four terms of form (8) contributed equally in the direct computation from two-body forces. Here instead only two terms remain: that contribution is cut in half. This reduction is partially compensated by that part of the Van Vleck potential which arises from like-particle forces. Thus the overall Van Vleck result is simply the earlier Levinger-Bethe result multiplied by a numerical factor;

$$\frac{(\sum' f_{0n})_{\mathrm{VV}}}{(\sum' f_{0n})_{\mathrm{LB}}} = \frac{(3/8)+x}{2x} \tag{13}$$

where x is the fraction of Majorana exchange potential in the total interaction. For a Serber mixture ($x = \frac{1}{2}$, half exchange, half ordinary) the results are

$$\text{for the potential } V\text{: } \sum f_{0n} = 1.4NZ/A,$$
$$\text{for the potential } \overline{V}\text{: } \sum f_{0n} = 1.35\,NZ/A.$$

These values are surprisingly close; it is worth while to emphasize that they are computed from expressions which differ in form, and that the agreement represents a partial compensation of errors.

A physical argument may suggest the nature of the difference. The missing

contribution in the Van Vleck procedure arises from the vanishing of the mixed commutators of (12). These vanish because the equivalent one-body potential for the protons, say, evaluated for the ground state, cannot depend on the momentum of any neutron in the nucleus. This independence is guaranteed by the summation over the neutron states throughout the whole of the Fermi sphere, as required by the Van Vleck prescription (10). But one may argue that the direct evaluation of the f sum, which with exact wave functions demands only a knowledge of the ground state wave function, physically arises from considering first the absorption of a gamma ray to form some excited state and then eliminating the particular excited state by an application of closure. From this point of view, one may be led to modify the Van Vleck potential. For the interaction with radiation empties a state within the Fermi sphere, and causes the occupation of another state. It might seem plausible to form the Van Vleck potential by summing then over the states actually occupied after such a transition, and not over the Fermi sphere. In such a procedure, the potential $\overline{V}_i$ would certainly depend on the neutron state involved, and therefore $\partial^2 \overline{V}/\partial k_i \partial k_j$ would no longer vanish. It seems possible in this way to recover f sums for the unlike-particle contributions, nearly identical with the result of the first procedure. But this type of calculation plainly surrenders the accuracy and generality claimed by the f sum, which ought to depend only upon the ground state. The whole matter reinforces the idea that there is an essential arbitrariness in the application of the sum rules when only approximate wave functions are available.

4. Conclusions

We have considered the two simple paths to the evaluation of the f sum, through the relation (4), which seem useful when an independent particle model of a dynamical system is a useful approximation. In general these cannot agree, and neither is entirely defensible. If the actual interactions are used it is necessary to use a correlated wave function for the ground state, some error being made if an uncorrelated wave function is used instead. If we attempt to circumvent this error by using in conjunction with the uncorrelated shell-model-type wave function the appropriate ground state equivalent one-body potential, a new error certainly is made: the velocity dependence of the equivalent potential tends to add a new contribution to the f sum. But such an addition is physically absent. It seems plausible that this second kind of error would be unimportant only if the shell model wave functions and potential were reliable in some sense not only for the lowest energy states of the system but even for those lying at excitations where the bulk of the oscillator strength in photo-absorption is found. The unanswered question is just what test exists for this reliability. The generally valid sum rules are by themselves insufficient.

It may still be hoped that the sum can be computed for nuclei using independent particle wave functions and the empirically-founded velocity-dependent "optical" potentials, such as those of Taylor [14]) or of Saxon *et al.* [15]). If these do arise from static potentials between two nucleons, it is possible that the sum so evaluated will lie close to the true value, as does the Van Vleck to the LB result in the computation above. It is to be stressed that there is no known theoretical foundation for such a hope; it is based entirely on the incomplete analogy with this rough computation. No such conclusion can be stated if the optical potentials should be consequences of a theory like that of Johnson and Teller [16]), and of Rand [17]), in which the nucleons in a nucleus partially lose their individual identities. For such a theory the radiation interaction can be understood only from the fundamental many-body hamiltonian of the theory.

References

1) A. Siegert, Phys. Rev. **52** (1937) 787
2) W. Panofsky and M. Phillips, Classical Electricity and Magnetism (Addison-Wesley, Cambridge, Mass., 1955)
3) F. Reiche and W. Thomas, Zeitschrift f. Physik **34** (1925) 510
4) R. Sachs and N. Austern, Phys. Rev. **81** (1951) 705
5) J. S. Levinger and H. A. Bethe, Phys. Rev. **78** (1950) 115 (cited as LB)
6) V. Fock, Zeitschrift f. Physik **89** (1934) 744
7) D. Wilkinson, Proceedings of the Glasgow Conference on Nuclear Physics (Pergamon Press, 1954); Physica **22** (1956) 1039
8) J. S. Levinger and D. C. Kent, Phys. Rev. **91** (1953) 420
9) J. S. Levinger, Phys. Rev. **97** (1955) 122
10) J. S. Levinger, Phys. Rev. **101** (1956) 733
11) J. L. Burkhardt, Phys. Rev. **91** (1953) 420
12) J. Van Vleck, Phys. Rev. **48** (1935) 367
13) H. A. Bethe, Phys. Rev. **103** (1956) 1353
14) T. Taylor, Phys. Rev. **92** (1953) 831
15) Melkanoff, Moszkowski, Nodvik and Saxon, Phys. Rev. **101** (1956) 507 (L)
16) M. Johnson and E. Teller, Phys. Rev. **98** (1955) 783
17) S. Rand, Phys. Rev. **99** (1955) 1620
18) V. Weisskopf, Nuclear Physics **3** (1957) 423

Nuclear Physics **3** (1957) 465—470; *North-Holland Publishing Co., Amsterdam*

ELECTRON CAPTURE IN ARSENIC 74 AND ARSENIC 76

J. SCOBIE

Department of Natural Philosophy, University of Glasgow

Received 1 February 1957

Abstract: The radiations of As^{74} and As^{76} have been studied, using proportional tube spectrometers with gaseous sources of radioactive arsine. Peaks have been observed in the As^{74} pulse spectrum, corresponding to the K and L radiations of germanium emitted in the electron capture decay to Ge^{74}. From the number of counts in the observed peaks and the total number in the pulse spectrum the ratio of electron capture to electron emission was found to be 0.67 ± 0.04. The ratio of L-capture to K-capture, determined from the relative areas under the electron capture peaks, is 0.085 ± 0.020, in agreement with the theoretical value of 0.095.

A search has been made for electron capture in As^{76}, using a proportional counter with an internal anti-coincidence system to reduce wall-effect. No K-capture was observed with an intensity greater than 0.02 % of the negatons.

1. Introduction

The radioactive isotopes As^{74} and As^{76} lie on either side of the only stable isotope of arsenic and from isobaric triplets with stable isotopes of germanium and selenium. They are therefore both unstable with respect to electron capture to Ge^{74} and Ge^{76} respectively.

Arsenic 74 is known to decay, with a half-life of about 18 days, by negaton emission to Se^{74}, and by positon emission and electron capture to Ge^{74}. The most recent work [1]) reports the presence of two negaton groups and two positon groups leading to the ground states and excited states of the respective stable isotopes. An accurate measurement of the relative probabilities of electron capture and electron emission, combined with the known intensities of the electron groups, would lead to a value for the ratio of electron capture to positon emission. In particular, it is of interest to compare the ratio for the first forbidden ($\Delta I = 0$, yes) transition with the theoretical allowed value. The experimental limits on the previous estimate of this ratio were such that a comparison was not attempted [1]). Robinson and Fink have pointed out, in a recent review [2]), that very few direct measurements have been made of the L-capture to K-capture ratio where the transition energy is known, and that a large proportion of the measured values are in disagreement with the theory. In the present work the relative intensity of electron capture and the ratio of L-capture to K-capture were determined.

Arsenic 76 is known to decay [3]), by the emission of four negaton groups, to the ground state and excited states of Se^{76}, with a half -life of 26 hours.

The energy available for the transition to Ge^{76} is reported to be 1.1 ± 0.1 MeV [3]), and attempts to observe positon emission have been made by several workers, resulting in an upper limit of 0.07 % of negaton emission [4]). No search for electron capture has been reported, and, in view of the large energy difference, it seemed desirable to carry out such a search.

For accurate work involving low energy Auger electrons and X-rays the proportional counter, with internal gaseous source, is the most suitable type of spectrometer, eliminating the large errors, due to scattering and absorption, associated with solid sources. Accordingly this technique was employed in the present work.

2. Electron Capture in As^{74}

The As^{74} was made by (γ, n) reaction on arsenic using the photon beam from the Glasgow 350 MeV electron synchrotron. Arsenious oxide was compressed in a ring of glass tubing and fixed in a position in front of and concentric with the beam collimator. In this way the source was left in position for five weeks without disturbing other workers using the machine. Arsine gas was made by dropping magnesium turnings on a solution of the radioactive arsenious oxide in dilute hydrochloric acid.

Part of the arsenious oxide was mounted, as an internal solid source, on the walls of a small proportional counter, and the decay of the total counting rate and of the K-capture counting rate observed for six half-lives. The counting rates decayed together with a half-life of 18 days. A long-lived component, with an intensity of about 1 % of the As^{74} activity, was observed in the decay of the total counting rate, and the experimental results were adjusted accordingly.

In the experiments on As^{74} the proportional counter used had a diameter of 14 cm and a sensitive length of 35 cm, defined by field correcting tubes. Arsine to a pressure of about 1 mm Hg was introduced into the counter, and methane to a pressure of 7 cm Hg and argon to two atmospheres, were added. The presence of the arsine in the counter did not appreciably affect the energy resolution, as defined by the width of the peak due to the 9.2 keV X-rays from the external Ge^{71} source used for calibration.

That part of the pulse spectrum in the energy region between 2 keV and 20 keV was examined with a Hutchinson-Scarrot multichannel kicksorter, and a prominent peak was observed whose energy, by comparison with the Ge^{71} calibration peak, was found to be 11.1 keV, corresponding to the K absorption energy of germanium. The amplifier gain was increased by a factor of eight, and the pulse spectrum between 0.2 keV and 3 keV was analysed as before. Another peak was observed at about 1.3 keV, corresponding to the L absorption energy of germanium. Fig. 1 shows that part of

the pulse spectrum in the energy region between 0.2 keV and 18 keV and includes both electron capture peaks.

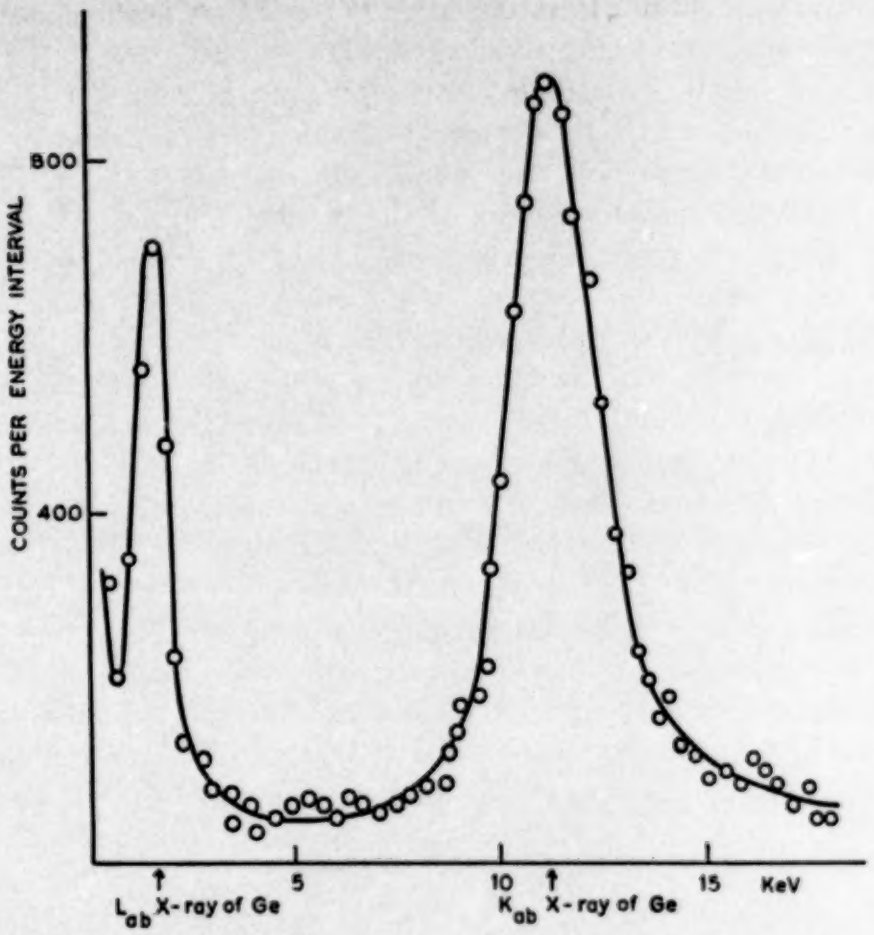

Fig. 1. Part of the proportional counter pulse spectrum of As^{74} including both electron capture peaks. This has been constructed from separate curves of the K and L peaks.

The relative intensity of electron capture was determined from the number of counts in the two peaks and the total number of counts in the spectrum. It was calculated that only 3.2 % of K-captures yielded K X-rays which escaped completely and did not lead to a count in either peak. The number of electrons, obtained from the total number of pulses recorded, was corrected for those particles entering the sensitive volume from the ends of the counter. This correction was calculated to be 7.5 % of the number of electrons. A similar correction, calculated to be 1 %, was applied to the observed number of K X-rays.

On completion of the measurements the proportional counter was pumped out and refilled with an argon-methane mixture as before. The pulse spectrum was analysed as before, and it was found that 18 % of the As^{74} activity had been deposited on the walls of the counter. Total counting rates, and the areas under K and L peaks taken at different times, in-

dicated that no loss of source occurred during the measurements, so it may be assumed that adsorption takes place immediately after filling. The difference between the observed spectra, after allowing for decay, is the pulse spectrum due to the gaseous source.

After applying these corrections, and taking into account the uncertainty in estimating the areas of the capture peaks, the branching ratio of electron capture to electron emission was found to be 0.67 ± 0.04. Using the latest values of the relative intensities of the electron groups [1]) the ratio of electron capture to positon emission becomes 1.42. Combining this result with the theoretical ratio (0.8) for the low intensity first forbidden unique transition to the ground state, a value of 1.49 is obtained for the first forbidden ($\Delta I = 0$, yes) transition to the first excited state. This is an increase over the theoretical allowed value (1.2) of about the same magnitude as that observed recently for a similar transition in Rb^{84} [5]).

From the relative areas of the observed peaks the L/K capture ratio can be obtained. The observed L peak arises from L-captures and from K-captures which are followed by the escape of K_α X-rays from the sensitive volume. Since the sensitive volume is a right cylinder the fraction of K X-rays escaping can be calculated with an accuracy depending only on the accuracy of the X-ray absorption coefficients of argon [6]). This escape fraction was calculated to be 29 % and 42 % for the K_α and K_β radiations respectively, using values of 65 gm/cm^2 and 49 gm/cm^2 for the absorption coefficients [7]). A value of 0.52 was used for the K fluorescence yield of germanium [8]), and the ratio of K_α intensity to total K X-ray intensity was taken as 0.85 [7]).

Using these values it was calculated that 12.8 % of the K-captures give rise to pulses in the L-peak. The ratio of counts in the L-peak to counts in the K-peak was observed to be 0.250 ± 0.025, giving a ratio of L-capture to K-capture of 0.085 ± 0.020, in agreement with the theoretical value of 0.095 [9]). This result is comparatively insensitive to variations in the value assumed for the fluorescence yield, a change of 10 % in the latter giving rise to a change in the L/K ratio of 0.017.

3. Search for Electron Capture in As^{76}

The main difficulty in the use of gaseous sources in proportional counters for the measurement of low intensity electron capture transitions, in competition with electron emission, is due to the steep rise in the electron pulse spectrum at low energies due to wall effect. Previous work with a conventional proportional counter had shown that this rise would have obscured any electron capture peak with an intensity less than 0.4 % of the negaton disintegrations.

Recently, Drever, Moljk and Curran [10]) have constructed proportional

counters with very small wall effects, obtained by surrounding the main counter with a ring of anti-coincidence proportional counters within the same tube, the cathodes of the ring counters consisting of a system of wires at the same potential as the case. The counter used in the present work was similar to these, but was considerably smaller and simpler. Perspex was used for all insulators and no guard tubes were used on the twelve ring counters. The total diameter was 7.5 cm and the sensitive length was 50 cm. The electronic system used was similar to that described by Drever *et al.* and the pulse spectra were analysed with the multichannel kicksorter. A cross-section through the proportional counter is shown in fig. 2.

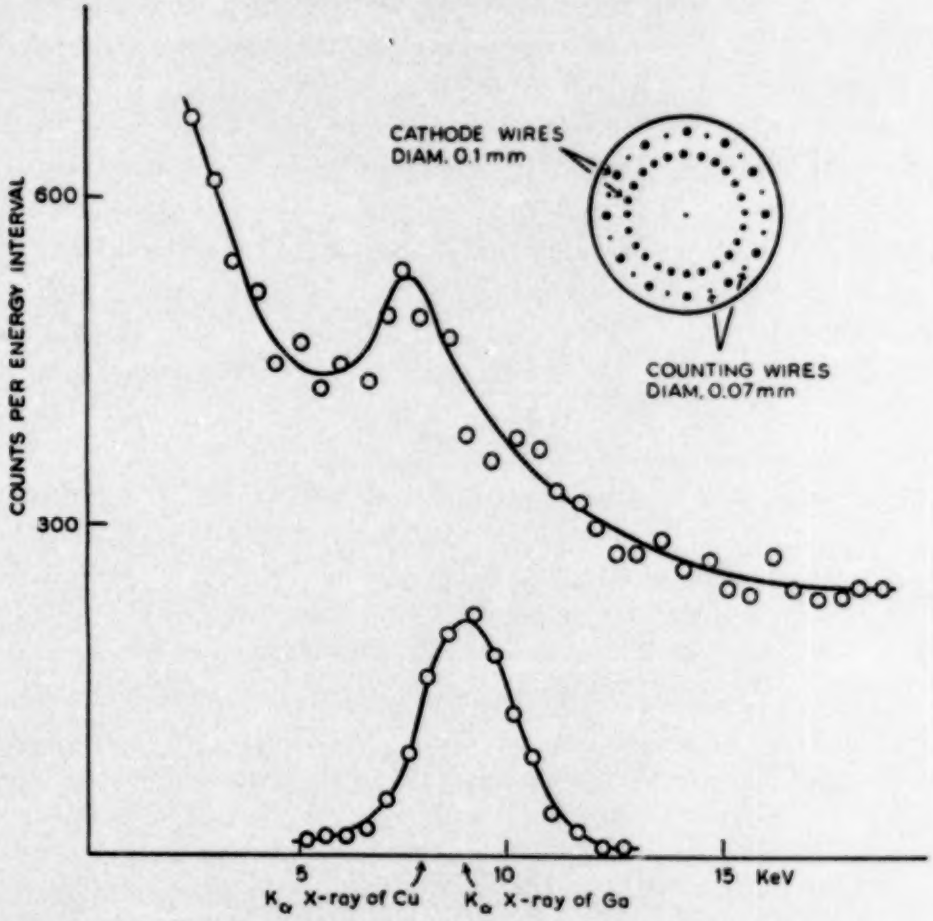

Fig. 2. Part of the proportional counter pulse spectrum of As^{76}. The lower curve is the peak due to the 9.2 keV X-rays from an external Ge^{71} source. Inset is a cross-section of the proportional counter used.

The As^{76} was obtained from A. E. R. E. Harwell in the form of arsenious oxide and the radioactive arsine was made as before. A trace of arsine was introduced into the counter which was then filled to a total pressure of two atmospheres with an argon-methane mixture. The operation of the counter was checked by the resolution of the 9.2 keV X-ray peak from an

external Ge^{71} source which was used for energy calibration. To confirm the identity of the As^{76} source the total counting rate in the proportional counter was observed for several half-lives, and the characteristic gamma rays were observed in a NaI scintillation spectrometer. After pumping out and refilling the counter it was found that 6 % of the source had been deposited on the counter wall.

That part of the pulse spectrum in the energy range between 2.5 and 17.5 keV is shown in fig. 2. A small peak at about 8 keV is superimposed on the continuous electron spectrum, which has been greatly reduced by the operation of the anti-coincidence system. This peak is interpreted as due to K X-rays of copper produced by the excitation of atoms in the counter wall by gamma rays originating in the insensitive regions at the ends of the counter. The lower curve in fig. 2 shows, on a different vertical scale, the peak due to the 9.2 keV X-rays of the Ge^{71} calibration source, observed under the same conditions. The width of this latter peak is about the same as that obtained with a conventional argon-methane filled counter, and it is clear that the presence of the arsine and the unusual construction of the counter have not seriously affected the energy resolution.

There is no evidence of a peak at 11.1 keV, the K absorption energy of germanium, and, comparing the statistical uncertainty at that part of the curve with the area under the copper peak, namely 0.035 % of the electron disintegrations, it is concluded that the upper limit for the probability of K-capture is 0.02 %.

A similar search, with negative result, was made for L-capture, although it is unlikely that the energy available for capture is so low as to make L-capture more probable than K-capture.

The author would like to thank Professor P. I. Dee for his interest and encouragement, Dr. G. M. Lewis for his supervision and advice, and Dr. A. Moljk and Mr. R. W. P. Drever for valuable discussions. The author is also grateful to Dr. W. McFarlane and the Synchrotron crew for their cooperation, and is indebted to the University of Glasgow for a scholarship.

References

1) S. Johansson, Y. Cauchois and K. Siegbahn, Phys. Rev. **82** (1951) 275
2) B. L. Robinson and R. W. Fink, Rev. Mod. Phys. **27** (1955) 424
3) Nuclear Level Schemes, United States Atomic Energy Commission (June 1955)
4) W. Mims and H. Halban, Proc. Phys. Soc. A **64** (1951) 311
5) J. P. Welker and M. L. Perlman, Phys. Rev. **100** (1955) 74
6) J. M. Hammersley, Proc. Roy. Soc. A **210** (1951) 98
7) A. H. Compton and S. K. Allison, X-rays in Theory and Experiment (Macmillan Company, London, 1935)
8) C. D. Broyles, D. A. Thomas and S. K. Haynes, Phys. Rev. **89** (1953) 715
9) H. Brysk and M. E. Rose, Oak Ridge National Lab. Report O.R.N.L. — 1830 (1955)
10) R. W. P. Drever, A. Moljk and S. C. Curran, Nuclear Instruments **1** (1957)

Nuclear Physics **3** (1957) 471—475; *North-Holland Publishing Co., Amsterdam*

SOME REMARKS ON DECAY RATES OF HEAVY MESONS

B. D'ESPAGNAT, R. OMNES†, J. PRENTKI

CERN, *Geneva*

Received 18 February 1957

Abstract: The lifetimes of particles and their antiparticles are discussed under different assumptions. It is shown that if P · C is conserved these lifetimes are rigorously equal, but in practice their equality is no evidence for P · C conservation even when strong final state interactions do exist. The P · C conservation is best tested by the K^0 modes of decay. A description of $K\mu\nu$ interaction by means of a direct coupling only (Yukawa type) is shown to be impossible.

Lee and Yang [1]) have considered the possibility of parity non-conservation in weak interactions. This proposal has recently received experimental confirmations [2, 3]).

Pauli [4]) and Lüders [5]) have shown that invariance of a Lagrangian under proper Lorentz transformation — the connection between spin and statistics being taken into account — automatically yields the invariance of the theory under P · C · T (product of P = parity, C = charge conjugation and T = time reversal). Thus in the reactions induced by weak interaction Hamiltonians which are not invariant under P there is non-conservation either of C or T or both. As, on the other hand, the results of the Columbia experiments [2, 3]) seem to imply C non-conservation, two possibilities have to be considered:

A) T is conserved but not C; this hypothesis is clearly equivalent to the assumption that P·C is conserved.

B) Neither T nor C are conserved.

In the present paper, weak couplings of the usual types (without derivatives of the fermion fields) are considered. The following propositions can then be proved.

1) *If* P·C *is conserved the lifetimes of a particle and its antiparticle are rigorously equal.*

If P · C commutes with the Hamiltonian H it also commutes with the T matrix, which is a function of H:

$$(PC)^{-1}T(PC) = T.$$

The T matrix, on the other hand, can always be split into two parts

$$T = T^{(+)} + T^{(-)}$$

such that

$$P^{-1}T^{(\pm)}P = \pm T^{(+)}. \qquad (1)$$

† On leave from C. E. A. Saclay, France.

Then

$$\begin{aligned}\langle b|T^{(\pm)}|a\rangle &= \langle b|P^{-1}C^{-1}T^{(\pm)}PC|a\rangle \\ &= \langle \bar{b}|P^{-1}T^{(\pm)}P|\bar{a}\rangle \\ &= \pm\langle \bar{b}|T^{(\pm)}|\bar{a}\rangle\end{aligned} \tag{2}$$

where $\langle \bar{b}| = \langle b|C^{-1}$ and $|\bar{a}\rangle = C|a\rangle$ are the charge conjugate states of $\langle b|$ and $|a\rangle$ respectively. The (exact) partial decay rate for the decay of a particle $|a\rangle$ into the state $|b\rangle$ is given, apart from a density of state factor, by

$$|T_{ba}|^2 = |T^{(+)}_{ba}|^2 + |T^{(-)}_{ba}|^2 + 2\,\mathrm{Re}\,(T^{(+)}_{ba}T^{(-)*}_{ba}), \tag{3}$$

while, using (2), that of the corresponding antiparticle into state $|\bar{b}\rangle$ is given by

$$|T_{\bar{b}\bar{a}}|^2 = |T^{(+)}_{ba}|^2 + |T^{(-)}_{ba}|^2 - 2\,\mathrm{Re}\,(T^{(+)}_{ba}T^{(-)*}_{ba}) \tag{3'}$$

with a summation over angles, spins, etc. of states b and $\bar{b}$ respectively. Now it is easily seen that in such a summation the last term in (3) and (3') necessarily vanishes. (One can for example split the summation over b states into a sum over the states b' having the same parity as a, for which $T^{(-)}_{b'a} = 0$, and a sum over the states b'' having opposite parity, for which $T^{(+)}_{b''a} = 0$.) Thus $|T_{ab}|^2 = |T_{\bar{a}\bar{b}}|^2$. From the equality of the partial decay rates the equality of the total lifetimes follows.

2) *If* P·C *is conserved, a neutral complex boson field of a given type can describe two particles with different possible decay modes and thus with very different lifetimes.*

This is indeed a trivial generalization of the Gell-Mann-Pais theory [6]). Let us assume that K is a scalar (any other assumption on spin and parity could be treated in a similar way); then

$$(PC)^{-1}\theta(PC) = \theta^\dagger, \qquad (PC)^{-1}\theta^\dagger(PC) = \theta. \tag{4}$$

With the definitions

$$\theta_1 = \frac{1}{\sqrt{2}}(\theta+\theta^\dagger), \qquad \theta_2 = \frac{1}{i\sqrt{2}}(\theta-\theta^\dagger) \tag{5}$$

one has

$$(PC)^{-1}\theta_1(PC) = \theta_1, \quad (PC)^{-1}\theta_2(PC) = -\theta_2: \tag{6}$$

θ_1 and θ_2 correspond to the eigenvalues $+1$ and -1 respectively for P·C. As a two pion system has $P = C = (-1)^l$ and thus $P{\cdot}C = +1$, it follows that θ_2 cannot decay into two pions, whereas θ_1 does decay very rapidly into that mode †.

The assumption of P·C conservation thus leads quite naturally to two very different lifetimes, just as the Gell-Mann-Pais theory [6]). Of course, both θ_1 and θ_2 can decay into the modes $K_{\mu 2}$, $K_{\mu 3}$, K_{e3}, $K_{\pi 3}$. Although two lifetimes should exist [7]) even if P·C is not conserved, it is only with P·C

† Notice that the decay $\theta^0 \to 2\pi^0$ implies that θ has an even spin, independently of whether P and C are conserved or not.

conservation that the two corresponding particles have different possible decay modes and that, therefore, a lifetime ratio as large as the observed one [8]), i.e. about 100, fits in a natural way into the theory.

3) Let us consider the decays

$$\theta_2^0 \to e^+ + \pi^- + \nu \quad \text{(b state)} \tag{7}$$

$$\theta_2^0 \to e^- + \pi^+ + \bar{\nu} \quad (\bar{\text{b}} \text{ state}). \tag{7'}$$

As the θ_2^0 field is self conjugate one has (compare with eq. (2)), if P·C is conserved,

$$T_{\theta b}^{(\pm)} = \pm T_{\theta \bar{b}}^{(\pm)}. \tag{8}$$

Thus the decay rates are, apart from the common density-of-states factor,

$$|T_{\theta b}|^2 = |T_{\theta b}^{(+)}|^2 + |T_{\theta b}^{(-)}|^2 + 2 \operatorname{Re} (T_{\theta b}^{(+)} T_{\theta b}^{(-)*}) \tag{9}$$

$$|T_{\theta \bar{b}}|^2 = |T_{\theta b}^{(+)}|^2 + |T_{\theta b}^{(-)}|^2 - 2 \operatorname{Re} (T_{\theta b}^{(+)} T_{\theta b}^{(-)*}). \tag{9'}$$

These formulae immediately show that

(i) on the whole, one should observe the same amount of decays (7) as of decays (7') (the last term in (9) and (9') gives zero after integration);

(ii) if θ has spin zero, or is not polarised, the angular correlations between π and e should be identical for both decay modes (7) and (7') (this follows from the odd parity of the last term in eq. (9) and from the fact that, as the momenta of the three outgoing particles are not independent, the pseudoscalars that can be formed must involve a spin vector and thus give zero when the summation over final polarisations is performed);

(iii) under the same assumptions as in (ii) and if not only the directions but also the polarisations of the emerging leptons are measured, the corresponding angular correlations between π and e should be different in (7) and in (7');

(iv) if θ^0 had a spin and were polarised the angular distributions of the π's (or the e's) would be different in (7) and (7') (the odd powers of $\cos\theta$ would differ in sign).

All these considerations are of course equally valid for the $\pi + \mu + \nu$ decays. Thus a detailed study of the anomalous θ^0 may help to decide whether P·C is really conserved and could furthermore give some complementary indications about the θ^0 spin.

4) Under the assumption that P·C is not conserved, Lee, Oehme and Yang [7]) have shown that the lifetimes of a charged particle and of its antiparticle are still equal in lowest order approximation. We here extend their proof to the case that strong and electromagnetic interactions exist among the decay products. Only the case of initital spin zero is considered here.

Let a refer to the initial state, α, $\beta \ldots$ to the final states. The final state interactions are taken into account by use of the equations [9])

$$K_{\beta a} = H_{\beta a} + \mathrm{P} \sum_{\gamma} \frac{\mathscr{K}_{\beta\gamma} H_{\gamma a}}{E_a - E_\gamma} \tag{10}$$

$$T_{\beta a} = K_{\beta a} - i\pi \sum_{\gamma} \varrho_\gamma \mathscr{T}_{\beta\gamma} K_{\gamma a} \tag{11}$$

where $H_{\beta a}$ is the lowest order approximation for the process considered, $\mathscr{K}$ and $\mathscr{T}$ being the reaction matrix and T matrix for final state interactions. The H, K and T matrices can still be split in the same way as in eq. (1). Then (see ref. [7]))

$$H^{(\pm)}_{\bar{\beta}\bar{a}} = \pm H^{(\pm)*}_{\beta a}. \tag{12}$$

As $\mathscr{K}_{\beta\gamma}$ conserves parity and C, it follows from (10) that

$$K^{(\pm)}_{\bar{\beta}\bar{a}} = \pm K^{(\pm)*}_{\beta a}. \tag{13}$$

Splitting now eq. (11) into two equations (for $T^{(+)}$ and $T^{(-)}$), writing the corresponding equations for antiparticles and using (13), one gets

$$T^{(\pm)}_{\beta a} = K^{(\pm)}_{\beta a} - i\pi \sum_{\gamma} \varrho_\gamma \mathscr{T}_{\beta\gamma} K^{(\pm)}_{\gamma a} \tag{14}$$

$$\pm T^{(\pm)}_{\bar{\beta}\bar{a}} = K^{(\pm)*}_{\beta a} - i\pi \sum_{\gamma} \varrho_\gamma \mathscr{T}_{\beta\gamma} K^{(\pm)*}_{\gamma a}. \tag{15}$$

For final states of total angular momentum zero it can be shown by using the invariance of strong and electromagnetic interactions under time reversal that

$$\mathscr{K}_{\alpha\beta} = \mathscr{K}_{\beta\alpha} = \mathscr{K}^*_{\alpha\beta} \qquad \text{(real and symmetric)}, \tag{16}$$

$$\mathscr{T}_{\alpha\beta} = \mathscr{T}_{\beta\alpha} \qquad \text{(symmetric)}. \tag{17}$$

Eqs. (14), (15), (17) and $\mathscr{T}^+\mathscr{T} \propto \mathscr{T}^+ - \mathscr{T}$ (unitarity of the $\mathscr{S}$ matrix) then give

$$\sum_{\beta} |T^{(\pm)}_{\beta a}|^2 = \sum_{\beta} |T^{(\pm)}_{\bar{\beta}\bar{a}}|^2.$$

The partial decay rates are, just as in § 1, proportional to expressions (3) and (3′) (with the change of notation $\mathrm{b} \to \beta$) and it is shown by the same argument as above that the cross-term vanishes. Thus the lifetimes are again equal in this approximation. In view of the smallness of the weak interaction coupling constants the equality of lifetimes of θ^+ and θ^- is not therefore an argument in favour of P·C conservation.

5) Finally we would like to point out that, independently of whether P·C is conserved or not, *the existence of both* $K \to \mu + \nu$ *and* $K \to \pi + \mu + \nu$ *decays and the assumption that only one type of K meson exists, make it impossible to describe K, μ, ν interactions by means of Yukawa type couplings* $(\bar{\psi}\psi\varphi)$; this result being rigorous if the K meson has zero spin. The proof [10])

lies in the fact that the graph of fig. 1 is not possible because of parity conservation in strong interactions. If the spin is not zero this proof is no longer valid; however, the experimental ratios $K_{\mu 2} : K_{e2}$ and $K_{\mu 3} : K_{e3}$ would still be extremely difficult to interpret by means of these interactions. It

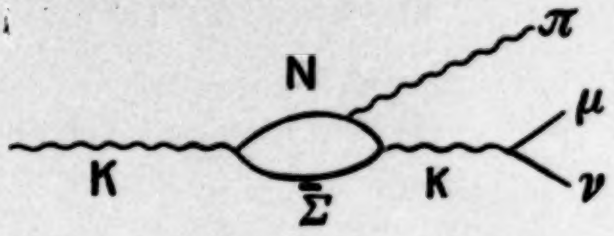

Fig. 1

thus turns out that the violations of parity and strangeness conservation rules and the necessity of introducing interactions other than $\bar{\psi}\psi\varphi$ (and the derived electromagnetic ones) all appear simultaneously in the weak interactions.

References

1) T. D. Lee and C. N. Yang, Phys. Rev. **104** (1956) 254; see also L. D. Landau, Nuclear Physics **3** (1957) 127
2) C. S. Wu, E. Ambler, R. W. Hayward, D. D. Hoppes and R. P. Hudson, Phys. Rev. (to be published)
3) R. L. Garwin, L. M. Lederman and M. Weinrich, Phys. Rev. (to be published)
4) W. Pauli, in Niels Bohr and the development of physics (Pergamon Press, London, 1955)
5) G. Lüders, Mat. Fys. Medd. Dan. Vid. Selsk. **28** (1954) no. 5
6) M. Gell-Mann and A. Pais, Phys. Rev. **97** (1955) 1387
7) T. D. Lee, R. Oehme and C. N. Yang, Phys. Rev. (to be published)
8) K. Lande *et al.*, Phys. Rev. **103** (1956) 1901
9) B. d'Espagnat et J. Prentki, Nuovo Cimento **3** (1956) 1045
10) B. d'Espagnat et J. Prentki, Nuovo Cimento **4** (1956) 1572

Nuclear Physics **3** (1957) 476—478; *North-Holland Publishing Co., Amsterdam*

POLARISATION IN THE ELASTIC SCATTERING OF NEUTRONS BY HELIUM

R. E. WHITE AND F. J. M. FARLEY

Auckland University College, Auckland, New Zealand

Received 26 January 1957

Abstract: The polarisation of neutrons in elastic scattering by helium is studied using polarised neutrons from a D—D source and observing the left-right asymmetry of recoil tracks in a helium-filled proportional counter. The polarisation is 0.46 ± 0.18 for 3 MeV neutrons.

The large spin-orbit coupling observed in studies of He^5 have led several workers to suggest the use of helium as a polarizer or analyser for fast neutrons [1, 2, 3]). This idea is strengthened by the calculations of Adair [1]) and Seagrave [4]) on neutron scattering by helium which predict large polarizations of order 30—80 per cent. These predictions do not however appear to have been tested experimentally, although the polarization of protons by scattering in helium has been verified in double scattering experiments [5]).

In the present experiment partially polarized neutrons derived from the D—D reaction are used, and the polarization properties of scattering by helium can then be established by a single scattering experiment.

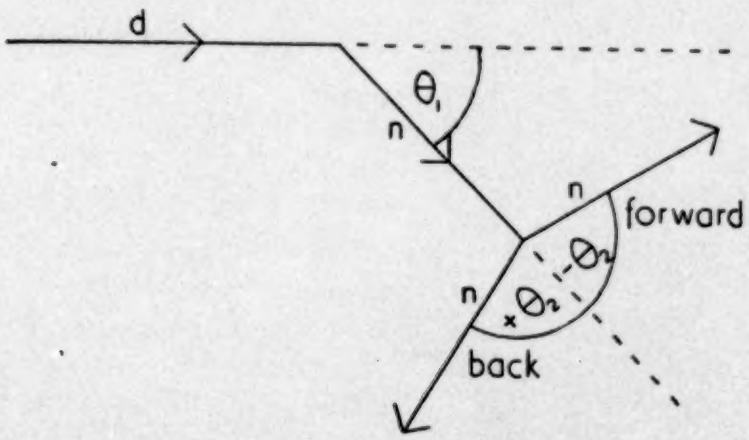

Fig. 1.

In our experiment we do not attempt to detect the neutrons after scattering, but instead look for a right-left asymmetry in the number of recoil alpha particles using a gaseous helium scatterer. A helium recoil counter with directional properties is used for the measurements.

The geometry of the experiment is shown in the figure. Neutrons from the D—D reaction are emitted at laboratory angle θ_1 to the direction of the incident deuterons and are then scattered by helium through laboratory angles $+\theta_2$ or $-\theta_2$ as shown.

If the polarization of the neutrons from the D—D reaction is $P_1(\theta_1)$ and if neutrons of this energy (initially unpolarized) would receive a polarization $P_2(\theta_2)$ on scattering by helium, then the ratio of left-right intensities in the above experiment is

$$R = \frac{I(+\theta_2)}{I(-\theta_2)} = \frac{1+P_1P_2}{1-P_1P_2} \quad (1)$$

i.e.

$$P_1P_2 = \frac{R-1}{R+1}. \quad (2)$$

In our experiment R is obtained from the number of alpha-particle recoils corresponding to neutrons scattered through $+\theta_2$ and $-\theta_2$. In theory a maximum polarization P_2 is obtained when $\theta_2 = 76°$ corresponding to scattering through 90° in centre of mass space. This corresponds to alpha-particles recoiling at 45° with respect to the direction of the incident neutrons, and therefore the left and right directions of the recoil alpha-particle are at right angles to each other and can readily be distinguished in a helium recoil counter with directional properties. The angle θ_1 is 45°, the angle at which most of the measurements of the D—D polarization have been made. The neutron energy with 300 keV deuterons incident on a heavy ice target is 2.9 MeV, giving recoil alpha-particles at 45° of energy 1.0 MeV.

A helium recoil counter with directional properties is achieved simply by arranging that the track length in the counter gas is larger than the diameter, and orienting the counter with its axis at 45° to the incident neutrons. The desired recoil tracks then travel more or less parallel to the axis of the counter and give a pulse-height corresponding to their energy, but the recoil tracks it is desired to exclude are perpendicular to the axis of the counter, and therefore can only dissipate a fraction of their energy in the counter gas giving a smaller pulse. Tracks around 45° in the undesired direction are therefore completely excluded. In the desired direction the exact range of angles around 45° is defined by means of the energy range accepted in the channel of a pulse height analyser.

In these experiments a proportional counter of diameter 2.5 cm and sensitive length 5.5 cm was used and the filling pressure was such that 1.0 MeV alpha particles gave a track of length 5.0 cm. The analyser was set to accept alpha particles with energy in the range 0.8—1.0 MeV, corresponding to angles from 50°—45°. To make measurements of the asym-

metry the counter was oriented with its axis alternately at $+45°$ and $-45°$ to the direction of the incident neutrons, a fixed stilbene scintillator being used to monitor the neutron intensity. The ratios of intensities of neutrons scattered backwards $(+\theta_2)$ and forwards $(-\theta_2)$ were as follows:

θ_1	R, back/forward
0°	1.02 ± 0.08
45° left	0.87 ± 0.07
45° right	0.90 ± 0.06
45° down	0.85 ± 0.08

The result at $\theta_1 = 0^0$, for which the incident neutrons are unpolarized shows no asymmetry as expected. The other three results agree within statistical error and give a mean value $R = 0.87\pm0.05$. It follows from equation (2) that $P_1P_2 = -0.069\pm0.026$, and taking $|P_1| = 0.15$ [6, 12]) we find $|P_2| = 0.46\pm0.18$ in agreement with the predicted values for 3 MeV neutrons of 0.4 (Adair) and 0.2 (Seagrave).

The negative value obtained for P_1P_2 implies that the sign of the polarizations P_1 and P_2 given by the two reactions are opposite. Adopting the sign convention of Wolfenstein [7]) and of Meier, Scherrer and Trumpy [8]) (which is opposite to that used by Schwinger [3]), Lepore [2]), Seagrave [4]) and, presumably, Adair [1])) the polarization P_1 is negative for $\theta_1 = 45°$ [8]). Our experiment therefore confirms the positive value of P_2 predicted by Adair and by Seagrave for 3 MeV neutrons.

We wish to thank Dr. D. Brown and Mr L. M. Delves for their contributions in discussion, and one of us (R. E. White) is indebted to the University of New Zealand for a Senior Research Fund Fellowship.

Note added in proof: Similar experiments, carried out in the U.S.S.R., have recently come to our attention [9, 10]).

Editor's Note. See further ref. [11, 12]).

References

1) R. K. Adair, Phys. Rev. **86** (1952) 155
2) J. V. Lepore, Phys. Rev. **79** (1950) 137
3) J. Schwinger, Phys. Rev. **69** (1946) 681
4) J. D. Seagrave, Phys. Rev. **92** (1953) 1222
5) M. Heusenkveld and G. Freier, Phys. Rev. **85** (1952) 80
6) P. von Huber and E. Baumgartner, Helv. Phys. Acta **26** (1953) 40
7) L. Wolfenstein, Phys. Rev. **75** (1949) 1664
8) R. W. Meier, P. Scherrer and G. Trumpy, Helv. Phys. Acta **27** (1954) 577
9) I. I. Levintov, A. V. Miller and V. N. Shamshev, Dokl. Akad. Nauk. SSSR. **103** (1955) 803
10) I. I. Levintov, A. V. Miller, V. N. Shamshev and E. Z. Tarumov, Physica **22** (1956) 1181
11) I. I. Levintov, A. V. Miller and V. N. Shamshev, Nuclear Physics **3** (1957) 221
12) I. I. Levintov, A. V. Miller, E. Z. Tarumov and V. N. Shamshev, Nuclear Physics **3** (1957) 237

Nuclear Physics **3** (1957) 479—490; *North-Holland Publishing Co., Amsterdam*

THE ENERGY LEVELS OF Hf^{177} AND THE UNIFIED MODEL

S. OFER

Department of Physics, Hebrew University, Jerusalem

Received 31 January 1957

Abstract: A study of the γ-ray transitions between levels of Hf^{177} resulting from the β-decay of Lu^{177} has been made using fast-slow coincidence technique. The results and the proposed spin and parity assignments are discussed in the light of the unified model. A value of 0.2 is derived for the gyromagnetic ratio associated with the collective rotational motion.

1. Introduction

In the following work a study of the γ-ray transitions between levels of Hf^{177} resulting from the β-decay of Lu^{177} has been made. The work was in particular concerned with aspects of the γ-ray transitions which could yield information on those specific properties of levels which are connected with the deformed character of nuclei in this part of the periodic table. From the experimental results of the E2/M1 mixing ratios combined with the results of the magnetic moment of the ground state, a value for the gyromagnetic ratio associated with the rotational motion could be obtained, assuming the strong coupling unified model.

The interpretations of the decay schemes of Lu^{177} which have been proposed hitherto [1, 2]) have been based on the assumption that the spin of Hf^{177} in the ground state is less than or equal to 3/2. Recent spectroscopic research on hafnium enriched in Hf^{177} has shown that the spin of the ground state is 7/2 [3]). When this value is inserted in the formula giving the energy separation between rotational levels as excited by Coulomb excitation [4]), excellent agreement is obtained. The strong coupling calculation of Nilsson and Mottelson [5]) also predicts that the ground state of Hf^{177} should be 7/2—. In this work the spin and parity assignments of the excited levels were made in the light of this latter conclusion.

The disintegration of Lu^{177} was investigated by Marmier and Boehm [2]) who used a curved crystal γ-ray spectrometer. Their decay scheme, which was completely confirmed in this work, is given in fig. 1. The intensity of the 72 keV—250 keV cascade is about 1 % of the strong 208 keV—113 keV cascade. In this work the angular correlation of the strong cascade 208 keV —113 keV was measured for different liquid sources of different viscosities. In addition, the anisotropy of the weak cascade was measured. The K-con-

version coefficient of the 72 keV γ-ray was also measured. The last two experiments served to determine the spin and parity of the 321 keV level above the ground state. The experiments were carried out using two NaI scintillators in a fast-slow coincidence arrangement; the fast resolving time was 7×10^{-8} sec.

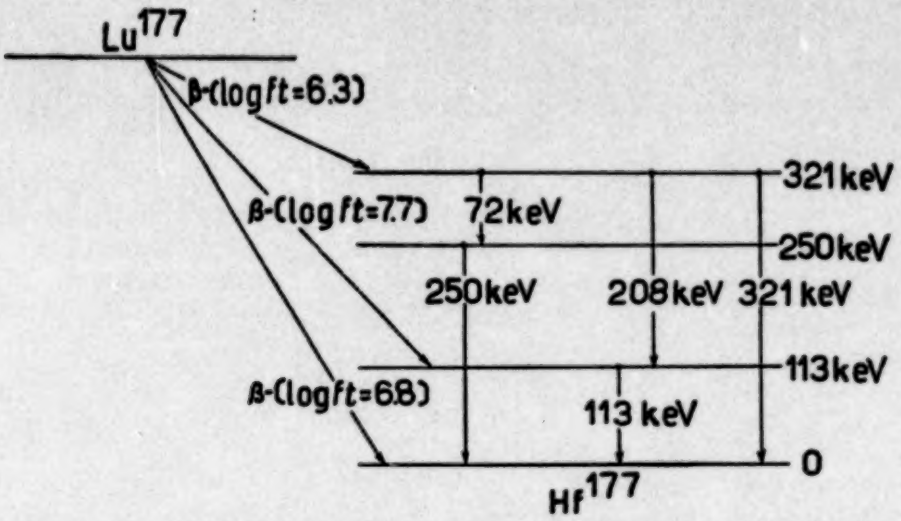

Fig. 1. Decay scheme of Lu^{177} as proposed by Marmier and Boehm [2]).

2. Measurement of the Angular Correlation of the 208 keV-113 keV Cascade

Two single channel pulse analysers were used in the slow channels to select the full peaks of each γ-ray. The distance between source and crystals was 10 cm. The measurements of the angular correlation were carried out for three liquid sources of Lu^{177} — a very dilute aqueous solution of $LuCl_3$ and two mixtures of the same aqueous solution with glycerine in different ratios.

The results are summarized in table 1, which gives the dependence of the angular correlation on the viscosity of the solutions. The anisotropy coefficients were calculated by least squares from the measured angular correlations and were corrected for finite solid angle effects.

TABLE 1
Anisotropy of 208 keV—113 keV cascade
for sources of different viscosities

Percentage of glycerine	Viscosity in c.g.s units	Experimental anisotropy	Coefficient of $P_2(\cos\theta)$ corrected for geometry	Attenuation of correlation
0	0.01	-0.186 ± 0.006	-0.130 ± 0.010	1
50	0.05	-0.194 ± 0.010	-0.135 ± 0.010	1
85	0.50	-0.142 ± 0.010	$-0.10\ \pm0.01$	0.75 ± 0.05

An inspection of the results shows, almost certainly, that the correlation measured in the purely aqueous source is unperturbed by time dependent

quadrupole interactions and can thus be relied upon in order to fix the spins of the levels and multipolarity of the radiations. On the other end, the correlation in the most viscous source is definitely perturbed.

3. Measurement of the K-conversion Coefficient of the 72 keV γ-ray

The K-conversion coefficient of the 72 keV γ-ray was measured by comparing the intensity of the 72 keV γ-rays and the KX-rays ($\approx$ 55 keV) resulting from this K-conversion. It is impossible to detect the low intensity

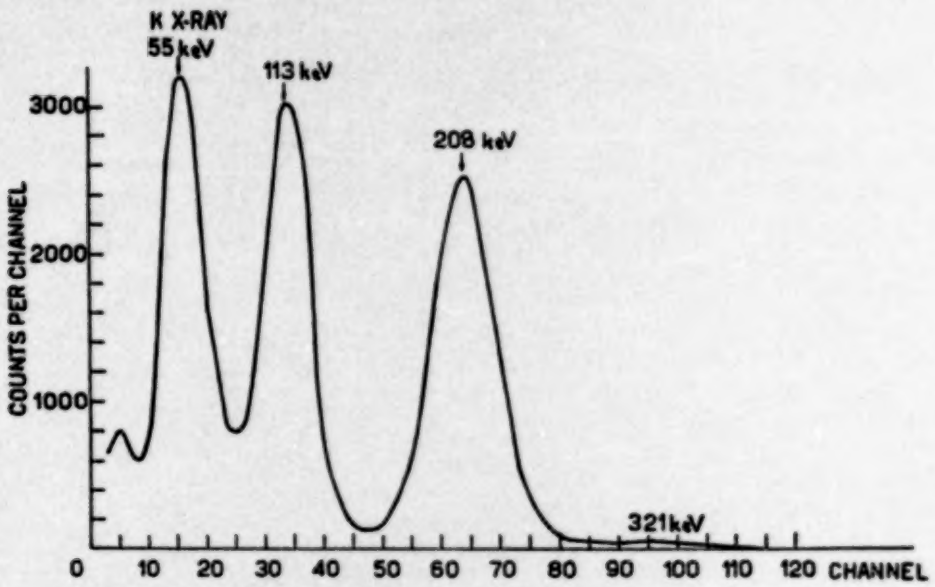

Fig. 2. "Singles" spectrum of γ-rays.

72 keV γ-ray in the "singles" spectrum which is shown in fig. 2 (the main γ-rays, 113, 208 and 321 keV show up clearly, as also does the X-ray peak at about 55 keV). It is possible, however, to compare the 72 keV γ-ray intensity

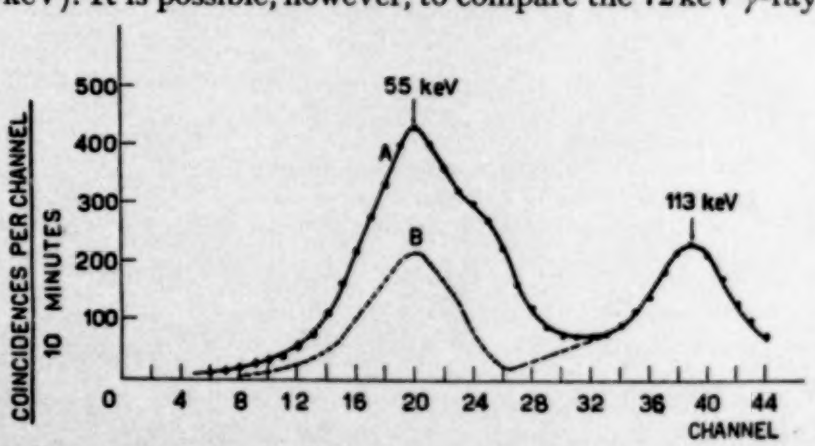

Fig. 3. A) Spectrum of pulse heights corresponding to γ-ray energies in the region of 0—150 keV obtained in one crystal when measured in coincidence with pulses in the second crystal falling in channel between 250 and 275 keV.
B) Corresponding coincidence spectrum when channel of second crystal is on the photo-peak of 208 keV γ-ray.

with the X-ray intensity in the spectrum of coincidence with the weak 250 keV γ-ray with which it is in cascade. (The 250 keV γ-ray is also not visible in the "singles" spectrum.) The spectrum of pulse heights corresponding to γ-ray energies in the range 0-150 keV obtained in one crystal was measured in coincidence with the pulses from the second crystal falling in a channel between 250 and 275 keV. The centre of this channel was chosen to be higher than the maximum of the photo-peak of the 250 keV γ-ray, in order to reduce the contribution of pulses from the tail of the 208 keV γ-ray photo-peak which would give coincidences with 55 keV X-rays and 113 keV γ-rays. The coincident spectrum was recorded by a 80 channels pulse analyser gated by the output of the fast-slow coincidence circuit. Curve A in fig. 3 shows the spectrum obtained in this way. From this figure it can be seen that there is a serious contribution to the coincidences arising from the 218 keV—113 keV cascade. Curve B in fig. 3 shows the coincidence spectrum in the same range

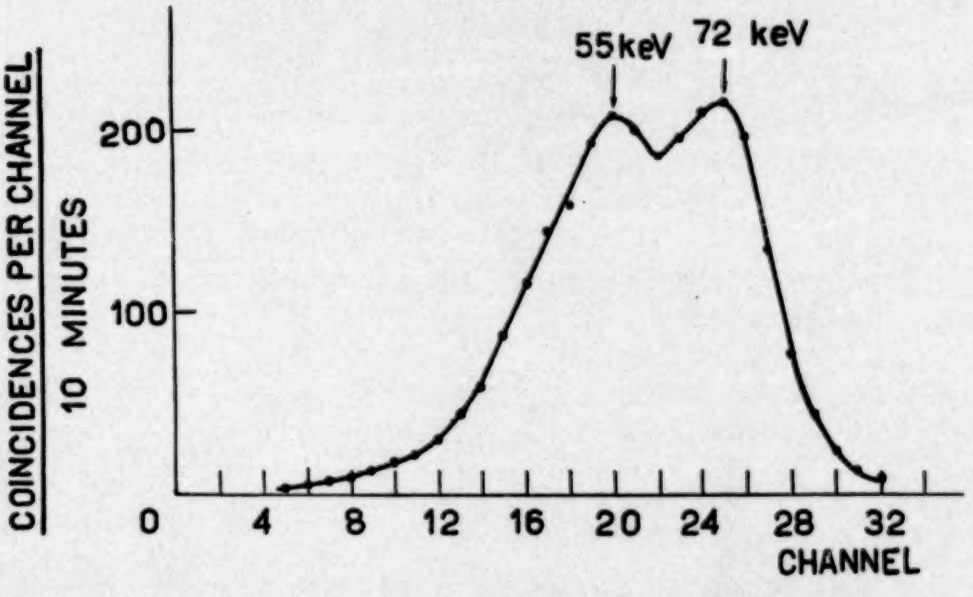

Fig. 4. Spectrum of γ-rays coincident with the 250 keV γ-ray obtained by subtracting curve B from curve A in fig. 3.

obtained when the second channel is placed on the photo-peak of the 208 keV γ-rays; the curves are normalised so that the 113 keV peaks are of the same intensity. For this normalisation, it is clear that the difference between these two curves gives the spectrum coincident with the 250 keV γ-rays. Fig. 4 shows this difference and displays the two close peaks arising from the K X-rays and the 72 keV γ-rays. From the ratio of intensities of these two peaks, taking into account the standard corrections for efficiencies and iodine X-ray escape probabilities and taking a value of 0.9 for the K fluorescent yield, we obtain a value of 1.0 ± 0.3 for the K-conversion coefficient for the 72 keV transition.

4. Measurement of the Anisotropy of the 72 keV-250 keV Cascade

In this measurement, one channel was chosen as above (between 250 keV and 275 keV), and the other channel was chosen between 65 keV and 80 keV to include the 72 keV γ-ray. The anisotropy in the 72 keV—250 keV cascade is diluted to a considerable extent, however, by the isotropic contributions of the 250 keV—55 keV and the 208 keV—55 keV cascades to the coincidences obtained with the above choice of channels. From the work described in the previous paragraph, it was concluded that 55 % of these coincidences belong to the 250 keV—72 keV cascade and 45 % originate in coincidences with the K X-rays. The latter obviously must clearly give an isotropic distribution. It is thus possible to correct the experimental results to obtain the anisotropy of the 72 keV—250 keV cascade.

The distance between source and crystals was 6 cm. Coincidences were measured only at angles of 90° and 180°. The coincidence rate was about 30/min, and at each angle about 20000 coincidences were recorded (changing the angle every five minutes). Lead absorbers were suitably disposed to prevent coincidences arising from Compton scattering of the higher energy γ-rays from one counter into the other; the lead was sheathed with copper to prevent the escape of lead X-rays from these absorbers into the counters. Measurements of the anisotropy were carried out for two liquid sources — a dilute aqueous solution of $LuCl_3$ and a mixture of this solution with glycerine having a viscosity of about 0.5 poise. The experimental results are given in table 2. In this table are also shown the anisotropies obtained after correcting for the presence of the isotropic X-ray cascade and geometrical

TABLE 2

Anisotropy of 72 keV—250 keV cascade for two sources of different viscosities

Viscosity	Experimental anisotropy	Anisotropy after corrections for X-ray cascade and geometrical effects
0.01	-0.09 ± 0.01	-0.20 ± 0.02
0.50	-0.08 ± 0.01	-0.18 ± 0.02

effects. The agreement between the anisotropies obtained with the two liquid sources imply that the correlations are not perturbed by quadrupole interactions, within the experimental error.

5. Spin and Parity Assignments

As mentioned in the introduction, the ground state spin of Hf^{177} has recently been found to be 7/2 [3]) and in accordance with the theoretical work of Mottelson and Nilsson [5]) which has been successful in predicting the spin and parity of nuclear ground states in the region of large nuclear deformations, we take the parity of the state to be negative. The ground state of

Lu^{177} is almost certainly 7/2+, since the experimental value for the spin of stable Lu^{175} is 7/2, and 7/2+ is the Mottelson-Nilsson prediction [5]). The two levels of Hf^{177} at 113 keV and 250 keV can undoubtedly be identified with the two first rotational levels which are obtained by Coulomb excitation [4]), and therefore these levels are 9/2− and 11/2− respectively.

According to the work of Marmier and Boehm [2]) in which the conversion coefficient of the 113 keV transition is measured, this transition is mostly E2 with not more than about 3 per cent admixture of M1. The K and L conversion coefficients obtained by Marmier and Boehm for the 208 keV transition show as can be seen from table 3, that this transition is mostly E1 with no more than 2 per cent admixture of M2. The value of the K conversion coefficient of the 72 keV transition obtained in this work is 1.0 ± 0.3. In view of the low energy of the transition, the value proves conclusively that the transition is essentially electric dipole. The cross-over transition of 250 keV must be E2.

TABLE 3

Experimental and theoretical values for the conversion coefficients of the 208 keV γ-line

	Experimental value	E1 theoretical value (according to Rose)	M2 theoretical value (according to Rose)
K	0.044	0.046	2.2
L_1	0.007	0.005	0.5

From the fact that the 72 keV and the 208 keV transitions are both essentially E1, it follows that the 321 keV state is either 9/2+ or 11/2+. The latter value is untenable for two reasons. The theoretical anisotropies for the

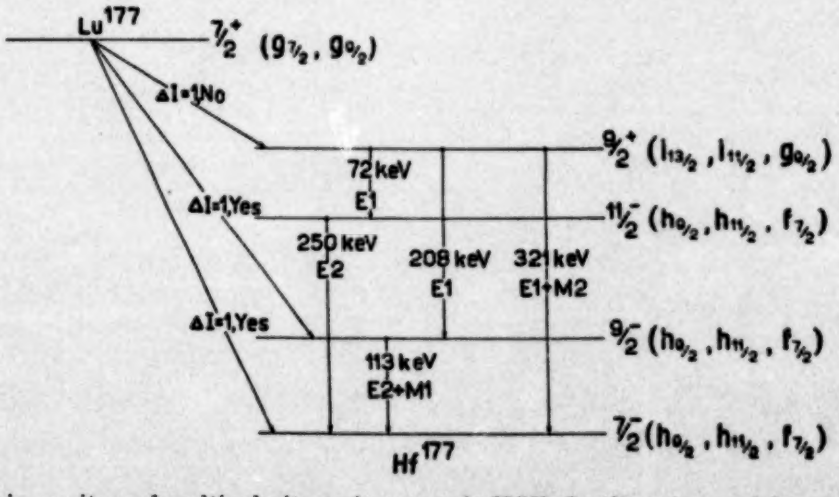

Fig. 5. Spin, parity and multipolarity assignments in Hf^{177}. On the extreme right are indicated the component single-particle shell model states in order of decreasing strength, according to the tables of Nilsson.

cascade 11/2(E1) 9/2(E2) 7/2 is +30 % and for the cascade 9/2(E1) 9/2(E2) 7/2 is −19 %. The present experimental value is -20 ± 2 %. Also, a spin of 11/2 for the 321 keV level would lead to a second forbidden β-transition to this level. This is not the case ($\log ft = 6.3$). The 321 keV level must therefore be 9/2+. In the light of this assignment to the 321 keV level and taking into account the experimental value of 0.2 for the K conversion coefficient of the 321 keV γ-ray, obtained by Marmier and Boehm [2]), it may be concluded that this transition, between the 9/2+ level at 321 keV and the 7/2− ground state is a mixture of about two-thirds E1 and one third M2. Fig. 5 shows the suggested spin and parity assignments for the levels and the multipole nature of the transitions. The spin and parity assignments are also in agreement with the experimental $\log ft$ values.

6. The E2/M1 Ratio in the 113 keV Transition

Accurate estimates of the E2/M1 mixing ratios cannot be obtained from measurements of the conversion coefficients because of the unreliability (particularly for the M1 transitions) of present theoretical values of the conversion coefficients due to finite nuclear size effects, and also because of the difficulty of making precise measurements. Large errors must be ascribed to some measurements which have been made of the E2/M1 ratios from the

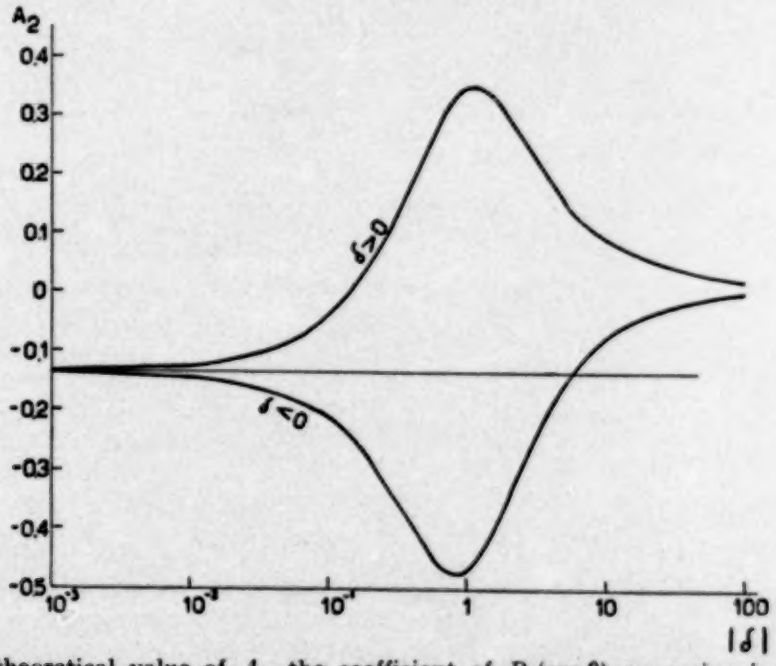

Fig. 6. The theoretical value of A_2, the coefficient of $P_2(\cos\theta)$ appearing in the angular correlation function for a 9/2(E1) 9/2(E1+M2) 7/2 cascade as a function of δ, where δ^2 is the E2/M1 mixing ratio. The horizontal line corresponds to the experimental value of A_2 equal to −0.135.

conversion coefficients. Under favorable circumstances, measurements of the angular correlation can yield reliable estimates.

In this work, the mixing ratio for the 113 keV transition was derived from the measurements of the angular correlation of the 208 keV−113 keV cascade described earlier. Fig. 6 shows the theoretical value for A_2, the coefficient of $P_2(\cos\theta)$ appearing in the correlation function for a 9/2(E1)9/2 (E1+M2)7/2 cascade, as a function of δ, where δ^2 is the ratio between E2 and M1 transition probabilities in the second transition of the cascade, on the assumption that the first component is pure electric dipole. The experimental value of A_2 is -0.135 ± 0.010. From this figure we see that δ can be 0 or -5.8. The value of zero would imply a pure M1 transition which is clearly excluded in the light of the conversion coefficients mentioned earlier. We are left with $\delta = -5.8$ or $\delta^2 = 34\pm4$, i.e. the magnetic dipole transition probability is 3 ± 0.5 percent of the electric quadrupole transition probability. It might be thought that since angular correlation can be sensitive to small amounts of multipole mixing, possible small admixtures of M2 radiation in the predominantly E1 radiation of 208 keV might invalidate the previous calculation which was made on the assumption that the E1 transition is pure. This point was examined and it was found that an assumption of 2 % M2 mixture in the 208 keV E1 transition leads to a value of 2.8 % or 3.2 % (depending on the sign of δ for the E1+M2 transition) for the ratio of M1 to E2 in the 113 keV transition. That is to say, in our case where the M1/E2 mixing ratio in the second component of the cascade is small, the correlation is not sensitive to a small M2 admixture in the first component.

7. Discussion of the Results in the Light of the Unified Model

7.1. THE 9/2 + LEVEL AT 321 keV

Nilsson and Mottelson [5]) predict the order of the single particles states in the deformed nucleus as a function of the nuclear deformation. For Hf^{177}, the nuclear deformation parameter as obtained from the measured quadrupole of the ground state [6]) is about 0.26. For this value, the next single particle state above the 7/2− state, should be, according to Nilsson and Mottelson, a 9/2+ state which agrees with the present result. The theoretical energy separation is about 400 keV which is to be compared with the experimental 321 keV.

7.2. BRANCHING RATIOS OF BETA AND GAMMA TRANSITIONS TO THE ROTATIONAL STATES OF Hf^{177}

It is one of the elegant predictions of the collective model that the ratio of the reduced transition probabilities for either β or γ transitions of the same multipolarity to different levels of a rotational band is given by a purely geometrical factor involving Clebsch-Gordan coefficients, as follows [6])

$$\frac{B(L, I_1 \to I_f)}{B(L, I_1 \to I_{f'})} = \frac{\langle I_1 L K_1 K_f - K_1 | I_1 L I_f K_f\rangle^2}{\langle I_1 L K_1 K_f - K_1 | I_1 L I_{f'} K_f\rangle^2}, \qquad (1)$$

where L denotes the multipolarity of the radiation and f and f′ denote levels belonging to the same rotational band.

Using the above formula, one obtains that the ratio between the ft value of the β-transition from Lu^{177} to the first rotational level of Hf^{177} and the ft value for the β-transition to the ground state is 3.5, taking $L = 1$ for both transitions. The experimental value deduced from the measurements of Marmier and Boehm is about 8. The explanation invoked by Chase and Wilets [7]) in order to account for a very similar discrepancy in the decay of Yb^{175} to the levels of Lu^{175} also serves very well in the present instance. Following Nilsson [8]), we may resolve the wave function of the 7/2+ ground state of Lu^{177} into two component single-particle shell model wave functions, the main component being $g_{7/2}$ with a small admixture of $g_{9/2}$. Similarly, the 7/2− ground state of Hf^{177} may be resolved into three shell model wave functions — a main component $h_{9/2}$ and two weak components of $h_{11/2}$ and $f_{7/2}$. (see fig. 5). The ground to ground β-transition will go not only by a $L = 1$ transition ($g_{7/2} \rightarrow h_{9/2}$) but also by a $L = 0$ transition ($g_{7/2} \rightarrow f_{7/2}$ and $g_{9/2} \rightarrow h_{9/2}$), whereas the transition from Lu^{177} to the first excited state of Hf^{177} can only go by a $L = 1$ transition ($L = 0$ forbidden since ΔI is not equal to zero). The presence of an $L = 0$ component in the β-transition to the ground state will increase the ratio of the ft values as defined above.

From the 9/2− level at 321 keV there are three competing E1 transitions to the three levels of the rotational band. Using equation (1) and taking into account the dependence of the transition probability on the third power of the energy, we obtain for the branching ratios to the ground state, first excited level and second excited level respectively, the values 4000 : 250 : 1. The experimental values obtained in the present work are about 10 : 150 : 1. There is a discrepancy of a factor of a hundred between the theoretical and experimental values for the branching ratio to the ground level and first rotational level. As pointed out by Chase and Wilets [7]) this kind of discrepancy is not surprising in light of the fact that the E1 transitions are almost completely forbidden (as can be seen in this work, for example, from the abnormally high M2/E1 ratio for the 321 keV γ-transition), so that small perturbations of the intrinsic nucleonic motion caused by the rotational motion may produce large changes in the E1 transition probabilities.

7.3. LIFE-TIME OF THE 113 keV LEVEL

Since we see that 113 keV transition is largely E2, the transition probability for the E2 transition fixes, essentially, the life-time of the 113 keV level. This may be calculated on the basis of the Bohr-Mottelson theory for a rotational transition, in terms of the intrinsic quadrupole moment Q_0 according to the formula [9]),

$$\tau_{\frac{1}{2}} = \frac{0.693\hbar L[(2L+1)!!]^2}{(1+\alpha)8\pi(L+1)B(\mathrm{E2}, I_1 \rightarrow I_f)}\left(\frac{c}{\omega}\right)^{2L+1}, \qquad (2)$$

where

$$B(\mathrm{E2}, I_1 \to I_f) = \frac{5}{16\pi} e^2 Q_0^2 \langle I_1 2K0/I_1 2I_f K\rangle^2. \tag{3}$$

After inserting the numerical values we obtain

$$\tau_{\frac{1}{2}} = \frac{2.50\times 10^{-58}}{Q_0^2} \text{ sec.}$$

Q_0, from recent measurement of the quadrupole moment of the ground state [10]) is 6.5×10^{-24} cm^2, and from measurements of the cross-section for Coulomb excitation [11]) is $(8\pm 2)\times 10^{-24}$ cm^2. From these values, one obtains for $\tau_{1/2}$ a value of about 5×10^{-10} sec. This is not in contradiction with the experimental upper limit of 5×10^{-10} sec obtained for the lifetime of this level [1]).

7.4. PERTURBATIONS OF THE ANGULAR CORRELATIONS

As is seen from table 2, the correlation of the 72 keV—250 keV cascade in a viscous liquid source is not perturbed, within the experimental errors whereas the correlation of the 208 keV—113 keV cascade is certainly perturbed for a liquid source with the same viscosity. This finds a ready interpretation in view of the fact that both the intermediate states in these cascades are rotational levels. According to the theory of Pound and Abragam [12]), the attenuation R of the coefficient of $P_2(\cos\theta)$ in the angular correlation caused by the time dependent interaction of the quadrupole moment of the gradient of the electric field in a liquid source is given by the formula $R = 1/(1+\lambda_2\tau)$ where τ is the lifetime of the intermediate state and λ_2 is given by

$$\lambda_2 = \frac{3}{80}\left(\frac{eQ}{\hbar}\right)^2 \left\langle \left(\frac{\partial^2 V}{\partial z^2}\right)^2 \right\rangle_{\mathrm{Av}} \cdot \tau_c \cdot \frac{6[4I(I+1)-7]}{I^2(2I-1)^2}. \tag{4}$$

If the transition probabilities and from them the lifetimes of the rotational levels are calculated on the basis of the unified model as given by formulae (2) and (3) above and if Q is derived from Q_0 by means of the formula [9])

$$Q = \frac{3I_0^2 - I(I+1)}{(I+1)(2I+3)} Q_0, \tag{5}$$

one can calculate the ratio of $\lambda_2\tau$ for the 250 keV and the 113 keV rotational levels. In the calculation of the ratio, the intrinsic quadrupole moment Q_0, the average square of the field gradient at the nucleus $\langle(\partial^2 V/\partial z^2)^2\rangle_{\mathrm{Av}}$ and the liquid correlation time τ_c, cancel out. The value obtained from this ratio is about 800. This, together with the experimental results for the perturbation of the 208 keV—113 keV cascade implies that the 72 keV—250 keV cascade should not be perturbed, even in a very viscous liquid source, as indeed was found to be the case.

7.5. CALCULATION OF GYROMAGNETIC RATIOS ACCORDING TO THE UNIFIED MODEL

According to the strong coupling collective model, the E2/M1 mixing ratio occurring in a rotational transition in an odd nucleus is related to both, the intrinsic quadrupole moment Q_0 and the difference between the intrinsic and the rotational gyromagnetic ratios $(g_k - g_r)$ according to the formula [13])

$$\delta^2 = \frac{3}{20I(I+2)} \left(\frac{Q_0 \cdot \Delta E \cdot M_0}{\hbar^2 (g_k - g_r)} \right)^2, \tag{6}$$

where I is the spin of the lower level, ΔE is the transition energy and M_0 is the nucleon mass. If Q_0 and ΔE are known, $|g_k - g_r|$ may be calculated. Another linear relation between g_k and g_r is provided by the expression for the magnetic moment of the ground state [9])

$$\mu = \frac{I_0^2}{I_0^2+1} g_k + \frac{I_0}{I_0+1} g_r . \tag{7}$$

From both these expressions g_k and g_r can be obtained separately. From equation (6), we obtain from the present measurements of for the 113 keV transition $|g_k - g_r| = 0.03 \pm 0.01$. The sign of $(g_k - g_r)$ is as the sign of Q_0/δ. It follows that $g_k - g_r = -0.03 \pm 0.01$. (In a recent work [14]) on Coulomb excitation of Hf^{177}, it was noted from a measurement of the ratio of the cross-over transition to the cascade transition from the 250 keV level that g_k is approximately equal to g_r, assuming the unified model.) From equation (7) and the recent measurement by optical methods of the magnetic moment of the ground state of Hf^{177} giving $\mu = 0.61$ [10]), we obtain $2.7 g_k + 0.78 g_r = 0.61$. Solving these equations, we obtain $g_r = 0.20 \pm 0.02$ and $g_k = 0.17 \pm 0.02$, neglecting errors in the magnetic moment measurements which are unknown to the author. Since $g_k - g_r$ is very small, the final estimate for g_r is not sensitive to errors arising in the determination of the mixing ratios. As discussed by Huus, Bjerregaard and Elbek [13]), most of the E2/M1 values for transitions from rotational states obtained from conversion coefficient measurements are very uncertain and values of $(g_k - g_r)$ derived from them are unreliable. A trustworthy estimate of g_r in an odd mass nucleus has been obtained by them for Ta^{181}. The value obtained was 0.17, which it is interesting to see is close to the present value.

One would expect a value of g_r equal to Z/A (0.4 for H^{177}) for the gyromagnetic ratio associated with the rotating nuclear matter, on the base of the Bohr-Mottelson theory. The values obtained experimentally, as described above, are about half this value. It will be easier to assess the significance of these results when the results of direct measurements of the gyromagnetic ratios for excited rotational states in even nuclei, which are now in progress[15]) will be known. It is interesting, however, to note that Blin-stoyle [16]) has suggested that low values of the nuclear gyromagnetic ratio associated with

rotational motion might be accounted for by a lower proton to neutron ratio in the outer rotating part of the nucleus.

The value of g_k equal to 0.17 obtained by the above analysis is to be compared with the value 0.43 obtained by using the formula for the intrinsic gyromagnetic ratio given by Nilsson [8]), together with his tables giving the amplitude of the single-particle isotropic oscillator functions which determine the wave functions in the deformed oscillator potential. It is perhaps not surprising that the agreement is not good, since the theoretical values of the magnetic moments are very sensitive to the form assumed for the nuclear wave functions. On the other hand, the formulae (6) and (7) from which our results for g_k and g_r are derived are only based on the assumption that it is possible to separate the intrinsic nucleonic motion and the collective rotational motion.

The author would like to thank Dr. S. G. Cohen for his continued interest and guidance.

References

1) F. K. McGowan, E. D. Klema and P. R. Bell, Phys. Rev. **85** (1952) 152
2) P. Marmier and F. Boehm, Phys. Rev. **97** (1955) 103
3) D. R. Speck and F. A. Jenkins, Phys. Rev. **101** (1956) 1831
4) H. P. Heydenburg and G. M. Temmer, Phys. Rev. **100** (1955) 150
5) B. R. Mottelson and S. G. Nilsson, Phys. Rev. **99** (1955) 1615
6) G. Alaga, K. Alder, A. Bohr and B. Mottelson, Dan. Mat. fys. Medd. **29** (1955) No. 9
7) D. M. Chase and L. Wilets, Phys. Rev. **101** (1956) 1040
8) S. G. Nilsson, Dan. Mat. fys. Medd. **29** (1955) No. 16
9) A. Bohr and B. Mottelson, Dan. Mat. fys. Medd. **27** (1953) No. 16
10) D. R. Speck and F. A. Jenkins, Bull. Am. Phys. Soc. **1** (1956) 282(C3)
11) P. H. Stelson and F. K. McGowan, Phys. Rev. **99** (1955) 112
12) R. N. Pound and A. Abragam, Phys. Rev. **90** (1953) 993
13) T. Huus, J. Bjerregaard and B. Elbek, Dan. Mat. fys. Medd. **30** (1956) No. 17
14) G. Goldring and G. T. Paulissen, Phys. Rev. **103** (1956) 1316
15) G. Goldring and P. R. Scharenberg (private communication)
16) R. J. Blin-stoyle, Rev. Mod. Phys. **28** (1956) 92

Nuclear Physics **3** (1957) 491—492; *North-Holland Publishing Co., Amsterdam*

BOOK REVIEWS

T. ROCKWELL (Editor), *Reactor Shielding Design Manual* (Mc Graw-Hill Book Co, New York, Toronto, London 1956. xii-481 pages, 43 s.)

The methods and data published in this handbook were developed for the design and construction of the shielding required for the United States Naval Reactors Project, and the Pressurised Water Reactor Project. A score of workers from these projects have contributed to the volume, but thoughtful editing has produced a unified handbook rather than a disconnected symposium. The design methods used in the above two projects are here generalised and systematised as far as present knowledge permits. In addition to the immediate problems of core shielding, coolant shielding, and shut-down access, the writers treat plant layout and shielding irregularities as major problems. A long chapter is devoted to the geometry of the radiation source.

Information is presented in full page graphs when this form is most useful to the designer, and its use illustrated where necessary by worked examples in the text. Reassuring comparisons are given between the theoretical methods of the handbook and experimentally obtained results. Many of the references are to U.S.A.E.C. reports, some of which are classified; it is unlikely that the practical designer would need to consult them. The writers admit that this manual is not a complete treatment of the subject, and express the hope that improvements can be made in a second edition to appear in the course of a year or so. This first edition is an extensive handbook of unclassified information, but the sections on, for example, gamma absorption, or shield fabrication and installation, could usefully be extended.

Since the methods described in this handbook have been tested in practice, it is claimed that they now permit a direct approach to shield design, obviating the need for preliminary tests on a full scale mock-up. The methods should also assist the designer in his search for the shield of lowest weight, volume, or cost. This is a most vital factor in the design of a propulsion reactor, and important in the case of a static installation.

J. Diamond

The physics of nuclear reactors (Supplement No. 5, British Journal of Applied Physics) (The Institute of Physics, London. 1956. 112 pages. 25 s.)

In July 1956, the Institute of Physics, in collaboration with the British Nuclear Energy Conference, arranged in London a conference for the purpose of surveying the scientific problems raised by the development of nuclear reactors. The present volume, issued as a Supplement to the British Journal of Applied Physics, in the same style and format as this journal, reproduces the introductory lectures to the various sessions (save one), as well as the main points of the following discussions. Since these lectures were given by authorities in the respective topics and were chosen so as to cover all aspects of the subject in a very comprehensive way, this record of the conference proceedings is a document of lasting value. Its usefulness is by no means limited to the specialists: it provides all those who are interested in the scientific aspects of this expanding branch of technology with a concise and reliable exposition of the present state of the development. After a general survey by Sir John Cockroft, the topics successively discussed are:

advanced reactors (J. R. Dietrich, Argonne Lab.)
experimental reactors (P. W. Mummery, Harwell)
the breeder reactor ‚Zephyr' (L. R. Shepherd, Harwell)
effects of irradiation on solids (A. H. Cottrell, Harwell)

shielding problems (G. C. Laurence, Chalk River)
control problems (A. J. Salmon, Aldermaston)
instrumentation (W. Macrae, Newcastle upon Tyne)
chemistry (R. Spence, Harwell) and metallurgy (L. Rotherham, Risley)
uses of reactors (W. B. Lewis, Chalk River and F. W. Fenning, Harwell).

There was also a lecture on nuclear theory by Prof. R. E. Peierls, but we are denied its substance and only presented with its skeleton. All lectures are technical in style, with abundant diagrams, formulae and tables; highly informative, yet not too forbidding for the non-specialist. But why must these wonderful achievements, which reach truly epic proportions, be described in such a horrible jargon? When will scientists have the courage to write about their work in a human, and, above all, in a *personal* way?

L. R.

NEWS ITEM

CONFERENCE ON LIQUID SCINTILLATION COUNTING (EVANSTON, AUGUST 20-22, 1957)

August 20-22, 1957, Northwestern University will hold a conference on Liquid Scintillation Counting at the Technological Institute, Evanston, Illinois. A wide range of topics on the theory and application of liquid scintillators is covered by invited papers: Coincidence counters, single channel counters, chemistry of liquid scintillators, and applications in biology and medicine, industry, archaeology, physics, chemistry and engineering.

Abstracts of non-solicited papers should be sent to the Program Chairman, Dr. F. Newton Hayes, Los Alamos, New Mexico, by June 1, 1957.

APPEAL TO CONTRIBUTORS

Among the factors delaying the appearence of a paper, the most serious is the unsatisfactory presentation of the typescript. An appeal is made to contributors to follow the simple rules and conventions laid down in the instruction sheet which has already been widely distributed and copies of which are available on request from the publishers or the members of the Editorial Board. Attention is called in particular to the writing of formulae. Authors are especially requested *not* to typewrite formulae, but to write them in long hand, very carefully, since the compositor cannot guess the meaning of a symbol which is not legible. In future, the Editor will be forced to return unsatisfactory typescripts to the authors for the necessary material improvements.

It frequently happens that after a paper has been communicated, the author sends substantial corrections or alterations. Since the publisher and printer spare no effort to achieve prompt publication, such late alterations often arrive after the paper has already been set, and inflict on them much unnecessary trouble and cost. Contributors should realise that a too hasty writing-up of a paper thus defeats the prospect of a quick publication.

Editor and publisher trust that the authors will not shun the slight trouble which the careful preparation of the typescript entails and thank them in advance for their cooperation.

JUST OUT

QUANTUM MECHANICS

by

H. A. KRAMERS

Late-Professor of Theoretical Physics, University of Leiden

Translated by D. TER HAAR, *Clarendon Laboratory - Oxford*

This book is an English translation of the well-known pre-war monograph on Quantum Theory.

The author was closely connected with Niels Bohr's institute from 1912 until 1926, during which period quantum theory was developed, to a large extent by the Copenhagen school, into essentially its present form. Among Kramers' own contributions to this development one may mention the so-called W-K-B method, the symbolic method for calculating intensities of spectral lines, the derivation of the wave equation for a relativistic electron (independent of and practically simultaneous with Dirac's derivation), and the idea of mass renormalisation. As a consequence, the presentation of quantum theory in the present textbook is more lively and less stereotyped than in most texts on the subject and often sheds light on details which are usually overlooked. Also, there are in this monograph a number of those mathematical gems which were so typical of Kramers.

6×9″, xvi +496 pages

Guilders 45.— (90 s.)

CONTENTS:

I. Quantum theory of free particles.
II. Non relativistic quantum theory of bound particles.
III. The non-relativistic treatment of the many-body problem.
IV. Transformation theory.
V. Perturbation theory.
VI. The spinning electron.
VII. The exclusion principle.
VIII. Electromagnetic radiation.

Sole distributors for U.S.A.: Interscience Publishers, Inc. - New York

NORTH-HOLLAND PUBLISHING COMPANY - AMSTERDAM

Send your order to your bookseller or directly to the publisher